HYDRAULIC MODELLING OF A SHARP CRESTED LABYRINTH WEIR

ADOLF TOMMY SITOMPUL

NOTICE

The quality of this microform is heavily dependent upon the quality of the original thesis submitted for microfilming. Every effort has been made to ensure the highest quality of reproduction possible.

If pages are missing, contact the university which granted the degree.

Some pages may have indistinct print especially if the original pages were typed with a poor typewriter ribbon or if the university sent us an inferior photocopy.

Reproduction in full or in part of this microform is governed by the Canadian Copyright Act, R.S.C. 1970, c. C-30, and subsequent amendments.

AVIS

La qualité de cette microforme dépend grandement de la qualité de la thèse soumise au microfilmage. Nous avons tout fait pour assurer une qualité supérieure de reproduction.

S'il manque des pages, veuillez communiquer avec l'université qui a conféré le grade.

La qualité d'impression de certaines pages peut laisser à désirer, surtout si les pages originales ont été dactylographiées à l'aide d'un ruban usé ou si l'université nous a fait parvenir une photocopie de qualité inférieure.

La reproduction, même partielle, de cette microforme est soumise à la Loi canadienne sur le droit d'auteur, SRC 1970, c. C-30, et ses amendements subséquents.

Canada

HYDRAULIC MODELLING OF
A SHARP CRESTED LABYRINTH WEIR

By

©ADOLF TOMMY SITOMPUL

A Thesis Submitted to the School of Graduate Studies

in Partial Fulfilment of the Requirements for

the Degree of Master of Engineering

FACULTY OF ENGINEERING AND APPLIED SCIENCE

MEMORIAL UNIVERSITY OF NEWFOUNDLAND

DECEMBER, 1993

ST JOHN'S NEWFOUNDLAND CANADA

ISBN 0-315-91601-X

Canada

Abstract

A labyrinth weir is an attractive alternative for water level control in flat land where the head is usually limited. It is also useful in a river where the weir width is confined by the topography. The advantages occur because the crest length of a labyrinth weir is significantly longer than the width of the river. This is achieved by having a plan form which consist of repeating geometric cycles, typically trapezoidal in form. As a result large flows can be released at relatively low heads. Trapezoidal and triangular forms have become the favoured geometric cycles for designers.

This study on a labyrinth weir was undertaken to confirm the operating parameters as well as to investigate different plan shapes including rectangular, rectangular with a semi-circular connection and reverse trapezoidal. Experimental and theoretical results confirmed that the trapezoidal shape with the side wall angle, α = 0.68 $\alpha_{max.}$ and the length magnification, l/w = 2.65 gave the best hydraulic performance among other labyrinth weir plan forms which were tested in this study. The effect of varying the crest width was also investigated in this study. This part of the study focused on the trapezoidal shape. It was shown that increasing the width of the crest up to 10 mm (in this case 10% of weir height, P) was not significant in decreasing the flow despite some frictional losses on the crest. Such a crest is useful when a river has a large quantity of debris.

The economic advantages of labyrinth weirs were also studied with reference to the Ciwadas trapezoidal labyrinth weir which was constructed in Indonesia in 1988. This labyrinth weir was designed to handle the flood flows of 200 m^3/s and control water depths between 1.6 m and 2.35 m. Comparison with a typical weir with gate shows that this labyrinth weir was more than 25% less expensive.

A computer code for analytical studies was also established. It was shown that for trapezoidal plan forms, a good agreement between theoretical results and experimental data could be achieved. This also confirms the previous theoretical solution proposed by Hay and Taylor although there is a little difference (0.1) in defining the value of the energy loss coefficient (contraction) at the entry to the weir.

Acknowledgements

It is my very pleasant duty to express my gratitude to my supervisor, Professor DR. J.J. Sharp, for his continual reinforcement, patience, very valuable advice and comment, and guidance in preparing this thesis and conducting the laboratory experiment.

I am also thankful to DR. L.M. Lye, for his very useful advice in preparing the Chapter 2 of my thesis.

The writer wish to express his thanks to DR. N. Hay of the Department of Mechanical Engineering, University of Nottingham for sending me the details of computer program of the theoretical solution of DR. Taylor's thesis.

The writer would like to acknowledge the financial support of the Government of Canada which is administired by the Canadian International Development Agency (CIDA). A part of the model test facility was financed by the Natural Sciences and Engineering Research Council of Canada (NSERC) to DR. J.J. Sharp. This assistance is gratefully acknowledged.

I gratefully acknowledge to the Ministry of Public Works of the Republic of Indonesia and to the Memorial University of Newfoundland for providing the opportunity to study in Canada.

The author wish to thank Mr. J. Andrews, Mr. S. Foster, and technical services staff of Faculty of Engineering for their help in the construction of the experimental apparatus. I am also indebted to Mr. D. Sparks of the Hydraulic Laboratory of Faculty of Engineering for his assistance during the experimental works in the laboratory.

Finally, I am much indebted to my wife, Evalina S.M. Pasaribu, and my parents, Mr. & Mrs. A.M. Sitompul, and Mr. & Mrs. A.S. Pasaribu for their patience and encouragement.

Table of Contents

List of Tables

List of Figures

List of Symbols

Symbol	Description	Dimensions
a	a half length of tip sections of labyrinth weir normal to the main flow direction	L
A	the area of the cross section of flow	L^2
b	the length of one side wall of labyrinth weir	L
C_d	discharge coefficient of a weir	-
C_{LH}	discharge coefficient of a labyrinth weir proposed by Lux and Hinchliff	-
C_{sc}	the coefficient of energy loss due to sudden contraction	-
C_w	discharge coefficient of a labyrinth weir proposed by Darvas	-
E	water surface elevation relative to crest	L
g	the acceleration due to gravity	LT^{-2}
H	the flow depth	L
H_v	the velocity head, $V^2/2g$	L
H_o	the total head, $H + H_v$	L
H/P	the ratio of the flow depth over the weir crest to the height of the weir	-
H_o/P	the ratio of the total head over the weir crest to the height of the weir	-
l	the developed crest length of one-cycle labyrinth weir	L
l/w	the length magnification, a ratio of length of one-cycle labyrinth weir to the length of corresponding presumptive	

	straight weir	-
L	the total developed crest length of a labyrinth weir regardless the number of cycle	L
L/W	the length magnification, a ratio of length of the labyrinth weir to the length of corresponding presumptive straight weir regardless the number of weir cycle	-
n	the number of labyrinth weir cycles in plan	-
P	the height of the weir	L
Q_L	the total flow over one-cycle labyrinth weir	L^3T^{-1}
Q_{TL}	the experimental total flowrate at the labyrinth weir regardless of the number of cycles	L^3T^{-1}
Q_{TN}	the theoretical flowrate at the presumptive straight weir, calculated on the basis of full channel width	L^3T^{-1}
Q_N	the total flow over a straight weir with a crest length equal to the channel width of one-cycle	L^3T^{-1}
Q_L/Q_N	the flow magnification, a ratio of discharge over a sharp crested labyrinth weir to the discharge over a sharp crested presumptive straight weir	-
O+M	operation and maintenance	-
s_{cb}	the slope of the channel bed between the sections	-
s_{sw}	the slope of side wall	
S_f	the friction slope between the sections	-
S_o	the slope of the river bed	-
w	the width of one-cycle of labyrinth weir	L
w/P	the vertical aspect ratio, a ratio of the width of one-cycle of the labyrinth weir to the height of the labyrinth weir	-
W	the total width of a labyrinth weir regardless the number of cycle	L
X	the transverse distance along the channel	L
α	the angle of the side wall of the labyrinth weir to the	

	main direction of the flow	-
β	the energy coefficient	-
μ_w	discharge coefficient of a labyrinth weir proposed by Magalhães	-
μ	viscosity	L^2T^{-1}
ρ	density of water	ML^{-1}
σ	surface tension	MT^{-2}

Chapter 1

Introduction

1.1. Weirs as control structures

Weirs are constructed to increase water levels by the effect of the backwater They can also be used to change the distribution of a river's discharge through its branches, and to provide suitable conditions for recreation and fisheries, etc. In addition to this, weirs are also utilized to pass the flood flows by allowing water to overtop. Raising the water level of a river allows water to enter the intake of an irrigation system, as well as the intake of a domestic or industrial water supply.

Straight weirs and barrages are two types of control structures which have wide application in irrigation systems. Although the purpose of both is to increase water levels, straight weirs differ from barrages in structure. A straight weir is built to maintain satisfactory water levels behind the weir. When the flood occurs, the water is allowed to flow over the crest and a gate is not provided (Figure 1-1). A barrage, consisting of a weir with an undershot gate, is usually built on the flatland area of a river where the

ratio of maximum flow to minimum flow is quite high. A small, unrestricted, weir is provided to pass the maximum flow without excessive increase in depth. However water elevations are likely to be too low with the unrestricted weir at low flows and a gate is therefore provided (Figure 1-2). This can be closed as the flow reduces to ensure satisfactory water levels at all flows between minimum and maximum.

1.2. The sharp crested labyrinth weir

The sharp crested labyrinth weir performs the same function as a barrage in the sense that an acceptable minimum elevation is maintained at low flows without having excessively high elevations at large flows. However no gate is required and, unlike a straight weir, a labyrinth weir is distinguished by the plan shape. The geometric design is not linear. Rather it is varied by using a repeating plan form (see Figure 1-3). As a result, the weir will consist of a number of cycles. Hence, the water flow is presented with a greater length of crest as compared with a straight weir occupying the same space. Because the crest length of a labyrinth weir is significantly longer than that of a straight weir, the discharge for a given operating head is significantly increased.

The development of labyrinth weirs has been supported by these following advantages :

a). Due to the increase in the crest length, it provides a lower operating head than a conventional weir. Thus, the inundation area can be decreased.

b). In case of a sudden change in the flow magnitude the fluctuation of water surface elevations can be reduced since this weir is suited for use where the ratio of flow

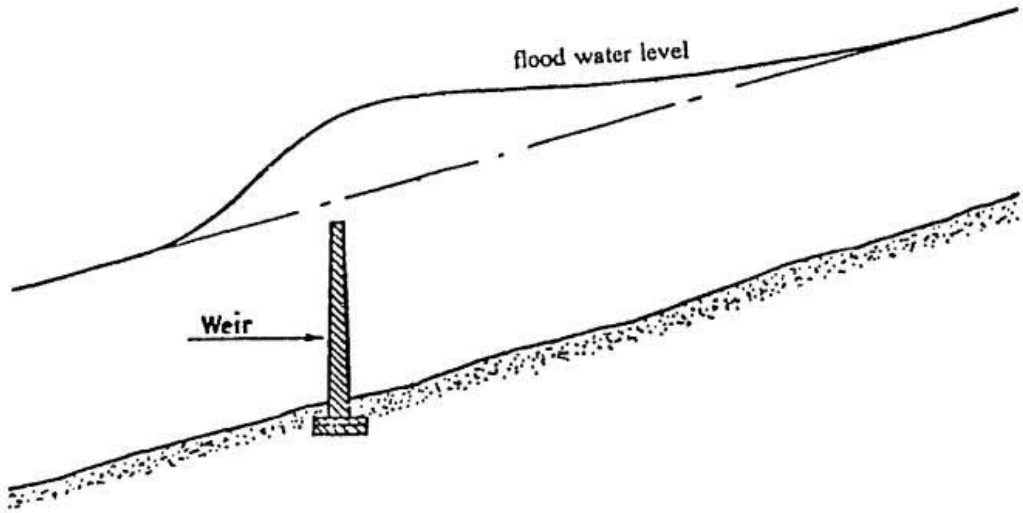

Figure 1-1 A straight weir
After Slagter (1975).

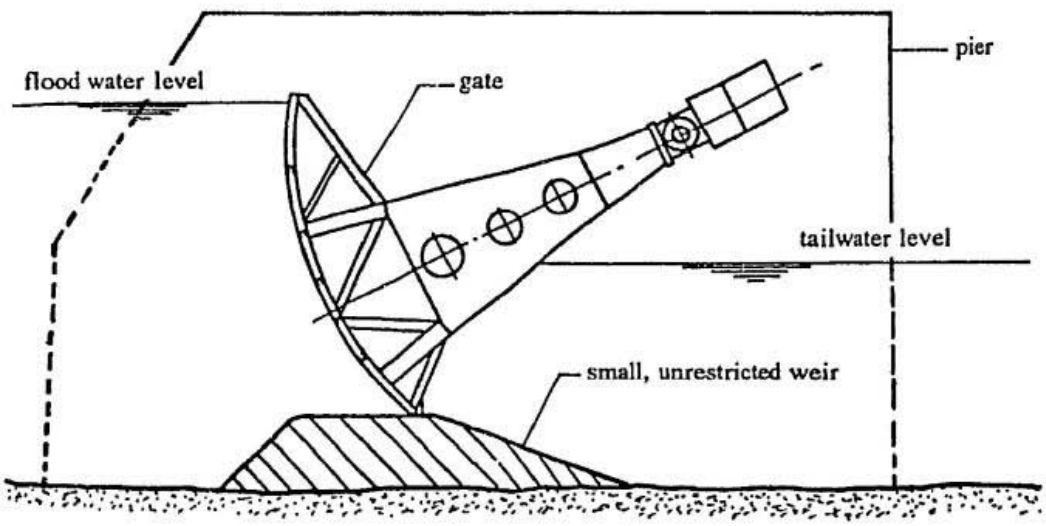

Figure 1-2 A barrage
After Slagter (1975).

maximum to minimum is quite high (see Figure 1-4).

c). The energy of the flow is partially dissipated by the interaction of the flows from adjacent cycles (see Figure 1-3). Therefore a simpler stilling basin floor can be designed. As a result, the costs of the stilling basin are reduced.

d). If the labyrinth weir is made of reinforced concrete, it will be a lighter structure than a conventional weir which is usually a massive structure. Consequently, a simpler foundation of the structure can be designed even though the bottom soils are poor.

e). Finally, it can be shown (see Chapter 2) that the labyrinth weir is more economical than a barrage.

1.3. The use of labyrinth weir in Indonesia

The Ciwadas labyrinth weir was the first, and is currently the only, labyrinth weir constructed in Indonesia. It is situated at Karawang, West Jawa, 300 km east of Jakarta, capital city of Indonesia, an area known for its shrimp products. Construction on the labyrinth weir began on November 27, 1987, and was completed on October 6, 1988, before the contract completion date on March 3, 1989. The contractor was P.T. Hutama Karya of Jakarta, Indonesia. The primary purpose of the weir is to provide 12 m^3/s freshwater for a shrimp pond area. For that purpose 1.6 m elevation of water is required by the intake. This reinforced concrete weir is able to pass the 50 year return period design flood of 200 m^3/s at a water surface elevation of 2.35 m.

Besides the Ciwadas weir, five other weirs have been designed but construction is currently on hold. These are, the Maloso Weir in South Sulawesi, Batanghari Weir in

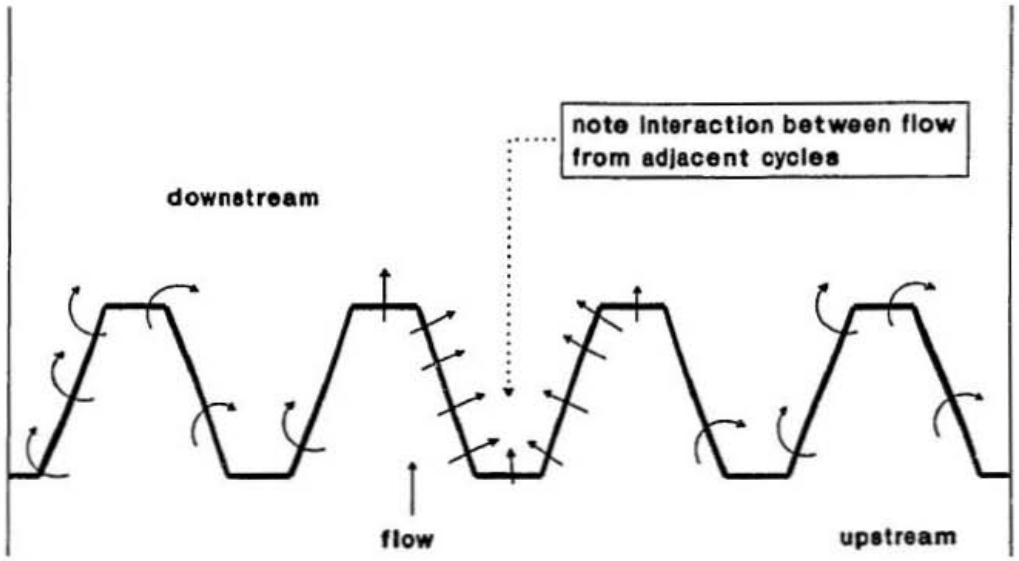

Figure 1-3 A typical 4 cycle trapezoidal shape labyrinth weir

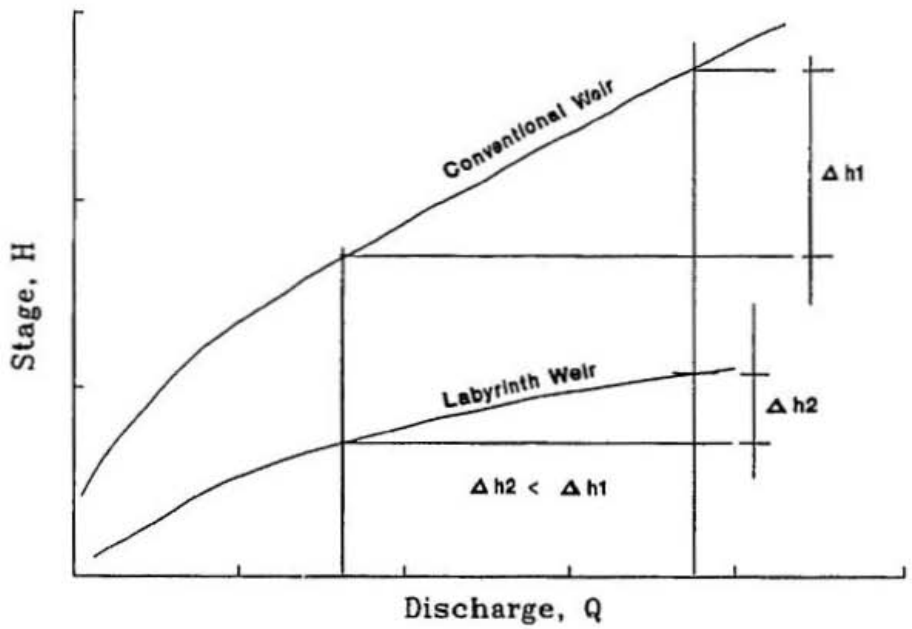

Figure 1-4 A stage-discharge (Q-H) relationship of the weirs

West Sumatra, Tami Weir in Irian Jaya, Ubrug Weir ,and Karedok Weir in West Jawa. Figure 1-5 shows the location of these labyrinth weirs. This study was designed to enhance the understanding, and therefore the further development, of labyrinth weirs in Indonesia.

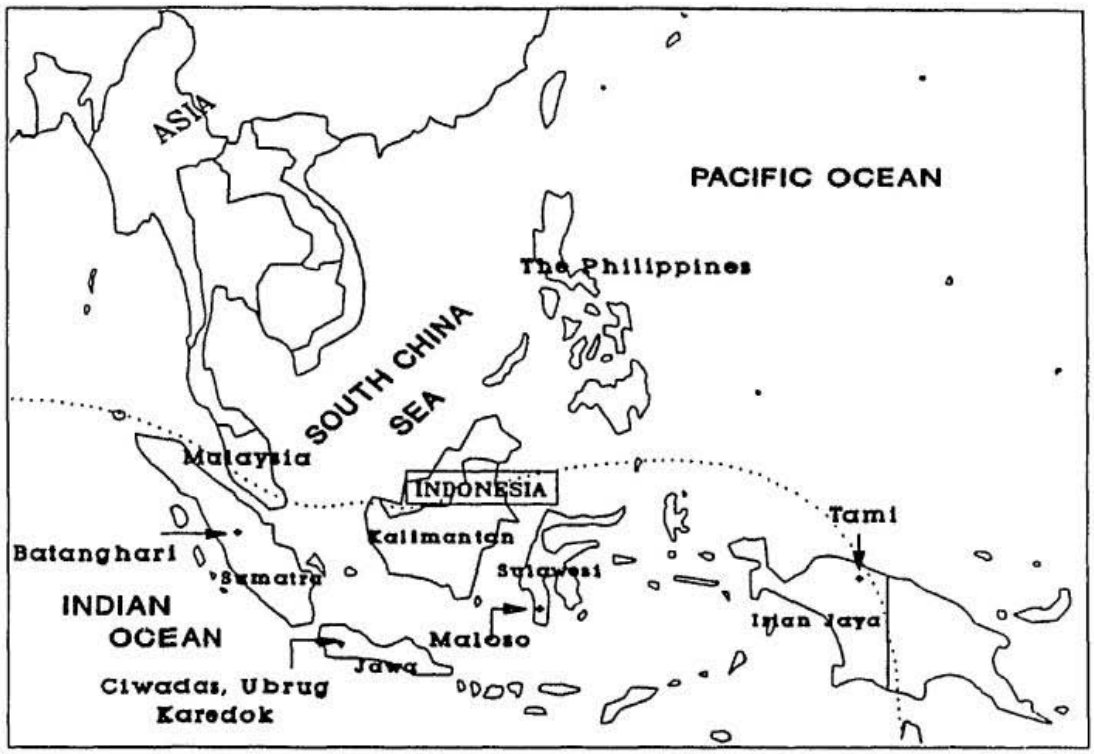

FIGURE 1-5 Location of the labyrinth weirs

1.4. The objective of this study

There are several objectives of the present study. The first is to check previous experimental data of the hydraulic model studies of labyrinth weirs which have been done by other researchers. The second is to consider and examine the combination of rectangular and half circle plan form as an alternative geometry (see Figure 1-6). A third

is to study the effect of variation in crest width for the trapezoidal plan form. All of these were based on experimental work. A further objective was to develop a spreadsheet analysis to provide an analytical solution of the flow over the labyrinth weir crest.

These original objectives were modified during the experimental work because of some initial findings. When a rectangular plan form was investigated at high flows, an undular jump was found to occurr over the crest (see Figure 1-7). This was thought to be due to blocking of the downstream flow. Therefore, a reverse trapezoidal plan form which increased the blocking was used to study this phenomenon (see Figure 1-8). It was also found that the spreadsheet analytical solution was cumbersome and time consuming and a computer program model was then developed in QuickBASIC to rectify the spreadsheet one.

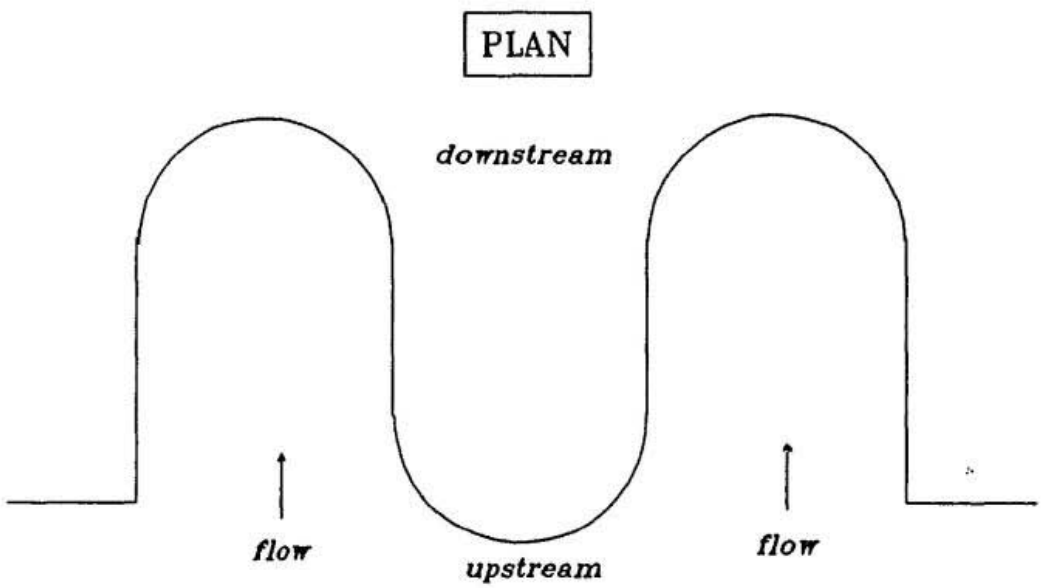

Figure 1-6 A combination of rectangular and half circle plan form

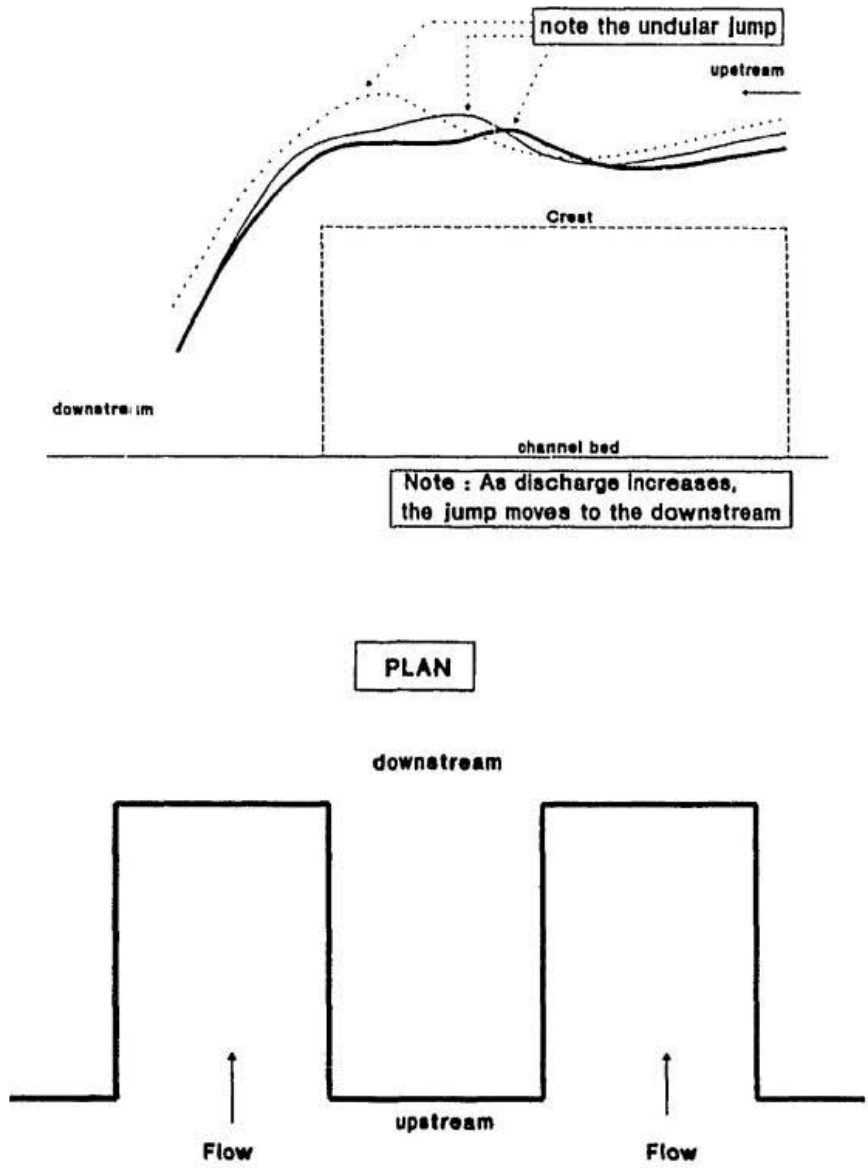

Figure 1-7 Flow description over the rectangular shape labyrinth weir at high flows

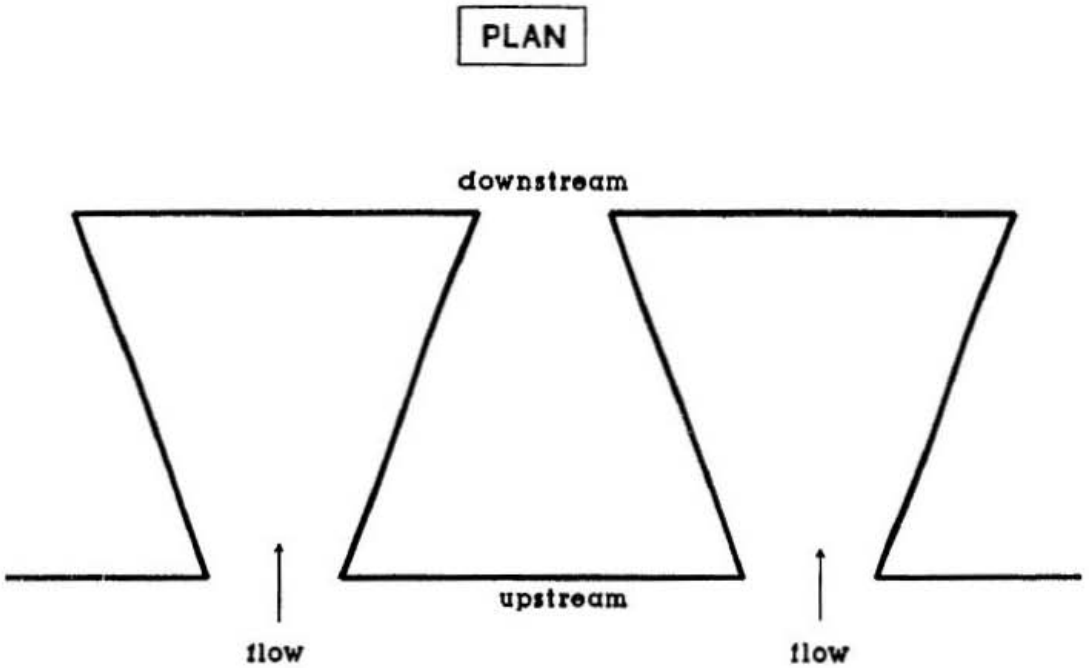

Figure 1-8 A reverse trapezoidal plan form

Chapter 2

Economic Analysis of a Labyrinth Weir

2.1. Introduction

Indonesia, the fifth most populous country in the world, has a population which is estimated to rise to not less than 196 million people by the end of 1995 (World Bank, 1990). According to a ministerial report (Indonesian Ministry of Transmigration, 1988), more than 80 percent of the people are dependent on agriculture. Water resources development and irrigation programmes therefore play an important role in improving the quality of life through a better income distribution and by helping the poor farmer. The important role of irrigation in increasing rice production is undoubted and was proved by the achievement of self sufficiency in rice production in 1984.

In 1985 the Ciwadas project was launched in accordance with planning and programming of water resources development to promote fish and shrimp cultivation through irrigation programmes. The project is situated at the Ciwadas River, Karawang, West Java, in the lowlands of Java, where the bulk of the rice is grown. Total annual

rainfall varies from about 1500 mm up to about 2500 mm (Water Resources Development, 1988). The rainy season, during which 70 percent of the rainfall occurs, extends from September to March (West monsoon) and the dry season from April to August (East monsoon) (Water Resources Development, 1988). This amount of rainfall is usually insufficient to grow a wet season crop. The onset of rains is sometimes delayed and much of the rainfall occurs in high intensity storms.

The Ciwadas River is situated on a flatland area with an average river bed slope of 4.84×10^{-4}. Fifty years of flow records on the Ciwadas River show that the maximum discharge was 196.25 m^3/s whereas the minimum was 4.15 m^3/s. Thus, the ratio of maximum to minimum flow is high (47.30). This is a typical value in most rivers in Indonesia (average value is in excess of 40). Based on those situations, it was decided that a barrage was the best structure to offer maximum water level control in these topographical and hydrological conditions. With a barrage, the water level behind the weir could be controlled at both low flows and high flows (Hutama Karya, 1985). However due to expensive construction costs, this alternative was not approved by the project steering committee.

An optimization cost analysis was carried out using a labyrinth weir as a second alternative because this weir results in a lower maximum water level than that of a conventional weir. From the analysis, it was estimated that the labyrinth weir could reduce the construction costs by 50 percent (Hutama Karya, 1985) and the labyrinth weir was therefore adopted in this project. As shown in Table 2.6, this estimate was, perhaps, too optimistic. The two alternative descriptions are displayed in Figure 2-1.

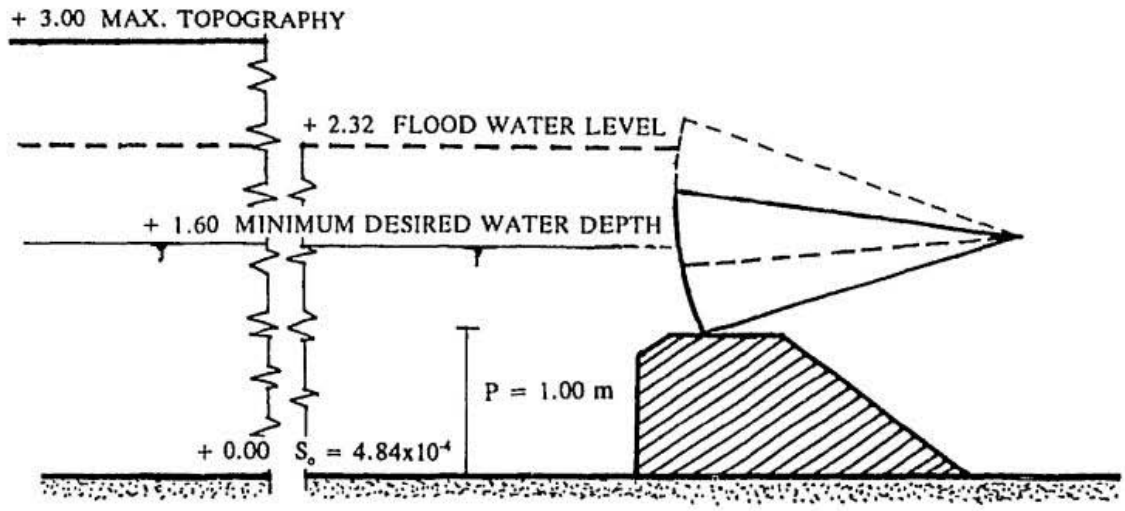

ALTERNATIVE 1 : *A BARRAGE*

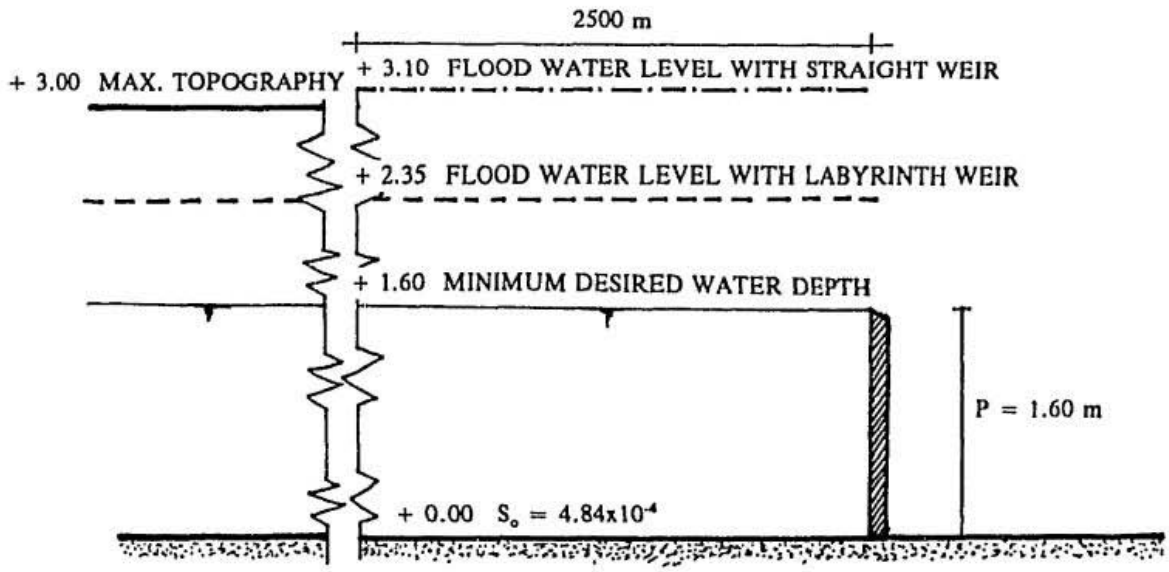

ALTERNATIVE 2 : *A LABYRINTH WEIR*

Figure 2-1 A description of two alternatives, barrage and labyrinth weir

A detailed economic analysis of a labyrinth weir is presented here to demonstrate the benefits of using this type of weir. Due to the availability of the Ciwadas project data, the Ciwadas labyrinth weir was selected as a study case.

2.2. The Ciwadas labyrinth weir and barrage description

2.2.1. Labyrinth Weir

The Ciwadas Labyrinth Weir was completed in 1988. As constructed the weir consists of seven cycles with a total crest length of 176.60 m within a river width of 61.00 m and has repeated, symmetrical trapezoidal shapes (Figure 2-2 and Figure 2-3). It is constructed of reinforced concrete with a crest width of 0.30 m and a crest height of 1.60 m. After the completion of this project, it became possible to provide freshwater for 600 ha of shrimp ponds by gravitational irrigation. The freshwater is conveyed by the primary freshwater channel and is distributed to two secondary channels through a distribution structure. Then, the freshwater is conveyed to several ponds where freshwater and seawater are mixed.

2.2.2. Barrage

Based on a 50 year return period, a design flood of 200 m^3/s and 1.6 m minimum water elevation required by the intake, were used to design the dimensions of the alternative system. Design calculations (Hutama Karya, 1985) showed that a 1.00 m height of unrestricted weir and 10 radial gates were required. Each gate would be 5.00 m wide and 1.00 m high (Figure 2-1).

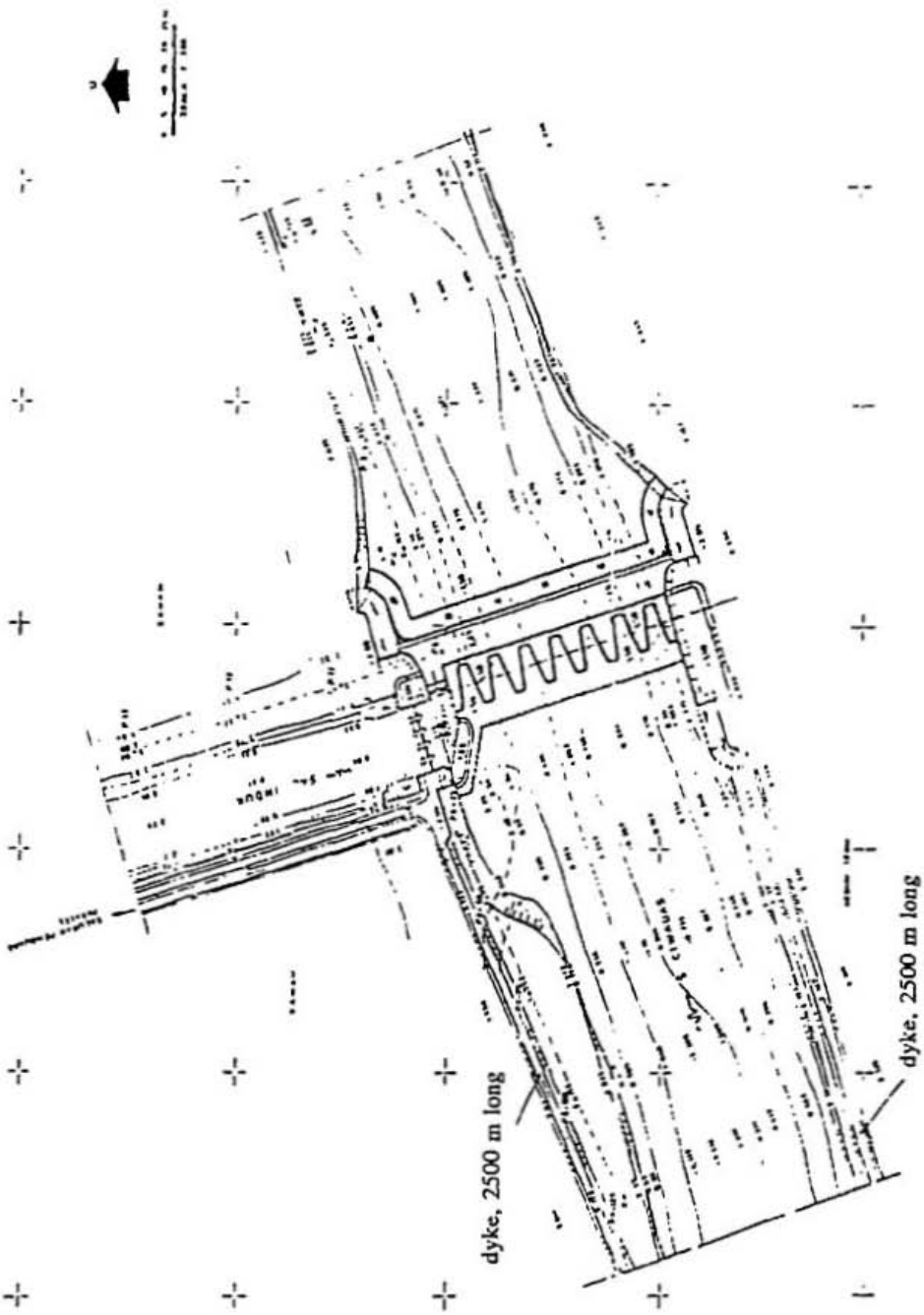

Figure 2-2 A situation of Ciwadas labyrinth weir
After Hutama Karya (1989).

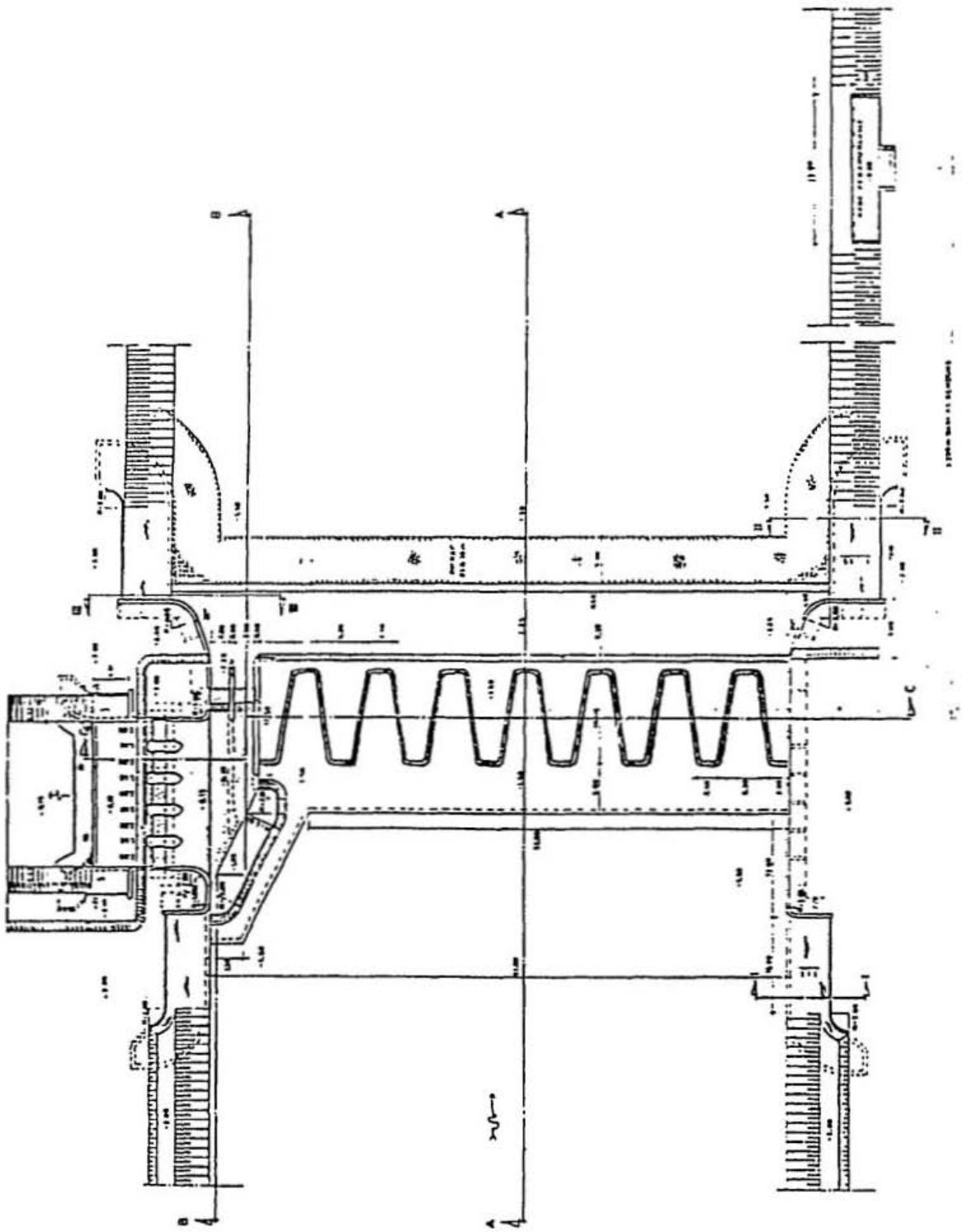

Figure 2-3 A plan of Ciwadas labyrinth weir
After Hutama Karya (1989).

2.3. Cost comparison of barrage and labyrinth weir

In this analysis, costs are defined in two ways. The first is in terms of construction costs while the second is in terms of operation and maintenance costs.

2.3.1. Construction Cost

The analysis of construction costs is broken into two parts. The first is for the labyrinth weir, and the second is for the barrage. The costs of two sluice gates (2.36 m x 1.75 m and 2.36 m x 2.35 m) for sediment flushing, removal of the existing weir, trash racks, an access road, lighting for works, a diversion channel, a cofferdam, dewatering, and a bridge for works were excluded from each analysis, because all of these were required both by a labyrinth weir and by a barrage. The contractor's report (Hutama Karya, 1989) showed that the actual construction costs for those works was US $ 377,094 (based on 1988 prices and an exchange rate of Rp.1650/US $).

Both designs would require dykes to be constructed upstream. These would be located on either side of the river and would protect the surrounding land against flooding at the higher water levels. However both alternatives were designed for the same maximum water level. The dykes required by the labyrinth weir and the barrage would therefore be of the same size. Design calculations (Hutama Karya, 1985) showed that a 3.00 m height and 2500 m length of dykes were required. The cross section of the dykes was trapezoidal with 2.00 m top width and 6.00 m base width for both alternatives. Costs would therefore be the same and dyke costs are therefore not given in this analysis. The contractor's report (Hutama Karya, 1989) showed that the actual construction costs for

a dyke was US $ 88,712 (based on 1988 prices and an exchange rate of Rp.1650/US $).

The labyrinth weir

Details of actual construction costs incurred by the labyrinth weir are listed in Table 2.1. The unit, number of units, unit price, and total costs were all taken from the contractor's final report (Hutama Karya, 1989). 'Extras', given in row 15 Table 2.1, refers to the costs discussed above. As shown in Table 2.1 the total specific cost of a labyrinth weir was US $ 659,432.36. When the extra costs noted above are added the real total cost of a labyrinth weir becomes US $ 1,036,527. Dyke costs would be in addition to this amount.

The barrage

The initial design report (Hutama Karya, 1985) which compared capital costs of a barrage with a labyrinth weir did not give detailed costs of the barrage. Total costs of a barrage were estimated without detailing the number of units and unit prices of each item of works. Instead of accepting these total costs, it was decided to attempt a more accurate estimate of unit numbers and unit prices. Therefore the design of the New Rentang barrage in Cimanuk River, West Java (Puslitbang Pengairan, 1973) was used as a reference to estimate the number of unit costs and some of the unit prices of a barrage. The numbers of units of each item of work were estimated by adjusting according to the dimensions of the Ciwadas barrage relative to that of the New Rentang barrage. These are shown as items 1, 2, 3, 5, 6, 7, 8, 13, 14, 15 and 16 in Table 2.2.

Some of the unit prices were taken from the final report of contractor (Hutama Karya, 1989) since some of the barrage works were also required for the labyrinth weir works, such as items 1, 6, 8, 14 and 15 in Table 2.2. The remaining unit prices, for items 2, 3, 5, 7, 13 and 16, were taken from the design of the New Rentang barrage (Puslitbang Pengairan, 1973) with an adjustment made to transfer from 1972 prices to 1988 prices.

The number of units and unit prices of items 4, 9, 10, 11, and 12 in Table 2.2 were estimated in consultation with the staff of P.T. Barata, an Indonesian metal works company (Wibowo, personal communication, 1993).

Estimated construction costs are displayed in Table 2.2. 'Extras', given in row 17 Table 2.2 again refer to the costs discussed in Section 2.3.1. As can be seen from Table 2.2 the total estimated cost required only by a barrage is US $ 826,827.68. If the extra costs detailed earlier are added the total estimated cost of a barrage becomes US $ 1,203,922. Dyke costs are again additional to this amount. The design calculation (Hutama Karya, 1985) estimated the total construction costs of a barrage at US $ 1,607,818 which is about 34 percent higher than author's estimation. Presumably this difference is because the contractor over-estimated the number of units in some works. It is considered that the estimate given here is more accurate since it is based on actual construction costs at another barrage which has been constructed in a similar area.

Discussion

As can be seen from Table 2.1 and Table 2.2 the capital costs of a labyrinth weir and a barrage are US $ 1,036,527 and US $ 1,203,922 respectively. Thus the capital cost

of the barrage is about 20 percent higher than that of the labyrinth weir. This assumes that both alternatives have the same life time. However, as shown in Table 2.2, one of the major costs relating to the construction is the cost of the gate and its facilities (items 4, 9, 10, 11, and 12) which amounts to US $ 362,341. This is approximately 30 percent of the cost of the barrage. These items are not required for the labyrinth weir. Whereas the labyrinth weir is comprised entirely of civil works (with the assumption of a life time of 50 years), part of the barrage (the gates and power equipment) is mechanical works with a life time of only 25 years (Lye, 1992). Therefore, the different life time should be taken into account, by reducing both capital costs to an annual cost of debt repayments.

The annual capital cost

In this calculation the capital costs of the barrage will be broken into two parts. Part one deals with the civil works, and part two deals with mechanical works. The total cost of these mechanical works, items 9, 11, and 12 in Table 2.2 is US $ 293,347. If the total costs for mechanical works are subtracted from the total then the estimated cost of the civil works of the barrage becomes US $ 910,575. The annual cost of both alternatives at different interest rates has been obtained and displayed in Table 2.3. As shown in Table 2.3, the cost ratio tends to decrease as the interest rate increases. It is likely that the difference of annual capital cost between both alternatives is significant at lower interest rates ($<8\%$).

TABLE 2.1

Table of actual construction cost of the labyrinth weir
(Based on 1988 prices and exchange rate of Rp.1650/US $)

No. (1)	I t e m (2)	Unit (3)	No. of units (4)	Unit Price (US $) (5)	Total (US$) (6)
	THE LABYRINTH WEIR				
	L = 176.6 m, W = 61 m, P = 1.6 m				
1.	Structure excavation works	m^3	23,892.00	5.43	129,733.56
2.	Soil improvement	m^3	3,764.00	13.19	49,647.16
3.	Wooden sheetpile works, constructing from circular piles 8 cm diameter and 5 m long.	no.	46,446.00	1.87	86,854.02
4.	Concrete works, 1:3:5 cement/sand/gravel mix	m^3	654.00	40.98	26,800.92
5.	Concrete works, 1:2:1 cement/sand/gravel mix	m^3	1,632.00	85.13	138,932.16
6.	Steel used as reinforcement	kg	237,755.00	0.39	92,724.45
7.	Wooden sheetpile for foundation, constructing from circular piles 10 cm diameter and 5 m long.	no.	2,875.00	2.85	8,193.75
8.	Masonary works for the flank walls, with 1:4 cement/sand mix as a filler material; stone 30 cm in diameter	m^3	596.00	31.72	18,905.12
9.	Finishing mortar, -1:2 cement/sand mix	m^2	831.00	1.31	1088.61
10.	Finishing mortar, -1:3 cement/sand mix	m^2	174.00	1.40	243.60
11.	Rip-rap; stone, diameter = 30 cm	m^3	686.00	30.15	20,682.90
12.	Backfill without compaction	m^3	5,910.00	1.43	8,451.30
13.	Bamboo weave wall	m^3	49.00	1.53	74.97
14.	Excavation of mud	m^3	16,096.00	4.79	77,099.84
			Sub Total		659,432.36
15.	Extra costs	-	-	-	377,094.00
			Total		1,036,527

Note : L = crest length; W = river's width; P = crest height Source : Hutama Karya, 1989.

TABLE 2.2

Table of estimated construction cost of the barrage
(Based on 1988 prices and an exchange rate of Rp.1650/US $)

No. (1)	Item (2)	Unit (3)	No. of units (4)	Unit Price (US $) (5)	Total (US $) (6)
	THE BARRAGE				
	W = 61.00 m, P = 1.00 m				
1.	Main structure excavation	m^3	26285.00	5.43	142727.55
2.	Steel sheetpile cut-off	m^2	1220.00	53.24	64952.80
3.	Concrete in the stilling basin floor, 1:2:3 cement/sand/gravel mix	m^3	762.50	55.66	42440.75
4.	Concrete in the piers, and the slabs -1:2:2 cement/sand/gravel mix	m^3	536.25	70.85	37993.31
5.	Concrete in the main weir, -1:2:2 cement/sand/gravel mix	m^3	468.75	70.85	33210.94
6.	Concrete in the bridge decks, 1:2:1 cement/sand/gravel mix,(61x8x0.3)m^3	m^3	146.40	85.13	12463.03
7.	Backfill & Compaction	m^3	4920.00	1.95	9594.00
8.	Masonary works	m^3	1260.00	31.72	39967.20
9.	The equipment to operate the 10 radial gates	no.	10.00	12130.0	121300.00
10.	Housing for control and operation of 10 radial gates	no.	10.00	3100.00	31000.00
11.	(a) 10 radial gates: 5 m x 1 m	kg	22530.00	4.55	102511.50
	(b) 10 gate hoists	kg	11265.00	6.09	68603.85
12.	Synthetic rubber waterstop	m	75.00	12.42	931.50
13.	Handrails	m	226.00	28.93	6538.18
14.	Excavation of mud	m^3	17705.60	4.79	84809.82
15.	Rip-rap; stone, diameter = 30 cm	m^3	823.50	30.15	24828.55
16.	Filter-materials	m^3	381.25	7.75	2954.70
			Sub Total		826827.68
17.	Extra costs	-	-	-	377094.00
			Total		1,203,922

TABLE 2.2 (continued)

Note : W = crest length; P = crest height
: Unit prices were taken from Hutama Karya, 1989 & Puslitbang Pengairan, 1973, and No. of units were calculated as indicated in text.

TABLE 2.3
Table of annual cost of the barrage and the labyrinth weir
(Based on 1988 prices and exchange rate of Rp.1650/US $)

Interest rate (%) (1)	Capital Recovery Factor n = 25 years (Riggs *et al.*, 1986). (2)	Annual Cost of Mechanical Works a barrage (US $) (3)	Capital Recovery Factor n = 50 years (Riggs *et al.*, 1986). (4)	Annual Cost of Civil Works a barrage (US $) (5)	Annual Cost of a barrage (US $) (3)+(5) (6)	Annual Cost of *a labyrinth weir* (US $) (7)	Cost Ratio (b/lw) (6):(7) (8)
3	0.05743	16846.92	0.03887	35394.05	52240.97	40289.80	1.30
5	0.07095	20812.97	0.05478	49881.30	70694.27	56780.95	1.25
7	0.08581	25172.11	0.07246	65980.26	91152.37	75106.75	1.21
8	0.09368	27480.75	0.08174	74430.40	101911.15	84725.72	1.20
9	0.10181	29865.66	0.09123	83071.76	112937.42	94562.36	1.19
10	0.11017	32318.04	0.10086	91840.59	124158.63	104544.11	1.19
11	0.11874	34832.02	0.11060	100709.60	135541.62	114639.89	1.18
12	0.12750	37401.74	0.12042	109651.44	147053.18	124818.58	1.18
13	0.13643	40021.33	0.13029	118638.82	158660.15	135049.10	1.17
15	0.15470	45380.78	0.15014	136713.73	182094.51	155624.16	1.17

Note : (3) = (2) * total cost mechanical works of a barrage.
(5) = (4) * total cost civil works of a barrage.
(7) = (4) * total cost of a labyrinth weir.

2.3.2. Operation and Maintenance Cost

Due to the absence of detailed actual costs for operation and maintenance of both alternatives, it was decided to use the costs for operation and maintenance of a labyrinth

weir given in the contractor's final report (Hutama Karya, 1989). These gave costs for the labyrinth weir directly but needed some interpretation to be used for the barrage.

Labyrinth Weir

Two people are required to operate and maintain the sluice gate (Hutama Karya, 1989). As displayed in Table 2.3, the estimated operation and maintenance costs for the labyrinth weir is only US $ 5,321. Most of this is for painting, grass cutting and salaries. All of the maintenance works (items 3 to 8) are usually contracted out since these works require many people and are part time in nature.

Barrage

An estimation of annual operation and maintenance costs of a barrage was not prepared by the contractor. All of the estimated unit prices in this analysis were then made with reference to the contractor's final report (Hutama Karya, 1989). This was decided because in general the operation and maintenance works required by a barrage are similar to those for the labyrinth weir except for operating the radial gates.

The number of units required in each item was considered to be the same as those calculated for the labyrinth weir except that it was considered that at least four people would be required to operate 10 radial gates as well as to maintain the sluice gate. In addition, the annual operation cost of the gate and hoist was estimated as 1.5% of the capital cost of gate and hoist (Lye, 1992). As shown in Table 2.4, the estimated cost is US $ 8,977, which about twice that of the annual costs of operation and maintenance for

the labyrinth weir. Most of this is for operation and maintenance of 10 radial gates, salaries, painting and grass cutting.

All of the maintenance works (items 4 to 9) are usually contracted out since these work require many people, and are again part time.

TABLE 2.4

Table of estimated annual operation and maintenance cost of the labyrinth weir (Based on 1988 prices and an exchange rate of Rp.1650/US $)

No. (1)	Item (2)	Unit (3)	No. of units (4)	Unit Price (US $) (5)	Total (US $) (6)
	THE LABYRINTH WEIR				
	Operation Cost				
1.	Lubrication oil	kg	20.00	3.03	60.60
2.	Personnel cost	no	2.00	544.50	1089.00
	Maintenance Cost				
3.	Painting works	m^2	200.00	9.08	1816.00
4.	Grass cutting	m^2	10000.00	0.16	1600.00
5.	Repair of masonary works	m^3	5.00	30.25	151.25
6.	Repair of soil works	m^3	100.00	1.51	151.00
7.	Sediment excavation	m^3	50.00	3.02	151.00
8.	Debris cleaning	m^3	100.00	3.02	302.00
			Total		**5,320.85**

Source : Hutama Karya, 1989.

TABLE 2.5

Table of estimated annual operation and maintenance cost of the barrage
(Based on 1988 prices and an exchange rate of Rp.1650/US $)

No. (1)	Item (2)	Unit (3)	No. of units (4)	Unit Price (US $) (5)	Total (US $) (6)
	THE BARRAGE				
	Operation Cost				
1.	Lubrication oil	kg	20.00	3.03	60.60
2.	Personnel cost	no	4.00 (author's estimation)	544.50	2178.00
3.	Gate & Hoist	-	-	-	2567.00 (Lye,'92)
	Maintenance Cost				
4.	Painting works	m^2	200.00	9.08	1816.00
5.	Grass cutting	m^2	10000.00	0.16	1600.00
6.	Repair of masonary works	m^3	5.00	30.25	151.25
7.	Repair of soil works	m^3	100.00	1.51	151.00
8.	Sediment excavation	m^3	50.00	3.02	151.00
9.	Debris cleaning	m^3	100.00	3.02	302.00
			Total		8,976.85

Source : Hutama Karya, 1989 except as noted.

Total Annual Cost

Since the annual operation and maintenance cost of each alternative is different, this difference should be taken into account by adding the annual cost to the annual operation and maintenance costs as shown in Table 2.6. Then the cost ratio of each alternative can be computed. As can be seen in Table 2.6, the cost ratio of the barrage to the labyrinth weir varies from 1.19 to 1.34. Again, the labyrinth weir would be a more attractive alternative than the barrage, especially when the interest rate is low. For

example, in Indonesia, the interest rate for water resources projects is usually about 7% (Water Resources Development, 1984). At that interest rate the total annual cost of the barrage is US $ 100,129 and that of the labyrinth weir is US $ 80,428 (Table 2.6.). The cost ratio of the barrage to the labyrinth weir is thus 1.24.

TABLE 2.6
Table of total annual cost of the barrage and the labyrinth weir
(Based on 1988 prices and an exchange rate of Rp.1650/US $)

Interest rate (%) (1)	Annual capital cost of a barrage (US $) (2)	Total annual cost of a barrage (US $) (3)	Annual capital cost of *a labyrinth weir* (US $) (4)	Total annual cost of *a labyrinth weir* (US $) (5)	Cost ratio (h/lw) (3):(5) (6)
3	52240.97	61217.82	40289.80	45610.65	1.34
5	70694.27	79671.12	56780.95	62101.80	1.28
7	91152.37	100129.22	75106.75	80427.60	1.24
8	101911.15	110888.00	84725.72	90046.57	1.23
9	112937.42	121914.27	94562.36	99883.21	1.22
10	124158.63	133135.48	104544.11	109864.96	1.21
11	135541.62	144518.47	114639.89	119960.74	1.20
12	147053.18	156030.03	124818.58	130139.43	1.20
13	158660.15	167637.00	135049.10	140369.95	1.19
15	182094.51	191071.36	155624.16	160945.01	1.19

Note : (3) = (2) + annual O+M cost of the barrage.
(5) = (4) + annual O+M cost of the labyrinth weir.

2.4. The prospect of applying the labyrinth weir

Table 2.6 showed that the total annual cost of debt repayments ratio of the barrage to a labyrinth weir is between 1.19 and 1.34. On average the labyrinth weir annual cost is about 25 percent lower than that of a barrage. This is less than the 50 percent

difference estimated by P.T. Hutama Karya as discussed in Section 2.1. Reasons for the difference were suggested in Section 2.3.1. Thus, it can be said that in situations where funding is the only consideration, the labyrinth weir is a better alternative because it requires a lower cost than a barrage. However, a barrage may be a better political alternative since it can help to develop and support the development of a metal works industry.

As a comparison, on a large project such as the Ute Dam in the United States of America, the United States Department of the Interior Bureau of Reclamation (USBR) estimated the cost for the labyrinth spillway (1984 prices) at US $ 10 million compared to a gated spillway costed at US $ 34 million (Hinchliff and Houston, 1984).

In conclusion, the benefits of using a labyrinth weir in a small project such as Ciwadas and in a large project such as Ute Dam are significant and it is likely that the benefits exist over a range of sizes.

Finally, it also can be concluded that a labyrinth weir is the best alternative for Indonesia, and its use should be encouraged in Indonesia due to a number of reasons. These include :

a). It requires a low technology of operation and maintenance.

b). It is easier to build than the barrage.

c). All materials and labour required by a labyrinth weir are available locally.

d). It requires a lower capital cost than that of a barrage as shown in Table 2.6. This capital cost in developing countries such as Indonesia is the main consideration since the funding is usually borrowed.

Figure 2-4 A close up of Ciwadas labyrinth weir

Figure 2-5 An upstream view of Ciwadas labyrinth weir

Chapter 3

Literature Review

The major papers, reports or investigations directly pertaining to labyrinth weirs which have been carried out prior to the current study will be reviewed separately in this chapter. Experimental work is emphasized in this chapter, and details of theoretical work are provided in chapter 4. Before the review of prior works is discussed, it is useful to describe briefly the existing labyrinth weirs which have been installed up to now. At the end of this chapter, a discussion is provided to summarize previous work.

3.1. Labyrinth weirs which have been constructed

Among the geometries of labyrinth weirs, the symmetrical triangular and trapezoidal plan form have been developing since the 1940s. However, the trapezoidal plan is the form most used in many countries, because it is easiest to construct. Table 3.1 presents some trapezoidal planform labyrinth weirs which have been built to date.

TABLE 3.1
Existing trapezoidal shape labyrinth weir installations

No. (1)	Name of Location (2)	Year of completion (3)	n (4)	P (m) (5)	w (m) (6)	l (m) (7)	Reference (8)
1.	Avon Dam, Sydney New South Wales Australia	1970	10	3.00	13.54	26.46	Darvas, (1971)
2.	Hyrum Dam Hyrum, Utah USA	-	2	3.66	9.14	45.72	Houston, (1983)
3.	Mercer Dam Dallas, Oregon USA	1972	4	4.57	5.49	17.60	Lux III,and Hinchliff, (1985)
4.	Ute Dam Logan, New Mexico USA	1984	14	9.14	18.29	73.16	Houston, (1982)
5.	Ciwadas Weir Karawang, Jawa Barat Indonesia	1988	7	1.60	7.70	25.00	Hutama Karya, (1989)
6.	South Heart Dam Northern Alberta, Alberta-Canada	1988	2	4.00	11.75	60.20	Tacail *et al.*, (1990)

Note : n = number of cycles; P = crest height; w = width of one-cycle; l = developed crest length.

3.2. N. Hay and G. Taylor experimental and theoretical works

Taylor (1968) performed a series of experiments using various labyrinth weir geometries : trapezoidal, triangular, and rectangular plan forms. Parameters which influenced the labyrinth weir flow and would be examined in the experimental study were determined before the model test was started (see Figure 3-1). These include :

- The flow magnification, Q_L/Q_N, which is the ratio of discharge over a sharp crested labyrinth weir, Q_L, to the discharge over a sharp crested straight weir, Q_N. The flow Q_N was calculated from a standard weir equation (Eq. 4.1) using the experimental values of

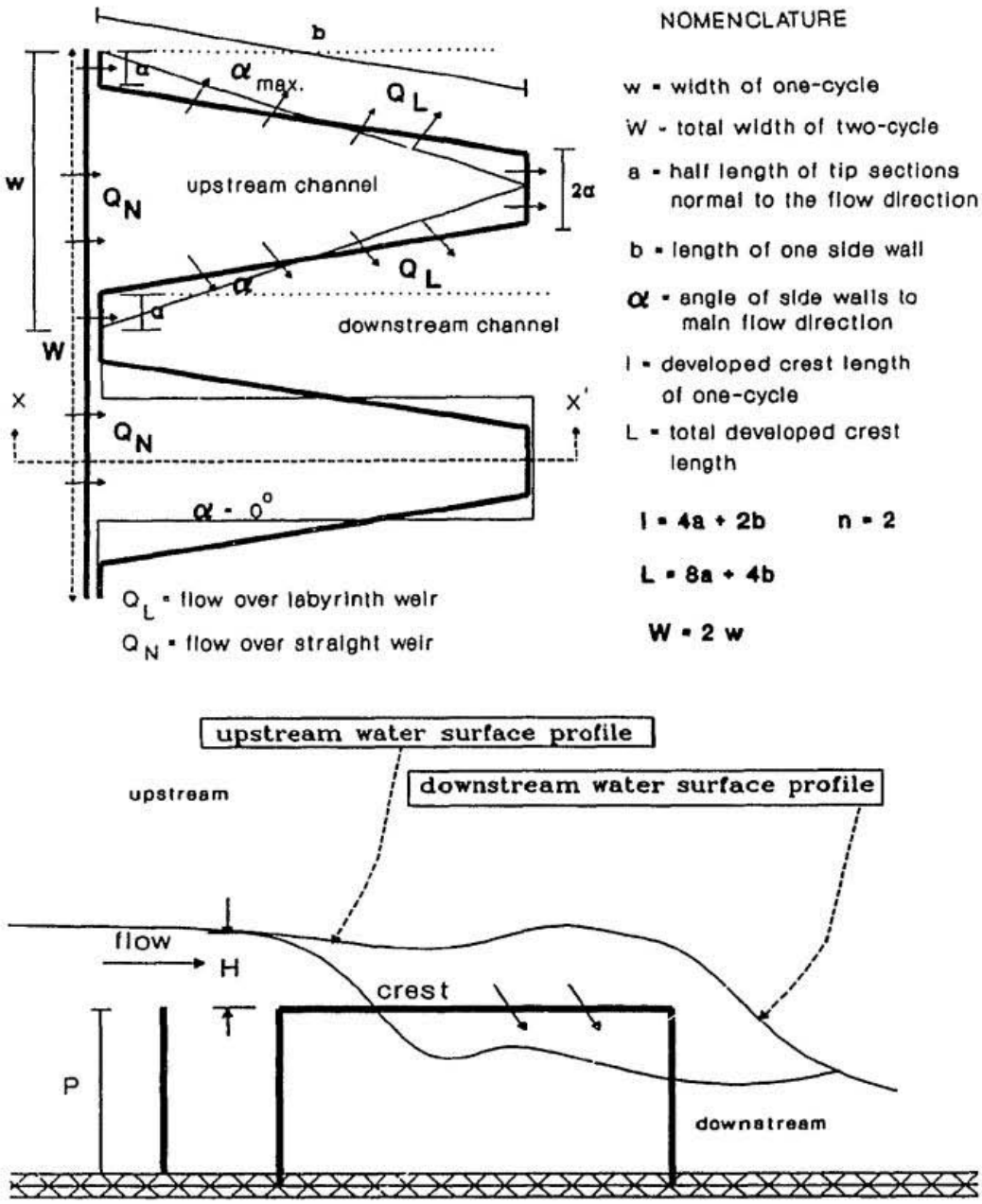

Figure 3-1 Diagram indicating the notation used in Hay and Taylor experimental and theoretical works. Modified from Taylor (1968).

H and P corresponding to the value of Q_L. Q_L was the experimental value of labyrinth weir discharge. This flow magnification will here be used to represent the performance of a labyrinth weir.

- The length magnification, L/W. This is the ratio of length of the labyrinth weir to the length of presumptive straight weir. Alternatively W may be considered as the width of the channel containing the labyrinth weir.
- The flow depth to weir height ratio, H/P, which is the ratio of the flow depth over the weir crest to the height of the labyrinth weir.
- The vertical aspect ratio, w/P, is the ratio of the width of one-cycle of the labyrinth weir to the height of the labyrinth weir.
- The side wall angle, α is the angle of the side wall of the labyrinth weir to the main direction of the flow. Rectangular geometry will result if $\alpha = 0°$.
- The number of weir cycles in plan, n.

The domain of Taylor's experiment is briefly described below :

a). The flow depth to crest height ratio (H/P) varied from 0 to 0.5.

b). The length magnification (L/W) ranged from 2 to 8.

c). The vertical aspect ratio (w/P) presented values between 2 and 4.5.

d). The side wall angle (α) tested varied from 0° to 20°.

e). The crest height (P) varied from 12.88 cm to 18.03 cm.

f). The number of weir cycles (n) observed varied from one to three.

They compared the flow over the labyrinth weir with the flow over a presumptive straight weir of a length equal to the total width of the labyrinth weir channel. Values

of Q_L/Q_N must always be in excess of 1.0. Half inch thick perspex sheet weir models were set in a test channel 4.9 m long, 0.91 m wide, and 0.36 m high. Developments to the models, such as change in channel bed elevation, presence of aprons, nappe interference, and alternative crest sections were noted.

The results of all model tests were plotted in the form of flow magnification (Q_L/Q_N) against depth to crest height ratio (H/P) for each value of the length magnification (L/W), vertical aspect ratio (w/P), side wall angle (α), and number of weir cycles (n).

From the experimental work, the following general conclusions can be drawn.

a). Generally, the flow magnification, Q_L/Q_N of all labyrinth weirs tends to decrease as the value of flow depth to crest height ratio increases (Figure 3-2 and Figure 3-3). This is as expected, since at low flow depth the interaction between flow from adjacent cycles is not significant. On the other hand, as the flow depth increases, the interference of the flow from adjacent cycles is serious. As a result the flow capacity of each cycle reduces. Hence the flow magnification decreases. However, in the rectangular plan form, it was found that a small increase in flow magnification value occured at particular points on the curves.

b). As the length magnification increases, the effectiveness of the weir's performance declines. Also, it was observed that the weir behaves best when the value of the length magnification, L/W = 2. This is because at L/W = 2, the labyrinth weir acts almost as a straight or linear weir for which L/W = 1.

c). The effect of the vertical aspect ratio, w/P is not significant in changing the labyrinth

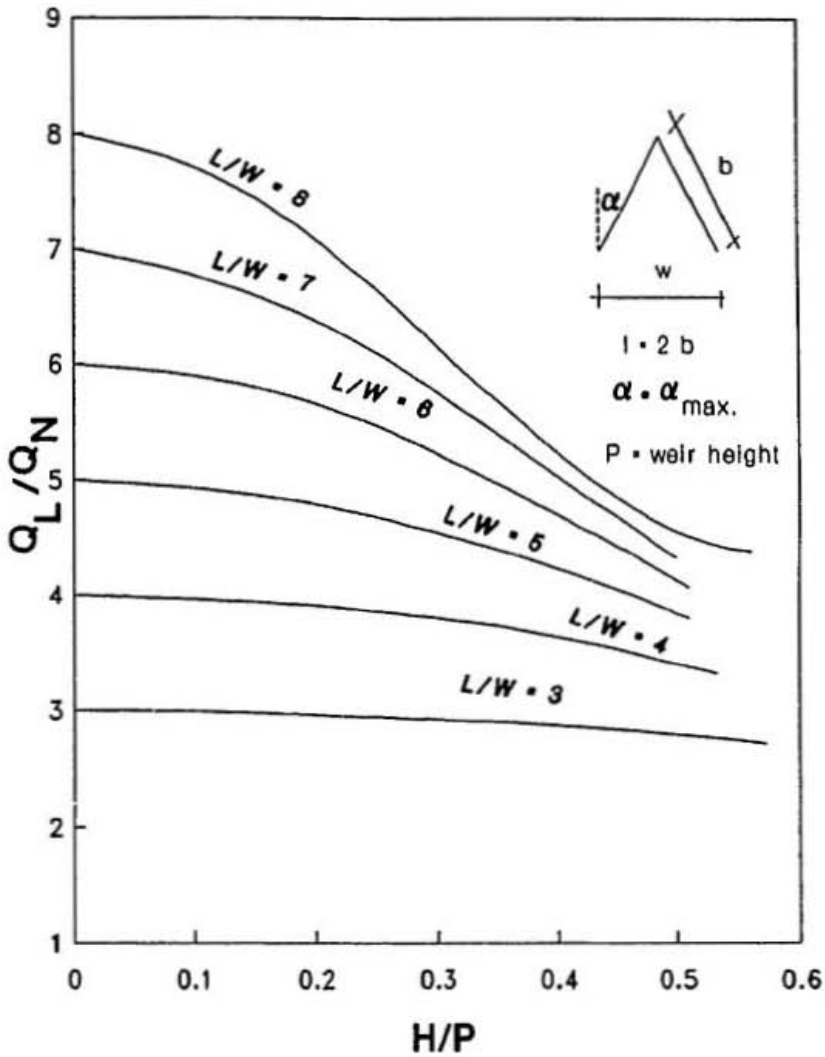

Figure 3-2 Hay and Taylor design chart for triangular plan form labyrinth weirs constructed without aprons, $w/P \geq 2.5$, with downstream interference (zero change in bed elevation), side wall angle, $\alpha = \alpha_{max.}$.
After Hay and Taylor (1970).

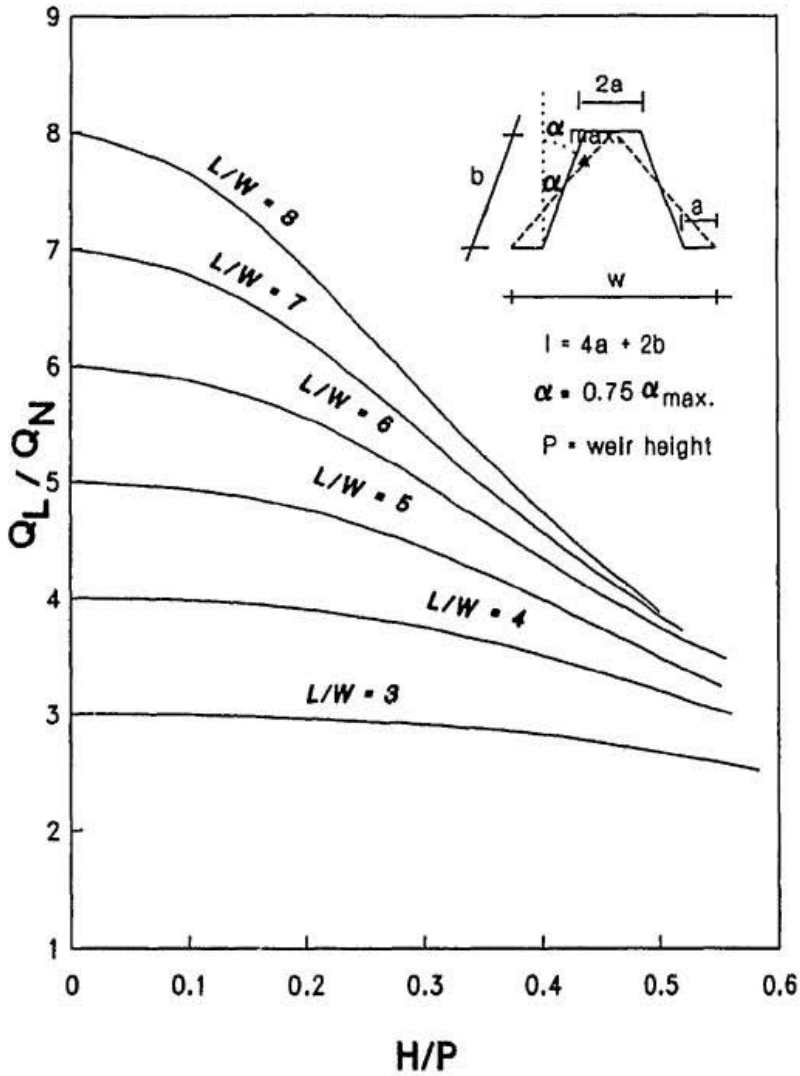

Figure 3-3 Hay and Taylor design chart for trapezoidal plan form labyrinth weirs constructed without aprons, $w/P \geq 2.0$, with downstream interference (zero change in bed elevation), side wall angle, $\alpha = 0.75\ \alpha_{max.}$. After Hay and Taylor (1970).

weir's performance if the value of $w/P \geq 2.5$ for a triangular plan form, and if the value of $w/P \geq 2.0$ for trapezoidal geometry.

d). The flow magnification value improves with a rise in the value of α for a given L/W. It was recommended, for maximum performance, that the side wall angle, α should be as large as possible. The maximum value, $\alpha_{max.}$, is the angle produced by a triangular shape.

e). The number of weir cycles, n does not effect the value of Q_L/Q_N.

f). The presence of aprons in both upstream and downstream channels (Figure 3-4) decreases the magnitude of the flow magnification.

g). A decrease in channel bed elevation downstream (Figure 3-5) causes a small improvement in performance.

h). An alteration in crest section shape from sharp to semi-circular (Figure 3-6) improves the performance by up to 20 percent compared to that of a sharp crest. This increase occurred under conditions of full aeration when the flow springs free over the total length of the labyrinth weir crest (Tacail *et al.*, 1990).

In addition, Hay and Taylor (1969) developed a computer program to predict the performance of labyrinth weirs. Results from the computation agreed with the results from the model tests with a difference between theoretical and experimental around 4 percent except for a rectangular geometry. One of these comparisons is given in Figure 3-7. The computer model analysis was based on a momentum approach given by Nimmo (Taylor,1968), and was coded in ALGOL. This computer model was proposed to help designers in pre-design of the labyrinth weir. Details are given in Chapter 4.

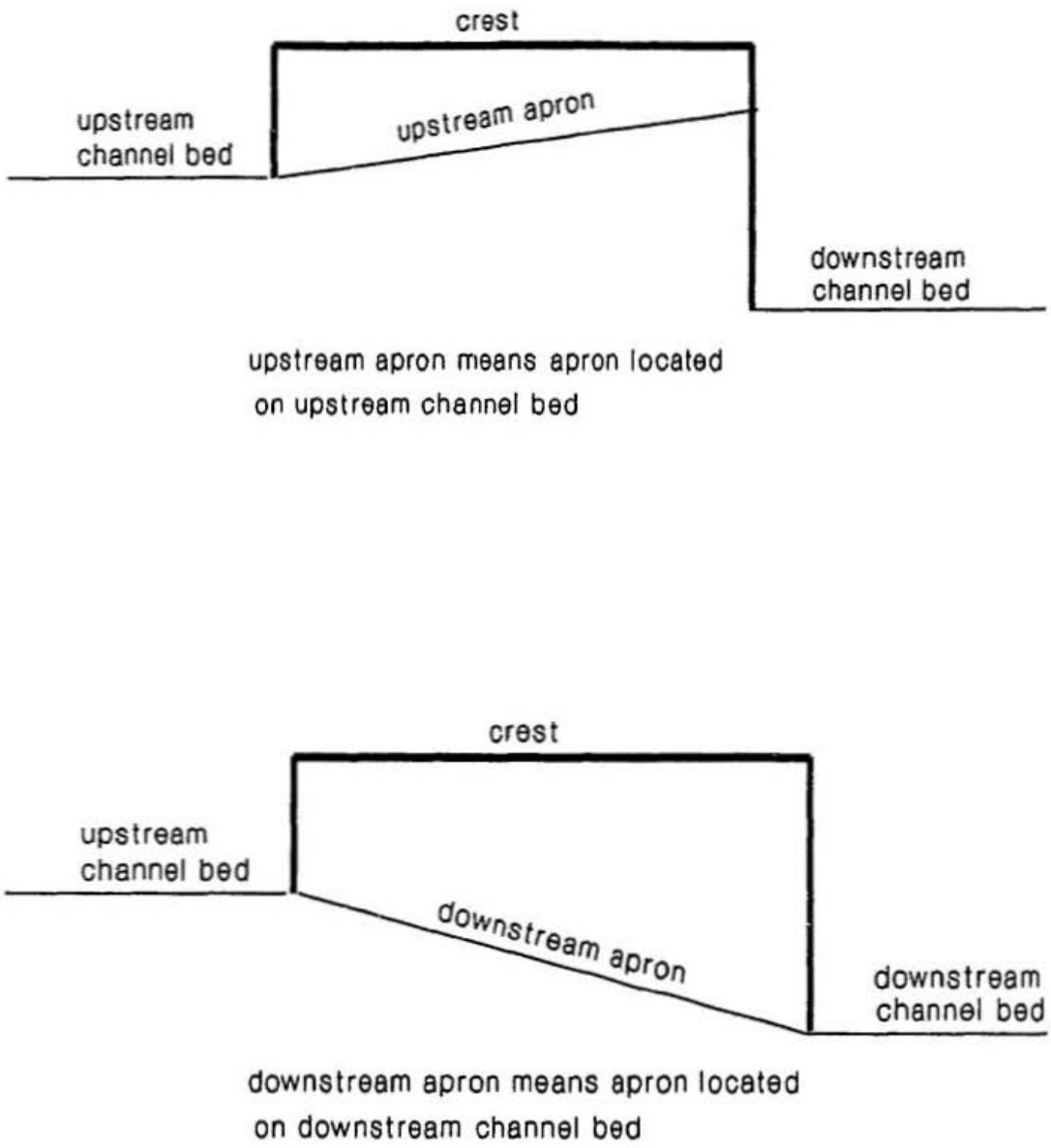

Figure 3-4 Sketch illustrating the presence of aprons in both upstream and downstream channel. Modified from Taylor (1968).

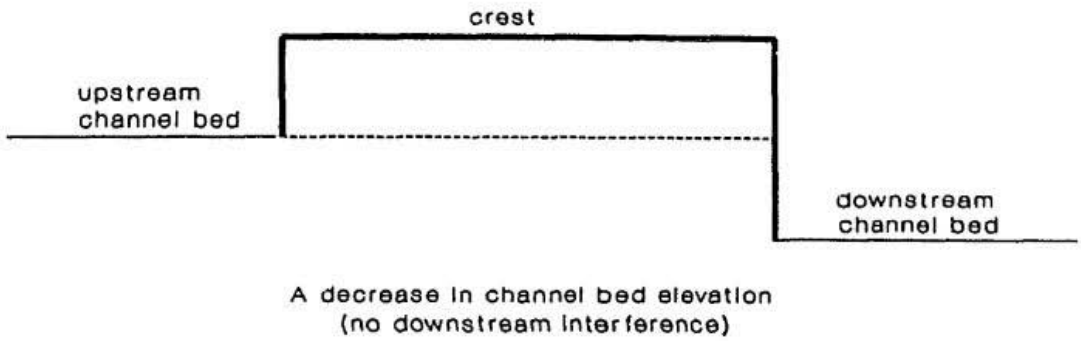

Figure 3-5 Sketch illustrating a decrease in channel bed elevation. Modified from Taylor (1968).

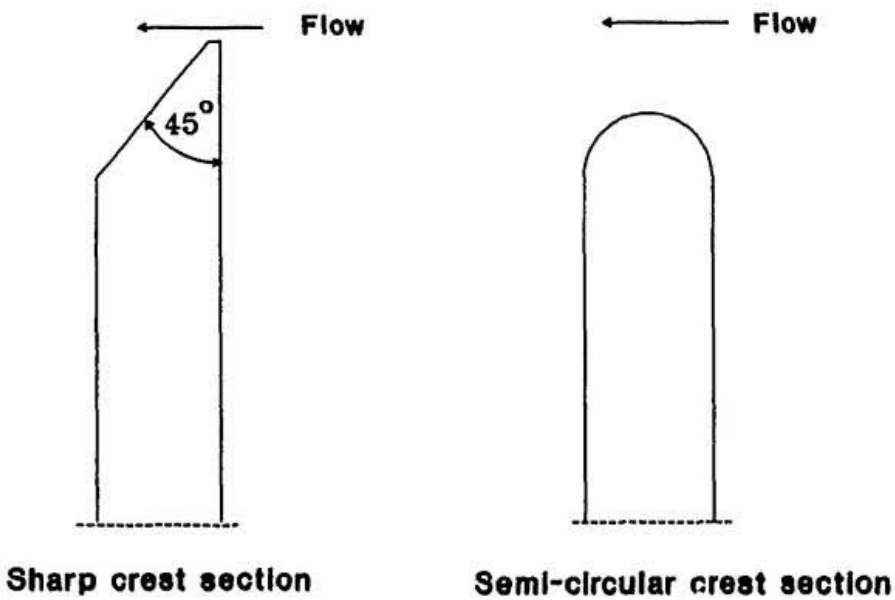

Figure 3-6 Model crest sections tested in Taylor's experimental work. Modified from Taylor (1968).

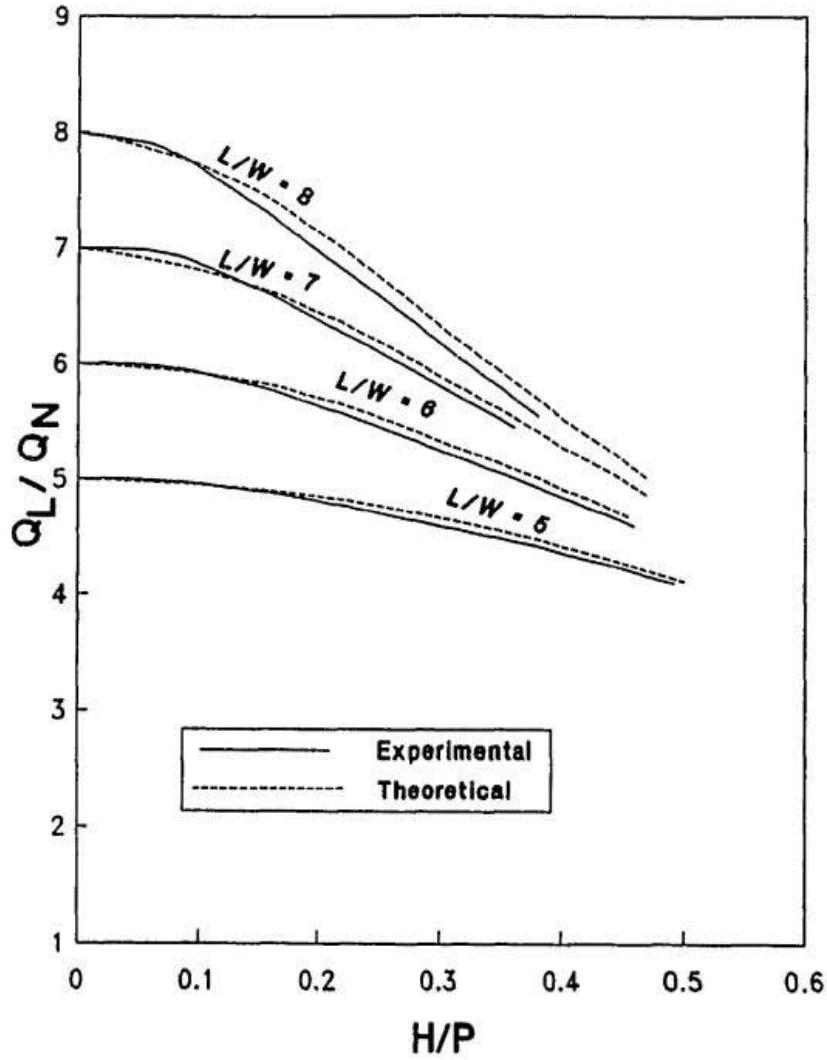

Figure 3-7 A comparison of experimental and theoretical results with energy loss due to contraction of the flow at entry to the upstream channel equal to $0.2\ V^2/2g$ in which V is velocity, for triangular plan form labyrinth weirs and no downstream interference. After Hay and Taylor (1969).

Due to the better performance of triangular and trapezoidal plan forms compared to rectangular geometry and a close agreement between theoretical and experimental results for both geometries, Taylor recommended the use of triangular and trapezoidal plan forms for the design of a labyrinth weir. Two design charts were provided for triangular ($\alpha = \alpha_{max.}$) and trapezoidal ($\alpha = 0.75\ \alpha_{max.}$) plan form sharp crested labyrinth weirs constructed without aprons as shown previously in Figure 3-2 and 3-3.

3.3. Discussion by Louis A. Darvas

To some extent Darvas (1971) agreed with Hay and Taylor's analysis that parameters L/W, w/P, α, and H/P determined the flow capacity of the labyrinth weir. However, he criticized the method of presentation which was proposed by Hay and Taylor as an indirect presentation of the performance of the labyrinth weir. In particular he criticized the use of a presumptive linear weir to calculate the flow magnification values. Thus he proposed to simplify the method of calculation by excluding the presumptive linear weir.

As an alternative he promoted a more direct design chart in which a labyrinth weir discharge coefficient, C_w is plotted against the length magnification, L/W for a series of constant values of the flow depth to crest height ratio, H/P. In other words, he preferred to express the efficiency of a labyrinth weir in terms of the discharge coefficient, C_w rather than by flow magnification, Q_L/Q_N as can be seen in Figure 3-8. Then, the labyrinth weir discharge was obtained using (Darvas, 1971) :

$$Q_L = C_w W H^{1.5} \quad (3.1)$$

where Q_L is the discharge over the labyrinth weir crest in ft^3/s, C_w is Darvas' discharge coefficient, W is the total width of the labyrinth weir in ft, and H is the flow depth over the crest of the labyrinth weir in ft.

This design chart was based on three dimensional hydraulic model studies of Avon and Woronora labyrinth weir spillways. These were conducted at the Metropolitan Water Sewerage and Drainage Board (MWS&DB) Hydraulic Laboratory, Sydney, Australia. Darvas showed that the results of these model tests were in close agreement with the results given by Hay and Taylor.

Darvas' tests were carried out under the following conditions :

a). The length magnification (L/W) ranged from 1 to 8.

b). The flow depth to crest height ratio (H/P) covered was from 0.2 to 0.6.

c). The side wall angle (α) was greater than 0.80 times α_{max}.

d). The vertical aspect ratio (w/P) was greater than 2.0.

e). There was free flow over the weir.

f). The shape tested was a trapezoidal plan form with a horizontal channel bed and a quarter of a circle crest (see Figure 3-9).

Darvas only proposed an alternative way of presentating the labyrinth weir's performance rather than further improvement of the labyrinth weir design. Darvas' design chart however can be used in a straightforward manner without knowledge of the flow over the linear weir.

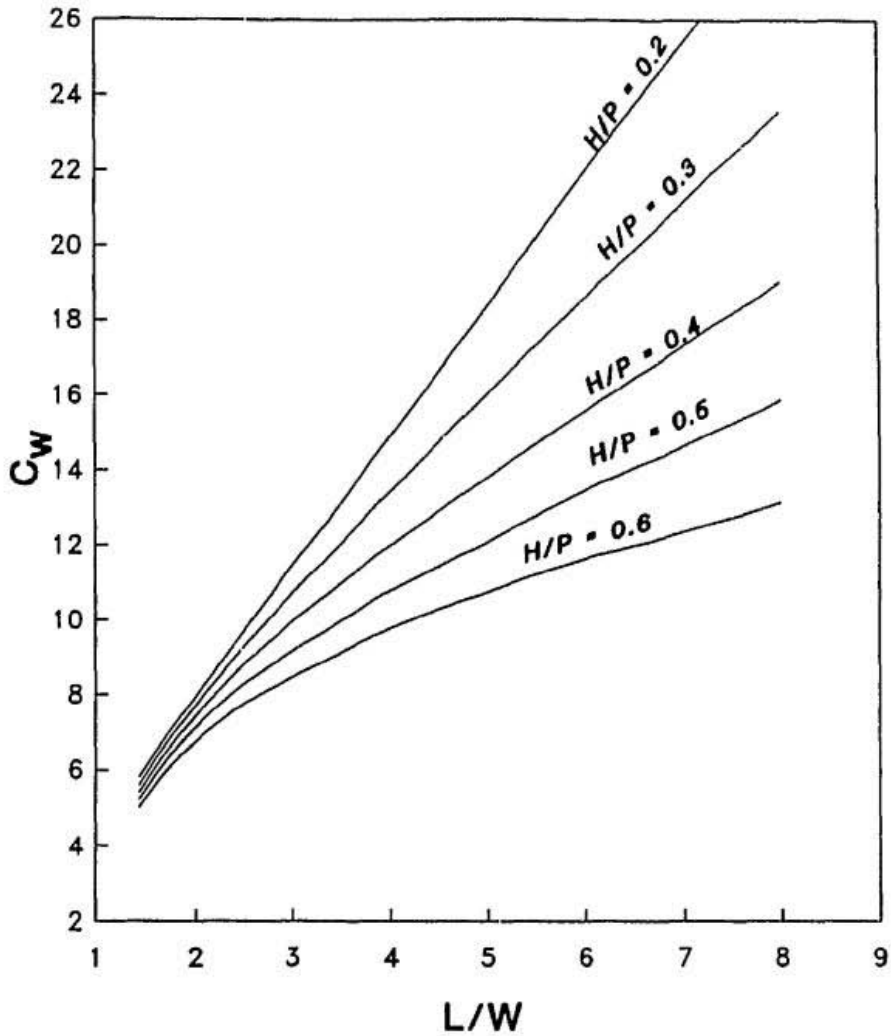

Figure 3-8 Darvas design chart for quarter-round crest trapezoidal plan form labyrinth weirs constructed without aprons, w/P $\geq$ 2, and side wall angle, $\alpha \geq 0.8\ \alpha_{max.}$. After Darvas (1971).

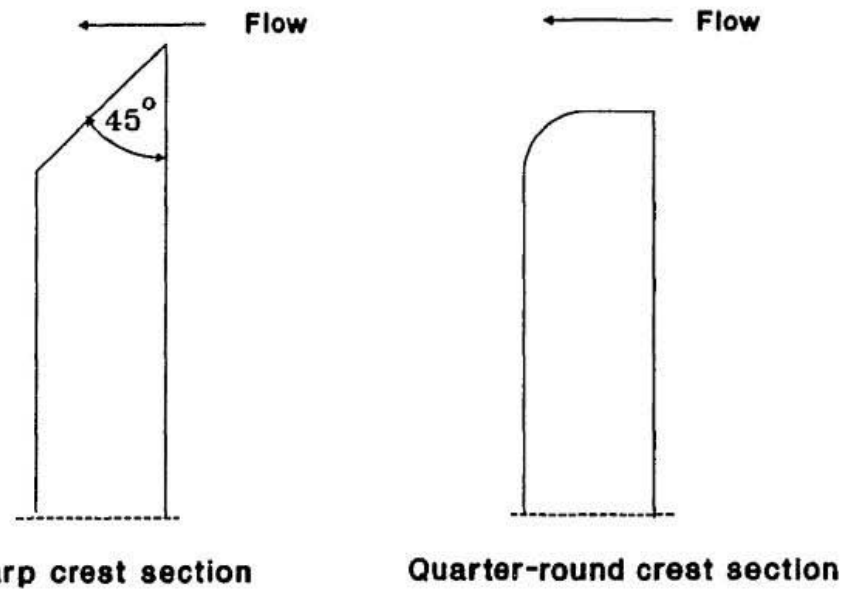

Figure 3-9 Sketch illustrating sharp crest section and quarter-round crest section. Modified from Houston (1982 and 1983).

3.4. USBR Hydraulic Model Study of Ute Dam Labyrinth Spillway

Along with a hydraulic model study of the Ute Dam Labyrinth Spillway, the United States Department of the Interior Bureau of Reclamation (USBR) reviewed the Hay and Taylor design curve (Houston, 1982). Two points regarding the previous design curve were criticised by them. The first was the use of only one depth measurement (H) without consideration of the velocity head ($H_v = V^2/2g$) when the design curves were developed. The second was the limitation in using these design curves, since they only covered H/P values from 0 to 0.5 (Figure 3-2 and Figure 3-3).

Because of these criticisms half inch thick and 0.1524 m high aluminum labyrinth weir models were tested in a flume 10.97 m long, 0.76 m wide, and 0.61 m high. The

model tests were run for trapezoidal and triangular planform sharp crested labyrinth weirs. The results of all model tests were also plotted in the same way as Hay and Taylor's design curves. Modified design curves were then developed for the value of w/P = 2.5. The Q_L/Q_N and L/W values ranged from 2 to 5, and the H_o/P values where $H_o = (H + H_v)$ were between 0 and 1.0 as shown in Figure 3-10. Because there was a different concept in determining the head values, the bureau design curves have a lower discharge magnification, Q_L/Q_N than Hay and Taylor's design curves at the same value of L/W and H/P. Houston attributed this difference entirely to the difference used in defining the value of H. In Hay and Taylor's work H was taken as the depth of flow above the crest whereas Houston used depth plus velocity head (H_o). These two head concepts were investigated in the present work (see Appendix E) and there was little difference in results.

From the experimental results, Houston also found that the triangular planform was the best geometry and recommended the use of this plan in the design of the labyrinth weir. The reason for this is that the triangular plan gave a slightly higher flow than the trapezoidal geometry under the same total head and length magnification.

The other interesting result from the model tests was the use of a splitter pier on the crest of each cycle of the labyrinth weir (Figure 3-11). The benefit of using this pier was to provide aeration along the full length of each side wall, so the negative pressure which usually occurs at a low discharge could be reduced.

A modified design curve then was used to design the 14-cycle Ute Dam labyrinth spillway. This labyrinth spillway was tested in a 1:80 scale model. The result of the

experimental study showed that this 14-cycle labyrinth spillway was able to pass the desired maximum discharge. The first 10-cycle labyrinth spillway designed using Hay and Taylor's (1970) design curves could not pass this maximum discharge.

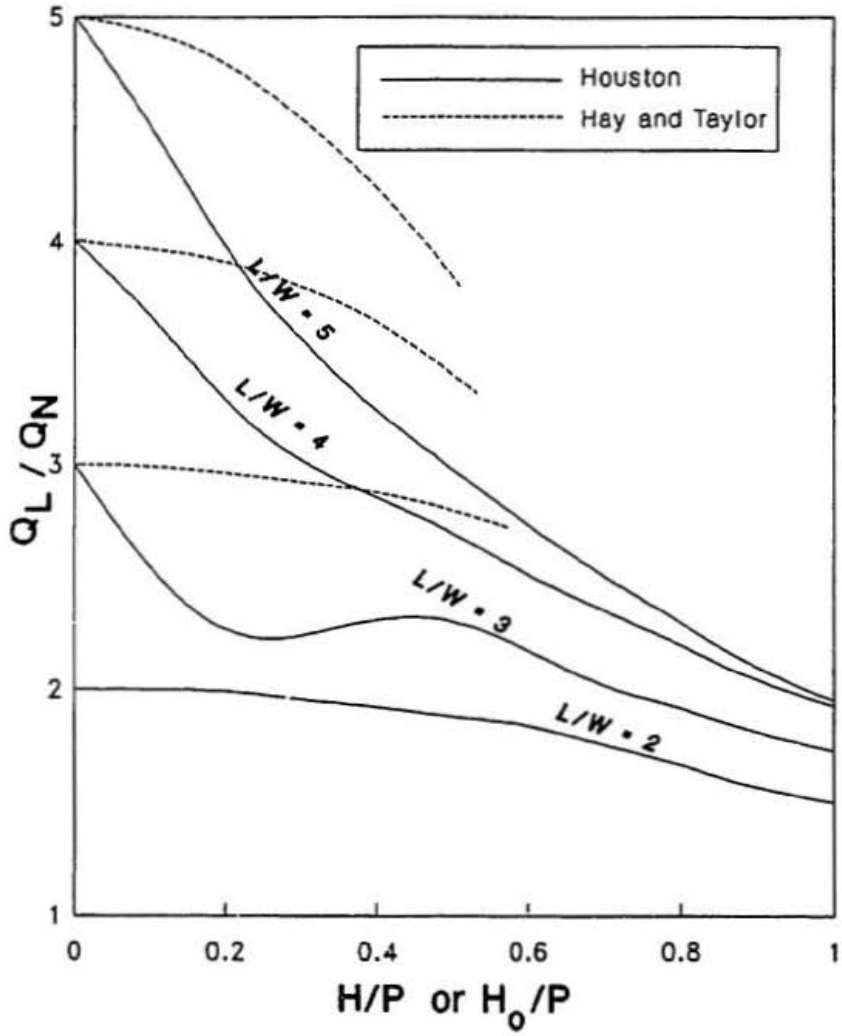

Figure 3-10 A comparison of USBR and Hay & Taylor design curves for triangular plan form weir, w/P = 2.5, side wall angle, $\alpha = \alpha_{max.}$, with downstream interference (zero change in bed elevation). After Houston (1982), Hay and Taylor (1970).

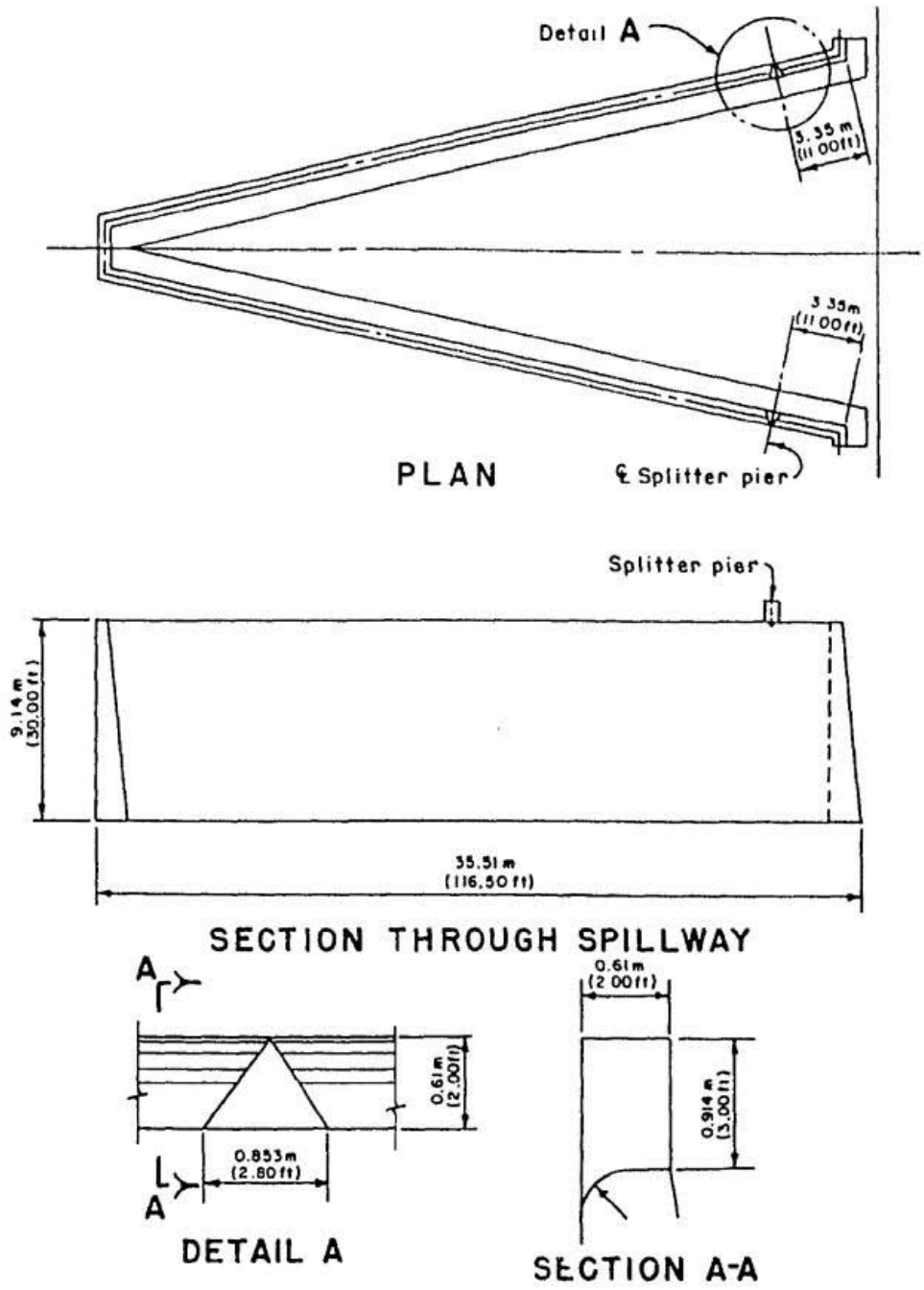

Figure 3-11 Splitter pier location and dimensions. After Houston (1982).

3.5. USBR Hydraulic Model Study of Hyrum Dam Auxiliary Labyrinth Spillway

The United States Department of the Interior Bureau of Reclamation (USBR) also performed 1:30 scale model tests on a two-cycle Hyrum Dam labyrinth spillway with a trapezoidal plan form of a crest height, P, equal to 3.66 m and length magnification, L/W equal to 5 (Houston, 1983). The study was initially focused on determining the effect of the direction of the labyrinth spillway, ie to locate one apex downstream and two apexes upstream or vice versa. The effect of approach conditions on the spillway orientation was also studied (Figure 3-12).

From the results of the investigation, it was shown that the labyrinth weir, which had a length magnification of five and two apexes located upstream, was less efficient hydraulically than the labyrinth weir with two apexes located downstream. Nevertheless, based on a study of the effect of approach conditions, it was concluded that the use of a good entrance condition had more significant effects on the efficiency of the spillway than the orientation of spillway. A good entrance condition is a curved approach as indicated in Figure 3-12. Thus the labyrinth spillway entrance conditions are more meaningful than the labyrinth spillway orientation.

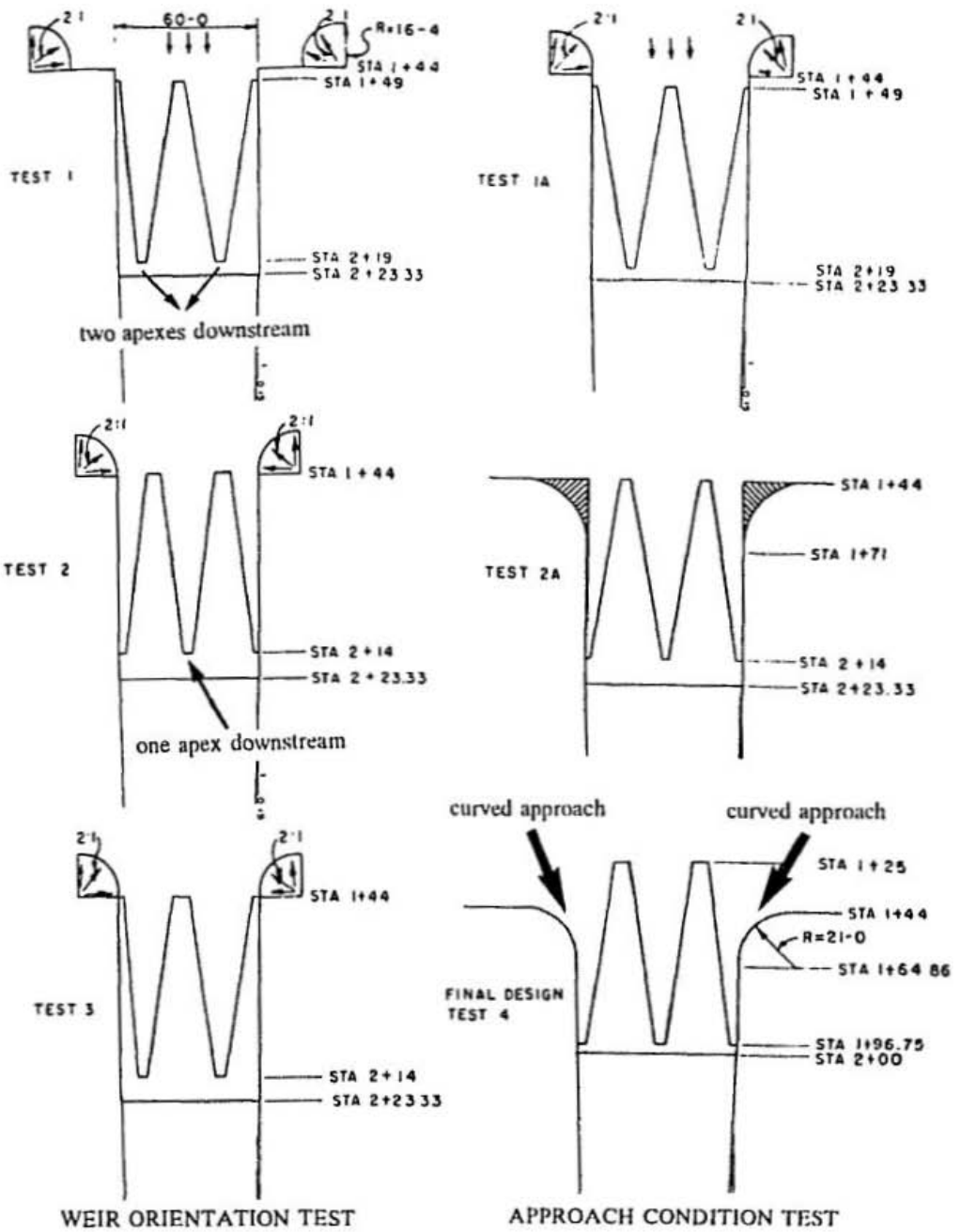

Figure 3-12 Schematic of the spillway approach condition and labyrinth weir orientation tested in the hydraulic model studies. (Flow direction from top to bottom). After Houston (1983).

3.6. J. Cassidy *et al.* on Hydraulic Model Study of Carty Dam Labyrinth Spillway

The main objective of this hydraulic model study was to verify the labyrinth spillway design for Carty Dam. This was based mainly on Hay and Taylor's work (Cassidy *et al.*, 1983). A triangular plan form with a semi-circular crest was chosen for the design of the Carty dam labyrinth spillway. Model tests were carried out by the Albrook Hydraulics Laboratory at Washington State University.

The results of the model test were plotted in the form of flow rate over the labyrinth spillway against the reservoir water surface elevation. The experimental results indicated that, at the higher flow depths, the flow capacity of the labyrinth spillway proved to be 20 percent to 25 percent lower than values extrapolated from the Hay and Taylor design curve. It was pointed out that the chute width of the labyrinth spillway depend on the developed length of labyrinth spillway. Increase in the developed length of the labyrinth spillway without increasing the chute width of the spillway reduced the effectiveness of the labyrinth spillway, particularly at higher flow. The model tests also agreed with the results of the hydraulic model study of Hyrum Dam (Houston, 1983) that the use of a curved approach channel is significant in increasing the weir's effectiveness, especially at higher flow rates.

3.7. A.P. Magalhães

In his paper, Magalhães (1985) reported the results of hydraulic model studies of Harrezza Dam, Dungo Dam, and Keddara Dam Labyrinth Spillways which were carried out at the Portuguese National Laboratory of Civil Engineering (LNEC) in 1980, 1981, and 1984 respectively (Magalhães,1985). In the case of the Harrezza Dam Labyrinth Spillway, for $H/P \geq 0.54$, the actual discharge was 17 percent lower than the predicted discharge from the Hay and Taylor, and the Darvas design curves. This difference underlined the necessity of hydraulic model tests to verify the design of labyrinth weirs.

Furthermore, Darvas' design chart was revised by Magalhães by presenting a dimensionless coefficient of discharge, μ_w as shown in Figure 3-13. Then, the discharge over the labyrinth weir was calculated using (Magalhães, 1985) :

$$Q_L = \mu_w W \sqrt{2g} H^{1.5} \tag{3.2}$$

Note that :

$$C_w = \sqrt{2g} \mu_w \tag{3.3}$$

in which C_w is Darvas' discharge coefficient, g is the acceleration due to gravity = 32.2 ft/s^2, (both Darvas and Magalhães presented their data in FPS units), and μ_w is Magalhães' discharge coefficient.

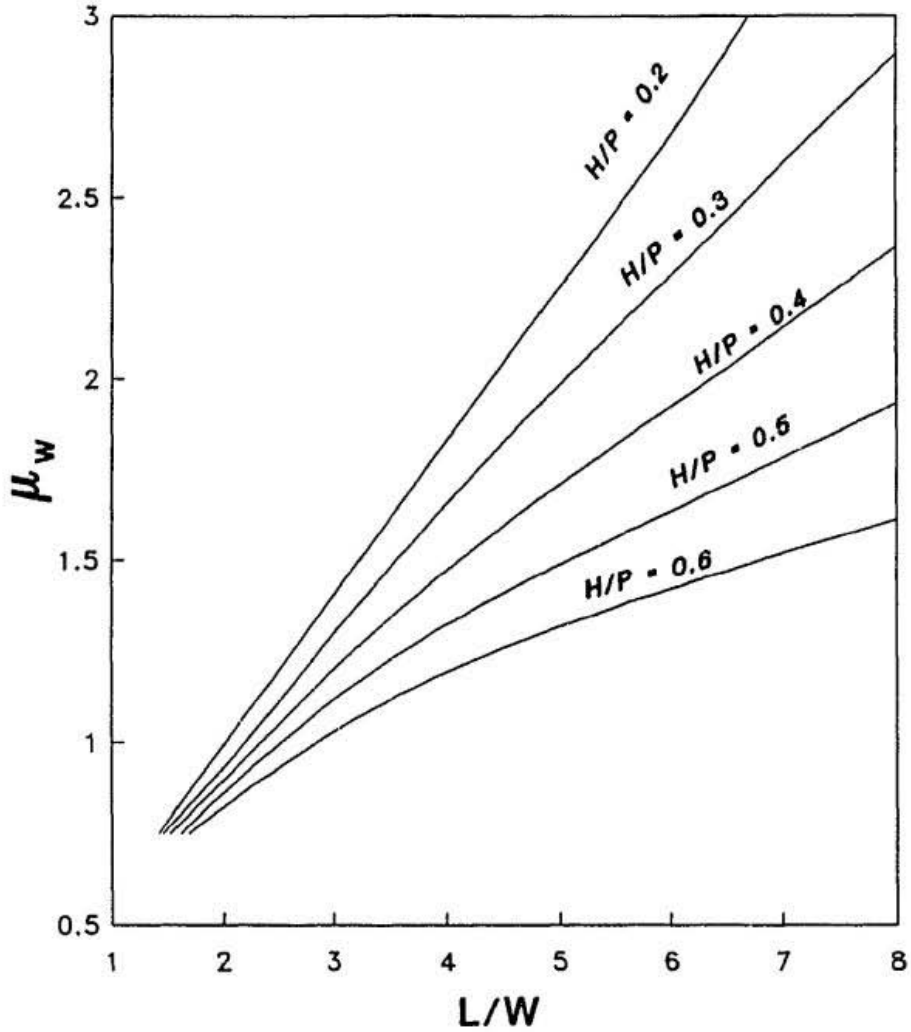

Figure 3-13 Discharge coefficient for quarter-round crest trapezoidal shape labyrinth weirs, constructed without aprons, w/P $\geq$ 2, and side wall angle, $\alpha \geq 0.8\ \alpha_{max.}$. After Magalhães (1985).

3.8. Frederick Lux III and David L. Hinchliff

In this paper (Lux and Hinchliff, 1985) the design and construction of labyrinth spillways was discussed. The work was based on the hydraulic model studies conducted by the USBR and tests by other investigators such as Taylor and Darvas. They pointed out that, in general, the main factors which influence the performance of the labyrinth weir are the plan form, the maximum discharge, and the design head. Usually, in the design stage, the maximum discharge and the design head are already settled. Therefore, the choice of the labyrinth geometry becomes important in order to obtain the best performance.

Normally, the flow pattern over a labyrinth weir passes through four basic stages as the upstream head increases. These stages were defined as : fully aerated, partially aerated, transitional, and suppressed (Figure 3-14). It was observed that the labyrinth weir behaves ideally in fully aerated stages when the flow falls freely over the total length of the labyrinth crest.

The general considerations for hydraulic design of a labyrinth spillway were summarized. These included spillway approach conditions and placement, upstream and downstream flow conditions, number of labyrinth cycles and nappe interference, and labyrinth low flow conditions.

In the design chart (Figure 3-14), C_{LH} was plotted against the total head to crest height ratio, H_o/P for a series of constant values of the length magnification, L/W. The value of C_{LH}, H_o/P and L/W were obtained from the hydraulic flume studies conducted by USBR (Houston, 1982) and Taylor (1968). Data were also obtained from site-specific

hydraulic models at Hyrum dam labyrinth spillway (Houston, 1983). Then, the discharge over the labyrinth weir could be estimated (for w/P $\geq$2) using (Lux & Hinchliff, 1985):

$$Q_L = C_{LH} \frac{(w/P)}{(w/P + k)} w H_o \sqrt{g H_o} \qquad (3.4)$$

where k has the value of 0.18 for triangular and 0.10 for trapezoidal (with a/w = 0.0765) plan forms. It was shown that the use of a quarter-round crest increased the discharge coefficient, C_{LH} above that of a sharp crest. This is shown in Figure 3-15. An increase of discharge coefficient, C_{LH} occurred under conditions of full aeration when the flow springs free over the total length of the weir crest (Tacail *et al.*, 1990).

Lux and Hinchliff presented this result using a discharge coefficient as indicated in equation 3.4. This is somewhat similar to Darvas' approach. However Lux and Hinchliff's discharge coefficient, C_{LH} differed from Darvas' discharge coefficient, C_w according to :

$$C_{LH} = \frac{(w/P + k)}{(w/P)\sqrt{g}} C_w \qquad (3.5)$$

In addition the method of presentation was similar to that of Hay and Taylor except that the head term included the velocity head, H_v (see Figures 3-14 and 3-15).

Finally, the structural design and construction considerations for a labyrinth spillway were discussed on the basis of the USBR's experience with Ute Dam. For structural design, the stability analysis of a labyrinth cycle should be investigated. This includes overtuning, sliding, and foundation bearing pressures subject to normal load at normal water surface level and extreme load at maximum water surface level.

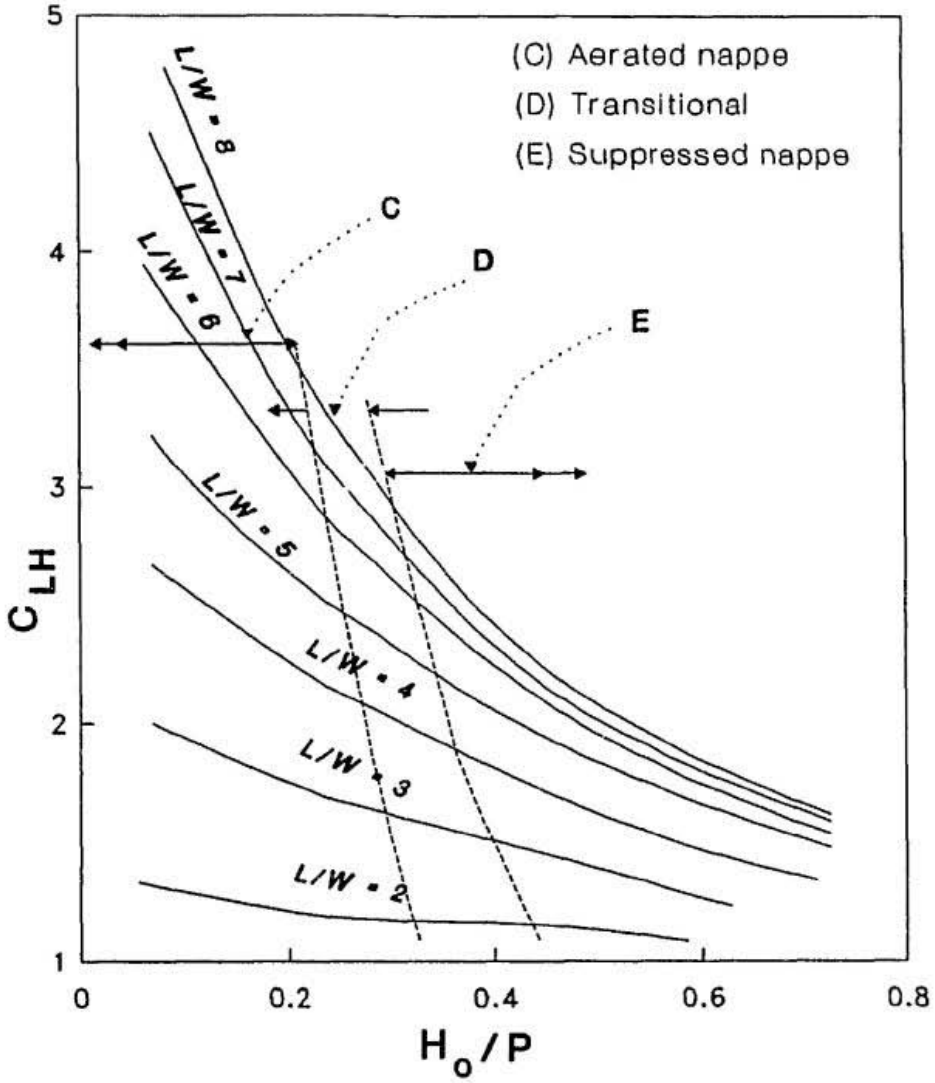

Figure 3-14 Design curves for sharp crest trapezoidal labyrinth weirs. After Lux & Hinchliff (1985).

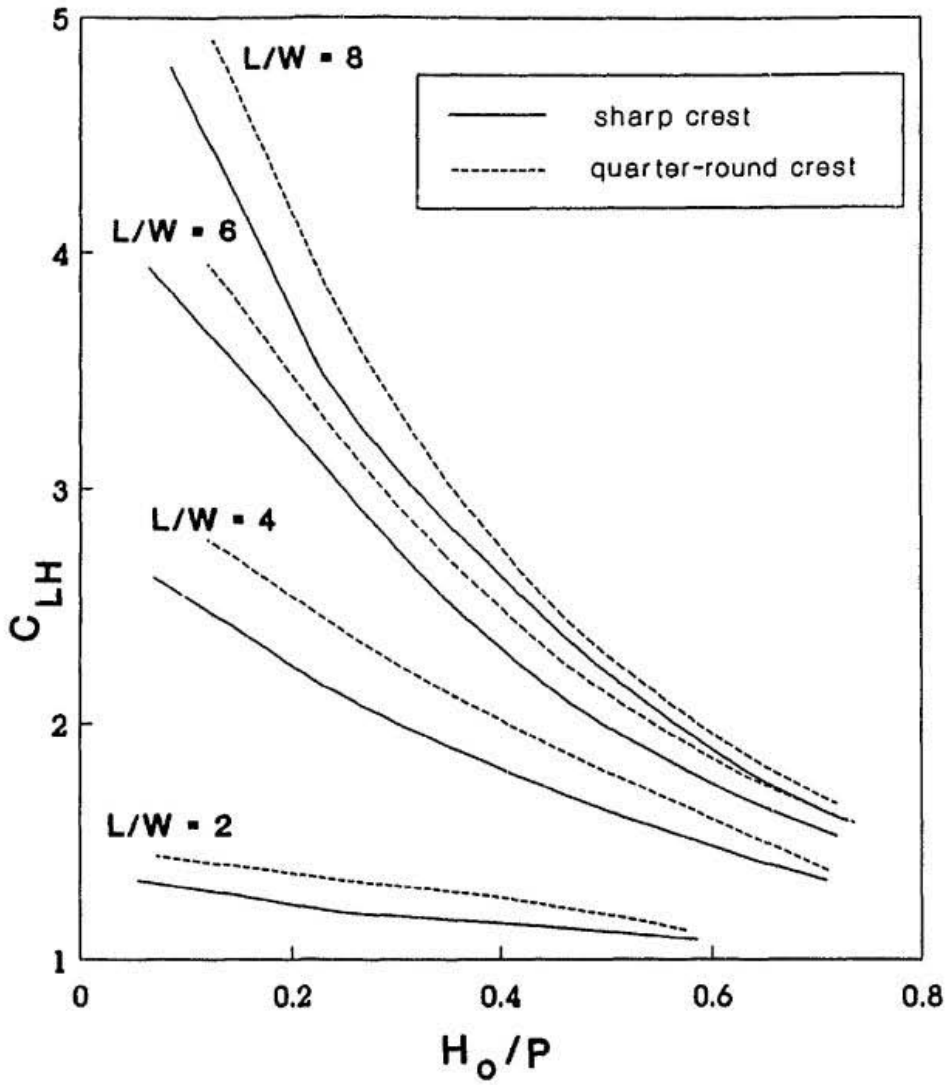

Figure 3-15 A comparison of discharge coefficient, C_{LH} between quarter-round crest and sharp crest trapezoidal plan labyrinth weir. After Lux and Hinchliff (1985).

3.9. A. Afshar

In his paper entitled "The development of labyrinth spillway designs", Afshar (1988) discussed the development and the benefits of using a labyrinth spillway mainly by reviewing the Lux and Hinchliff paper (Lux & Hinchliff, 1985). The Hay and Taylor

works (Hay & Taylor, 1970) and Darvas discussion paper (Darvas, 1971) were also discussed in this paper.

Moreover, some examples of the main characteristics of some labyrinth spillways which have been constructed to date were stated briefly. Afshar emphasized the economic value of labyrinth spillways. He also recommended the use of this spillway in situations where the head is limited or the spillway width is confined by the topography.

3.10. Indonesian Institute of Hydraulic Engineering (IIHE), Bandung-Indonesia experimental works

The aim of this study was to find the most suitable geometry of labyrinth weir for use in Indonesia (Memed and Sadeli, 1990; Puslitbang Pengairan, 1991). This took into account the need for a low cost design giving good flow capacity with a small length magnification. The range of the experimental work is described below :

a). The flow rates ranged from 0.1 m^3/s to 1 m^3/s.

b). The labyrinth weirs were tested for one, two, four, and eight cycles.

c). Triangular and trapezoidal shapes were observed.

A mahogany labyrinth weir, with a crest height of 0.20 m was used on the model tests. Modifications to the models, such as change in the crest sections, alteration of the different crest heights, and the effects of sedimentation downstream of the weirs were also examined.

The results of all model tests were as follows :

a). The most suitable geometry was established as shown in Figure 3-16.

b). Alteration in crest sections from 2.0 cm to 3.0 cm top width, and 3.0 cm to 4.0 cm top width slightly decreases the flow over the labyrinth weir. They recommended that a crest section with 1.0 cm top width gives the maximum flow capacity under the same operating depth.

c). As the number of weir cycles increases while the value of L/W held constant, the flow over the labyrinth weir falls (Figure 3-17).

d). Change in crest height is not significant in changing the flow capacity of the labyrinth weir.

e). Effects of sedimentation with an increased depth of sediment of 5 cm up to 10 cm in the upstream channel, do not influence the flow capacity of labyrinth weir.

In the end of the study, a design chart was established for practical use in the field. This is reproduced in Figure 3-17. The design chart was developed for the most suitable geometry which proved to be a trapezoidal plan form with $\alpha=0.68\alpha_{max.}$ as indicated in Figure 3-16. The discharge over the weir crest, Q was plotted against the total head of the approaching flow, H for various values of the number of cycles as shown in Figure 3-17.

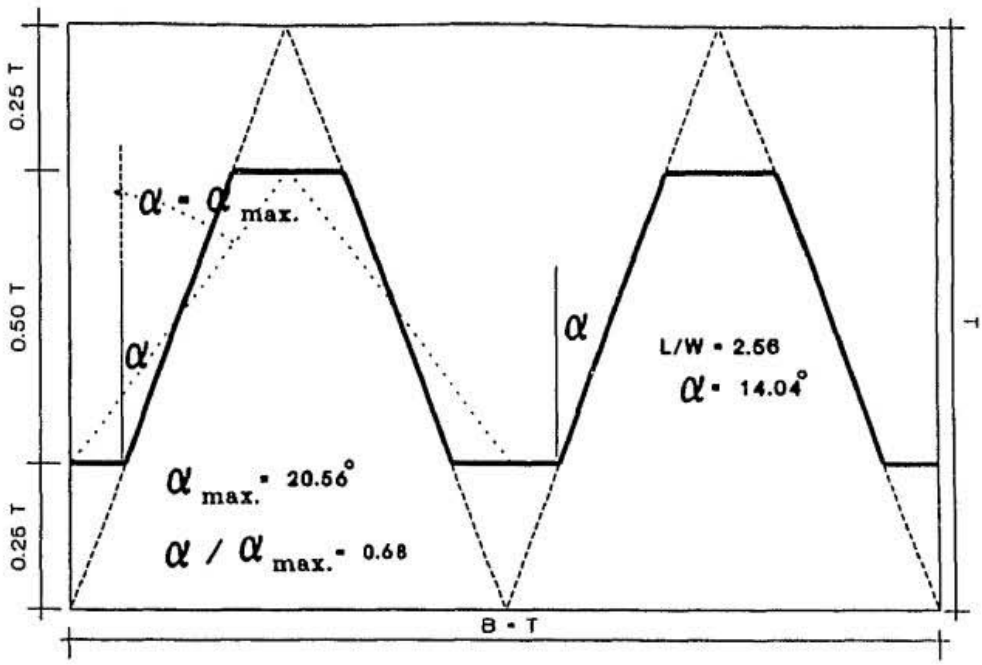

Figure 3-16 A most suitable geometry of the labyrinth weir. Modified from Puslitbang Pengairan (1991).

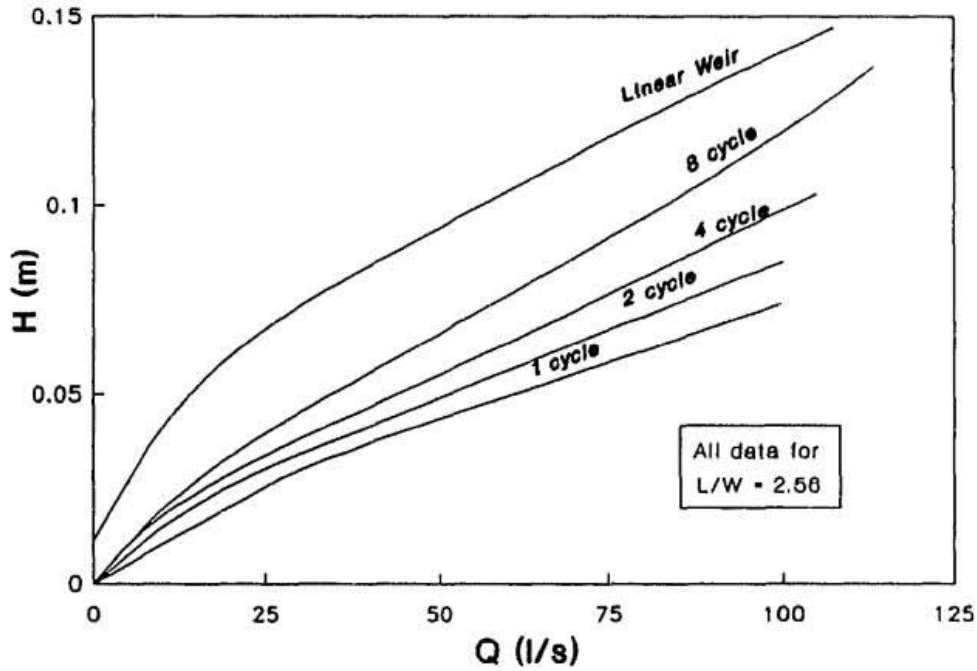

Figure 3-17 IIHE design chart for trapezoidal shape labyrinth weirs, l/w=2.56, side wall angle, α = 14.04°. After Puslitbang Pengairan (1991).

3.11. Tacail *et al.* on hydraulic model study of South Heart Dam Labyrinth Spillway

This paper (Tacail *et al.*, 1990) reported experience in the design and hydraulic model study of South Heart Dam Labyrinth Spillway in northern Alberta, Canada. The objective of the laboratory experiment was to investigate different weir cycles including two cycles and three cycles. Experiments were also done to study the effects of changing the crest height and shape.

From their experiments, they summarized some important factors relating to the labyrinth weir performance. These include :

a). An increase of vertical aspect ratio, w/P was able to eliminate the effect of downstream interference and submergence. Thus, the labyrinth weir capacity increased. This was proved by reducing the number of weir cycles from three to two, thus increasing the w/P value. The increase in discharge occured because increasing the value of w/P provides a larger space in the downstream channel.

b). An increase in weir height, P while keeping the head constant was significant in increasing the labyrinth weir discharge. This increase occurred when the value of H/P ranged from 0.25 to 0.33.

c). An increase in the side wall angle, α was significant in increasing the labyrinth weir flow capacity. This was shown by reducing the number of cycles and therefore increasing the value of α. It was emphasized then that the side wall angle is an important factor in influencing the flow capacity of labyrinth weir. Also, the model study corroborated Hay and Taylor's recommendation to adopt the side wall angle, $\alpha \geq 0.75\ \alpha_{max.}$.

d). The effect of changing the crest shape increased the discharge 23 percent above that of a sharp crested labyrinth weir. It was observed that the labyrinth weir flow capacity is sensitive to a change in crest shape and height only under free-flow conditions.

It was concluded that for the same spillway width, the two-cycle was better than the three-cycle labyrinth weir. Thus the two-cycle was adopted in the South Heart Dam labyrinth spillway. The study also underlined the importance of hydraulic model studies in confirming the parameters influencing the flow capacity of a labyrinth weir.

3.12. Discussion

In general it has been shown that the discharge over the labyrinth weir is not determined only by the crest shape and depth or total head to weir height ratio (H/P or H_o/P) as at straight weir. Other parameters are also important. These include the length magnification (L/W), and the side wall angle (α) which depends on the labyrinth weir shape (Hay and Taylor, 1970; Darvas, 1971; Houston ,1982 and 1983; Lux and Hinchliff, 1985; and Magalhães, 1985).

Hay and Taylor (1970) observed that for a value of the length magnification, L/W $<$ 2 the performance of the weir was relatively unaffected by changes in the value of H/P. Memed and Sadeli (1990) found similar results for the trapezoidal shape shown in Figure 3-16 with a length magnification, L/W $<$ 2.56.

Lux & Hinchliff (1985) insisted that the choice of the labyrinth weir shape was an important step in the design of the weir. Most authors recommended the use of a triangular or trapezoidal shape in the design of labyrinth weir plan form. Hay and Taylor

(1970) suggested the use of a triangular shape with $\alpha=\alpha_{max.}$ or a trapezoidal geometry with $\alpha \geq 0.75\alpha_{max.}$. The USBR also suggested the use of a triangular shape (Houston, 1982) and Darvas (1971) recommended the use of trapezoidal geometry with $\alpha \geq 0.8\alpha_{max.}$. The Indonesian Institute of Hydraulic Engineering (IIHE) Bandung, Indonesia also proposed the use of a trapezoidal shape (Figure 3-16). A trapezoidal plan form with $\alpha=0.68\alpha_{max.}$ was established and recommended in the design of the weir geometry (Memed & Sadeli, 1990; Puslitbang Pengairan, 1991). These studies showed that the flow capacity of the specified triangular and trapezoidal plan forms increases in direct proportion to an increase in crest length.

It was shown that, in general, the flow capacity of a labyrinth weir decreases as the depth or total head over the crest increases. This was thought to be due to the limitation of space either in the approach channel at the upstream side or in the receiving channel downstream. Hydraulic model studies have been carried out to improve these conditions. Taylor (1968) showed that a decrease of channel bed elevation downstream slightly increases the flow over the labyrinth weir. The USBR (Houston, 1983) also showed that the use of a curved approach in the spillway entrance, upstream channel (Figure 3-12) was significant in improving the labyrinth spillway's flow capacity. Cassidy *et al.* (1983) agree that the use of this curved approach in the spillway entrance increases the discharge over the labyrinth spillway as discussed in Section 3.6.

Some authors added that the choice of the number of weir cycles (n) will affect the quantity of the flow over the labyrinth weir. Two hydraulic model studies (sections 3.10 and 3.11) showed that an increase in the number of weir cycles decreases the flow

capacity of each cycle. Thus the overall performance of labyrinth weir with a smaller number of cycles would be better than a greater one. This did not confirm the result obtained earlier by Taylor (1968) that the behaviour of the labyrinth weir is independent of the number of weir cycles (Section 3.2.).

Among the previous works, only Hay & Taylor developed a theoretical solution to predict the flow capacity of a labyrinth weir. Other workers relied on the results of hydraulic model studies. However Taylor's model was based on ALGOL which is now seldom used. Thus in this thesis an attempt is made to develop the theoretical solution as done by Hay and Taylor but using different code and revised theory. When no funding is available for hydraulic model testing, this theoretical solution will be very useful for designers.

The importance of hydraulic model studies was also emphasized by some authors (Magalhães, 1985; Lux and Hinchliff, 1985; and Tacail *et al.*, 1990). Hydraulic model studies will confirm the important parameters influencing the labyrinth weir flow capacity and will confirm design estimates of discharge.

The economic value of labyrinth weirs was discussed by some authors (Hay and Taylor, 1970; Hinchliff and Houston, 1984; and Afshar, 1988). However none of them provided an economic analysis for a labyrinth weir. This thesis has shown the economic advantages by giving the case of one labyrinth weir which has already been constructed in Indonesia (see Chapter 2).

Finally, a number of generalized design curves for pre-design purposes were proposed. Hay and Taylor's (1970) design curves express the flow magnification as a

function of the length magnification and the flow depth to crest height ratio (Figure 3-2 and 3-3). On the other hand Darvas' (1971) design chart describes a discharge coefficient as a function of the length magnification and the flow depth to weir height ratio (Figure 3-8). Magalhães (1985) revised Darvas' design chart by presenting a dimensionless coefficient of discharge as indicated in Figure 3-13. The USBR (Houston, 1982) also promoted design curves in which the velocity head (H_v) was taken into account as shown in Figure 3-10. Using the experimental data from Taylor (1968), Darvas (1970), and Houston (1982), Lux and Hinchliff presented design curves expressing the relationship between the discharge coefficient and the total head ($H_o = H + H_v$) to crest height ratio for a constant value of the length magnification. This design curve was completed for the four basic stages of the flow over a labyrinth weir (Figure 3-14). Finally, IIHE Bandung, Indonesia advanced the design chart for a particular size of trapezoidal geometry (Figure 3-17).

Chapter 4

Theoretical Background and Computer Modelling

4.1. Theoretical background

4.1.1. The general weir equation

To best understand how much water can flow over a sharp crested weir, normal and labyrinth, one must be aware of the following equation used in calculating water flow (Daily and Harleman, 1973; Vennard and Street, 1975; Daugherty and Franzini, 1977; and Chadwick and Morfett, 1986) :

$$Q = C_d \frac{2}{3} \sqrt{2g}\ L\ H^{1.5} \qquad (4.1)$$

in which Q is the discharge over the weir crest in m^3/s, L is the net crest length in m, C_d is the weir discharge coefficient, H is the depth of the approaching flow in m, and g is the acceleration due to gravity = 9.81 m/s^2. Many textbooks suggest that C_d should be predicted by the Rehbock equation (Daugherty and Ingersoll, 1954; Vennard and

Street, 1975; Daugherty and Franzini, 1977) as shown below :

$$C_d = 0.605 + 0.08\,\frac{H}{P} + \frac{1}{305\,H} \qquad (4.2)$$

where H is in feet. In order to use the S.I. system, equation (4.2) should be modified to become :

$$C_d = 0.605 + 0.08\,\frac{H}{P} + \frac{1}{1000.7\,H} \qquad (4.3)$$

From equation (4.1), the total discharge overtopping the weir is proportional to the length of crest. Therefore, the flood flows which pass the weir can be increased without increasing the depth by extending the length of the crest. However, on a narrow-width river, it is impossible to make the crest longer. In periods of high discharge, the raised water level may cause unwanted inundations in the flood plain, and require local protective action by raising the crest of a levee. These problems could not be prevented through the use of a normal weir where the crest length cannot be increased. Those problems however can be solved by the use of a labyrinth weir in which the crest length can be increased. This weir is particularly suited for use at sites where the depth over the crest is limited or the weir width is restricted by the topography.

4.1.2. Theoretical solution

Hay and Taylors' (1969) theoretical solution.

Nimmo's momentum equation (Nimmo, 1928) was applied by Hay and Taylor (1969) in their theoretical solution. They chose this equation because it described the

general case of side weir flow. A sloping channel with the channel width and side wall slope varying from section to section (Figure 4-1) was considered in Nimmo's equation (Taylor, 1968). The equation was based on consideration of momentum principles and is given below :

$$\frac{Q^2}{g\,A} + \frac{Q\,\Delta Q}{g\,A} - \frac{(Q + \Delta Q)^2}{g\,(A + \Delta A)} = \frac{(W + \Delta W)\,(H^2 + 2\,H\,\Delta h)}{2}$$

$$+ (s_{sw} + \Delta s_{sw})\,\frac{(H^3 + 3\,H^2\,\Delta h)}{3} - \frac{W\,H^2}{2} - \frac{s_{sw}\,H^3}{3} - \frac{\Delta W\,H^2}{2}$$

$$- \frac{\Delta s_{sw}\,H^3}{3} - \Delta x\,(S_f - s_{cb})\,(W\,H - s_{sw}\,H^2) \qquad (4.4)$$

where : Q is the flow past a downstream section across the channel; ΔQ is the overflow between the sections; A is the area of cross section of flow at downstream section; ΔA is the difference in area of cross section of flow between the sections; g is the acceleration due to gravity; W is the width of channel bed at downstream section; ΔW is the difference in channel width between the sections; H is the flow depth at downstream section; Δh is the difference in depth between the sections; s_{sw} is the slope of side wall at downstream section; Δs_{sw} is the difference in slope of side wall between the sections; S_f is the friction slope between the sections; and s_{cb} is the slope of the channel bed between the sections.

Since this original equation was general, Taylor simplified it in order to be used in the case of labyrinth weir flow (Figure 4-2). The final equation is expressed by :

$$\frac{\Delta h}{\Delta x} = \frac{2Q\ (H+P)}{w}\ \frac{(Q \tan \alpha - \frac{w\ C_d\ H^{\frac{3}{2}}}{\cos \alpha})}{(w^2\ (H+P)^3\ g - Q^2)} \qquad (4.5)$$

where : Δh is the predicted difference in depth between 2 sections; Δx is a transverse element of channel length; Q is the discharge over the weir crest downstream of the section; H is the depth downstream of the section; P is the crest height; w is the average channel width between two sections; α is the side wall angle; C_d is the coefficient of discharge between two sections; and g is the acceleration due to gravity.

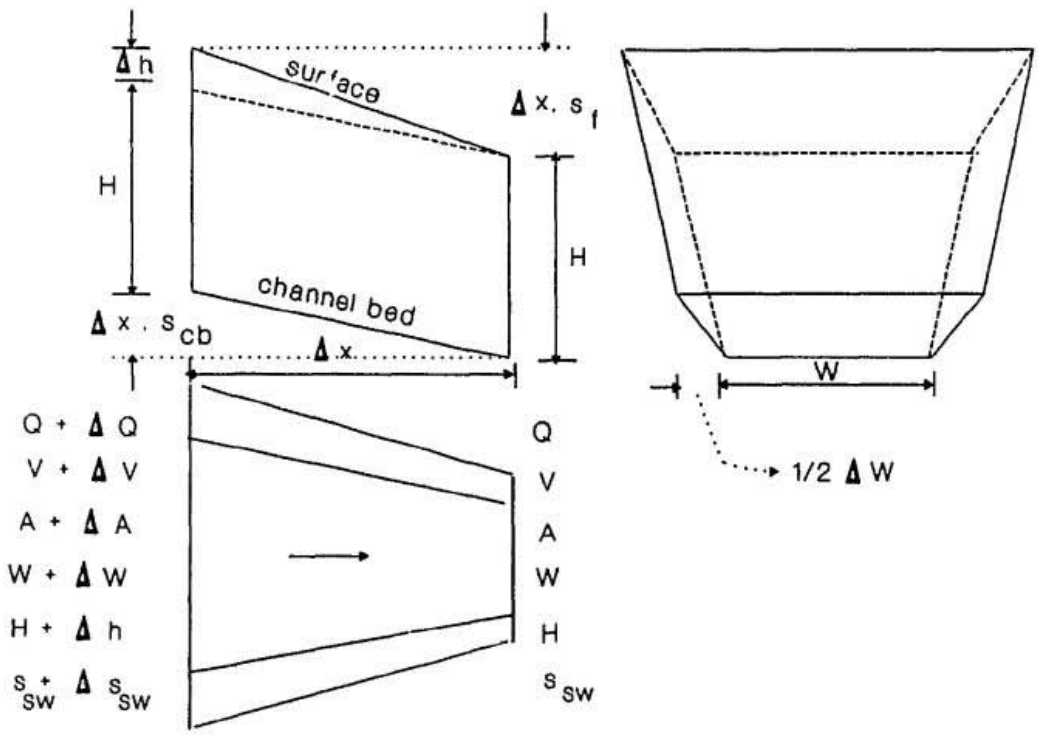

Figure 4-1 Sketch illustrating the notation used in Nimmo's equation. After Taylor (1968).

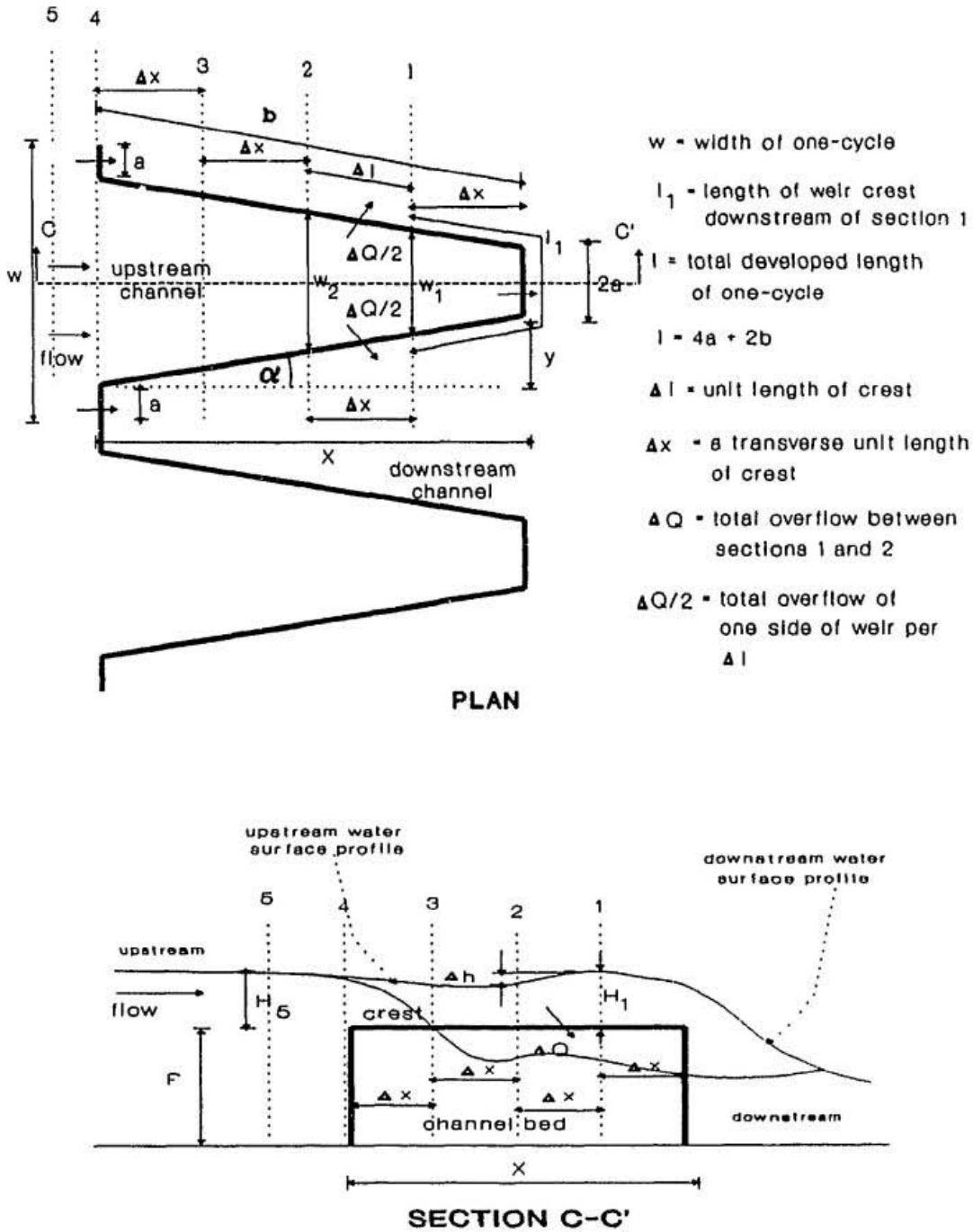

Figure 4-2 Flow description over the trapezoidal shape labyrinth weir. (modified from Hay and Taylor, 1969).

If the depth, H and flow, Q are known at one particular section, then the water surface profile throughout the channel and the total flow can be determined by equation (4.5). This solution was obtained by a marching method using finite differences as described below.

(1) Consider the flow over the labyrinth weir shown in Figure 4-2. The channel is divided into a number of sections each separated by Δx.

(2) Assume that the flow depth, H_1 at section 1 is known. Therefore, Q_1 can be calculated from the standard weir equation (equation 4.1) using the local depth at section 1 and the crest length downstream of section 1, ie l_1.

(3) Calculate the slope of the water surface at section 1 using equation (4.5). Then, Δh_{12} can be determined by defining the value of Δx. Then $H_2 = H_1 + \Delta h_{12}$.

(4) The average depth between two sections $= (H_1 + H_2)/2$, and the overflow between sections 1 and 2 is given by :

$$\Delta Q_{12} = \frac{2\, C_d\, \Delta x}{\cos \alpha}\, \frac{2}{3}\, \sqrt{2\, g}\, \left(\frac{H_1 + H_2}{2}\right)^{\frac{3}{2}} \qquad (4.6)$$

then, $Q_2 = Q_1 + \Delta Q_{12}$.

(5) Using geometrical considerations,

$$\frac{\Delta w}{\Delta x} = \frac{w_2 - w_1}{\Delta x} = 2 \tan \alpha \qquad (4.7)$$

or

$$w_2 = w_1 + 2\, \Delta x \tan \alpha \qquad (4.8)$$

The flow conditions are then known at section 2. The procedure is repeated in a similar

way to determine the flow and depth at the next section (section 3, Figure 4-2) and so on for the entire length of labyrinth weir crest or until the end of the upstream channel entry section (section 4, Figure 4-2).

Finally, energy conditions are satisfied between sections 4 and 5. Therefore,

$$H_5 = H_4 + C_{sc} \frac{V_4^2}{2g} \tag{4.9}$$

where C_{sc} is a coefficient of energy loss due to sudden contraction of the flow at entry to the upstream channel, and V_4 is the flow velocity at section 4, Figure 4-2. From Hay and Taylors' (1969) investigation C_{sc} was found to be equal to 0.2. The theoretical values agree very well with experimental results as discussed previously in Chapter 3.

Author's theoretical solution.

Basically, the flow over the labyrinth weir is a typical case of flow over a side channel spillway since the discharge along the labyrinth crest changes in the direction of the flow. In determining the side channel spillway flow characteristics, the theory of spatially varied flow with decreasing discharge has been applied by many experimenters. Therefore, in this theoretical works, the momentum equation for spatially varied flow with decreasing discharge will be adopted to predict the water surface profile. Figure 4-2 shows the flow description over a labyrinth weir. The momentum equation (Chow, 1959) for the control volume between sections 1 and 2 Figure 4-2 can be written as follows :

$$\Delta h = \frac{\beta\, Q_1\, (V_1 + V_2)\, \Delta V}{g\, (Q_1 + Q_2)} \left(1 - \frac{\Delta Q}{2Q_1} \right) + S_f\, \Delta x \qquad (4.10)$$

where Δh is the predicted difference in depth between sections 1 and 2; β is the energy coefficient; Q_1 is the total discharge over the labyrinth weir crest downstream of section 1; $\Delta Q/2$ is the discharge over one side of the labyrinth weir per unit length of the crest between sections 1 and 2; Q_2 is the total discharge over the labyrinth weir crest downstream of section 2 (equal to $Q_1 + \Delta Q$); g is the acceleration due to gravity; V_1 is the velocity at section 1; V_2 is the velocity at section 2; ΔV is the difference between velocities at sections 1 and 2; S_f is the friction slope; and Δx is the distance between sections 1 and 2 measured along the center line of the channel (Figure 4-2).

Some assumptions are made in this solution. These include :

1). The flow is uniform and steady.

2). The energy coefficient, β in equation (4.10) is taken equal to one. For greater accuracy the value of β must be obtained experimentally from the velocity distribution in the channel cross section.

3). At any section, the water surface across the section is horizontal.

4). Frictional forces are negligible provided Δx is small. Then the friction slope, S_f in equation 4.10 can be neglected.

5). The overflow per unit of crest length at any section may be calculated from the standard weir equation using the local depth at that section.

Equation (4.10) can then be simplified to :

$$\Delta h = \frac{Q_1 (V_1 + V_2) \Delta V}{g (Q_1 + Q_2)} (1 - \frac{\Delta Q}{2Q_1}) \qquad (4.11)$$

The solution is started by defining the local depth at a particular section. Section 1 in Figure 4-2 was chosen as a starting point of this solution. Let the local depth at section 1 be H_1, and the crest length up to section 1 be l_1. The total flow up to section 1, Q_1 thus can be determined using :

$$Q_1 = C_{d_1} \frac{2}{3} \sqrt{2\,g}\; l_1 H_1^{1.5} \qquad (4.12)$$

in which :

$$C_{d_1} = 0.605 + 0.08 \frac{H_1}{P} + \frac{1}{1000.7\, H_1} \qquad (4.13)$$

and :

$$l_1 = 2\,a + 2 \frac{\Delta x}{\cos \alpha} \qquad (4.14)$$

Then the flow velocity V_1 at section 1, can be calculated using :

$$V_1 = \frac{Q_1}{A_1} \qquad (4.15)$$

where A_1 is the area of the cross section of flow at section 1 and is given by :

$$A_1 = (H_1 + P) (2\,a + 2\,\Delta x \tan \alpha) \qquad (4.16)$$

Let, the overflow between sections 1 and 2 be ΔQ_{12}. Then $\Delta Q_{12}/2$ is the flow over one side of the weir and can be calculated from the standard weir equation using the average local depth between sections 1 and 2 as expressed by :

$$\frac{\Delta Q_{12}}{2} = C_{d_{sc}} \frac{2}{3} \sqrt{2\,g}\ \frac{\Delta x}{\cos\,\alpha} \left(\frac{H_1+H_2}{2}\right)^{1.5} \qquad (4.17)$$

The flow depth H_2 at section 2 is unknown but can be obtained by assuming a value of Δh and adding this to the value of H_1. The difference in flow, ΔQ, between sections 1 and 2 can then be obtained from equation 4.17, thus giving the total flow Q_2 at section 2. From H_2, Q_2 and the known geometry it is then possible to calculate V_2. Equation 4.11 can then be used to calculate Δh which can be compared to the assumed value. If the calculated value differs from the assumed value a new estimate must be made and the procedure must be repeated until the calculated value agrees with the assumed value. The calculation can then move as to obtain conditions between sections 2 and 3, and so on. This procedure is repeated in a similar way until the channel upstream entry section is reached (section 4 in Figure 4-2). To obtain the flow depth at section 5, Figure 4-2, the energy condition must be satisfied between sections 4 and 5. In this solution, Hay and Taylor's approach was adopted. However, the value of the coefficient of energy loss due to sudden contraction, C_{sc} was found to be equal to 0.1. This value is lower than the value of 0.2 determined by Hay and Taylor (1969).

4.2. Dimensional Analysis

Dimensional analysis is used to provide guidance to experiments and presentation of experimental results by incorporating all of the relevant variables into a dimensionless equation (Sharp, 1981). The experimental investigation presents either the design charts or the numerical constants, and assists in checking the correctness of the analysis.

The total discharge per cycle, Q_L (Figure 4-2) can be expressed by the function:

$$Q_L = \phi\ (\ l,\ a,\ w,\ P,\ H,\ \rho,\ g,\ \mu,\ \sigma\ ) \qquad (4.18)$$

where :

Q_L = total flow over one-cycle of the labyrinth weir

l = developed crest length of one-cycle

a = half length of tip section normal to the flow

w = cycle width

P = crest height

H = upstream depth above the crest

ρ = density of water

g = gravitational acceleration

μ = viscosity

σ = surface tension

Since the flow in nature is turbulent, and occurs at a relatively large head, it can be assumed that viscosity μ, and surface tension σ are insignificant variables (Sharp, 1981). Therefore, they can be dropped from equation (4.18). Thus, equation (4.18) becomes :

$$Q_L = \phi\ (\ l,\ a,\ w,\ P,\ H,\ \rho,\ g\ ) \qquad (4.19)$$

In order to make the equation dimensionally homogenous, the density should be eliminated since it is the only variable which has a mass dimension. Then, equation

(4.19) becomes :

$$Q_L = \phi \ (\ l, \ a, \ w, \ P, \ H, \ g \ ) \qquad (4.20)$$

Using the Indicial Approach or Rayleigh's Method, several combinations of dimensionless numbers can be obtained from equation (4.20), so that equation (4.20) can be written in terms of the dimensions to give :

$$Q_L = k \ l^a \ a^b \ w^c \ P^d \ H^e \ g^f \qquad (4.21)$$

where k, a, b, c, d, e, and f are undefined constants. Rewriting the equation (4.21) in terms of the length [L] and time [T] dimensions gives :

$$\frac{[L]^3}{[T]} = k \ [L]^a \ [L]^b \ [L]^c \ [L]^d \ [L]^e \ (\frac{[L]}{[T]^2})^f$$

Equating exponents of [L], and [T] :

[L] $3 = a + b + c + d + e + f$

[T] $-1 = -2f \rightarrow f = ½$

$e = 2½ - a - b - c - d$

Substituting in equation (4.21), these values lead to :

$$\frac{Q_L}{g^{\frac{1}{2}} H^{\frac{5}{2}}} = \phi \ (\ \frac{l}{H}, \ \frac{a}{H}, \ \frac{w}{H}, \ \frac{P}{H} \ ) \qquad (4.22)$$

Compounding equation (4.22) , in order to have a convenient solution, gives :

$$\frac{Q_L}{g^{\frac{1}{2}} H^{\frac{5}{2}}} * \frac{H}{l} = \phi \left(\frac{l}{H} * \frac{H}{w} , \frac{a}{H} * \frac{H}{w} , \frac{w}{H} * \frac{H}{P} , \frac{H}{P} \right) \quad (4.23)$$

Therefore, equation (4.22) can be rewritten as :

$$Q_L = C_d \, l \, H \sqrt{g \, H} \quad (4.24)$$

where

$$C_d = f \left(\frac{l}{w} , \frac{a}{w} , \frac{w}{P} , \frac{H}{P} \right) \quad (4.25)$$

Equation (4.24) is the general weir equation. This equation uses the crest length per cycle, l, as the characteristic length for the labyrinth weir. In equation (4.25), all dimensionless ratios except the last one are fixed for a given labyrinth weir. Thus, C_d in this case is known as the coefficient of discharge of the labyrinth weir. In other words, the labyrinth weir discharge coefficient, C_d is given as a function of dimensionless parameters l/w, a/w, w/P, and H/P. If the values of l/w, a/w, and w/P are already fixed, then, equation (4.25) could be expressed by the function :

$$C_d = \phi \left(\frac{H}{P} \right) \quad (4.26)$$

Equation (4.26) is the Rehbock equation (see equations 4.2 and 4.3).

An alternative equation can be obtained to describe the performance of a sharp crested labyrinth weir of constant geometry in terms of flow magnification. The total discharge per cycle, Q_L (Figure 4-2) may be expressed by the function :

$$Q_L = \phi (Q_N , H, P, l , w) \quad (4.27)$$

where :

Q_N = total flow over a sharp crested normal or linear weir

H = upstream depth above the crest

P = crest height

l = crest length of labyrinth weir

w = crest length of linear or normal weir

Rearranging equation (4.27) as before gives :

$$Q_L = k\ Q_N^a\ H^b\ P^c\ l^d\ w^e \quad (4.28)$$

where k is a constant. Equation (4.28) in dimensional form can be rewritten as :

$$\frac{[L]^3}{[T]} = \left(\frac{[L]^3}{[T]}\right)^a [L]^b\ [L]^c\ [L]^d\ [L]^e \quad (4.29)$$

Equating exponents of [L] and [T] :

[T] $-1 = -a$

$a = 1$

[L] $3 = 3a + b + c + d + e$

$0 = b + c + d + e$

$b = - c - d - e$

Substitute these values into equation (4.28) gives :

$$\frac{Q_L}{Q_N} = \phi \left(\frac{P}{H} , \frac{l}{H} , \frac{w}{H} \right) \qquad (4.30)$$

Compounding, in order to have a convenient solution, gives :

$$\frac{Q_L}{Q_N} = \phi \left(\frac{H}{P} , \frac{l}{H} * \frac{H}{w} , \frac{w}{H} * \frac{H}{P} \right) \qquad (4.31)$$

Thus, equation (4.30) can be rewritten as :

$$\frac{Q_L}{Q_N} = \phi \left(\frac{H}{P} , \frac{l}{w} , \frac{w}{P} \right) \qquad (4.32)$$

From equation (4.32), the comparison of the labyrinth weir flow, Q_L, with the corresponding straight weir flow, Q_N is expressed directly. Hay and Taylor (1970) used equation (4.32) to present the results of their model test. On the other hand, Darvas (1971) expressed the results of his experiment by equation (4.25). In the present experiments, the results of the model test will be plotted in terms of flow magnification (Q_L/Q_N) against flow depth to weir height ratio (H/P) for a constant value of the length magnification (l/w) and vertical aspect ratio (w/P). This is similar to the way in which Hay and Taylor presented the results of their model tests.

4.3. Computer Modelling Programme

The momentum equation (eq. 4.11) describes one-dimensional steady, spatially varied flow. It can be used to compute the flow profile of a spatially varied flow with decreasing discharge based on a method of numerical integration. Because the numerical solution is repetitive, it was decided to develop a computer program to increase the speed

of the process. Then, numerical predictions of labyrinth weir performance could be made directly without model tests.

4.3.1. An attempt to develop a computer model

As discussed in the previous chapter, Hay and Taylor (1969) established a computer model to predict the performance of a labyrinth weir and compared their solution with experimental work.

Hay and Taylor's computer program in ALGOL is relatively complex and difficult to understand. Also, ALGOL has largely been replaced by other programming languages. Therefore, an alternative formulation was developed using equation (4.11). Initially, it was thought that the use of a spreadsheet, or tabular method, to compute the water surface profile would be easier than the use of computer program. Using a spreadsheet, the analysis could be developed easily by a trial and error procedure.

However following this development it was found that the use of spreadsheet was cumbersome and time consuming. A computer program in QuickBASIC was then set up based on the spreadsheet procedures.

4.3.2. Spreadsheet work

The computational procedures to get one value of H/P corresponding to one value of Q_L/Q_N are described below (see Figure 4-3 and Table 4.1) :

1). Specify the length of one-cycle, l; the width of one-cycle, w; half length of tip section normal to the flow, a; weir height, P; acceleration due to gravity, g; and number of

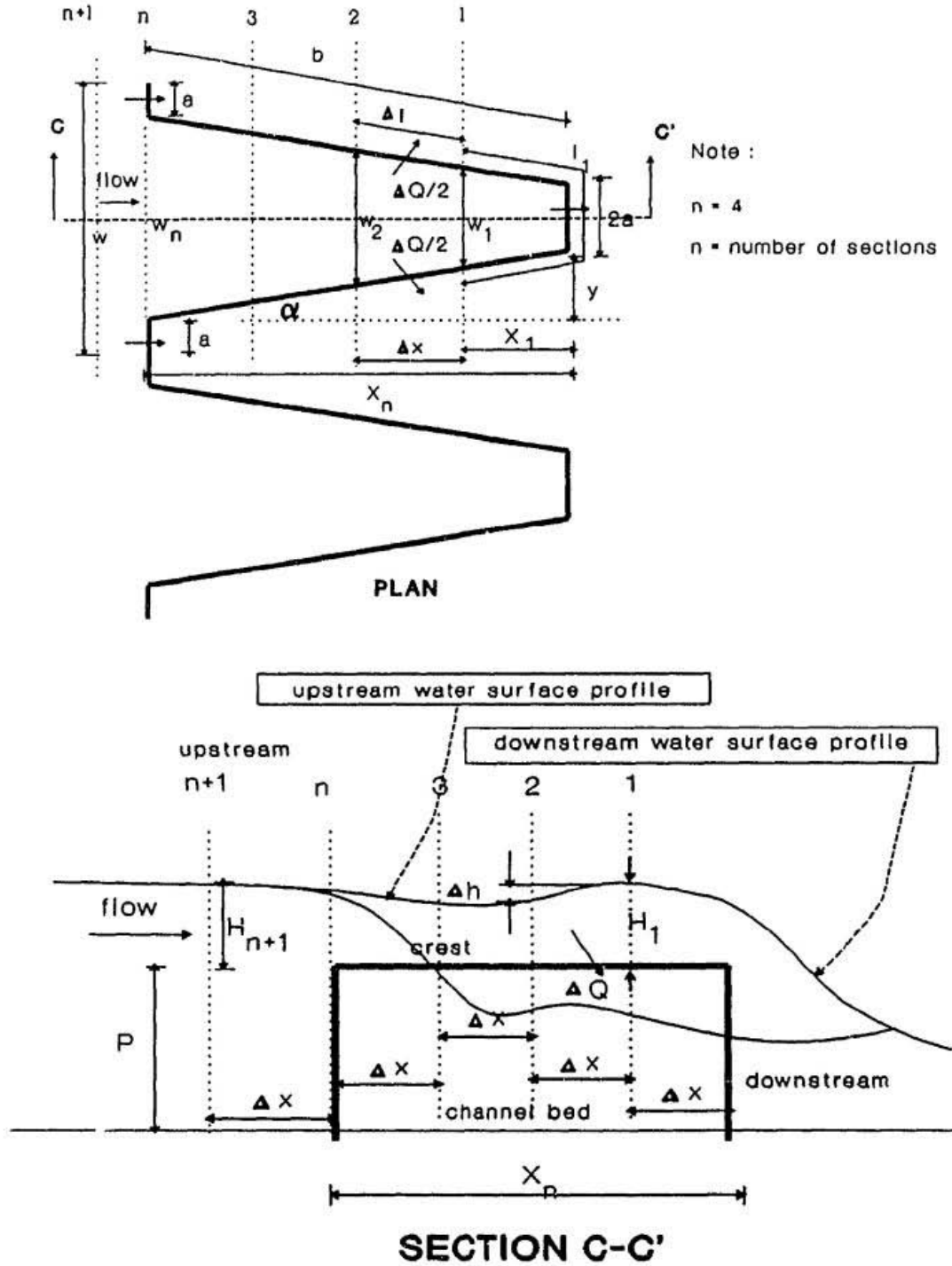

Figure 4-3 Sketch to illustrate the theoretical analysis of flow over the labyrinth weir. (modified from Hay and Taylor, 1969).

TABLE 4.1

Table of computation for the determination of discharge of each section

Data :

l =	71.9600 cm	g =	981.0000 cm/s ^ 2	delta l =	2.4138 cm	P =	10.0000 cm	X =	28.1002 cm
w =	28.1000 cm	alpha =	0.2450 radian						
a =	3.5125 cm	delta x =	2.3417 cm	y =	7.0250 cm	b =	28.9650 cm	alpha =	14.0362
n =	12								

Sec. No	x (cm)	H (cm)	Cd	l (cm)	Q (cm ^ 3/s)	delta Q (cm ^ 3/s)	Q1 + Q2 (cm ^ 3/s)	w (cm)	A (cm ^ 2)	V (cm/s)	(V1 + V2) (cm/s)	delta Q (cm ^ 3/s)	delta V (cm/s)	delta H (cm)	Sec. No
(1)	(2)	(3)	(4)	(5)	(6)	(7)	(8)	(9)	(10)	(11)	(12)	(13)	(14)	(15)	(16)
0	0.0000														0
1	2.3417	0.3048	0.9353	11.6525	55.0865	22.4396		8.1958	64.4564	0.8522				0.0001	1
2	4.6834	0.3049	0.9352		77.5260		132.6125	9.3667	96.5226	0.8032	1.4554	22.4396	0.1509	0.0001	2
2	4.6834	0.3049	0.9352		77.5260	22.4506		9.3667	96.5226	0.8032				0.0001	2
3	7.0250	0.3050			99.9767		177.5027	10.5375	108.5889	0.9207	1.7239	22.4506	0.1175	0.0001	3
3	7.0250	0.3050	0.9351		99.9767	22.4591		10.5375	108.5889	0.9207				0.0001	3
4	9.3667	0.3051			122.4358		222.4124	11.7083	120.6556	1.0148	1.9354	22.4591	0.0941	0.0001	4
4	9.3667	0.3051	0.9350		122.4358	22.4676		11.7083	120.6556	1.0148				0.0001	4
5	11.7084	0.3052			144.9033		267.3391	12.8792	132.7224	1.0918	2.1065	22.4676	0.0770	0.0001	5
5	11.7084	0.3052	0.9349		144.9033	22.4761		12.8792	132.7224	1.0918				0.0001	5
6	14.0501	0.3053			167.3794		312.2827	14.0500	144.7895	1.1560	2.2478	22.4761	0.0642	0.0001	6
6	14.0501	0.3053	0.9348		167.3794	22.4845		14.0500	144.7895	1.1560				0.0001	6
7	16.3918	0.3054			189.8639		357.2433	15.2208	156.8568	1.2104	2.3664	22.4845	0.0544	0.0001	7
7	16.3918	0.3054	0.9347		189.8639	22.4930		15.2208	156.8568	1.2104				0.0001	7
8	18.7335	0.3055			212.3570		402.2209	16.3917	168.9243	1.2571	2.4675	22.4930	0.0467	0.0001	8
8	18.7335	0.3055	0.9346		212.3570	22.4960		16.3917	168.9243	1.2571				0.0000	8
9	21.0751	0.3055			234.8530		447.2100	17.5625	180.9904	1.2978	2.5547	22.4960	0.0406	0.0000	9
9	21.0751	0.3055	0.9346		234.8530	22.4960		17.5625	180.9904	1.2978				0.0000	9
10	23.4168	0.3055			257.3490		492.2020	18.7333	193.0564	1.3330	2.6308	22.4960	0.0354	0.0000	10
10	23.4168	0.3055	0.9346		257.3490	22.4960		18.7333	193.0564	1.3330				0.0000	10
11	25.7585	0.3055			279.8450		537.1940	19.9042	205.1224	1.3643	2.6973	22.4960	0.0313	0.0000	11
11	25.7585	0.3055	0.9346		279.8450	22.4960		19.9042	205.1224	1.3643				0.0000	11
12	28.1002	0.3055	0.9346		302.3410	32.7383	582.1859	21.0750	217.1884	1.3921	2.7564	22.4960	0.0278	0.0000	12
12'	28.1002	0.3055			335.0773										12

*Trapezoidal geometry

CSC = 0.1000 / 0.1500 / 0.2000 / 0.2500 / 0.3000 / 0.3500

lw = 2.5616

w/P = 2.8100 *(1 cycle).*

*COMMODEL.WK3

@output1a.wk3

Check :

X12 = 28.1002 cm

l12 = 64.9650 cm

w12 = 21.0750 cm

TABLE 4.1 (continued)

Sec. No	X (cm)	H+ CSC*V^2/2*g (cm)	QL (cm^3/s)	Cd	QN (cm^3/s)	QL/QN	H/P
(17)	(18)	(19)	(20)	(21)	(22)	(23)	(24)
		0.3056		0.9345	130.9639	2.5580	0.0306
		0.3056		0.9344	131.0183	2.5575	0.0306
13	30.4419	0.3057	335.0773	0.9344	131.0427	2.5570	0.0306
		0.3057		0.9343	131.0671	2.5565	0.0306
		0.3058		0.9342	131.0915	2.5561	0.0306
		0.3058		0.9342	131.1159	2.5556	0.0306

INPUT		OUTPUT	
l (cm) =	71.9600	lw =	2.5616
w (cm) =	28.1000	w/P =	2.8100
a (cm) =	3.5125	QL/QN =	2.5580
P (cm) =	10.0000	H/P =	0.0306
g(cm/det^2) =	981.0000		
n =	12		
CSC =	0.1000		

* delta H (column 15) is quoted from Open-Channel Hydraulics, Ven Te Chow Pn D., page 346

**delta H = ((Q1*(V2 + V1) delta V)/(g (Q2 + Q1)) * (1 - (delta Q/2*Q1))

*CSC = energy loss coefficient due to sudden contraction

sections, n. As shown in Table 4.1, l = 71.98 cm; w = 28.1 cm; a = 3.5125 cm; P = 10 cm; g = 981 cm/s^2; and n = 12.

2). Then, l/w; w/P; y; b; X; α; Δx; and Δl are calculated. These notations are illustrated in Figure 4-3.

y is obtained by :

$$y = (\frac{w}{2} - 2\ a) \tag{4.33}$$

b is expressed by :

$$b = \frac{(l - 4\ a)}{2} \tag{4.34}$$

X is given by :

$$X = \sqrt{(b^2 - y^2)} \tag{4.35}$$

α is calculated by :

$$\alpha = \text{arc tan } (\frac{y}{X}) \tag{4.36}$$

Δx and Δl are estimated by :

$$\Delta x = \frac{X}{n} \quad ; \quad \Delta l = \frac{\Delta x}{\cos \alpha} \tag{4.37}$$

3). The solution is started from section 1 (column 1, row 1). The transverse distance of section 1 from the tip section at the downstream end of the labyrinth weir, X_1 is obtained by setting n = 1 in the general equation :

$$X_n = (n - 1)\ \Delta x + \Delta x \qquad (4.38)$$

The value of X_1 (equal to 2.3417 cm) is shown in column 2, row 1.

4). The flow depth H_1 at section 1, is specified. In this example H_1 was set equal to 0.3048 cm (column 3, row 1).

5). The coefficient of discharge, C_d is then predicted using the Rehbock equation with the depth = H_1. Experimental work will later (Chapter 6) be described regarding the use of the Rehbock equation to predict the theoretical discharge coefficient of the labyrinth weir. This is estimated by :

$$C_{d_n} = 0.605 + 0.08\ \frac{H_n}{P} + \frac{1}{10.006562\ H_n} \qquad (4.39)$$

Here $C_{d(n=1)} = 0.9353$ (column 4, row 1).

6). The length of weir crest l_1 downstream of section 1, is then calculated from :

$$l_1 = (\ 2\ a + \frac{2\ \Delta x}{\cos\ \alpha}\ ) \qquad (4.40)$$

In column 5, row 1, l_1 is shown equal to 11.8525 cm.

7). The flow Q_1 at section 1, is then estimated using the standard weir equation applied to the length of weir crest downstream of section 1, l_1. This is given by :

$$Q_1 = C_{d_1}\ \ l_1\ \ H_1^{1.5}\ \ \frac{2}{3}\ \ \sqrt{2\ g} \qquad (4.41)$$

From this equation $Q_1 = 55.0865\ cm^3/s$ (column 6, row 1).

8). Next the channel width w_1 at section 1 is calculated with n = 1 in the equation :

$$w_n = (2\ a + 2\ X_n \tan \alpha) \qquad (4.42)$$

Then, $W_{n=1}$ = 8.1958 cm (column 9, row 1).

9). The area A_1 of the cross section of flow at section 1, is calculated from :

$$A_n = (H_n + P)\ \ w_n \qquad (4.43)$$

giving $A_{n=1}$ = 84.4564 cm^2 (column 10, row 1).

10). Then the velocity V_1 at section 1, can be calculated by .

$$V_n = \frac{Q_n}{A_n} \qquad (4.44)$$

Then $V_{n=1}$ = 0.6522 cm/s as shown in column 11, row 1.

11). The solution of the momentum equation requires a trial and error procedure and it is necessary to estimate Δh. This assumption is specified at column 15, row 1. Once $\Delta h_{assumption}$ (0.0001 cm) was entered in column 15, row 1, $\Delta Q_{1\ to\ 2}$ (ie from n=1 to n=2) can be calculated using the standard weir equation given by :

$$\Delta Q_{(n)-(n+1)} = 2\ \ C_{d_{(n)-(n+1)}}\ \ \frac{\Delta x}{\cos \alpha}\ \ \left(\frac{H_n+H_{n+1}}{2}\right)^{1.5}\ \ \frac{2}{3}\ \ \sqrt{2\ g} \qquad (4.45)$$

in which :

$$C_{d_{(n)-(n+1)}} = 0.605 + 0.08\ \frac{\left(\frac{H_n+H_{n+1}}{2}\right)}{P} + \frac{1}{10.006562\ \frac{(H_n+H_{n+1})}{2}} \qquad (4.46)$$

and n = 1

This gave $\Delta Q_{1\text{-}2}$ = 22.4396 cm^3/sec (column 7, row 1).

12). Calculate $X_2 = X_1 + \Delta x$ (It is obtained by setting n = 2 in equation (4.38)). The value of X_2 (equal to 4.6834 cm) is shown in column 2, row 2.

13). Calculate the flow depth H_2 at section 2. This is estimated by :

$$H_{n+1} = H_n + \Delta h_{(n)-(n+1)} \qquad (4.47)$$

in which Δh above is the assumed value of Δh given in column 15, row 1. Thus H_2 = 0.3049 cm (column 3, row 2).

14). The discharge Q_2 at section 2, is estimated (n=1) from :

$$Q_{n+1} = Q_n + \Delta Q_{(n)-(n+1)} \qquad (4.48)$$

Then Q_2 = 77.5260 cm^3/s (column 6, row 2).

15). Sum $Q_1 + Q_2$. This is needed to simplify the calculation of Δh using the momentum equation (see step 22). Q_1 is the total flow at the downstream section 1 and Q_2 is the total flow at the upstream section 2. In column 8, row 2, $Q_1 + Q_2$ is shown equal to 132.6125 cm^3/sec.

16). Calculate the width w_2 at section 2 (see step 8).

17). Calculate the area A_2 of the cross section of flow at section 2 (see step 9).

18). Calculate the velocity V_2 at section 2 (see step 10).

19). Sum $V_1 + V_2$ (see step 15). V_1 is the velocity at the downstream section 1 and V_2 is the velocity at the upstream section 2.

20). Calculate the difference in flow ΔQ between the two sections. $\Delta Q = Q_2 - Q_1$ (column 13). Actually this equals to ΔQ at step 11 for all sections except the last row (see step).

21). Calculate the difference in velocity ΔV between sections 1 and 2. $\Delta V = V_2 - V_1$ (column 14).

22). Compute Δh using the momentum equation. This is calculated, with n=1, from :

$$\Delta h_{(n)-(n+1)} = \frac{Q_n\ (V_n+V_{n+1})\ \Delta V_{(n)-(n+1)}}{g\ (Q_n+Q_{n+1})}\ (1\ -\ \frac{\Delta Q_{(n)-(n+1)}}{2\ Q_n}) \qquad (4.49)$$

This equation gives $\Delta h_{computed}$ between sections 1 and 2, Δh_{1-2} and is entered automatically in column 15, row 2. The value calculated is 0.0001 and matches the assumed value of step 11 entered in column 15, row 1. Because of the match, the trial and error calculation is finished between sections 1 and 2. If $\Delta h_{computed}$ did not match $\Delta h_{assumption}$, it is necessary to return to step 11 and substitute $\Delta h_{assumption}$ by $\Delta h_{computed}$. Then step 11 would be repeated. This process continues until the calculated value of Δh printed in column 15, row 2 is equal to the assumed value entered in column 15, row 1.

The whole process is then repeated from section 2 to 3 and is started by entering the assumed value of Δh_{2-3} in column 15, row 3. The spreadsheet goes through the calculation and prints the calculated value of Δh in column 15, row 4. The operator checks and reenters as necessary. This is repeated for each section up to section 12 (shown as section n in Figure 4-3).

23). The total flow Q_{12} at section 12, is the total flow without including the flow over the two tip sections, each of length a, at the upstream end of labyrinth weir crest. Thus the total flow $Q_{12'}$ at section 12, becomes :

$$Q_{12'} = Q_{12} + C_{d_{11}} \quad (2\ a) \quad (H_{12})^{1.5} \quad \frac{2}{3} \quad \sqrt{2\ g} \qquad (4.50)$$

This gives $Q_{12'}$ = 335.0773 (column 6, row 12' and column 20, row 13).

24). Calculate $X_{13} = X_{12} + \Delta x$ (It is obtained by setting n = 13 in the equation (4.38)). This gave X_{13} = 30.4419 cm (column 18, row 13). It is necessary to satisfy energy conditions between sections 12 and 13 to obtain the depth H_{13} at section 13. This is given by :

$$H_{13} = H_{12} + C_{sc} \frac{V_{12}^{\ 2}}{2\ g} \qquad (4.51)$$

where C_{sc} is the energy loss coefficient due to sudden contraction. A number of C_{sc} values were investigated. This was required in order to match the author's theoretical results with the Hay and Taylor's theoretical results. The author assumed that Hay and Taylor's theoretical solution was the correct one. However author's theoretical solution will also be compared to author's experimental results. As shown in Table 4.1, C_{sc} values equal to 0.1, 0.15, 0.2 and 0.25 were tried and gave depths H_{13} at section 13 as shown in column 19. These depths (column 19) were then used (step 5) to calculate the discharge coefficients shown in column 21.

25). The total flow over the normal or straight weir applying the local depth H_{13} at section 13, and the width of one-cycle labyrinth weir, w is given by :

$$Q_N = C_{d_{11}} \quad w \quad \frac{2}{3} \quad \sqrt{2\ g} \quad (H_{13})^{1.5} \qquad (4.52)$$

These results are given in column 22.

26). Finally, the flow magnification, Q_L/Q_N was calculated along with the depth to weir height ratio, H/P. These results are given in columns 23 and 24 respectively. Note that the whole procedure only provides one value of Q_L/Q_N and one corresponding value of H/P depending on the value specified for C_{sc}. To get another value of Q_L/Q_N and H/P for the same dimension of labyrinth weir, steps 4 to 26 except step 6 must be repeated. If the dimensions are changed, then the solution must be started from step 1.

A comparison of results with Hay and Taylor's theoretical solution showed that a value of C_{sc} equal to 0.1, gave the best fit. Details of the comparison are given in section 4.3.5.

Table 4.1 provides only one example of the spreadsheet calculation and gives data for H/P = 0.0306. Other examples are provided in Appendix A where Tables C.1 to C.8 give data for eight different values of H/P with values varying from 0.03 to 0.58. In each case the dimensions of the labyrinth weir are given by l = 71.98 cm, w = 28.1 cm, a = 3.51 cm, and α = 14.04°.

4.3.3. Flow charts

A flow chart to illustrate the operations which must be carried out by the computer was developed for the QuickBASIC program. This is shown in Figure 4-4. This flow chart is designed to obtain a series of values of Q_L/Q_N and a series of corresponding values of H/P for particular design dimensions. The range of H/P values is set from 0 to 0.6. The flow charts consist of three nested loops. The inner loop represents the iteration of flow depth at a section. The middle loop repeats this

calculation over the length of the labyrinth weir to provide one value of H/P and one corresponding value of Q_L/Q_N. The outer loop repeats the entire calculation for a range of specified values of H/P.

The flow chart starts with the specification of the design dimensions of the labyrinth weir. These include : the developed length of one-cycle (l), the width of one cycle (w), the half length of tip section (a), and the weir height (P). It is then necessary to specify the number of sections (n), gravitational acceleration (g), and energy loss coefficient due to sudden contraction (C_{sc}). Next the labyrinth weir parameters are calculated. These include : the length magnification (l/w), width to weir height ratio (w/P), and side wall angle (α). The geometrical dimensions which will be required for the next calculation are also calculated.

The flow chart then comes to the outer loop which calculates the different values of H/P and corresponding values of Q_L/Q_N. This starts by defining the depth at the initial section (H_1), the initial assumption of difference of depth between the two sections ($\Delta h_{assumption}$), the level of acceptable error (E), and the amount by which this initial depth is increased for each repetition of the entire calculation. This outer loop will be re-executed automatically with different values of H_1 and will stop automatically when the value of H/P is greater than or equal to 0.6.

After that, flow chart comes to the middle loop which computes the different values of depth at each adjacent section. This middle loop will be re-executed automatically once Δh is established in the inner loop. The number of repetitions in this second loop depends on the number of sections, n, which were defined. Once the last

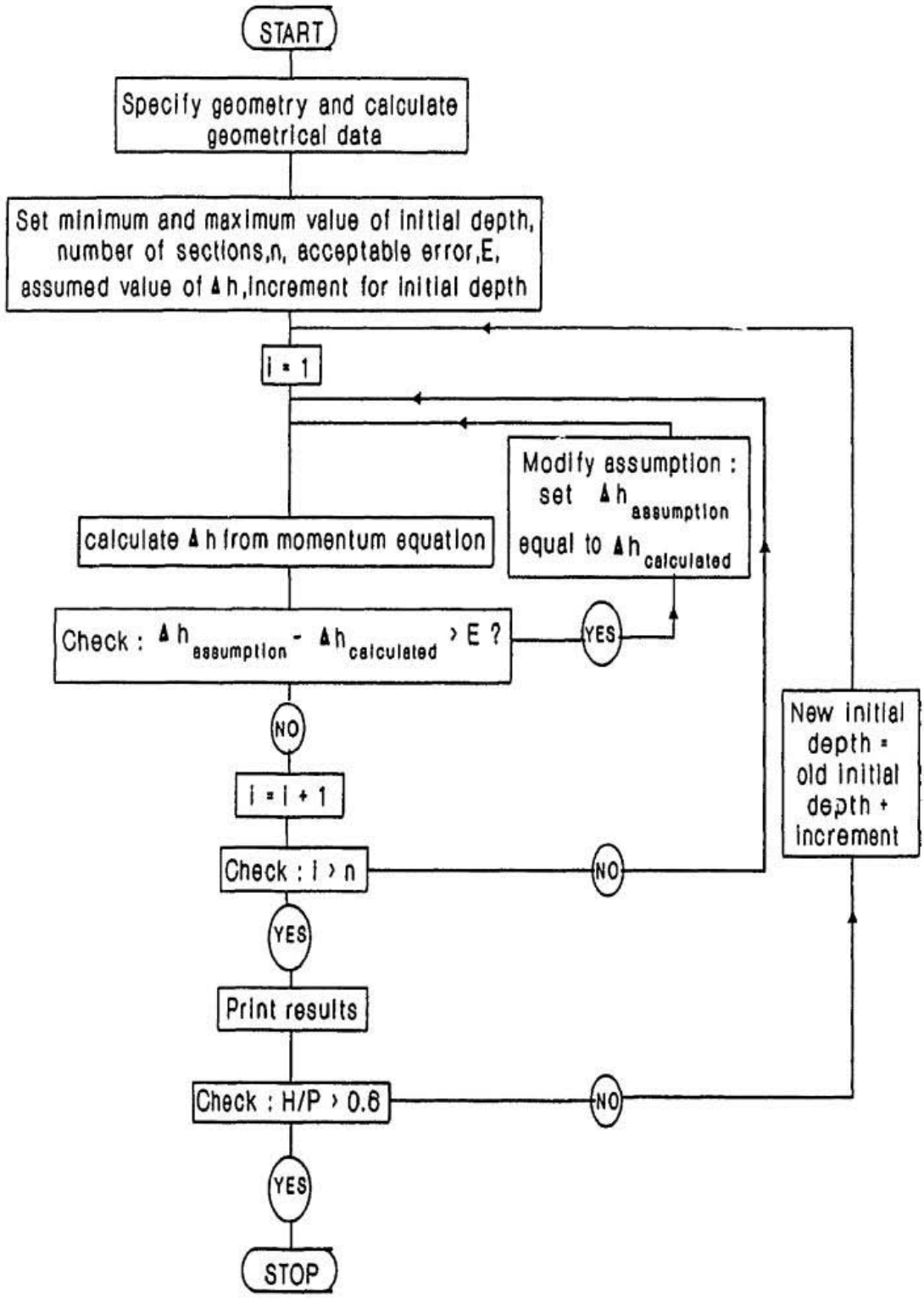

Figure 4-4 Flow charts for QuickBASIC program

section is reached, the computation goes back automatically to the outer loop.

Next, the flow chart comes to the inner loop. This loop repeats the calculation of the depth difference between two sections (Δh) until the computed value agrees with the assumed value. The calculation uses the momentum equation. If the error between $\Delta h_{assumption}$ and $\Delta h_{computed}$ is greater than the level of acceptable error (E), then this inner loop will be re-executed. This is done automatically by modifying the next estimation of Δh by setting the assumed value equal to the computed value. Once the value of $\Delta h_{assumption}$ agrees with $\Delta h_{computed}$ this inner loop will jump back automatically to the middle loop.

Finally, the output of the program is printed. This includes the flow magnification (Q_L/Q_N) and depth to weir height ratio (H/P) of one design dimension of labyrinth weir with one-cycle. A typical output of the QuickBASIC program is shown in Appendix C.

4.3.4. QuickBASIC Program

The computer program was designed for practical use in the design of labyrinth weirs and to compute the relationship between flow magnification values, Q_L/Q_N and depth to weir height ratios, H/P. These values are computed for one-cycle of the labyrinth weir. As shown in Appendix B, the program consisted of 142 lines. These include :

(1) Lines 10-90 clear screen, and give the program title.

(2) Line 100 is a dimension statement.

(3) Lines 110-210 print the heading.

(4) Lines 220-310 input data. This includes the developed length of labyrinth weir, width of one-cycle, half length of tip section, gravitational acceleration, weir height, number of increments, and energy loss coefficient due to sudden contraction.

(5) Lines 320-390 print the labyrinth weir geometry.

(6) Lines 400-510 calculate the length magnification, depth to weir height ratio, side wall angle, and other geometrical dimensions of labyrinth weir.

(7) Lines 520-600 print the labyrinth weir design parameters.

(8) Lines 610-720 print the heading of output.

(9) Lines 730-780 specify the initial value of the depth Δh difference between two sections, the level of acceptable error (E), the minimum value of initial depth (H_1), the maximum value of initial depth (H_1), and the desired increment of initial depth.

(10) Line 790 starts the calculation in loop 1 for different initial depths.

(11) Lines 800-920 calculate the total flow at the initial section.

(12) Line 930 starts the calculation in loop 2 for different adjacent depths until to the last section.

(13) Lines 940-960 stores $\Delta h_{input\ data}$ and calculates the width.

(14) Lines 970-1110 give the calculation in loop 3 to match $\Delta h_{input\ data}$ with $\Delta h_{computed}$.

(15) Line 1120 stores the adjacent depth after getting the matched Δh.

(16) Line 1130 is the end of loop 2.

(17) Lines 1140-1170 stores the depth, flow, discharge coefficient, and velocity at the last section.

(18) Line 1180 calculates the flow over two tip sections at the upstream end of the

labyrinth weir

(19) Line 1190 calculates the total flow of a labyrinth weir for one initial depth value.

(20) Lines 1200-1210 calculate the total depth in the approach channel.

(21) Lines 1220-1230 calculate the total flow over the normal weir.

(22) Lines 1240-1250 calculate the flow magnification and depth to weir height ratio.

(23) Lines 1260-1420 print output and stop the program.

4.3.5. Comment on Spreadsheet vs QuickBASIC

In the author's experience, five minutes was required to obtain one value of Q_L/Q_N and the corresponding value of H/P using the spreadsheet. This duration was largely because a trial and error method was applied. Thus, to get a series of values ($0.1 \leq H/P \leq 0.6$) would require, on average, half an hour.

Unlike the spreadsheet, QuickBASIC only requires a few seconds to obtain a series of values of Q_L/Q_N and H/P. Thus, QuickBASIC is more advantageous than the spreadsheet with respect to time.

The outputs of the spreadsheet and the QuickBASIC program are shown in Figure 4-5 and are very close. Further details of spreadsheet output are given in Appendix A. The output of the QuickBASIC program is shown in Appendix C. The QuickBASIC program is to be preferred as the method of obtaining a theoretical solution.

The author's results were compared with those of Hay and Taylor (1969). Three models in Taylor's work were reproduced in the author's theoretical solution. These were considered to be representative of Hay and Taylor's results and were considered to be

sufficient for comparison. The comparison is illustrated in Figure 4-6. This showed satisfactory agreement with the condition that the energy loss coefficient, C_{sc} was equal to 0.1 rather than 0.2 which was obtained earlier by Taylor (1968).

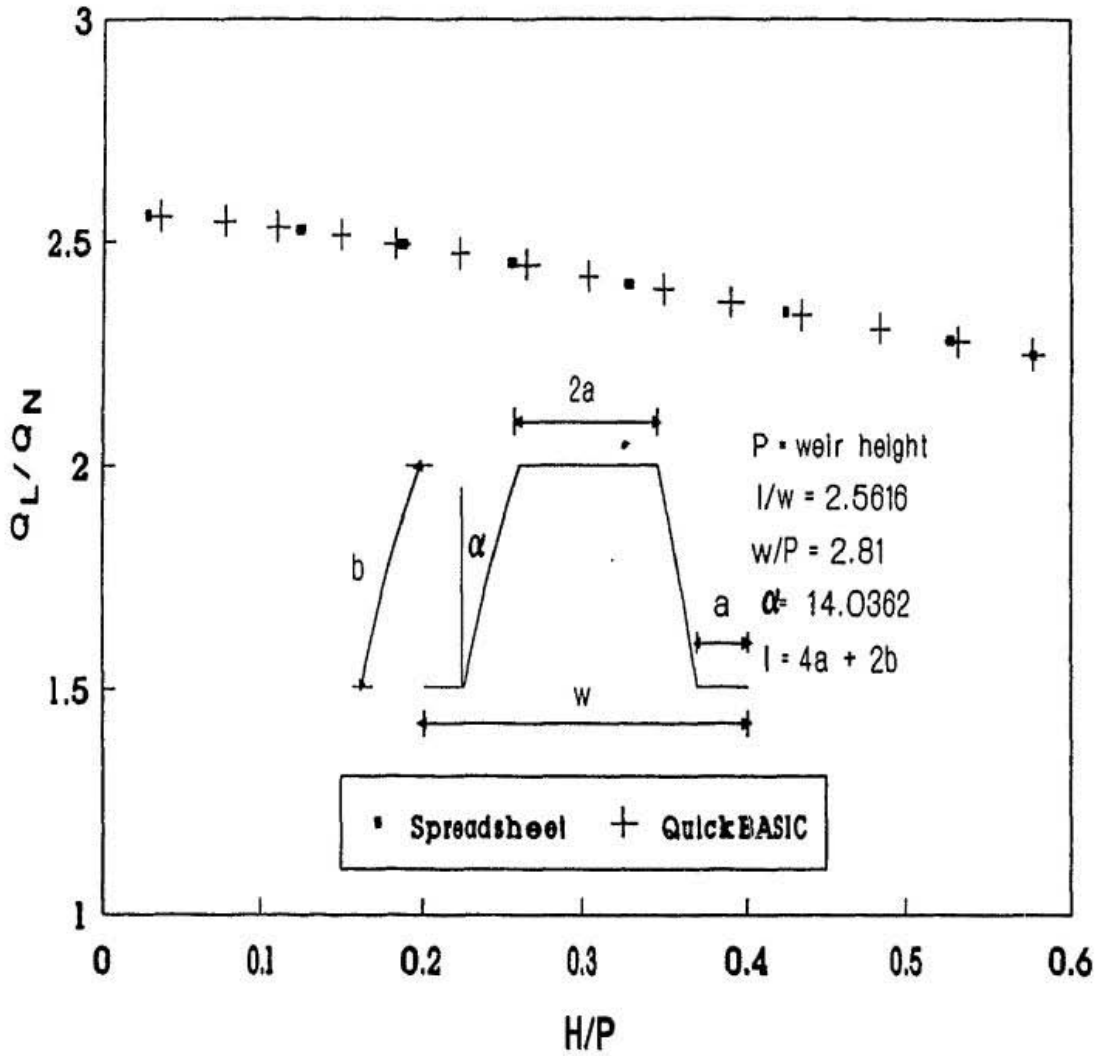

Figure 4-5 A comparison of the output obtained from spreadsheet and QuickBASIC.

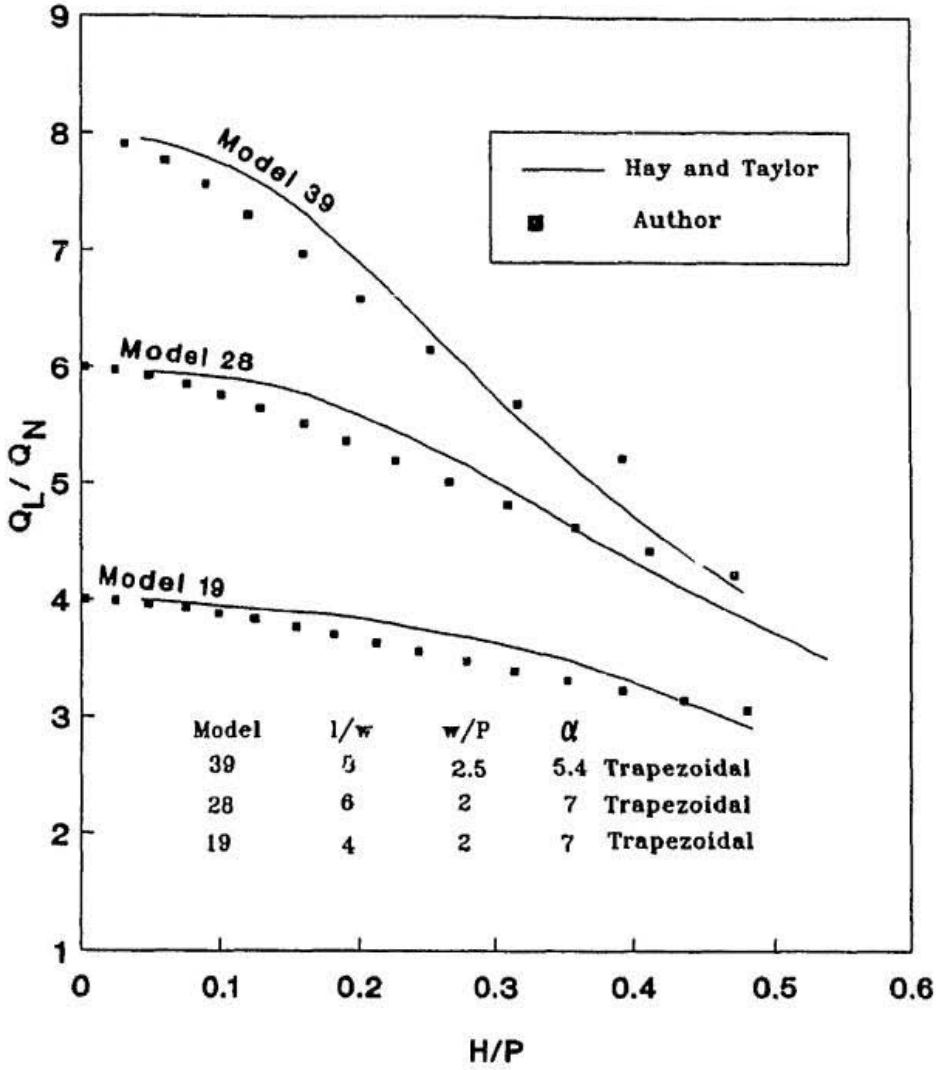

Figure 4-6 Comparison between Hay and Taylor theoretical results and author theoretical results for 3 trapezoidal planform labyrinth weirs with downstream interference (zero change in bed elevation). (modified from Hay and Taylor, 1969).

Chapter 5

Experimental Procedures

5.1. Weir models

The trapezoidal geometry (Figure 3-16) which was proposed by IIHE, Bandung-Indonesia, would be retested in this present experiment. Experiments were required to confirm previous experimental data obtained in hydraulic model studies of this weir. Based on the dimensions of the testing flume facility at the Hydraulics Laboratory, Memorial University of Newfoundland, the size of the trapezoidal geometry was designed. The resulting two-cycle trapezoidal plan form labyrinth weir had dimensions : w = 281 mm, l = 720 mm, a = 35 mm, α = 14.04°, and P = 100 mm as indicated in Figure 5-1 and noted as model no.1.

Based on the dimensions of this trapezoidal geometry, a rectangular geometry with a semi-circular connection between the two-cycles was developed by the author as an alternative geometry. It was thought that this might give a better performance than the trapezoidal plan form because the rectangular geometry with a semi-circular connection

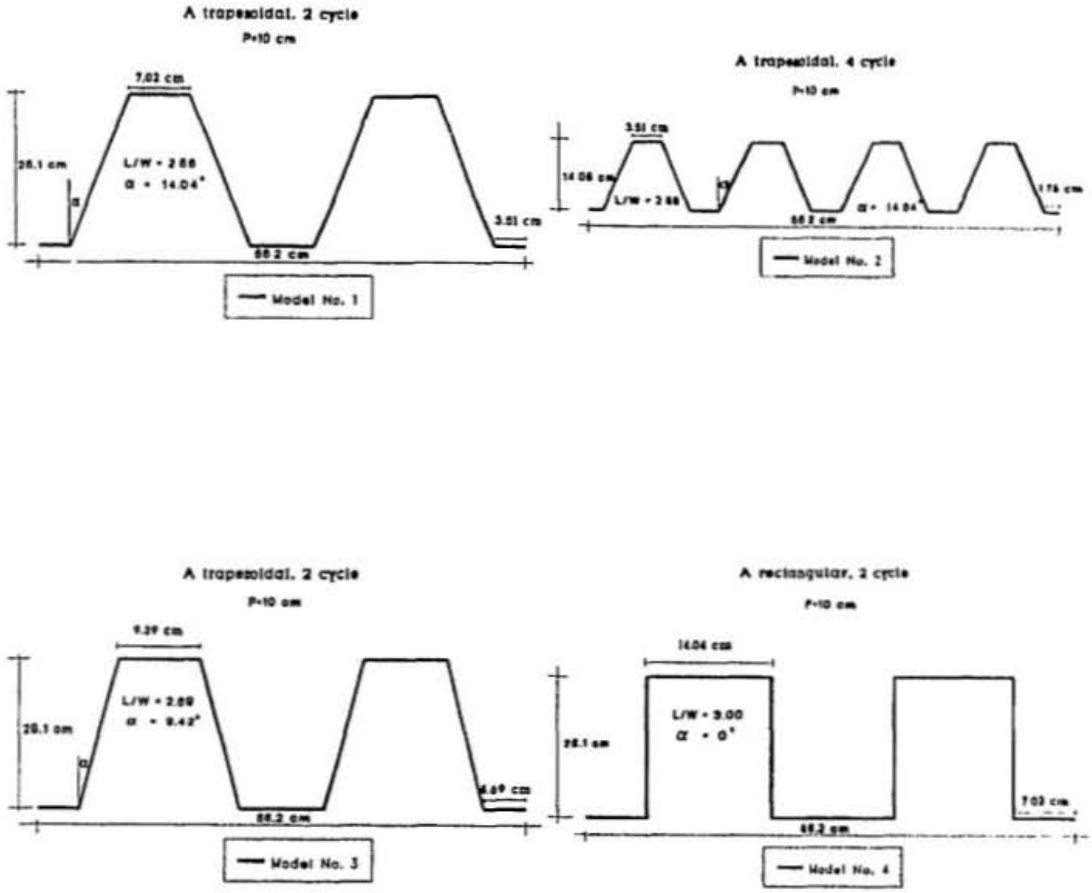

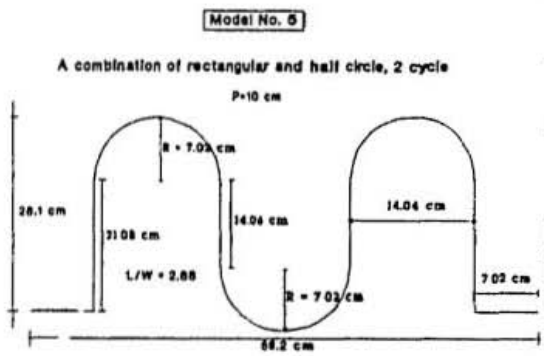

Legend :

- L/W = length magnification
- α = side wall angle
- P = crest height

Figure 5-1 Schematic of the sharp crested labyrinth weir plan forms tested in the flume. (Flow direction from bottom to top).

provides a longer crest than the trapezoidal shape. Thus it might give a larger flow than the trapezoidal shape at the same operating depth. The rectangular geometry with a semi-circular connection was designed with : w = 281 mm, l = 752 mm, a = 70 mm, R = 70 mm, α = 0°, and P = 100 mm as shown in Figure 5-1 and noted as model no.5. It was also considered necessary to retest the rectangular geometry in order to compare the performance of a rectangular geometry with that of a rectangular geometry with a semi-circular connection. This two-cycle rectangular geometry was designed with : w = 281 mm, l = 843 mm, a = 70 mm, α = 0°, and P = 100 mm as displayed in Figure 5-1 and noted as model no.4.

To avoid the possibility of scale errors a trapezoidal geometry similar to model no.1 was developed but with four-cycles. The shape was exactly the same as that of model no.1 but the size were reduced by a factor of 2.0. This is shown in Figure 5-1 and noted as model no.2.

A decrease in the side wall angle, α for a trapezoidal geometry also was examined by developing another trapezoidal shape with two-cycles. The dimensions were, w = 281 mm, l = 757 mm, a = 47 mm, α = 9.42°, and P = 100 mm as illustrated in Figure 5-1 and noted as model no.3. This model would confirm whether a decrease in the side wall angle, α for a trapezoidal geometry would also significantly reduce the flow capacity at the same operating depth conditions.

As discussed in section 4.2 the results of the model test would be presented in terms of flow magnification (Q_L/Q_N) against flow depth to weir height ratio (H/P) for a constant value of the length magnification (L/W) and vertical aspect ratio (W/P).

Therefore, to produce the correlation between them, the experiment should be conducted with a variation in the value of l, w, and P. Variation in l was obtained by developing models no.3, 4, and 5. A variation in w also was noted by developing model no.2. Variation in P was considered by developing model no.1a (see Figure 5-2). The dimensions were similar to model no. 1 except that the crest height, P was reduced to 50 mm.

It was decided to use 2 mm thick aluminum to construct the labyrinth weir models in this experimental study. This was chosen because aluminum is easy to fabricate and there is no warping problem. Also, since the thickness of the aluminum is 2 mm, it is not necessary to chamfer the downstream edges of the crest. Such material has already been considered as a sharp crested weir (Kraatz, 1975).

After initial tests (model no. 1) were run, it was observed that the value of Q_L/Q_N exceeded the value of L/W. This was peculiar, because the maximum Q_L/Q_N value of a labyrinth weir should be equal to the value of L/W (see section 3.2). It was thought that this might due to under estimation of the discharge coefficient using the Rehbock equation in calculating the total flow of a straight weir, Q_N, from the standard weir equation. This could have resulted in a lower value of Q_N than was expected and therefore a higher value of Q_L/Q_N than was expected. Consequently, it was necessary to evaluate the use of the Rehbock equation to predict the discharge coefficient in calculating Q_N. A straight weir (model no.6, Figure 5-2) then was established with crest length, L = 562 mm and P = 100 mm.

Further developments of weir shape were done again during the experimental

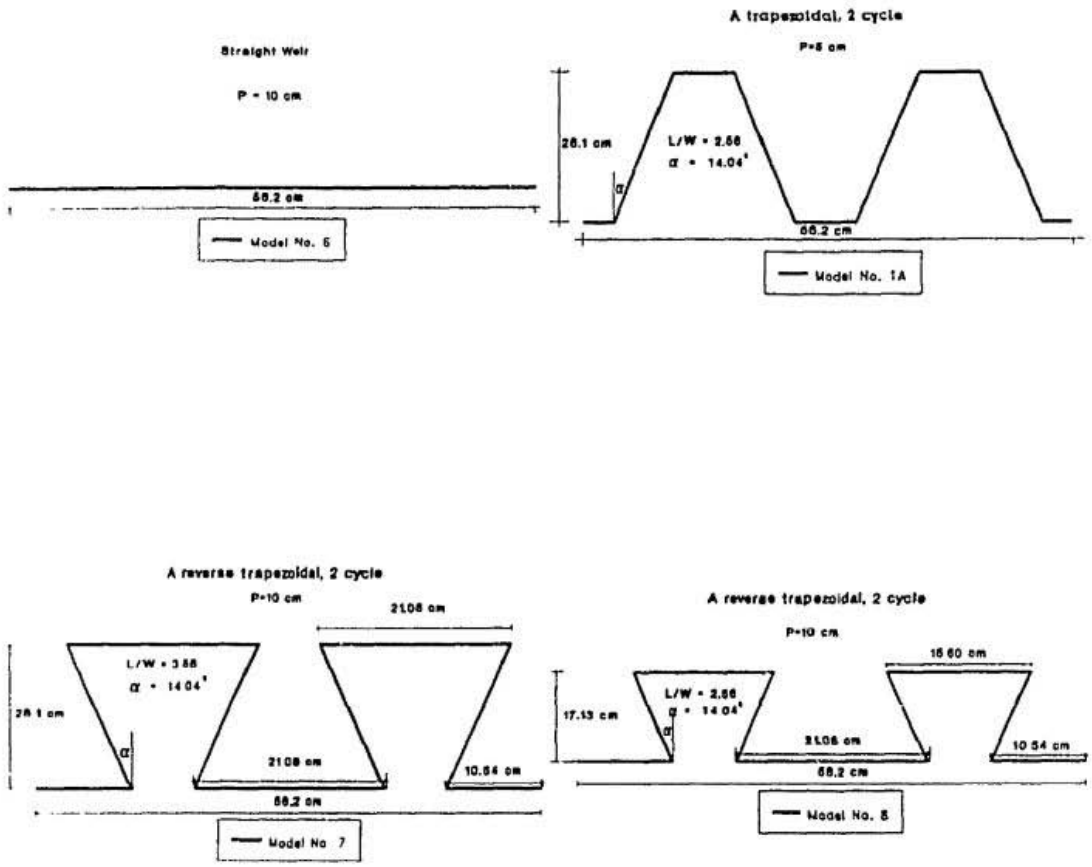

Legend :

- L/W = length magnification

- α = side wall angle

- P = crest height

Figure 5-2 Schematic of the sharp crested weir geometries tested in the flume. (Flow direction from bottom to top).

work because of some initial findings. When a rectangular geometry (model no.4) was investigated at high flows, a small undular jump was found to occur over the crest. This was thought to be due to blocking of the downstream flow due to insufficient cross sectional area in the downstream flow passages. Thus, a reverse trapezoidal shape (model no.7, Figure 5-2) which increased the blocking by further restricting the downstream width was used to study this phenomenon. After model no.7 was run, it was shown that the jump did indeed occur due to blocking of the downstream flow. Then, efforts were made to increase the area of the downstream receiving channel by developing another reverse trapezoidal shape (model no.8, Figure 5-2) and examining whether it would decrease the size of the jump or perhaps eliminate the jump altogether.

From past experience in the field, sharp crests are sensitive to large quantities of debris. Sometime this could damage the sharp crest and as a result, reduce the effectiveness of the weir to pass the flow. For this reason, it was thought necessary to study the effect of varying the crest thickness. Among the four models of labyrinth weirs (model no.1, 3, 4, and 5), model no.1 proved to be the model which gave the largest flowrate per unit of crest length. Therefore, model no.1 was retested with different values of the crest thickness. These are shown as models no. 1B, 1C, 1D, and 1E in Figure 5-3. A photograph of all weirs model is given in Figure 5-4.

5.2. Range of flows required

Based on the dimensions of the labyrinth weir models, the range of flows required could be determined by specifying the range of depths, H, which would be tested in this

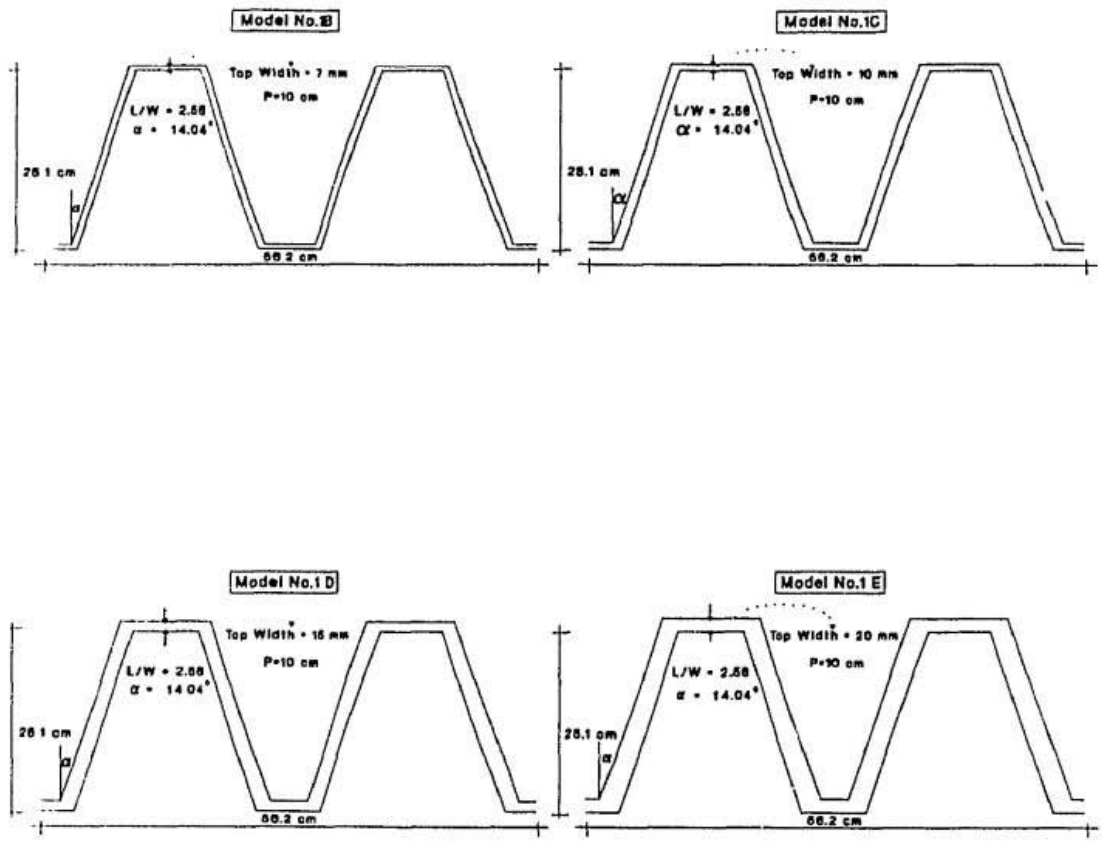

Legend :

- L/W = length magnification
- α = side wall angle
- P = crest height

Figure 5-3 Schematic of the trapezoidal labyrinth weirs with different top width tested in the flume. (Flow direction from bottom to top).

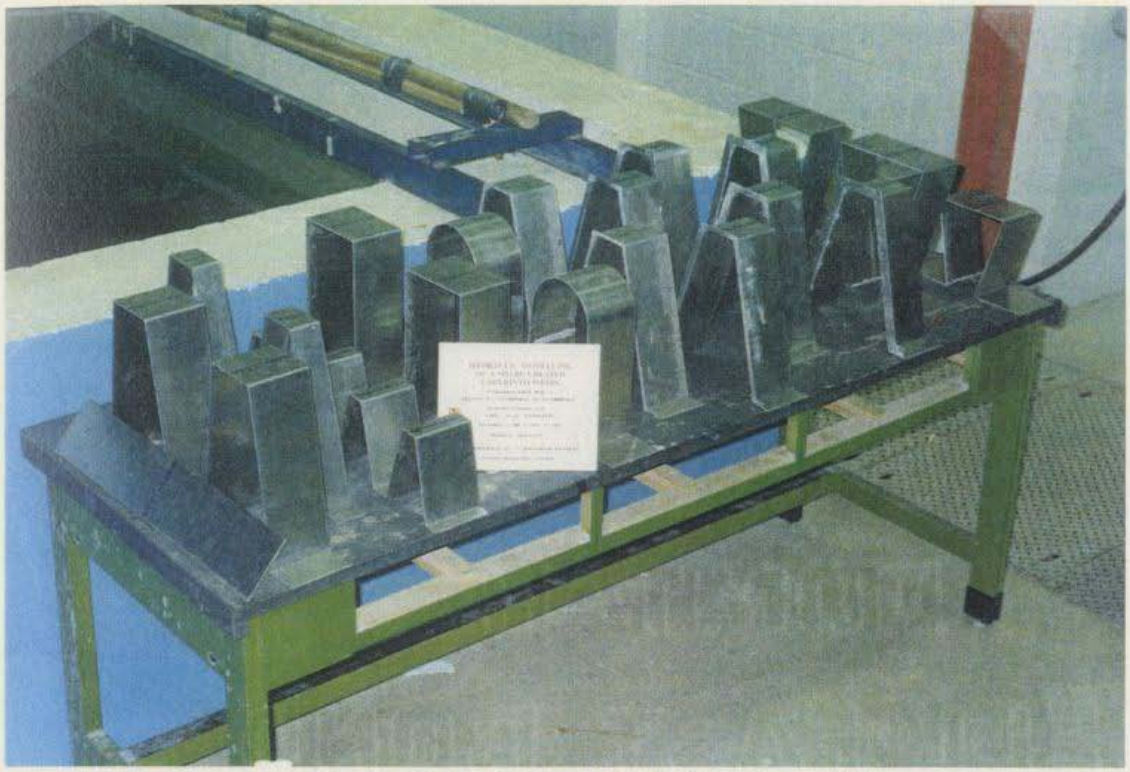

Figure 5-4 Photograph of all weir models

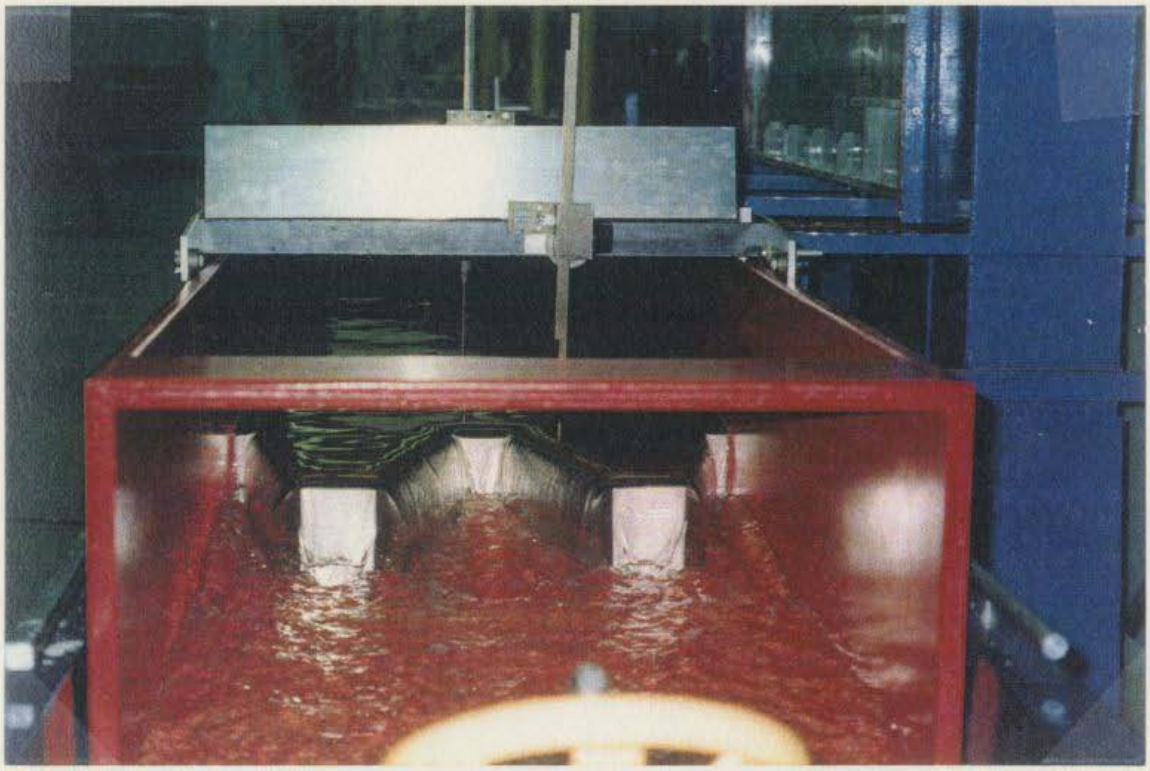

Figure 5-5 Initial test in progress

experiment. Initial tests (Figure 5-5) proved that the minimum depth which could be measured in the model was 10 mm. When a lower depth than 10 mm was run, it was found to be difficult to take the measurement since in this condition the depth fluctuated. In addition, it was also shown that the maximum depth which could be measured was 60 mm. When a higher depth than 60 mm was run, it was observed that a submerged flow occurred.

Therefore, the range of depth to weir height ratio, H/P which would be investiged in this experiment was between 0.1 and 0.6. Then the maximum depth, $H_{max.}$ which would be observed for all models was 60 mm except for model no.1a (P = 50 mm) $H_{max.}$ = 30 mm. The minimum depth, $H_{min.}$ which would be covered for all models was 10 mm. The range range of flows was estimated from the standard weir equation (equation 4.1) and is summarized in Table 5.1 below.

TABLE 5.1
Range of flows, Q required in the experiment

Model No.	Total crest length,L (cm)	$H_{min.}$ (cm)	$H_{max.}$ (cm)	Minimum flow, (l/s)	Maximum flow, Q (l/s)
1	143.96	1.0	6.0	3.03	41.84
2	143.95	1.0	6.0	3.03	41.84
3	151.49	1.0	6.0	3.19	44.03
4	168.60	1.0	6.0	3.55	49.00
5	150.51	1.0	6.0	3.17	43.74
6	56.20	1.0	6.0	1.18	16.33
7	200.16	1.0	6.0	4.21	58.17
8	143.96	1.0	6.0	3.03	41.84
1A	143.96	1.0	3.0	3.06	15.16

1B	143.96	1.0	6.0	3.03	41.84
1C	143.96	1.0	6	3.03	41.84
1D	143.96	1.0	6	3.03	41.84
1E	143.96	1.0	6	3.03	41.84

Note : Flow is estimated from standard weir equation (equation (4.1)).

5.3. Size and design of flume

The initial experimental arrangement attempted to make use of an existing facility. This facility was a recirculating sand flume and a new channel was constructed of wood to hold the model weirs. The intention was to place this new channel on top of the existing flume so as to make use of the pump, flow measurement device and recirculating pipework. The new channel was constructed to be 4.12 m long, 0.32 m deep and 0.56 m wide. Photographs are shown in Figures 5-6 and 5-7.

The initial experiments showed however that the maximum flow rate of the pump was not sufficient to cover the maximum flow rate required by this experiment. Therefore, the old wooden flume was modified and removed. A completely new flume was designed as shown in Figures 5-8 to 5-12. In this new set up, it was intended that water would be supplied to the flume from an underground tank by a constant speed centrifugal pump connected to the flume through an 203 mm diameter pipe with appropriate control valves. The exit flow from the flume was discharged into a tail flume fitted with a calibrated V-notch weir, from where it discharged into the main sump.

The flow entering the flume was led into the bottom of a vertical box with a trapezoidal cross section. Aluminum honeycomb was placed in this box to minimise

Figure 5-6 Photograph of initial testing facility (side view)

Figure 5-7 Photograph of initial testing facility (downstream view)

Figure 5-8 Photograph of the new testing facility (upstream view)

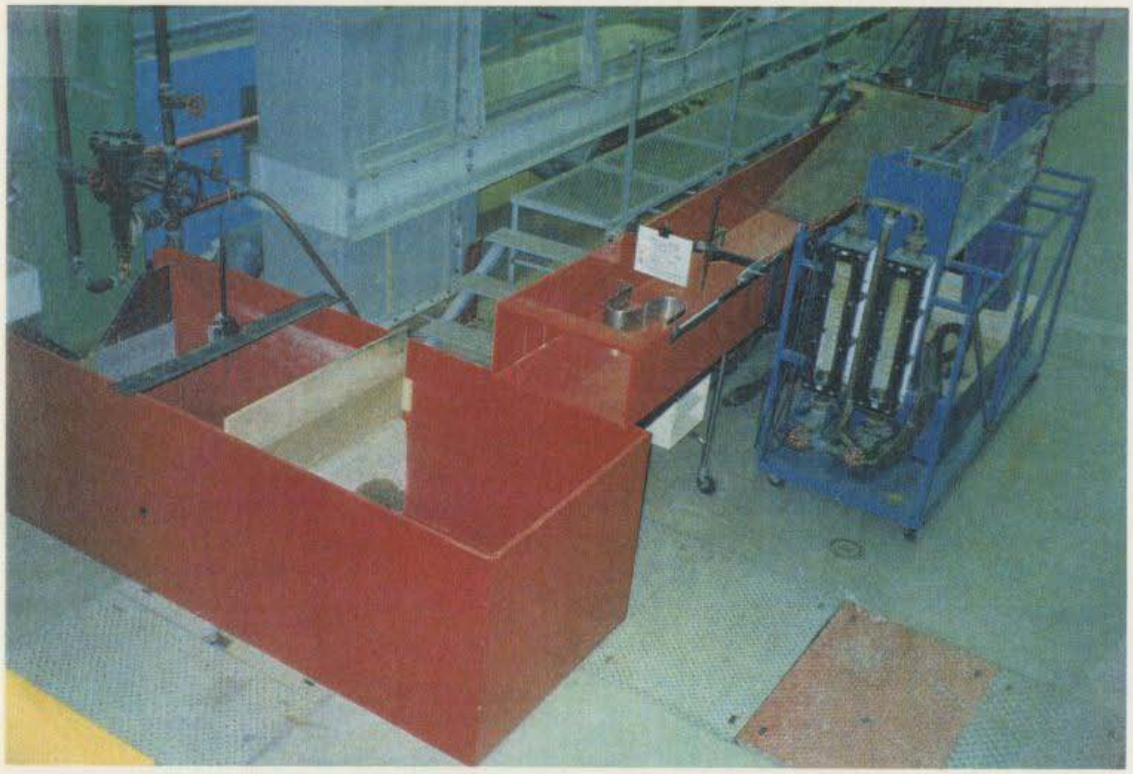

Figure 5-9 Photograph of the new testing facility (downstream view)

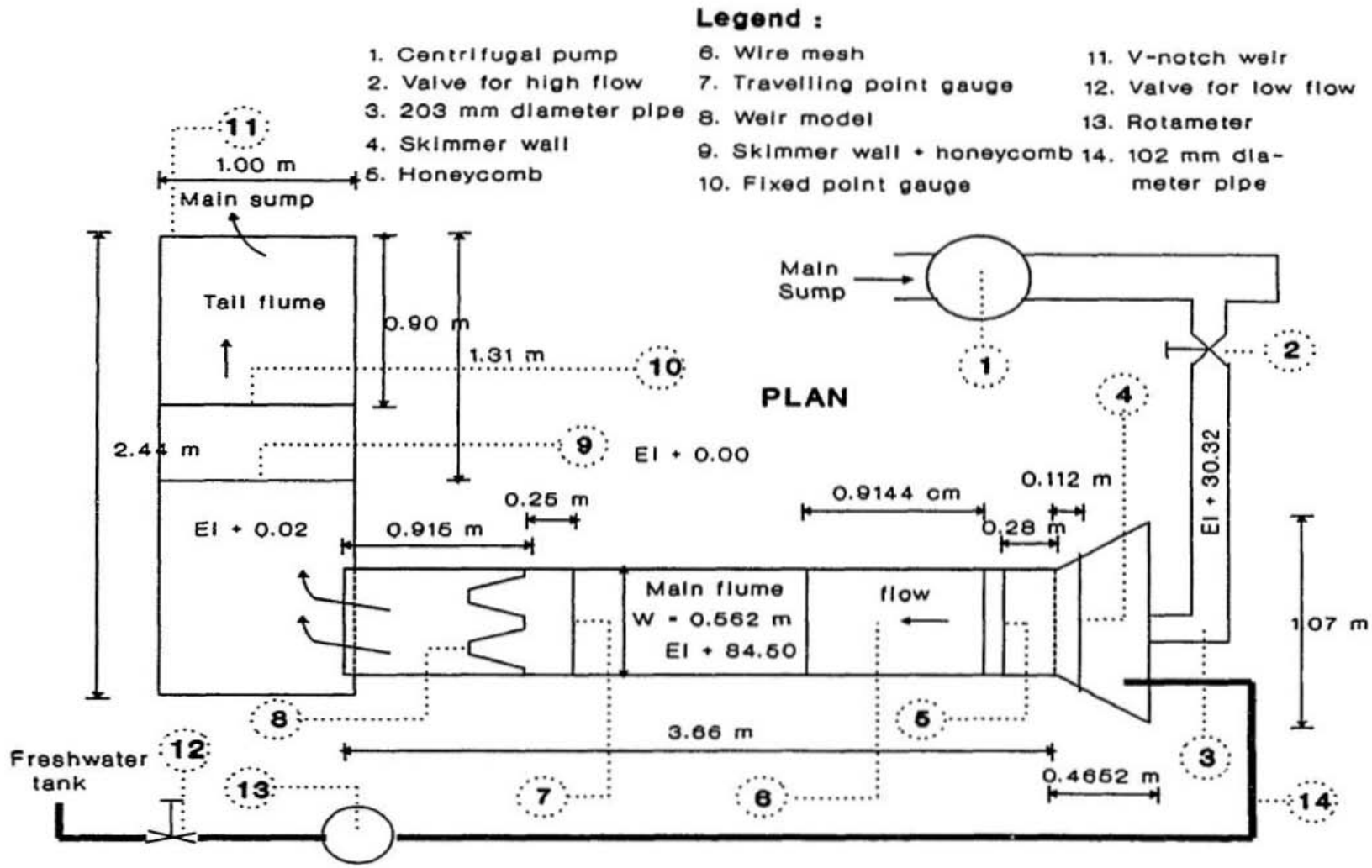

Figure 5-10 Layout experimental setup

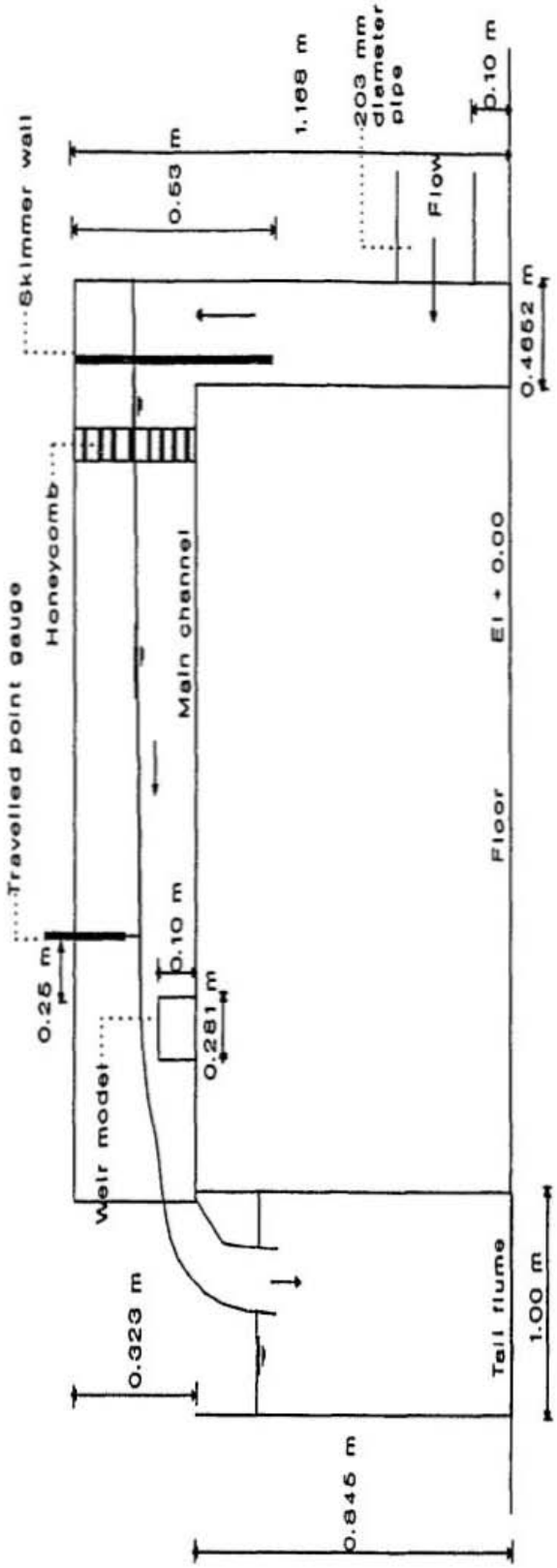

Figure 5-11 Side view of experimental setup

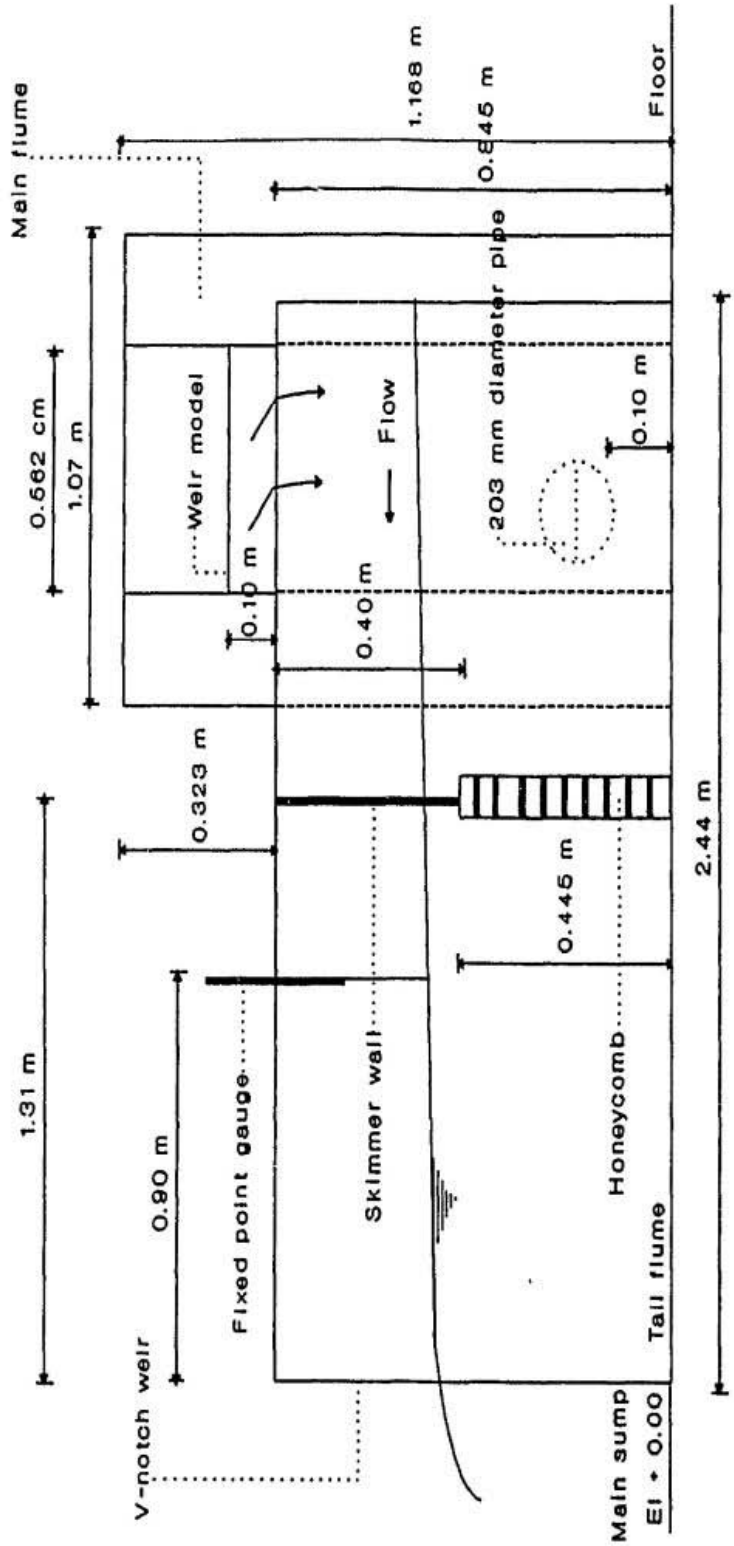

Figure 5-12 Front view of experimental setup

eddies as the water rose and to provide a smooth flow at the upstream end of the flume. This system later proved to be unsatisfactory, particularly at high flow, for it produced waves in the flume. Then, some sheets of wire mesh were placed beyond the honeycomb, and this new flow straightener resulted in a smooth ripple free surface (Figure 5-13).

The weir model was placed 915 mm from the downstream end of the main flume. To avoid leakage between the bottom and edges of the weir and the flume walls, the very small gaps between weir model and the channel bed were secured by a thin layer of duxseal along the bottom and sides (Figure 5-14). This did not affect the flow capacity of labyrinth weir.

Finally, depth measuring sections were determined (Figure 5-15), 25 cm ($\geq 4xH_{max.}$) from the weir model (Albertson *et al.*,1960; Kraatz,1975). This depth, H would then be used in equation (4.1) and would be plotted as the value of H/P. Also a survey was conducted of the channel bed to ensure that the flume had been set up with a horizontal bed.

5.4. Provision of flow

When the second run of the model test was being carried out, it was observed that the lowest flow rate of the centrifugal pump was too large to supply the minimum flow rate required by this experiment. Therefore, it was decided to use the centrifugal pump only for high flows. Under these conditions the flow rate would be adjusted by valve and the flow magnitude would be measured by the V-notch weir (Figure 5-16). Model tests showed that the range of these high flows varied from 8.20 l/s to 39.15 l/s.

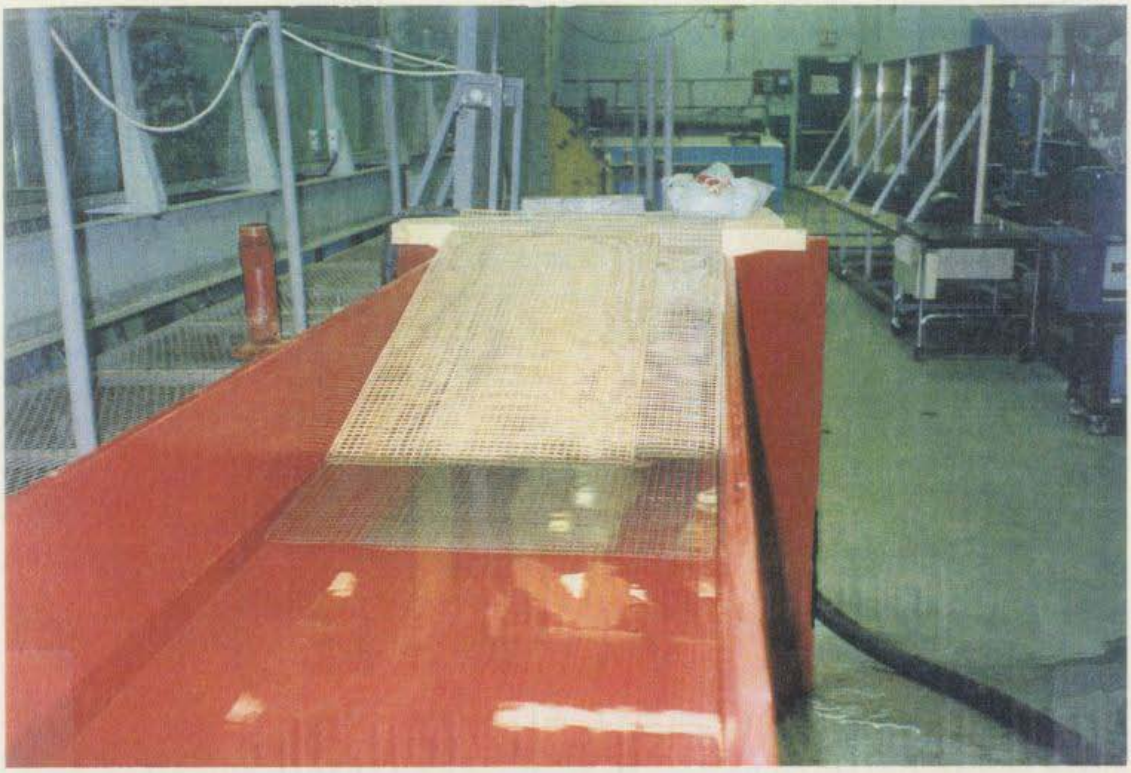

Figure 5-13 Photograph of the flow straightener system

Figure 5-14 Photograph of a thin layer of duxseal along the bottom and sides

Figure 5-15 Photograph shows the location of depth measuring section

Figure 5-16 Photograph of the V-notch weir

Following this it was decided to supply low flows using the laboratory freshwater supply. The flow rate could be adjusted by valve and the flow magnitude could be controlled by the rotameter. Flows from this rotameter were delivered to the flume through a 102 mm diameter pipe. Experiment showed that the range of the low flow was between 2.43 l/s to 8.1 l/s.

5.5. Flow measurement and depth measurement

5.5.1. Flow measurement

A sharp sided 90° V-notch weir (Figure 5-17) was designed to measure the discharge. This was chosen for ease of construction and for accuracy over the design range of flows (8.2 l/s to 39.15 l/s). The flow depths at the downstream end were measured 900 mm upstream from the weir crest by a fixed point gauge (Figure 5-18). A wooden board 20 mm thick, 400 mm high together with aluminum honeycomb approximately 100 mm thick, 445 mm high was set at 1.31 m from the downstream end to provide the necessary stilling.

5.5.2. Depth measurement

Water surface profiles over the model were measured by a movable point gauge to the nearest 0.001 ft (0.305 mm). This avoided the need for more than one point-gauge, since the measurement point varied along the length and width of the channel (Figure 5-19).

The flow depth upstream of the V-notch weir was measured by a fixed point

DETAIL OF V-NOTCH WEIR

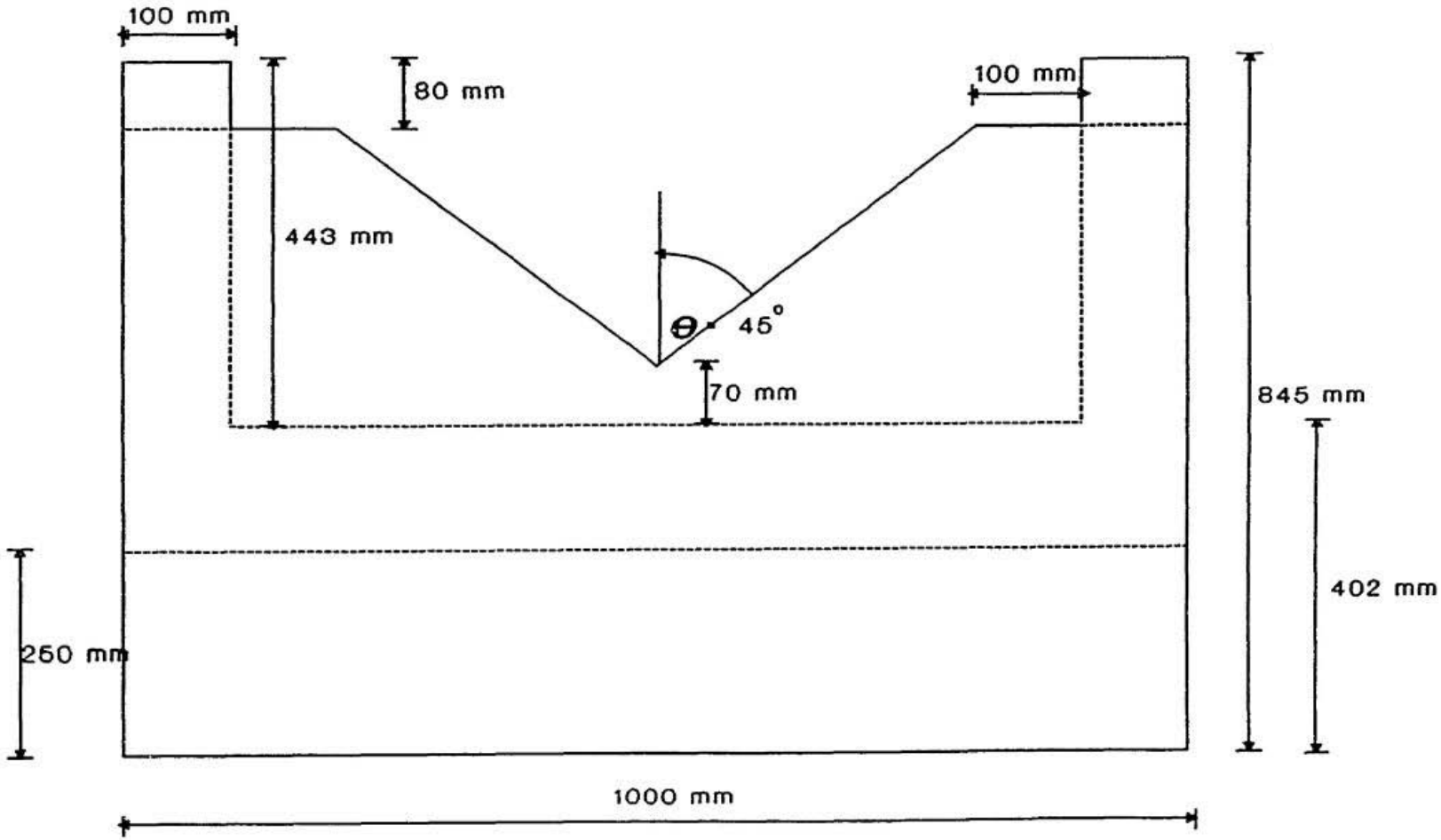

Figure 5-17 Detail of V-notch weir

Figure 5-18 Flow depth measurement at the V-notch weir in progress

Figure 5-19 Depth measurement at the weir model in progress

gauge to the nearest 0.001 ft (0.305 mm). This fixed point gauge was placed 0.9 m upstream of the weir crest.

5.6. Calibration works

Because the flow and depth measurements were the main data that would be collected in the model tests, it was very important to ensure accurate calibration of the point gauge, the rotameter, and the standard 90° V-notch weir.

5.6.1. Calibration and check on accuracy of the point-gauges

A calibration of point-gauges (see Figure 5-20) showed that 328 counts on the counter was equivalent to 100 mm. Alternatively each count measured 0.001 ft. Although a calibration of point-gauges was done, it is necessary to check the accuracy of the point-gauges. This was done by taking the flow depth measurement using the point-gauges and a vertical manometer connected to the tail flume (see Figure 5-21).

Several readings of the flow depth over the sharp sided 90° V-notch weir were taken 0.90 m upstream of the V-notch weir crest, together with readings of the vertical manometer. Comparisons showed that the maximum variation in the determination of the flow depth was 4.18 percent as displayed in Figure 5-22. Also, it can be seen that the error decreases with increasing discharge, Q.

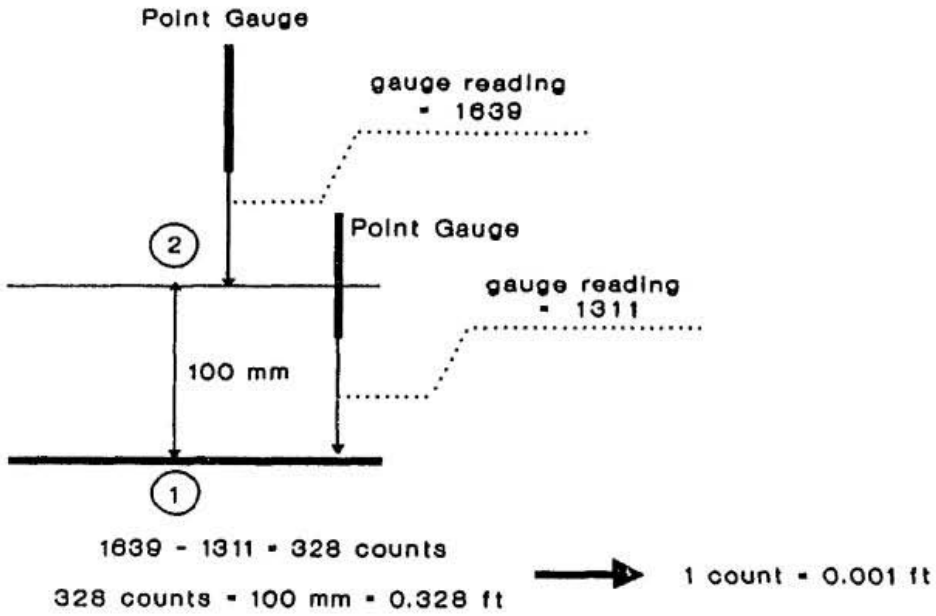

Figure 5-20 Sketch to illustrate a calibration of point gauge

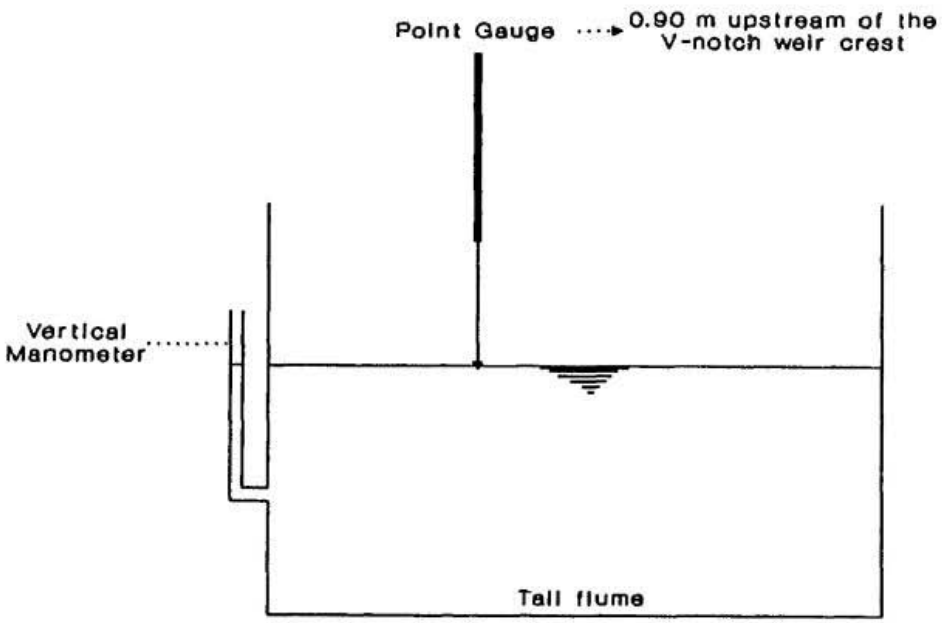

Figure 5-21 Sketch to illustrate a check an accuracy of point gauge using manometer

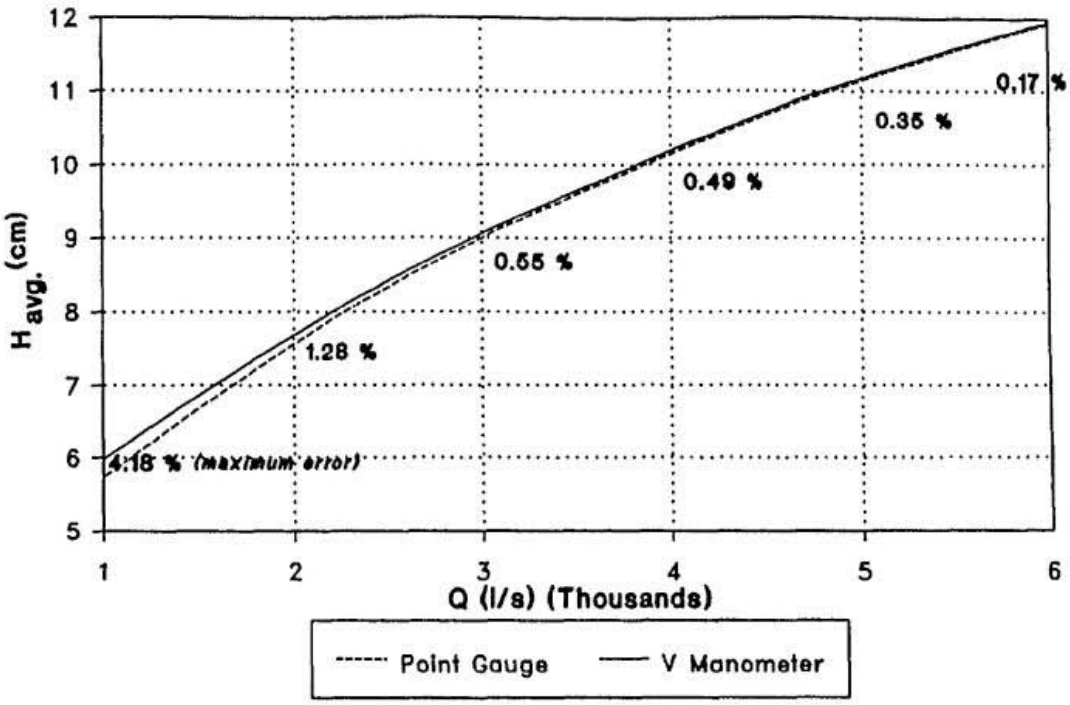

Figure 5-22 The discharge-depth (Q-H) relationship at the v-notch weir measured by point gauge and vertical manometer.

5.6.2. Calibration of rotameter

A number of flow rates were run and measured using the rotameter. These were compared with a volumetric measurement. This is a simple way to check the accuracy of the rotameter by discharging a measured volume of water within a particular time. This was done by discharging water into a tank of known cross sectional area and measuring the increase in depth over a measured time.

The test result is shown in Figure 5-23. It was observed that the maximum error of the rotameter was only 1.56 percent. A photograph to show the calibration of rotameter is given in Figure 5-24.

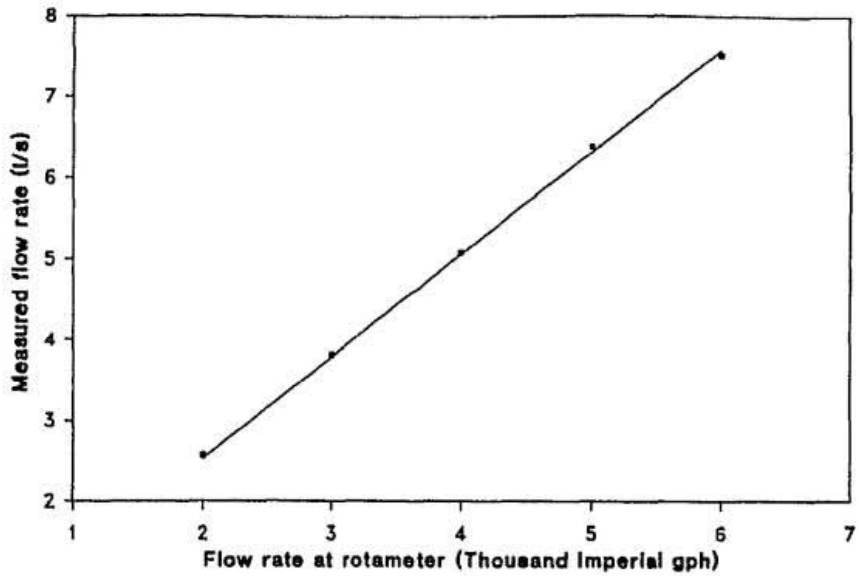

Figure 5-23 The calibration test result of rotameter

5.6.3. Calibration of the V-notch weir

A total of six flows were run to calibrate the V-notch weir using the rotameter (Figure 5-25). Four readings for each flow were taken using the fixed point gauge to measure the flow depth over the V-notch weir. Flowrates were measured using the rotameter. The results are presented in Figure 5-26 which shows the plot of flowrate, measured by rotameter, against head over the V-notch weir. This correlation gives the relationship for the V-notch weir as :

$$Q = 15.21\ H^{2.5} \tag{5.1}$$

where Q is discharge in l/s; and H is the depth over the crest in cm.

Equation (5.1) may be rewritten as :

Figure 5-24 Calibration of the rotameter in progress

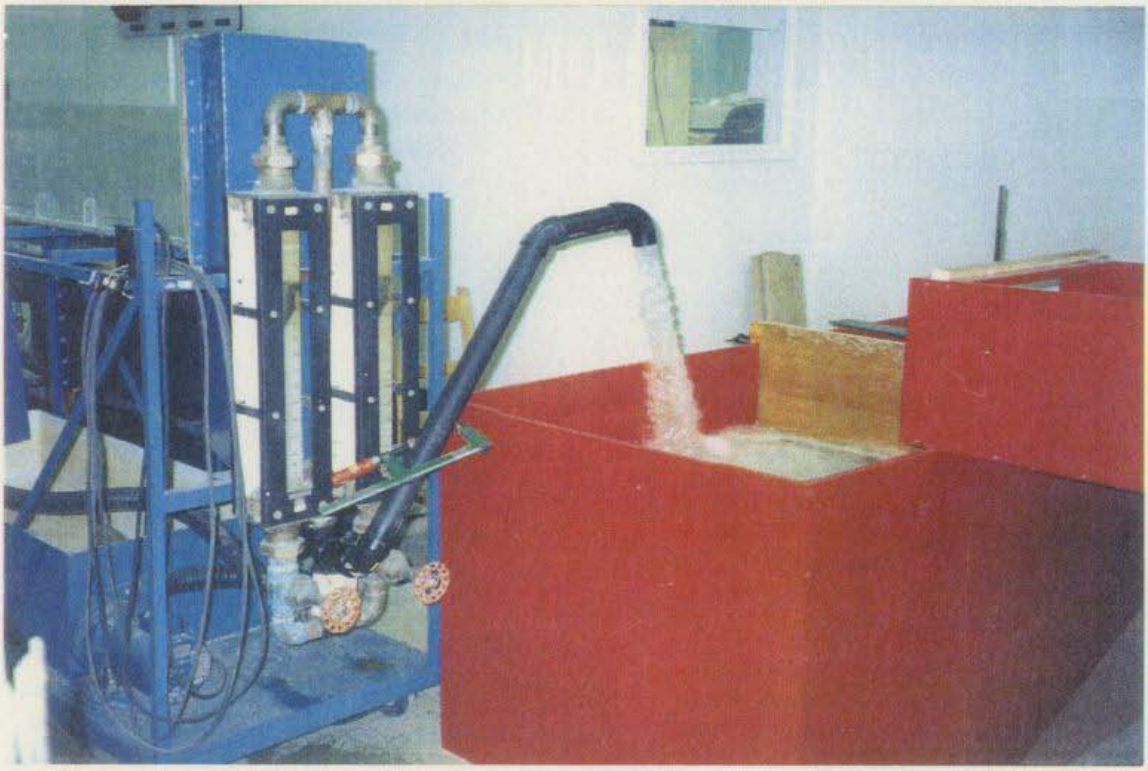

Figure 5-25 Calibration of the V-notch weir in progress

$$Q = \frac{8}{15}\sqrt{2g}\, C_d \tan\theta\, H^{2.5} \qquad (5.2)$$

where C_d is a discharge coefficient = 0.64 and θ is the angle of each side of the V-notch to the vertical = 45°. Usually C_d = 0.58-0.61 (Novak,1990)

Although equations 5.1 and 5.2 were obtained under the low flowrate condition, it was considered that they can be used also for the high flow condition, because of the known accuracy of V-notch weirs. Operational problems did not permit direct calibration of the higher flows.

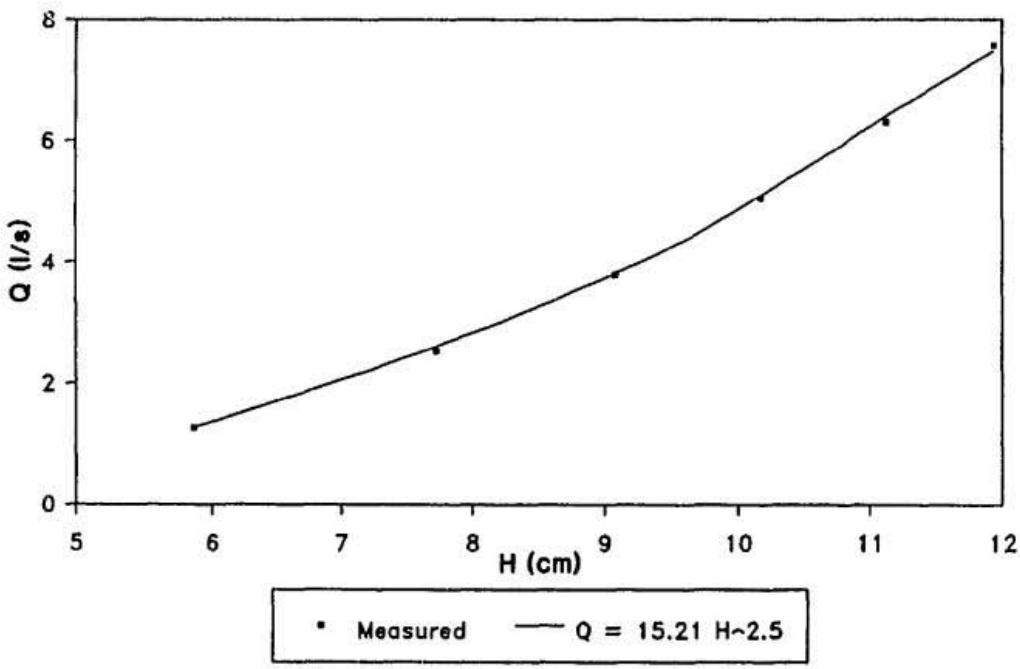

Figure 5-26 The discharge-depth (Q-H) relationship at the v-notch weir, a comparison of measured and predicted by $Q = 15.21\ H^{1.5}$.

5.7. Experiments

The general procedures used are described in this section which also includes some details of the model tests.

5.7.1. A typical experiment

Methods of collecting the experimental data will be discussed in two sections according to the magnitude of the flow (see section 5.4).

(1) Low flows

First, the valve at the freshwater supply was opened. Then, the flowrate Q_r at rotameter was set. The valve was adjusted until the flowrate at the rotameter was stable at the desired flowrate, Q_T. It was then necessary to wait until the water surface on the flume was stable. Usually, ten minutes was enough to get this condition. Then, the depths were measured using the point gauge 250 mm upstream from the weir model (discussed previously in section 5.3 and see Figure 5-27). Three depths were measured across the channel. The mean depth, H, was taken as the average value of these depth measurements. One value of Q_T and one value of H were obtained from each test.

(2) High flows

First, the valve downstream of the centrifugal pump was opened. Then, the depth over the weir crest was set. This was done by adjusting the valve until the depth over the crest was established at the desired flow depth. As before it was then necessary to wait about ten minutes until the water surface on the flume and tail flume were stable. Then, the flow depths were measured using the point gauge 250 mm upstream from the weir

model (discussed previously in section 5.3 and see Figure 5-27). Last, the flow depth was measured 900 mm upstream of the V-notch weir in order to obtain the flowrate, Q_T, which was calculated using equation 5.1. As before one value of Q_T and one value of H were obtained from each test.

The water surface profiles for low and high flows were obtained from depth measurements along the lines 1 and 2 shown in Figure 5-28. Typically, ten depth measurements were made along the line at 50 mm intervals. This was varied as necessary to give sufficient detail. Measured data are given in Appendix D.

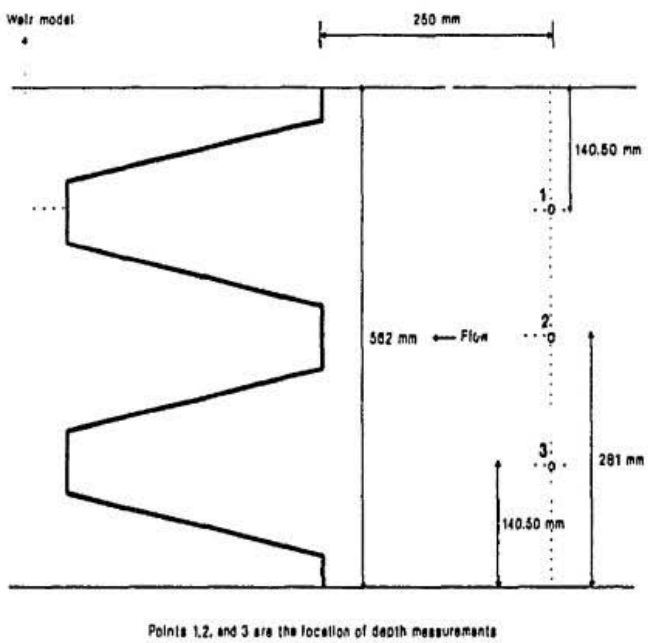

Figure 5-27 Measurement sections of depth, H

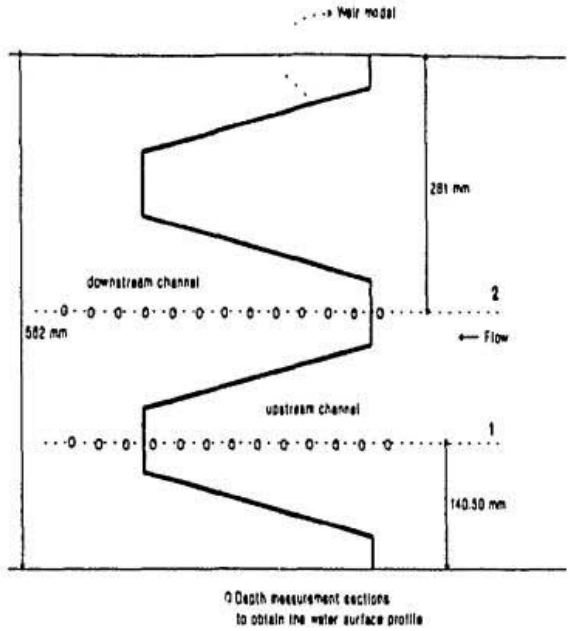

Figure 5-28 Measurement sections to obtain the water surface profile

5.7.2. Model test data

The number of flow runs and the flow ranges for each of the weir models is summarized in Table 5.2. As shown in Table 5.2 the maximum flow in these experiments was 39.15 l/s and the minimum flow was 2.43 l/s. Details of the flow and depth for each weir model are given in Appendix D which also summarises the calculations. A total of 205 experiments were run using the 8 basic models and the 5 modifications of model no.1.

TABLE 5.2
Range of flows for each weir model in the experiment

Model No. (1)	Number of tests (2)	Flow range (litre/second) (3)
1	21	3.53 - 37.92
2	15	3.86 - 29.31
3	11	4.73 - 35.27
4	24	4.24 - 37.00
5	24	3.37 - 36.87
6	15	2.43 - 17.66
7	14	5.07 - 23.80
8	14	4.73 - 24.19
1a	12	2.90 - 13.52
1b	13	4.84 - 38.00
1c	14	4.95 - 39.15
1d	14	4.92 - 38.89
1e	14	4.92 - 35.76

5.7.3. The range of the Froude and Reynolds number in the model test

Since the flow in open channels results under the action of gravitational forces which influence the resistance it is useful to check the values of the Froude, F, and Reynolds number, R_e (Sharp, 1981). However, it is not necessary to check the Froude and Reynolds number for each flow rate in all experiments. Rather it is possible to use minimum and maximum flow rates in order to obtain a range of values for F and R_e. In the experiments reported here the maximum flow was 39.15 l/s at a total flow depth

equal to 158 mm. The minimum flow was 2.43 l/s at a total flow depth equal to 115 mm. The Froude number, F is expressed by :

$$F = \frac{V}{\sqrt{g\,H}} \qquad (5.3)$$

in which F is the Froude number; V is velocity; g is gravitational acceleration; and H is the flow depth. Using equation (5.3) the maximum Froude number is 0.35 while the minimum Froude number is 0.035.

The Reynolds number, R_e can be estimated from :

$$R_e = \frac{V\ H}{\nu} \qquad (5.4)$$

where R_e is Reynolds number; V is velocity; H is the flow depth; and ν is kinematic viscosity assumed to be 10^{-6} m^2s^{-1}. Using equation (5.4) the maximum value of R_e was 6966 and the minimum value was 433. Thus it can be concluded that the model flows were rough turbulent since rough turbulent flow occurs when $R_e > 400$ to 800 (de Vries, 1971 quoted in Sharp, 1981).

Chapter 6

Results and Discussion

The results of the tests on each model will be given separately. A discussion to compare these results will also be provided in this chapter. As discussed in the previous chapter (4.2) the experimental results were plotted in terms of flow magnification, Q_L/Q_N and flow depth to weir height ratio, H/P. This will represent the performance of each labyrinth weir model. The results of the investigation however will also be plotted in terms of a relationship between the discharge coefficient, C_d and the flow depth to weir height ratio, H/P. This is to confirm the assumption made in the theoretical solution that the discharge coefficient could be predicted by the Rehbock equation (see section 4.1).

6.1. The linear weir (model no.6)

After fifteen flow runs (see Appendix D for experimental data in Table D.6) the results of the test were plotted in terms of discharge coefficient, C_d against depth to crest height ratio, H/P as shown in Figure 6-1. Three theoretical formulas to predict the C_d

values were compared to experimental values of C_d. These include :

(1) The Rehbock equation (modified from Daugherty and Ingersoll, 1954; and quoted in Vennard and Street, 1975; and Daugherty and Franzini, 1977).

$$C_d = 0.605 + 0.08\,\frac{H}{P} + \frac{1}{10.007\,H} \qquad (6.1)$$

in which H is in cm.

(2) The Rouse equation (quoted in Daily and Harleman, 1973).

$$C_d = 0.61 + 0.08\,\frac{H}{P} \qquad (6.2)$$

(3) The Kindsvater and Carter formula (modified from Albertson *et al.*, 1960).

$$C_d = 0.6019 + 0.0748\,\frac{H}{P} \qquad (6.3)$$

As shown in Figure 6-1, among those equations, the Rehbock formula showed the best agreement with the author's C_d experimental values, although the experimental discharge coefficients were slightly higher than theoretical values predicted by the Rehbock formula. This difference however was observed to be not more than 10% on average (see Table D.6). Thus the experimental values were considered to be still predicted reasonably well using the Rehbock equation. This confirms the previous assumption made in section 4.1. and this equation (6.1) was used to predict the value of C_d for a linear weir. This value of C_d was also required to estimate the theoretical flowrate over the straight weir (Q_N) using equation (4.1).

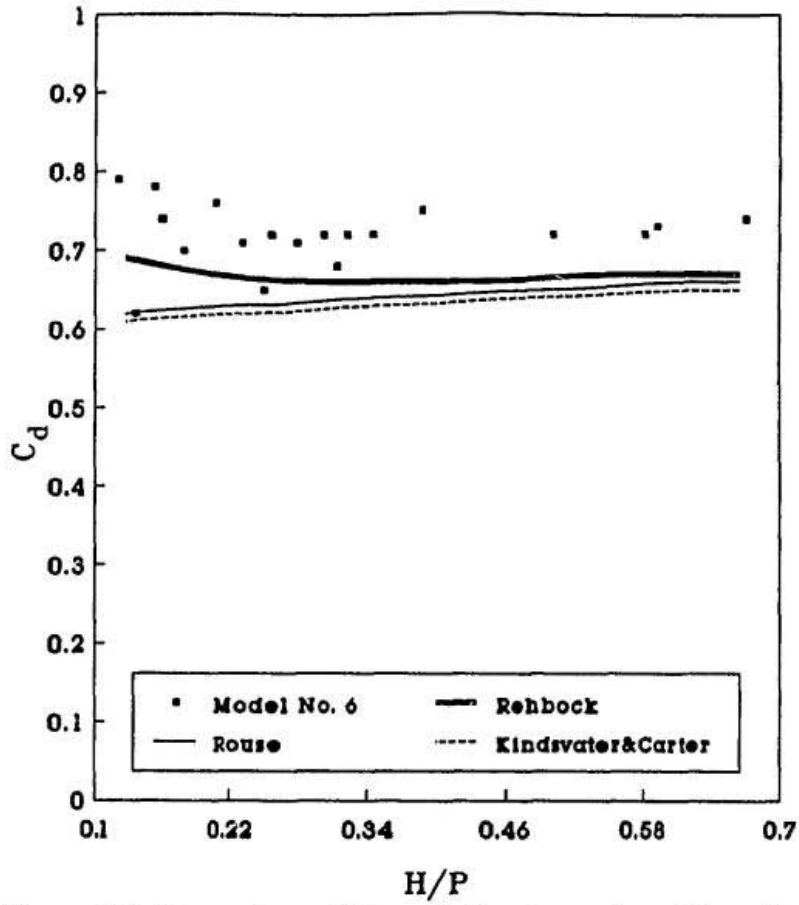

Figure 6-1 Comparison of theoretical and experimental results of discharge coefficient, C_d vs H/P of the straight weir (model no.6).

6.2. The trapezoidal labyrinth weirs (model no.1, 1a, 2, and 3)

6.2.1. Coefficient of discharge

The results of all the trapezoidal labyrinth weir model tests were plotted in terms of discharge coefficient, C_d against depth to crest height ratio, H/P as shown in Figures 6-2 (model no.1-data in Table D.1, model no.1a-data in Table D.9, model no.2-data in Table D.2, and model no.3-data in Table D.3). It can be seen that C_d results are scattered but still may be predicted reasonably well using the Rehbock equation.

However, when the value of H/P > 0.4 the experimental values of C_d decreased and could not be predicted by Rehbock formula. This was as expected. At higher values of H/P there is more interference in the flows leaving each cycle and as a result the discharge coefficient decreases.

The good agreement between theory and experiment for discharge coefficient values at H/P < 0.4 suggests that, provided L/W is also less than about 2.7, the discharge can be predicted by equation 4.1, the standard weir equation. At values of L/W > 2.7 and H/P > 0.4 the QuickBASIC program would give a more accurate solution.

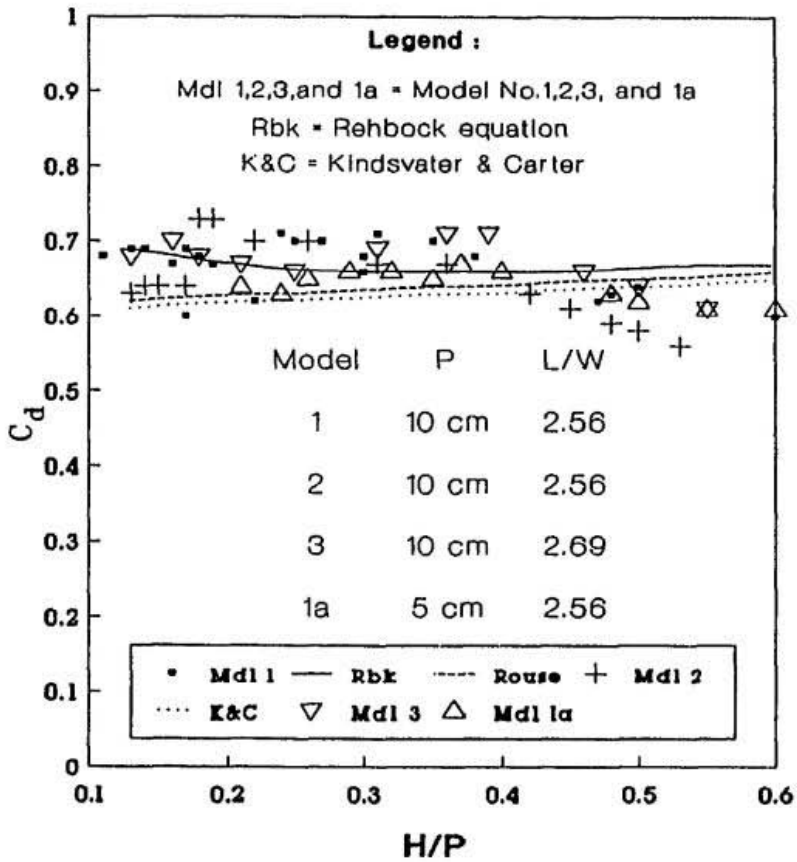

Figure 6-2 Comparison of theoretical and experimental results of discharge coefficient, C_d vs H/P of models no. 1, 2, and 3 (Figure 5-1) and model no.1a (Figure 5-2)

6.2.2. Scale errors

Scale effects were checked by comparing the values of flow magnification between model no.1 (data in Table D.1) and model no.2 (data in Table D.2). These weirs were geometrically identical (see Figure 5-1) but model no.2 was half the size of model no.1. As illustrated in Figure 6-3, scale effects or errors were insignificant and both models gave the same results. This suggested that the models were large enough to be used for prediction purposes.

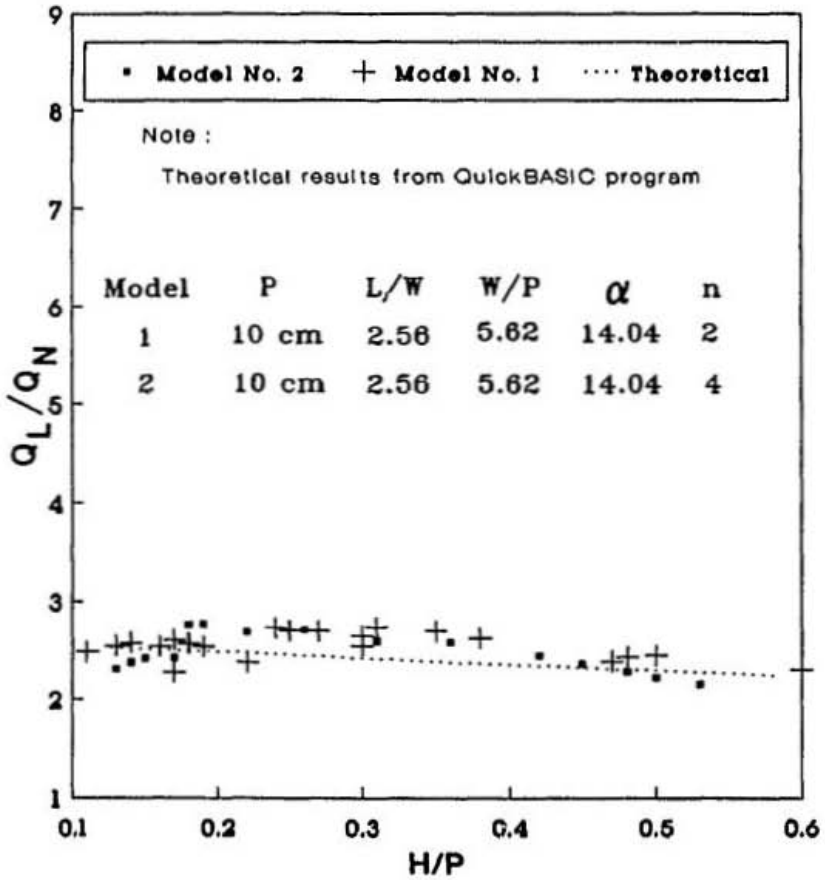

Figure 6-3 Comparison of flow magnification between model no.1 and model no.2 which have different sizes

6.2.3. Effect of changing the side wall angle (α)

The effect of changing the side wall angle (α) was observed by comparing the values of flow magnification of model no.1 (data in Table D.1) and model no.3 (data in Table D.3). Model no.1 had a side wall angle of 14.04° while the side wall angle in model no.2 was 9.42° (see Figure 5-1). As indicated in Figure 6-4, this change did not affect the flow magnification magnitudes significantly. Note however that there is a slight theoretical difference. This difference was smaller than the experimental scatter.

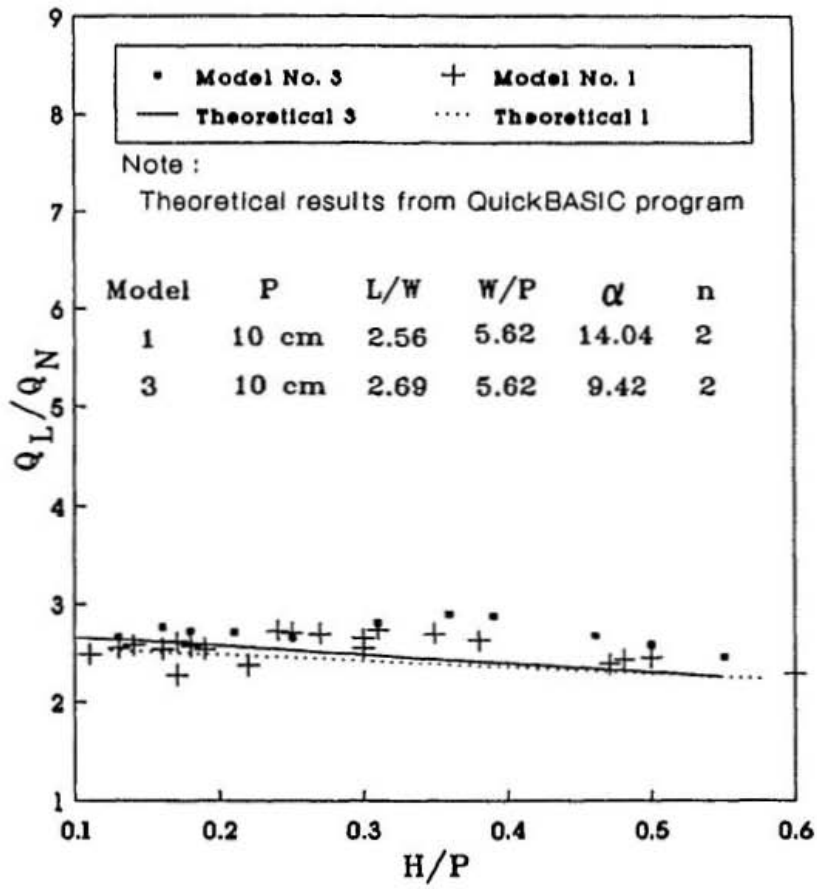

Figure 6-4 Comparison of flow magnification between model no.1 and model no.3 with different value of the side wall angle (α) and the length magnification (L/W).

6.2.4. Effect of varying the crest height (P)

Models no.1 (data in Table D.1) and no.1a (data in Table D.9) were identical geometrically except that the crest height of model no.1a (50 mm) was half that (100 mm) of model no.1 (see Figures 5-1 and 5-2). These models were used to investigate the effect of varying the crest height. As can be seen in Figure 6-5, it was obvious that the change of this parameter was not significant and there was no change in labyrinth weir performance either theoretically or experimentally.

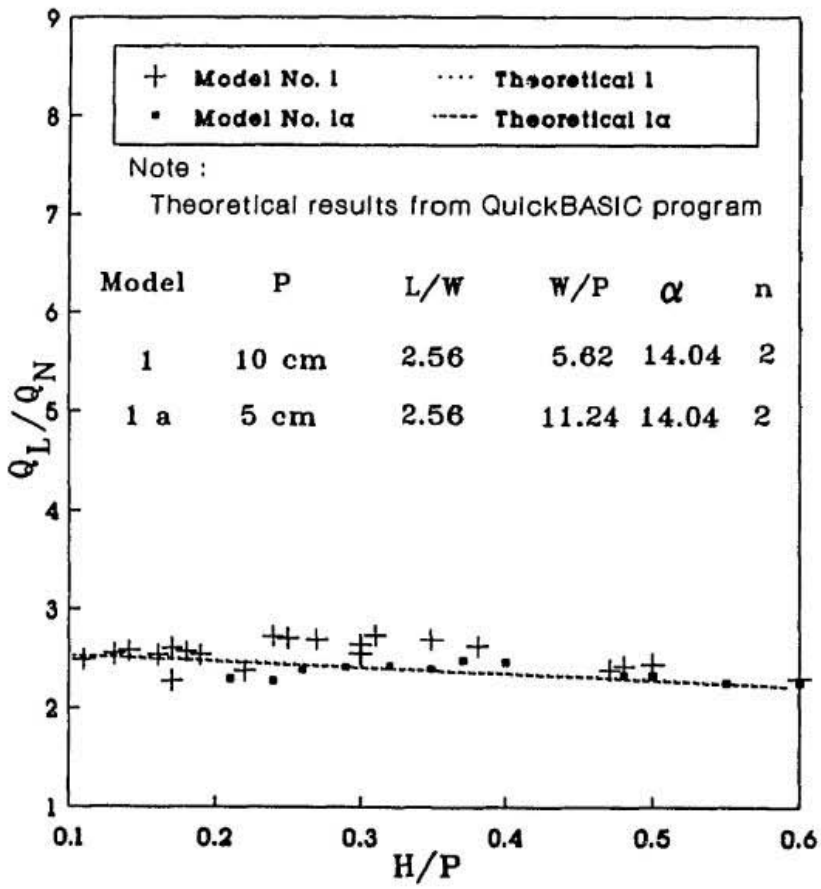

Figure 6-5 Comparison of flow magnification between model no.1 and model no.1a with different value of the weir height (P).

6.2.5. Discussion

In all trapezoidal labyrinth weir models, the coefficient of discharge, C_d, could be predicted reasonably well using the Rehbock equation except for H/P > 0.4 (see Figure 6-2). This confirmed the previous assumption that the Rehbock equation could be used to predict the theoretical values of C_d in a theoretical solution. It was also observed that the experimental values of flow magnification agreed very well with the theoretical values predicted by the QuickBASIC program.

In addition, the curve of Q_L/Q_N against H/P tends to be relatively flat at the low values of Q_L/Q_N studied in these experiments. This is as expected and confirms the results obtained by previous experimenters.

6.3. The rectangular labyrinth weir (model no.4, Figure 5-1)

6.3.1. The discharge coefficient (C_d)

As can be seen in Figure 6-6 (data in Table D.4), the experimental discharge coefficient for the rectangular geometry labyrinth weir decreased rapidly as the depth to crest height ratio, H/P, increased. Thus, the theoretical value of C_d could not be predicted very well either using the Rehbock, the Rouse or the Kindsvater & Carter formulas. This decrease in discharge coefficient is thought to be due to the weir's geometry. Because the sidewalls of the rectangular shape are parallel to the flow direction the flow over the side wall crests has a velocity component parallel to the crests and therefore the flow may be reduced.

6.3.2. The flow magnification

As displayed in Figure 6-7 (data in Table D.4), the experimental values of the flow magnification at this type of weir were satisfactorily predicted by the theoretical computer solution although the experimental values were slightly higher. This did not confirm Taylor's work (1968) which showed a significant discrepancy between theoretical and experimental results. However, the author's experiments were based on a lower length magnification value (l/w = 3) than Taylor's model (l/w = 6 and l/w = 8) and this may be the reason for the better agreement.

The trend of both theoretical and experimental values showed that the flow magnification decreases as the depth to crest height increases. This corroborated Taylor's experiment for a rectangular shape labyrinth weir.

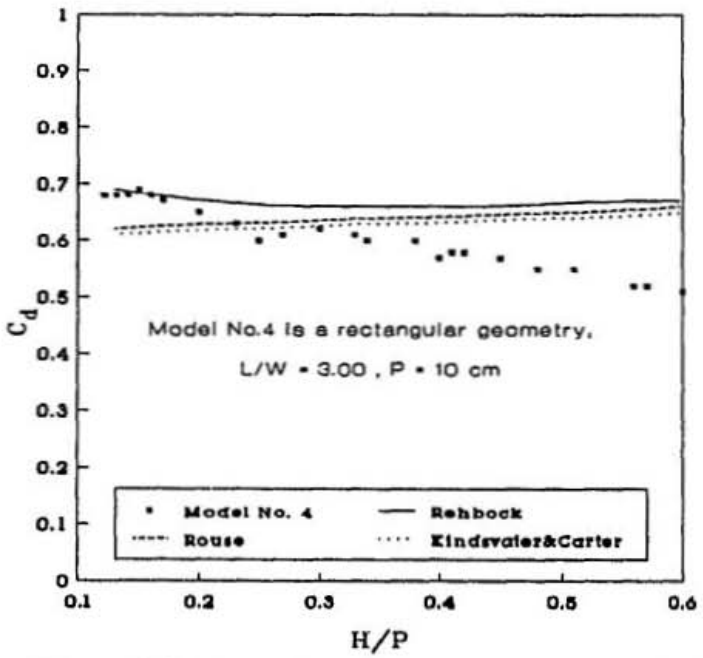

Figure 6-6 Comparison of theoretical and experimental results of discharge coefficient, C_d vs H/P of model no. 4 (rectangular shaped labyrinth weir, two-cycle).

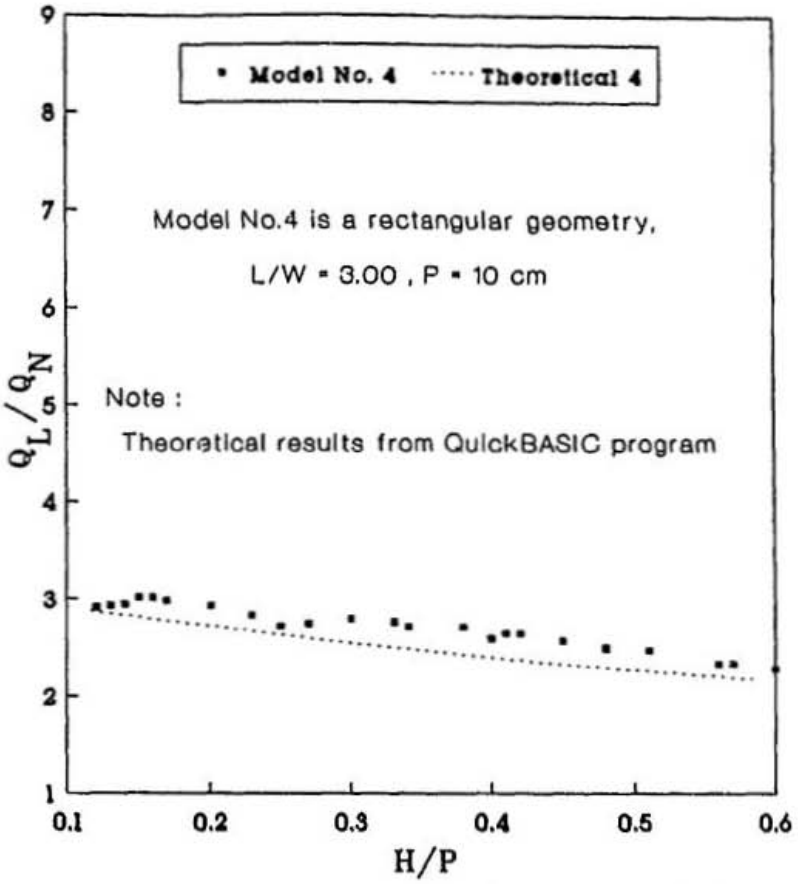

Figure 6-7 The flow magnification at rectangular shape labyrinth weir (model no.4, Figure 5-1), both experimental and theoretical values.

6.3.3. The water surface profile

The water surface profile along the centre line of one cycle is shown in Figure 6-8 (data in Tables D.14, D.15, and D.16). As can be seen from Figure 6-8, an undular jump occurred in this rectangular shape. The phenomenon was particularly noticable at high flows (H/P $\geq$ 0.40). Also the height of the jump rises as the flow increases. In addition the jump location moves in the downstream direction as the flow increases.

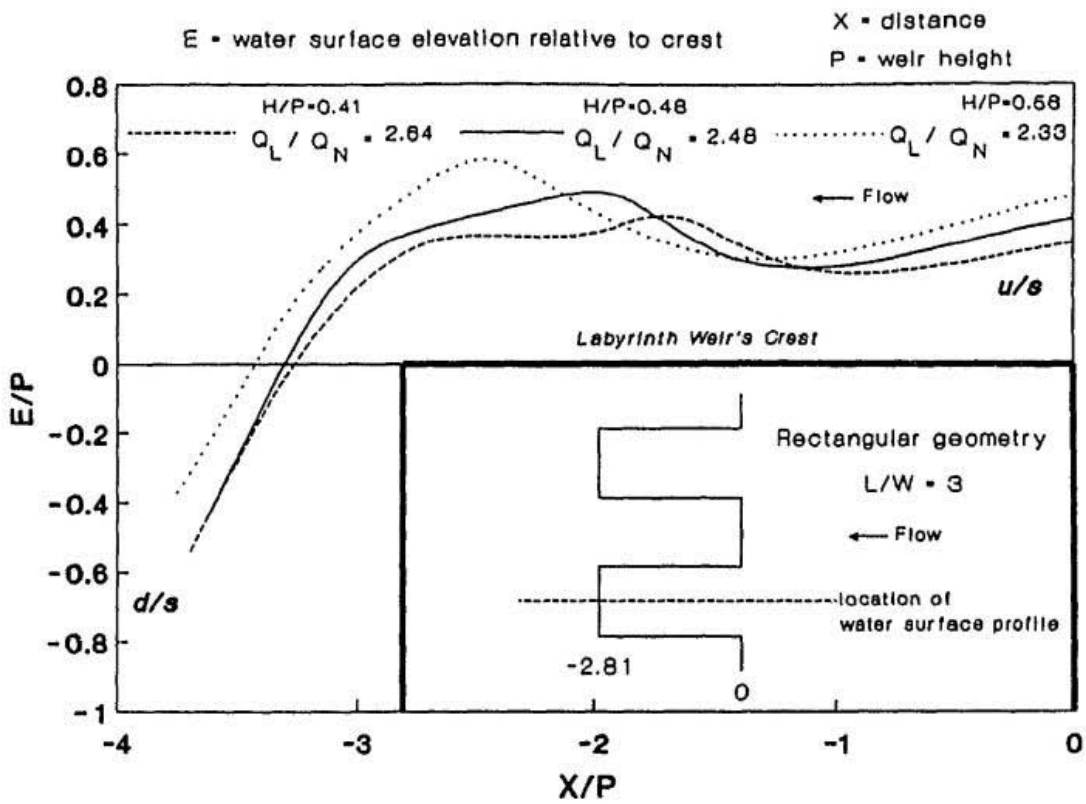

Figure 6-8 Water surface profile along the centre line of one-cycle on rectangular plan form labyrinth weir (model no.4, Figure 5-1).

6.4. The rectangular geometry with a semi-circular connection (model no.5, Figure 5-1)

6.4.1. The discharge coefficient, C_d

The relationship between the discharge coefficient, C_d, and the depth to crest height ratio, H/P, is shown in Figure 6-9. This indicates that the experimental values are in good agreement with the theoretical values predicted the by Rehbock equation except at higher flows ($H/P \geq 0.4$) where there is a discrepancy.

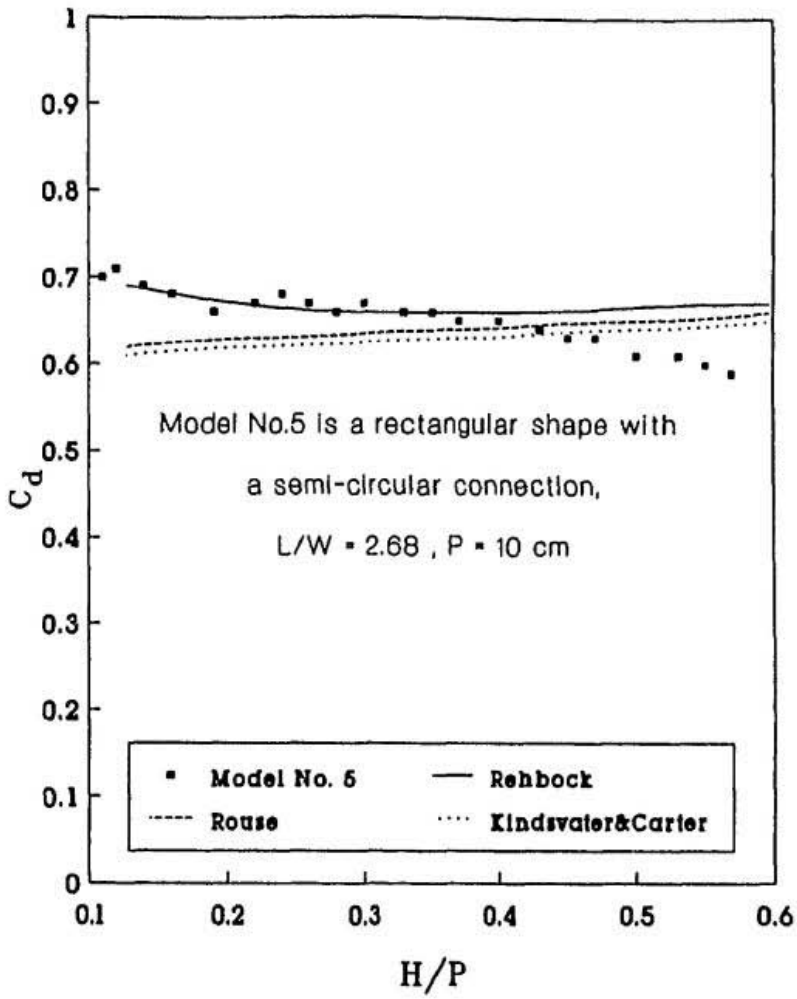

Figure 6-9 Comparison of theoretical and experimental results of discharge coefficient, C_d, vs H/P of model no.5 (rectangular geometry with a semi-circular connection, two-cycle labyrinth weir).

6.4.2. The flow magnification

The experimental data and computed results of the QuickBASIC program were plotted and displayed in Figure 6-10. As shown in Figure 6-10 (data in Table D.5), the computed results compared well with the experimental data. Note however that there is a discrepancy between the experimental and theoretical curves. This was not considered

to be significant since the difference was smaller than 10 percent.

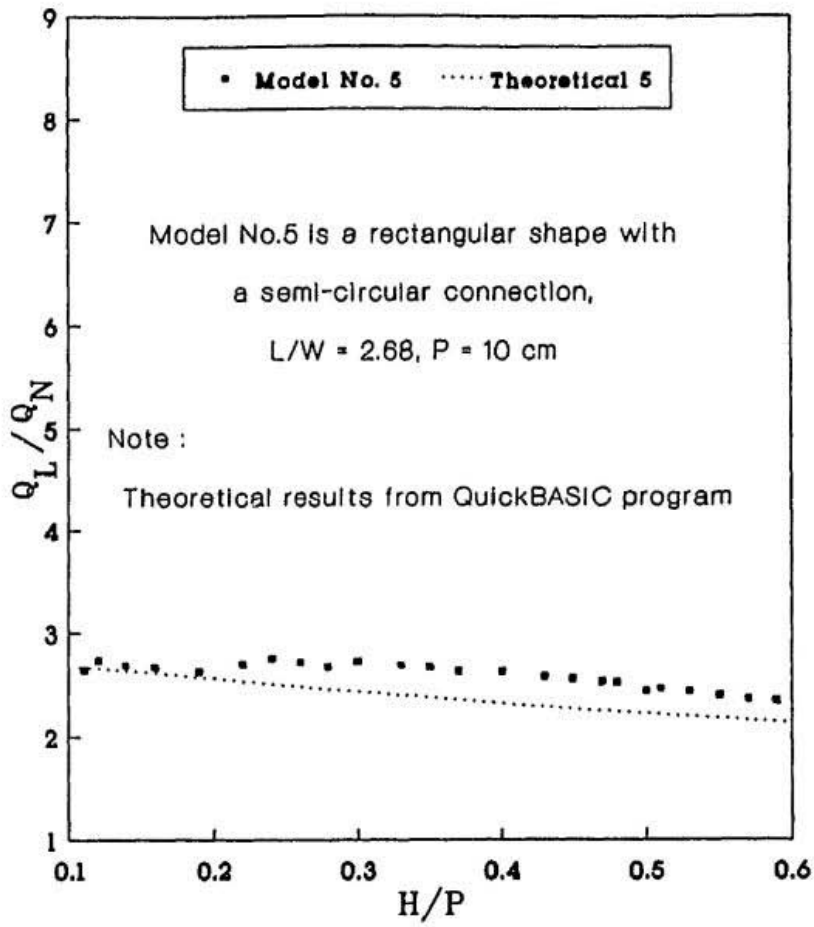

Figure 6-10 The flow magnification data at rectangular geometry with a semi-circular connection, two-cycle labyrinth weir (model no.5), both experimental and computed results.

6.4.3. The water surface profile

The water surface profile is shown in Figure 6-11. As can be seen from Figure 6-11 (data in Tables D.17, D.18, and D.19), an undular jump also occurred at this geometry especially at higher flows. Also the height of the jump rises as the flow increases and the jump location moves downstream as the flow increases.

Although this model behaved similarly to model no.4 (Figure 5-1) with respect to the jump, the height of the jump which occurred with this model was lower than that of a rectangular shaped labyrinth weir. A comparison is shown in Figures 6-12 (data in Tables D.15 and D.17) and 6-13 (data in Tables D.16 and D.19). Notice in Figure 6-13, that although model no.5 had a higher value of H/P and Q than model no.4, the height of the jump on model no.5 was slightly lower than that of model no.4. This suggests that the semi-circular connections help to increase the effectiveness of the sidewalls to pass the flow. As a result the height of the jump decreases.

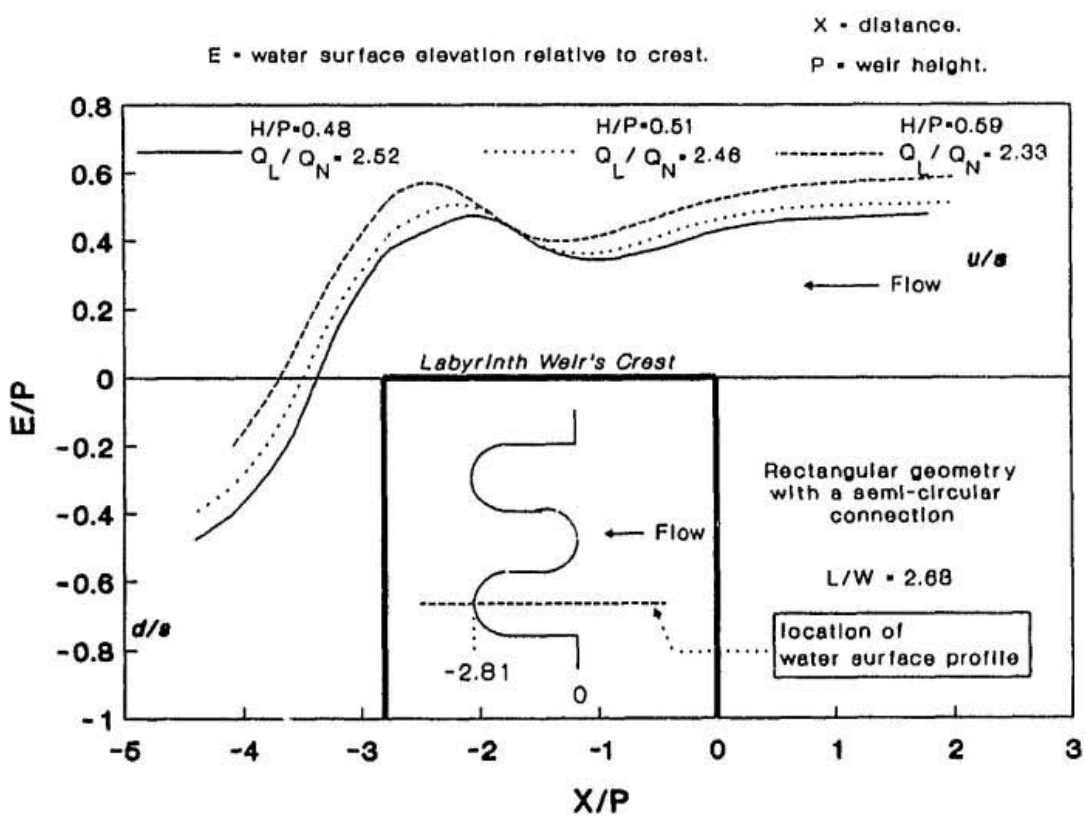

Figure 6-11 Water surface profile along the centre line of one-cycle on rectangular plan form with a semi-circular connection, two-cycle labyrinth weir (model no.5, Figure 5-1).

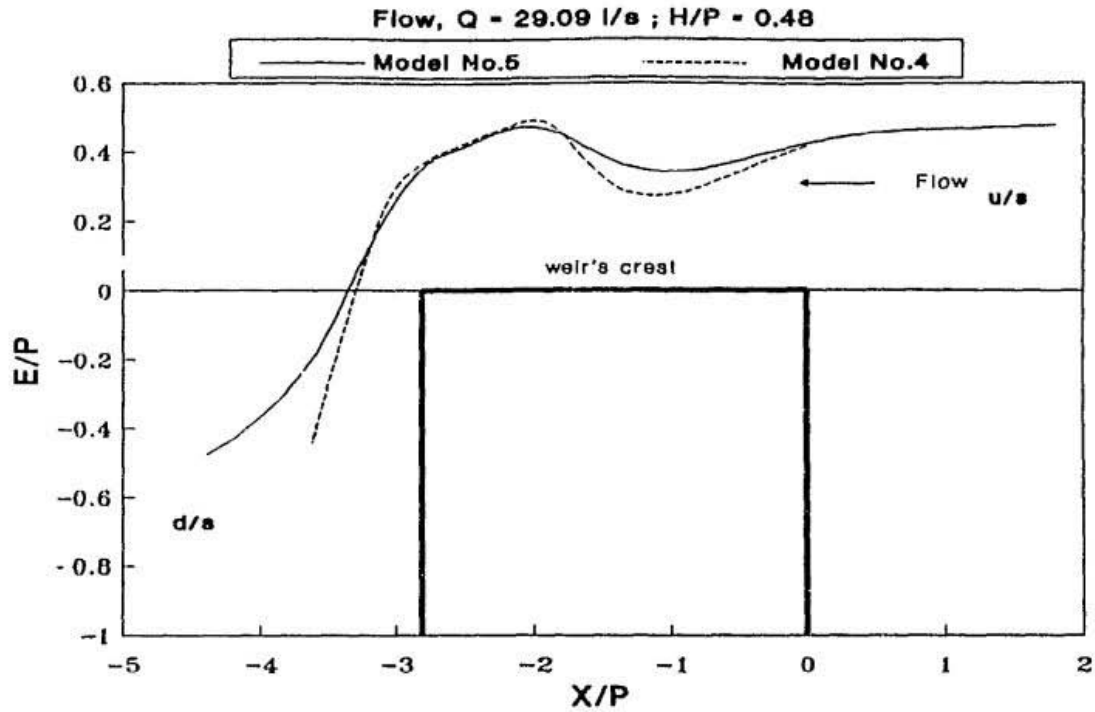

Figure 6-12 Water surface profiles on model no.4 and model no.5

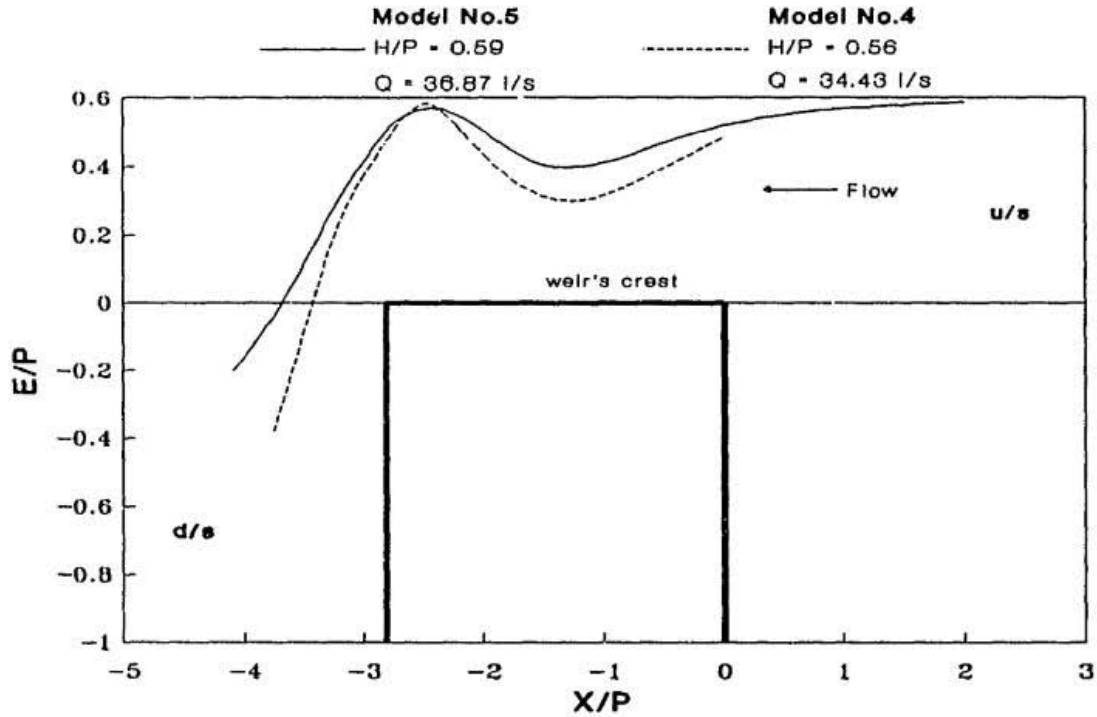

Figure 6-13 Water surface profiles on model no.4 and model no.5

6.5. The reverse trapezoidal shapes (model no.7 and no.8, Figure 5-2)

The primary purpose of these experiments was to study the undular jump. Also, this study investigated whether the undular jump occurred because of the blocking in the downstream channel or because of the angle of the side walls to the main flow direction. As in other experiments, flows and flow magnifications were also measured.

6.5.1. The discharge coefficient

As can be seen in Figure 6-14 (data in Tables D.7 and D.8), the effect of reversing the trapezoidal shape decreased the discharge coefficient rapidly and none of the proposed theoretical equations could predict this value. However, reducing the length of the side wall crest by constructing model no.8 was significant in increasing the discharge coefficient to some degree.

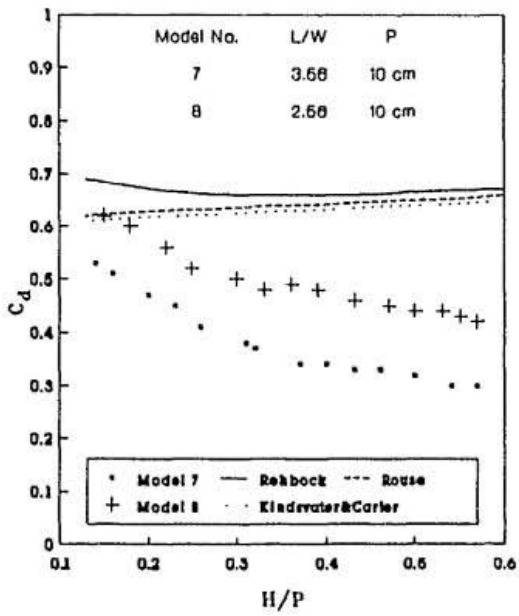

Figure 6-14 Comparison of discharge coefficient, C_d, between model no.7 and model no.8.

6.5.2. The flow magnification

As shown in Figure 6-15 (data in Tables D.7 and D.8), the reverse trapezoidal effect changed the trend of flow magnification. The labyrinth weir behaves ideally at low flow and as height increases the flow magnification decreases rapidly. This is because the effectiveness of the side walls to pass the flow decreased, especially at high flow.

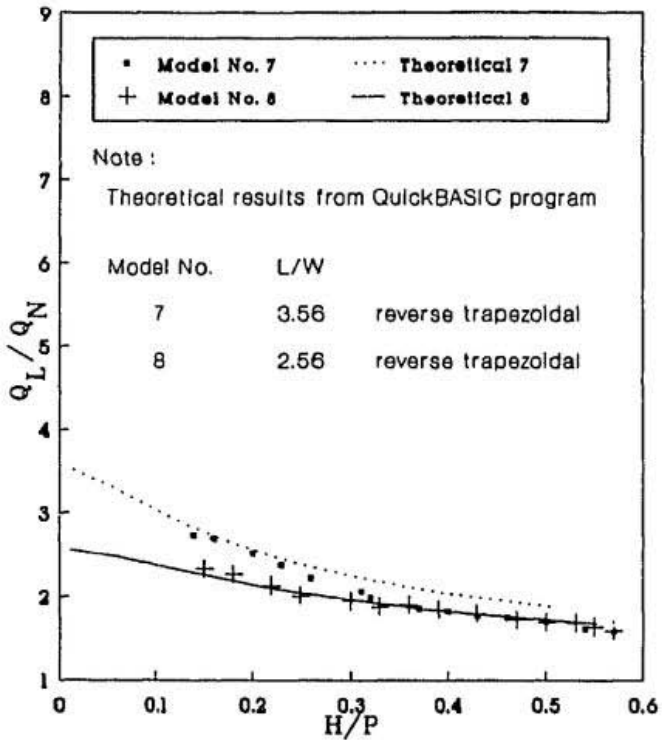

Figure 6-15 Comparison of flow magnification-depth to crest height ratio relationship between model no.7 and model no.8.

6.5.3. Water surface profile

The water surface profile at model no.7 is shown in Figure 6-16 (data in Tables D.20, D.21, and D.22). Similarly, the water surface profile at model no.8 is shown in Figure 6-17 (data in Tables D.23, D.24, and D.25).

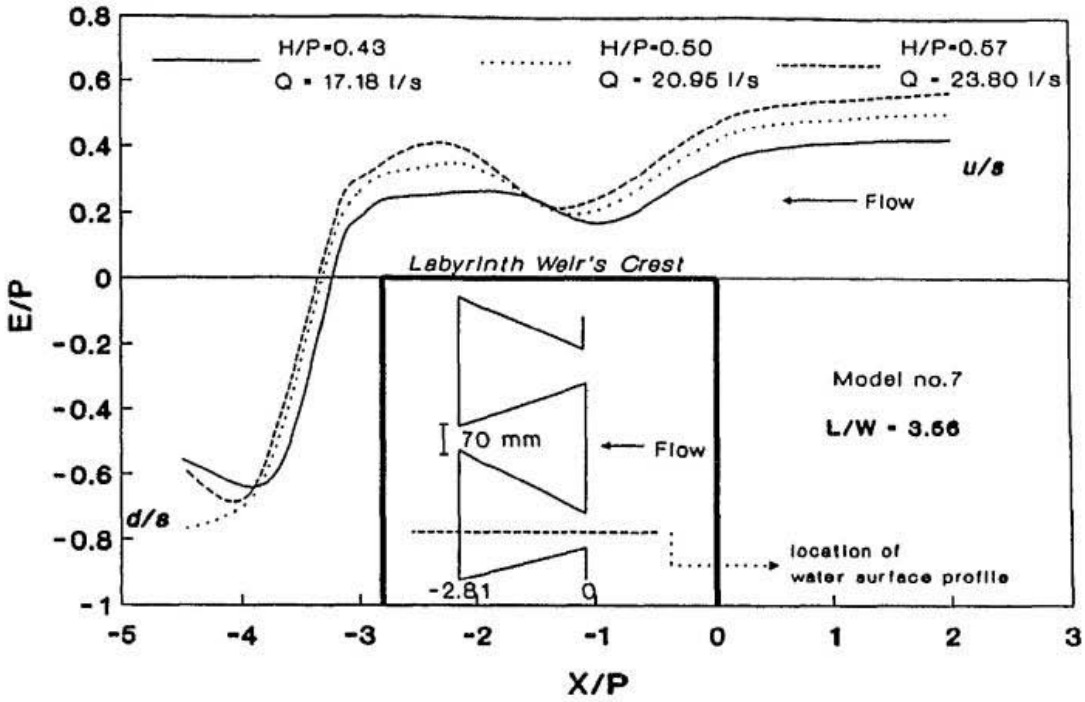

Figure 6-16 Water surface profile at model no.7

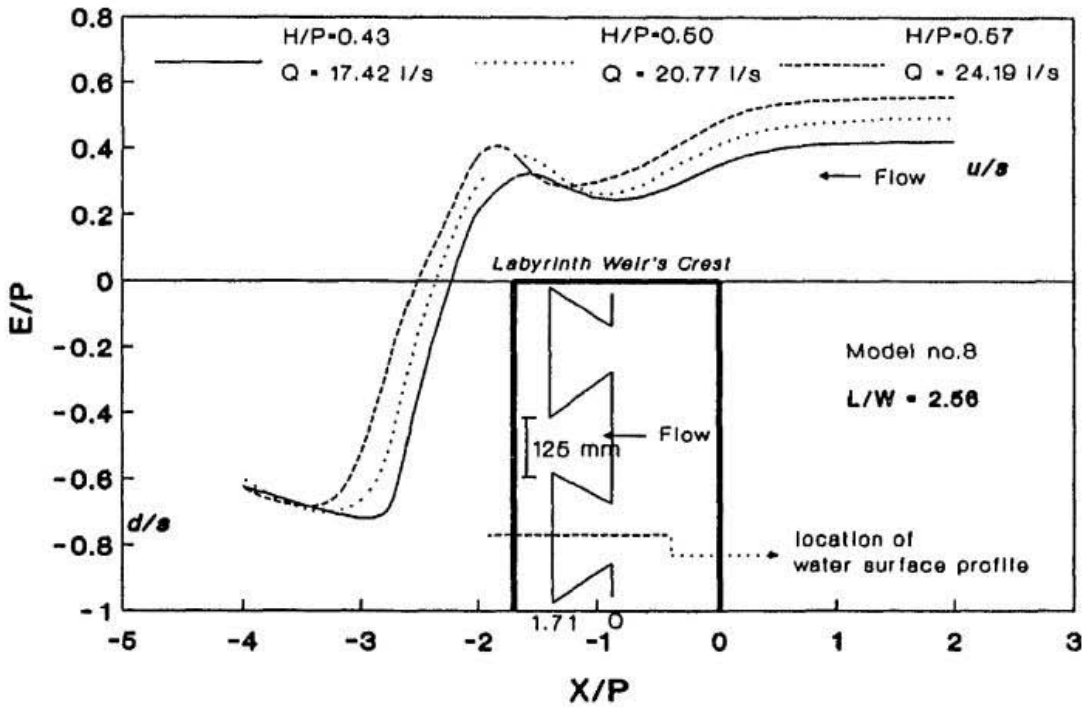

Figure 6-17 Water surface profile at model no.8

Model no.7 was designed to increase the blocking in the downstream flow by decreasing the size of the openings in the downstream channel (ie 70 mm in Figure 6-16). It was expected that this would increase the size of the jump. Model no.8 was similar in shape but had larger openings (125 mm in Figure 6-17). This was expected to decrease the jump size below that of model no.7. A comparison of the jumps on upstream channel for these shapes and for model no.4 (the rectangular planform) is shown in Figure 6-18 (data in Tables D.23, D.24, and D.25).

Jumps formed with all three models. There is little difference between the jumps which formed at models no.4 and no.7 but the jump which formed at model no.8 was much shorter. All jumps were of approximately the same height. This makes it difficult to draw any definite conclusion but the reduction in jump length when the downstream openings were increased (ie model no.8) does suggest that blocking was important. However a comparison of the jumps on downstream channel (see Figure 6-19-data in Tables D.26, D.27, and D.28) showed obviously that blocking was also important. Model no.7 which had openings 70 mm in the downstream channel had the highest and the longest jump, while model no.8 which had larger openings (125 mm) had a lower and a shorter jump than model no.7. The widest downstream opening occurs for the normal trapezoidal plan form in which jumps were never observed. It was concluded again that this shape (model no.1-see Figure 5-1) was the ideal shape for a labyrinth weir.

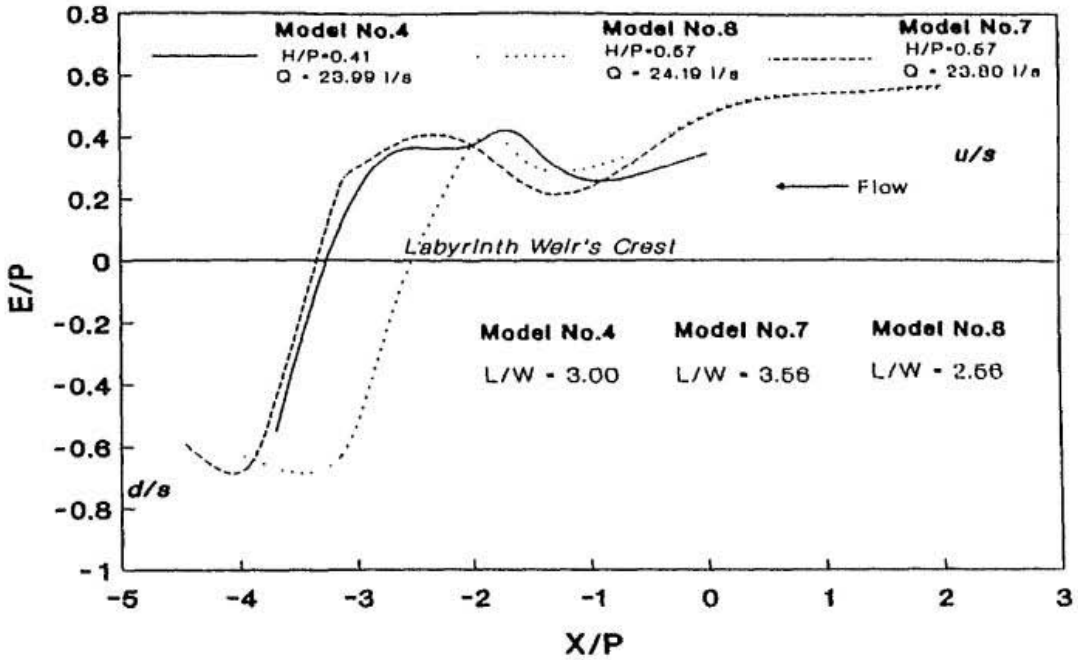

Figure 6-18 A comparison of watersurface profile at models no.4, 7 and 8 along the centre line of one-cycle (most on upstream channel).

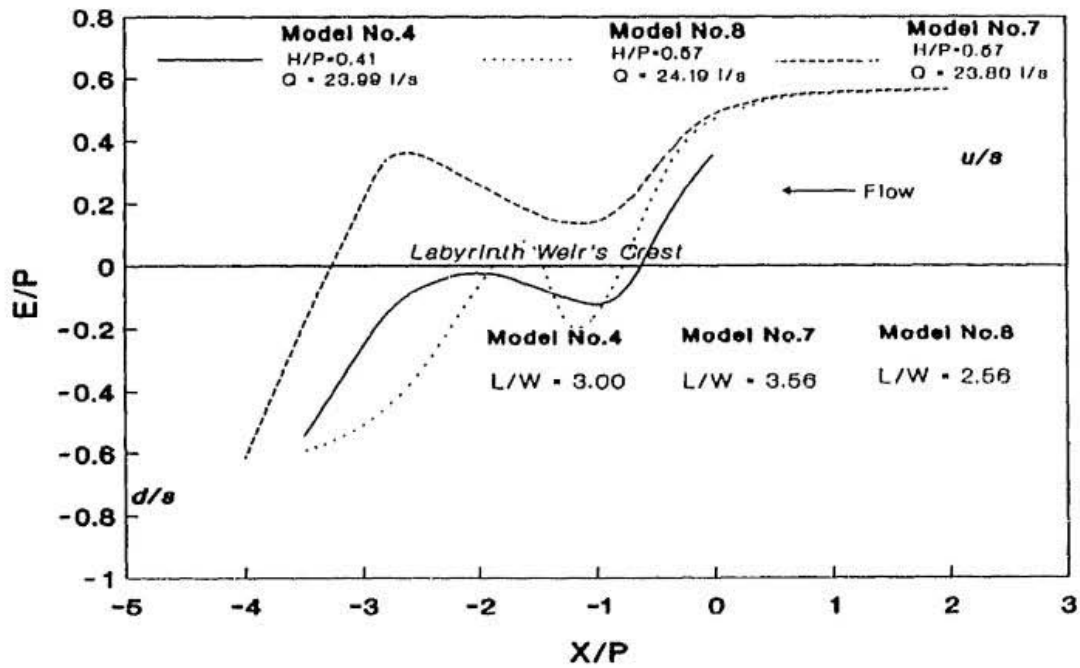

Figure 6-19 A comparison of watersurface profile at models no.4, 7 along the centre line between two cycles (most on dowmstream channel)

6.6. Comparison between model no.1, 4 and 5

A comparison between trapezoidal (model no.1), rectangular (model no.4) and rectangular with a semi-circular connection (model no.5) plan forms was made to evaluate those models in terms of total flowrate and flow magnification. In this comparison, model no.1 was chosen to represent the trapezoidal geometries.

As shown previously in Figure 5-1, model no.4 was 17% longer than model no.1, while model no.5 was 4% longer than model no.1. As can be seen from Figures 6-20 and 6-21 (data in Tables D.1, D.4, D.5 and D.6), the increase of the crest length at model no.4 and model no.5 was not significant in increasing the flow capacity over the labyrinth weir (see equation 4.1).

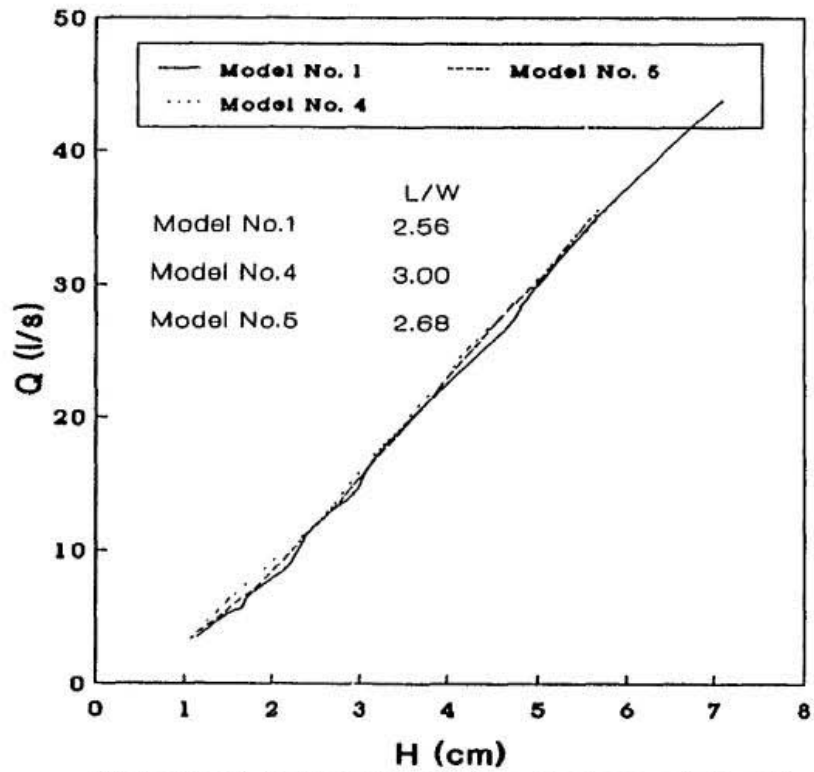

Figure 6-20 Comparison of stage-discharge relationship at models no.1, no.4, and no.5.

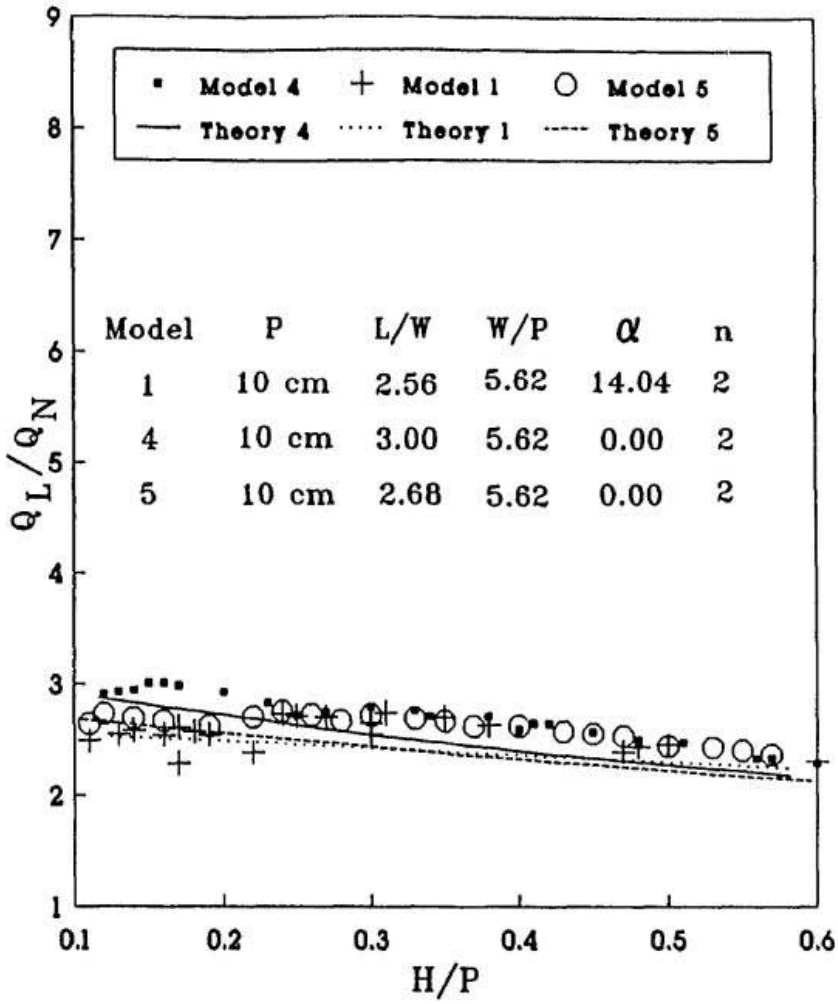

Figure 6-21 Comparison of flow magnification-depth to crest height ratio relationship at models no.1, no.4 and no.5.

As shown in Figure 6-21, the theoretical results from the QuickBASIC program show a small difference in values of the flow magnification, especially at low values of H/P. Similarly, the experimental results showed that the difference in the magnitude of flow magnification among the three models was small except at low values of H/P. These differences were not considered to be significant from a practical viewpoint.

Again, it can be concluded that the trapezoidal shape (model no. 1-see Figure 5-1) is the most suitable shape from a hydraulic point of view. Also it is easier and cheaper to build than rectangular shapes or rectangular shapes with semi-circular connection (models no.4 and no.5-see Figure 5-1).

6.7. The trapezoidal shapes with different crest widths (Model No.1b, 1c,1d, and 1e)

6.7.1. The discharge coefficient

As indicated in Figure 6-22, the increase of the crest width from 7 mm (model no. 1b, data in Table D.10) to 10 mm (model no. 1c, data in Table D.11) did not change the discharge coefficient significantly. The experimentally determined values were still predicted reasonably well using the Rehbock equation. However when the crest width was expanded to 15 mm (model no.1d, data in Table D.12) and 20 mm (model no. 1e, data in Table D.13), the discharge coefficient decreased. In this case, models no.1d and 1e did not act as a sharp crested weir. The frictional losses over the crest were significant and hence the discharge coefficient decreased.

6.7.2. The flow magnification

The flow magnification values were not affected by increasing the crest width when the width was smaller than 10 mm. However, as shown in Figure 6-23, for model no. 1d and no. 1e with crest width 15 mm and 20 mm respectively, the value of the flow magnification was likely to decrease at low flow.

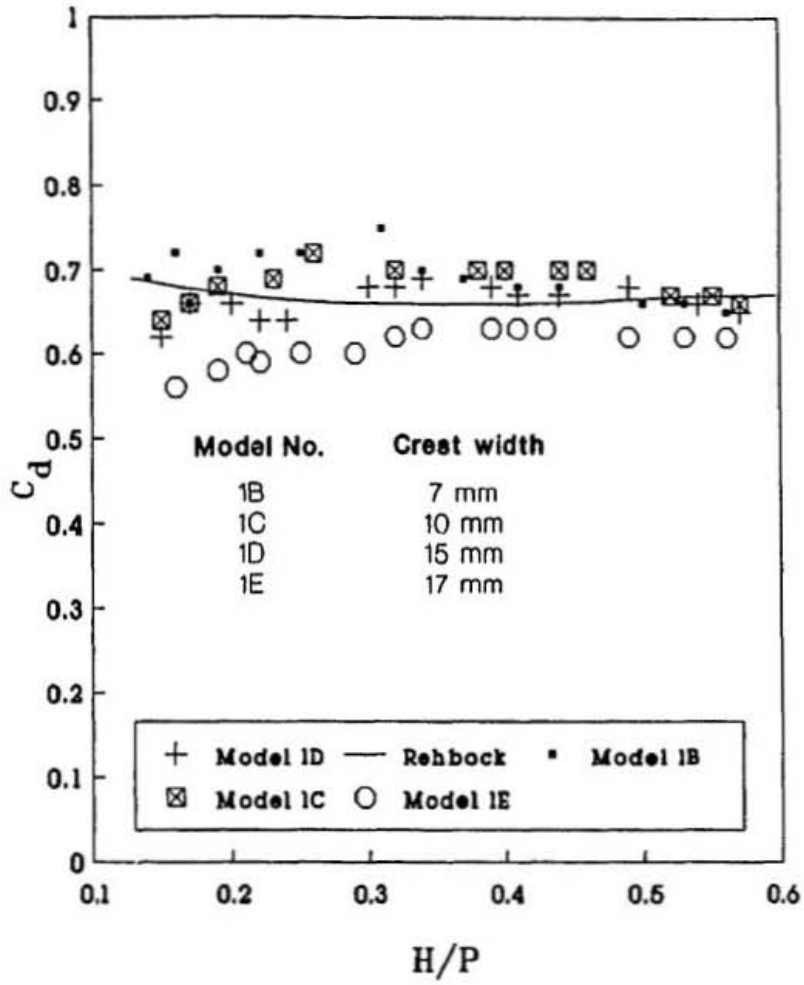

Figure 6-22 Comparison of discharge coefficient amongst model no.1b, 1c, 1d, and 1e with 7 mm, 10 mm, 15 mm, and 20 mm top width respectively.

6.7.3. Discussion

As indicated in Figure 6-22 and 6-23, it can be concluded that model no.1b and 1c with crest widths of 7 mm and 10 mm respectively still behave reasonably similar to model no.1 which had a crest width of 2 mm. In practice, a really sharp crest is seldom used since this would make the crest sensitive to damage by floating debris.

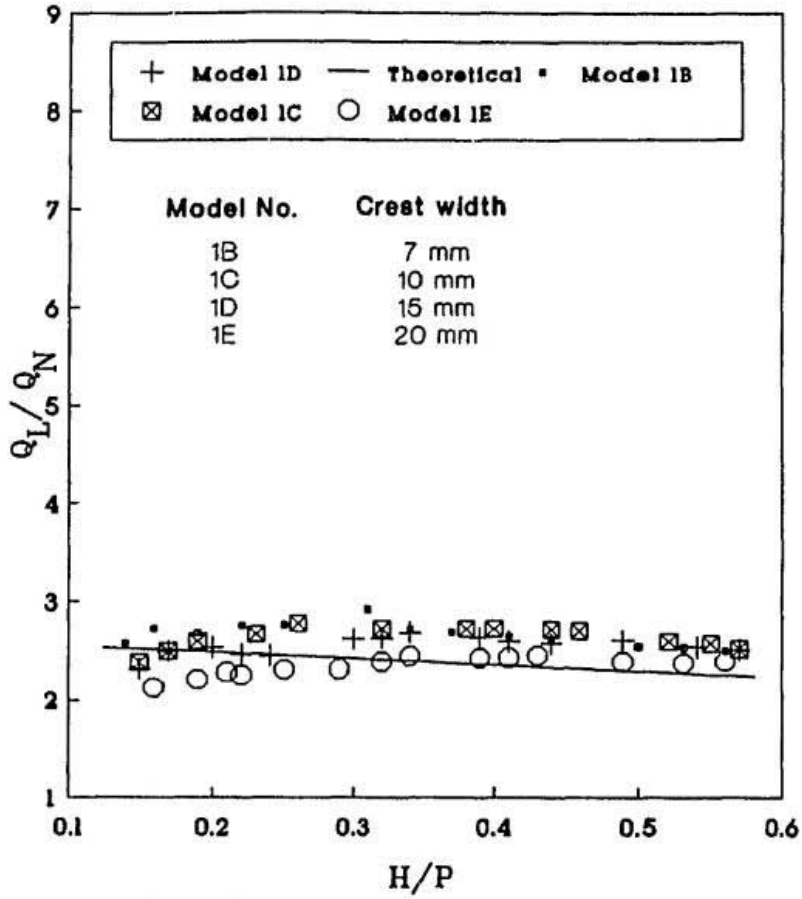

Figure 6-23 Comparison of the flow magnification amongst model no.1b, 1c, 1d, and 1e with 7 mm, 10 mm, 15 mm, and 20 mm top width respectively.

6.8. General discussion

The experimental results showed that the value of the discharge coefficient, C_d depends on the geometry of the labyrinth weir and the crest width of the labyrinth weir. It was shown that for all trapezoidal geometries (models no.1, 1a, 2, and 3) the experimental data were fitted reasonably well by the Rehbock equation, except for higher values of H/P (see Figure 6-2). The discharge coefficient for a rectangular geometry could not predicted by the Rehbock equation (see Figure 6-6). This was thought to be

because the sidewalls of the rectangular shape are parallel to the flow direction. The flow over the side wall crests then has a velocity component parallel to the crests and the discharge coefficient may therefore be reduced. However, for a rectangular geometry with a semi-circular connection (model no.5-see Figure 5-1), the experimental discharge coefficient was still predicted well by the Rehbock equation, except at higher values of H/P (see Figure 6-9). This was thought to be because the semi-circular connection helps to increase the discharge coefficient, C_d.

In addition, increasing the crest width from 2 mm (model no.1, data in Table D.1) to 10 mm (model no.1c, data in Table D.11), had little effect on the relationship between the experimentally measured values of the discharge coefficient and those given by the Rehbock equation. However the expansion of the crest width from 10 mm to 15 mm (model no.1d, data in Table D.12) and from 10 mm to 20 mm (model no.1e, data in Table D.13), showed that the experimental discharge coefficient did not fit the Rehbock equation for these crest widths.

It was also shown that the experimental flow magnification values generally have a good agreement with the theoretical results from the QuickBASIC program (see Figures 6-3, 6-4, 6-5, 6-15, 6-23). However at the rectangular geometry (model no.4) and the rectangular geometry with a semi-circular connection (model no.5), it was shown that the experimental flow magnification values are always slightly higher than the theoretical results obtained from the QuickBASIC program (see Figures 6-7, 6-10). Nevertheless both experimental and theoretical results show the same trend, namely that the flow magnification tends to decrease as the head over the weir increases.

Chapter 7

Conclusions and Recommendation

7.1. Conclusions

Within the limitations of this experimental work, the following conclusions can be advanced.

- The use of a labyrinth weir with a rectangular and semi-circular connection geometry (model no.5, see Figure 5-1) does not significantly increase the performance of a labyrinth weir relative to that with a trapezoidal plan form. Although theoretically the performance should be improved because the crest length of this labyrinth weir is 4% longer than the trapezoidal shape (model no.1, see Figure 5-1), the experiments showed that there were no significant differences between the two shapes.
- It was found that the trapezoidal geometry with the side wall angle, $\alpha = 0.68\ \alpha_{max.}$ (model no.1 or model no.2, see Figure 5-1) gave the best hydraulic performance among other labyrinth weir geometries which were tested in this study. This confirms the result obtained by IIHE, Bandung, Indonesia (Memed and Sadeli, 1990; Puslitbang Pengairan,

1991).

- The reverse trapezoidal geometries (models no.7 and no.8, see Figure 5-2) were used to show that the existence of the jump obtained with model no.4 (rectangular shape) and model no.5 (rectangular with a semi-circular connection geometry) was probably due to blocking of the flow in the downstream channel. Also it was shown that allowing a larger space in the downstream channel (model no.8) decreased the dimensions of the jump.
- The experimental discharge coefficient at weir models no.4 (rectangular geometry, L/W = 3.00), no.7 (reverse trapezoidal, L/W = 3.56), no.8 (reverse trapezoidal, L/W = 2.56), no.1D (trapezoidal geometry with crest width = 15 mm, L/W = 2.56), and no.1E (trapezoidal geometry with crest width = 20 mm, L/W = 2.56) could not be predicted well using Rehbock equation. Thus the QuickBASIC program would give a more accurate solution in predicting the performance of those models.
- However at weir models no.1 (trapezoidal geometry, L/W = 2.56), no.1a, no.2, no.3 (trapezoidal geometry, L/W = 2.69), and no.5 (rectangular plan form with a semi-circular connection, L/W = 2.68) when the value of H/P < 0.4, the discharge coefficient could be predicted well by the Rehbock equation. Thus when the value of the length magnification, L/W < 2.7 and the value of H/P < 0.4, the theoretical flowrate over the labyrinth weir can be estimated using the standard weir formula (equation 4.1) by applying the Rehbock equation (6.1) to predict the theoretical discharge coefficient. While the QuickBASIC program should be used to predict the performance of the labyrinth weir when the value of H/P > 0.4.
- The ability of the computer program to predict the performance of the labyrinth weir

has been demonstrated in this thesis. The results showed that in all cases the theoretical flow magnifications have close agreement with the experimental data. Also, the theoretical values showed a good agreement with the ones obtained earlier by Hay and Taylor (1969). This condition was achieved with the energy loss coefficient (due to a sudden contraction) equal to 0.1. This value differs from the value (0.2) obtained by Hay and Taylor.

- The economic advantages of labyrinth weirs have also been demonstrated in this thesis. It has been shown that the Ciwadas trapezoidal labyrinth weir, which was constructed in Indonesia, was more than 25% less expensive compared to the alternative of a straight weir with gate.

7.2. Recommendation

Based on the experimental results, it is possible to encourage the use of a trapezoidal geometry with : $\alpha = 0.68\ \alpha_{max.}$, length magnification l/w equal to 2.65, and the crest width approximately 10% of weir height P (see model no.1c, Figure 5-3). The increased width of the crest is not significant in decreasing the discharge coefficient despite some frictional losses on the crest. Such a crest is useful when a river has a large quantity of debris.

Since the QuickBASIC program was capable of predicting the performance of the labyrinth weir, especially for use with the trapezoidal geometry in this study, it is recommended that this QuickBASIC program is used in the preliminary design of labyrinth weirs in Indonesia.

References

Albertson, M.L., Barton, J.R., and Simons, D.B. (1960). *Fluid Mechanics for Engineers,* Prentice-Hall, Inc., 9th Ed., Englewood Cliffs, N.J.

Ackers, P., White, W.R., Perkins, J.A., and Harrison, A.J.M. (1978). *Weirs and Flumes for flow measurement,* John Wiley & Sons

Afshar, A. (1988). "The development of labyrinth spillway designs," *Water Power Dam and Construction,* pp.36-39

Cassidy, J., Gardner, C., and Peacock, R. (1983). "Labyrinth-Crest Spillway Planning, Design, and Construction," *International Conference on the Hydraulic Aspects of Floods & Flood Control,* London, England, pp.59-80

Chadwick, A., and Morfett, J. (1986). *Hydraulics in Civil Engineering,* Allen & Unwin, London, 492 p.

Chow, V.T. (1959). *Open channel hydraulics,* McGraw-Hill Book Co.,Inc., New York, N.Y., 680 p.

Daily, J.W., and Harleman, D.R.F. (1973). *Fluid Dynamics,* Addison-Wesley Publishing Company, Inc. Reading, Massachusetts, USA

Darvas, L.A. (1971). "Discussion of Performance and Design of Labyrinth Weirs, by N.Hay, and G. Taylor," *Journal of the Hydraulics Division, Proceedings of the ASCE,* No. HY8, pp.1246-1251.

Daugherty, R.L., and Ingersoll, A.C. (1954). *Fluid Mechanics,* McGraw Hill, 5th Ed., NY, 472 p.

Daugherty, R.L., and Franzini, J.B. (1977). *Fluid Mechanics with Engineering Applications,* McGraw-Hill, 7th Ed., 564 p.

Ellis, D.S. (1947). *Elements of Hydraulic Engineering,* Van Nostrand, NY, 277 p.

Hay, N., and Taylor, G. (1969). "A Computer Model for the Determination of the Performance of Labyrinth Weirs," *13th Congress of the International Association of Hydraulic Research,* Science Council of Japan, Kyoto, Japan, pp.361-378

Hay, N., and Taylor, G. (1970). "Performance and Design of Labyrinth Weirs," *Journal of the Hydraulics Division, Proceedings of the ASCE,* Vol.96, No. HY11, pp. 2337-2357

Henderson, F.M. (1966). *Open Channel Flow,* MacMillan Publishing Co., Inc., New York, N.Y., 522 p.

Hinchliff, D.L., and Houston, K.L. (1984). "Hydraulic Design and Application of Labyrinth Spillways," *Bureau of Reclamation,* Denver, Colorado, 24 p.

Houston, K.L. (1982). "Hydraulic Model Study of Ute Dam Labyrinth Spillway," Report No. GR-82-7, *Bureau of Reclamation,* Denver, Colorado, 41p.

Houston, K.L. (1983). "Hydraulic Model Study of Hyrum Dam Auxiliary Labyrinth Spillway," Report No.GR-82-13, *Bureau of Reclamation,* Denver, Colorado, 29p.

Hutama Karya, P.T. (1985). *Studi Perencanaan Proyek Pandu Tambak Udang Inti Rakyat (TIR) Ciwadas,* Jakarta, Indonesia

Hutama Karya, P.T. (1989). *Laporan Akhir Pelaksanaan Proyek Pandu Tambak Udang Inti Rakyat (TIR) Ciwadas,* Jakarta, Indonesia

Jaeger, C. (1956). *Engineering Fluid Mechanics,* Blackie & Son Ltd., London, United Kingdom, 529 p.

Kraatz, D.B. (1975). "Small Hydraulic Structures," *Irrigation and Drainage Paper FAO,* pp.182-187

Lux III, F., and Hinchliff, D.L. (1985). "Design and Construction of Labyrinth Spillways," *15th Congress of ICOLD,* Lausanne, Switzerland, Q.59-R.15, pp.249-274

Lye, L.M. (1992). *Engineering Economic Analysis, ENGR 9310,* Course Notes, Fall Term, Faculty of Engineering and Applied Science, Memorial University of Newfoundland, St.John's, Newfoundland, Canada

Magalhães, A.P. (1985). "Labyrinth-Weir Spillways," *15th Congress of ICOLD,* Lausanne, Switzerland, Q.59-R.24, pp.395-407

Memed, M., and Sadeli, L. (1990). "Optimasi Dimensi Hidrolis Bendung dan Spillway Tipe Gergaji," *Seminar on Theory and Application on Hydraulic Phenomena of Hydraulic Structures,* Bandung, Indonesia, 20p.

Novak, P., Moffat, A.I.B., Nalluri, C., and Narayanan, R. (1990). *Hydraulic Structures*, Unwin Hyman, Ltd., London, United Kingdom, 546 p.

Pusat Penelitian dan Pengembangan (Puslitbang) Pengairan, Badan Penelitian dan Pengembangan Pekerjaan Umum, Departemen Pekerjaan Umum, Republik Indonesia (1973). *New Rentang Barrage, Rentang, Jatibarang, West Java*, Bandung, Indonesia, 74 p.

Pusat Penelitian dan Pengembangan (Puslitbang) Pengairan, Badan Penelitian dan Pengembangan Pekerjaan Umum, Departemen Pekerjaan Umum, Republik Indonesia (1986). *Aturan Operasi Pintu Bendung Gerak Rentang Baru, Rentang, Jatibarang, Jawa Barat,* No. PA.1308-HAU, Bandung, Indonesia, 18 p.

Pusat Penelitian dan Pengembangan (Puslitbang) Pengairan, Badan Penelitian dan Pengembangan Pekerjaan Umum, Departemen Pekerjaan Umum (1991). "Bendung dan Pelimpah Tipe Gergaji," *Balai Penyelidikan Hidrolika*, Bandung, Jawa Barat, Indonesia, 8 p.

Quasney, J.S. (1992). *Programming in QuickBASIC*, Boyd & Fraser Publishing Company, Boston, M.A., 120 p.

Riggs, J.L., Rentz, W.F., Kahl, A.L., and West, T.M. (1986). *Engineering Economics*, McGraw-Hill Ryerson, Toronto, ON, Canada, 746 p.

Samuels, P.G. (1989). "Backwater lengths in rivers," *Proc. Instn Civ. Engrs.*, Part 2, 87, pp. 571-582

Sharp, J.J. (1976). "Discussion of A dimensionless number for the study of open channel flow, by O.N. Wakhlu," *Proc. Instn Civ. Engrs.*, Part 2, 61, pp.233-245

Sharp, J.J. (1981). *Hydraulic Modelling*, Butterworths, London, England, United Kingdom, 242 p.

Sharp, J.J. (1988). *BASIC fluid mechanics*, Butterworths, London, England, United Kingdom, 139 p.

Sharp, J.J. (1992). *Similarity and Model Tecniques, ENGR 9710*, Course Notes, Fall Term, Faculty of Engineering and Applied Science, Memorial University of Newfoundland, St.John's, Newfoundland, Canada

Sinha, C.P., and Singh, D.P. (1984). "Barrages on Alluvial Rivers," *Channels and Channel Control Structures, Proceedings of the 1st International Conference*, Southampton, England, Springer-Verlag, Berlin-Heidelberg-New York-Tokyo, ed. K.V.H. Smith, A Computational Mechanics Centre Publication, pp.1.19-1.32

Sitompul, A.T. (1992). "An application of dimensional analysis on hydraulic modelling of a sharp crested labyrinth weir," *Similarity and Model Tecniques, ENGR 9710,* Term Paper, Fall Term, Faculty of Engineering and Applied Science, Memorial University of Newfoundland, St.John's, Newfoundland, Canada, 15 p.

Sitompul, A.T. (1992). "A cost-benefit analysis of the Wonorejo Dam and Irrigation Project Tulungagung II, Brantas River Basin Development in East Jawa, Indonesia ," *Engineering Economic Analysis, ENGR 9310,* Project Report, Fall Term, Faculty of Engineering and Applied Science, Memorial University of Newfoundland, St.John's, Newfoundland, Canada, 19 p.

Slagter, J.C. (1975) *Weirs,* International Course in Hydraulic Engineering, Part 1-textbook, Delft, Netherlands

Smith, C.D. (1985). *Hydraulic Structures,* University of Saskatchewan Printing Services, 364 p.

Tacail, F.G., Evans, B., and Babb, A. (1990). "Case study of a labyrinth weir spillway," *Canadian Journal of Civil Engineering,* National Research Council Canada, Vol. 17, pp. 1-7.

Taylor, G. (1968). "The Performance of Labyrinth Weirs," *PhD. thesis,* University of Nottingham, Nottingham, England, U.K., 362 p.

Transmigration, Indonesian Ministry of. (1988). *Indonesia, Our People, Our Land, Our Future,* an official booklet publication

United States Department of the Interior, Bureau of Reclamation. (1987). *Design of Small Dams,* A Water Resources Technical Publication, 860 p.

Venit, S.M. (1991). *Programming in QuickBASIC:Problem Solving with Structure and Style,* West Publishing Company, St. Paul, M.N., 418 p.

Vennard, J.K., and Street, R.L. (1975). *Elementary Fluid Mechanics,* John Wiley & Sons, Inc., Toronto, Canada, 740 p.

Vittal, N., and Rastogi, N.K. (1984). "Comparative Discharge Performance of Side and Normal Weirs," *Channels and Channel Control Structures, Proceedings of the 1st International Conference,* Southampton, England, Springer-Verlag, Berlin-Heidelberg-New York-Tokyo, ed. K.V.H. Smith, A Computational Mechanics Centre Publication, pp.1.33-1.44

Wakhlu, O.N. (1975). "A dimensionless number for the study of open channel flow," *Proc. Instn Civ. Engrs.,* Part 2, 59, pp. 515-522.

Water Resources Development, Directorate General of., Ministry of Public Works. (1988). *Water Resources and its Development in Indonesia*, an official booklet publication, Jakarta, Indonesia, 47 p.

Water Resources Development, Directorate General of., Sub Directorate of Planning and Programming, Ministry of Public Works, Republic of Indonesia. (1984). *Guideline BP 12, The economic analysis of DGWRD Projects*, Jakarta, Indonesia

Wibowo, S. (1993). *Personal communication*, a long-distance call, St.John's, Canada - Jakarta, Indonesia

World Bank. (1990). *World Development Report 1990*, Washington D.C.

APPENDIX A

Input and output of spreadsheet

TABLE A.1

Table of computation for the determination of discharge of each section

Data :

l =	71.9800 cm	g =	981.0000 cm/s^2	delta l =	2.4138 cm	P =	10.0000 cm	X =	28.1002 cm
w =	28.1000 cm	alpha =	0.2450 radian						o
a =	3.5125 cm	delta x =	2.3417 cm	y =	7.0250 cm	b =	28.9650 cm	alpha =	14.0362
n =	12								

Sec. No	x (cm)	H (cm)	Cd	l (cm)	Q (cm^3/s)	delta Q (cm^3/s)	Q1 + Q2 (cm^3/s)	w (cm)	A (cm^2)	V (cm/s)	(V1 + V2) (cm/s)	delta Q (cm^3/s)	delta V (cm/s)	delta H (cm)	Sec. No.
(1)	(2)	(3)	(4)	(5)	(6)	(7)	(8)	(9)	(10)	(11)	(12)	(13)	(14)	(15)	(16)
0	0.0000														0
1	2.3417	0.3048	0.9353	11.6525	55.0865	22.4396		8.1958	84.4564	0.6522				0.0001	1
2	4.6834	0.3049	0.9352		77.5260		132.6125	9.3667	98.5226	0.8032	1.4554	22.4396	0.1509	0.0001	2
2	4.6834	0.3049	0.9352		77.5260	22.4506		9.3667	98.5226	0.8032				0.0001	2
3	7.0250	0.3050			99.9767		177.5027	10.5375	108.5889	0.9207	1.7239	22.4506	0.1175	0.0001	3
3	7.0250	0.3050	0.9351		99.9767	22.4591		10.5375	108.5889	0.9207				0.0001	3
4	9.3667	0.3051			122.4358		222.4124	11.7083	120.6556	1.0148	1.9354	22.4591	0.0941	0.0001	4
4	9.3667	0.3051	0.9350		122.4358	22.4678		11.7083	120.6556	1.0148				0.0001	4
5	11.7084	0.3052			144.9033		267.3391	12.8792	132.7224	1.0918	2.1065	22.4678	0.0770	0.0001	5
5	11.7084	0.3052	0.9349		144.9033	22.4761		12.8792	132.7224	1.0918				0.0001	5
6	14.0501	0.3053			167.3794		312.2827	14.0500	144.7895	1.1560	2.2478	22.4761	0.0642	0.0001	6
6	14.0501	0.3053	0.9348		167.3794	22.4845		14.0500	144.7895	1.1560				0.0001	6
7	16.3918	0.3054			189.8639		357.2433	15.2208	156.8568	1.2104	2.3664	22.4845	0.0544	0.0001	7
7	16.3918	0.3054	0.9347		189.8639	22.4930		15.2208	156.8568	1.2104				0.0001	7
8	18.7335	0.3055			212.3570		402.2209	16.3917	168.9243	1.2571	2.4675	22.4930	0.0467	0.0001	8
8	18.7335	0.3055	0.9346		212.3570	22.4960		16.3917	168.9243	1.2571				0.0000	8
9	21.0751	0.3055			234.8530		447.2100	17.5825	180.9904	1.2976	2.5547	22.4960	0.0405	0.0000	9
9	21.0751	0.3055	0.9346		234.8530	22.4960		17.5825	180.9904	1.2976				0.0000	9
10	23.4168	0.3055			257.3490		492.2020	18.7333	193.0564	1.3330	2.6306	22.4960	0.0354	0.0000	10
10	23.4168	0.3055	0.9345		257.3490	22.4960		18.7333	193.0564	1.3330				0.0000	10
11	25.7585	0.3055			279.8450		537.1940	19.9042	205.1224	1.3643	2.6973	22.4960	0.0313	0.0000	11
11	25.7585	0.3055	0.9346		279.8450	22.4960		19.9042	205.1224	1.3643				0.0000	11
12	28.1002	0.3055	0.9346		302.3410	32.7363	582.1859	21.0750	217.1884	1.3821	2.7564	22.4960	0.0278	0.0000	12
12'	28.1002	0.3055			335.0773										12

0.1000

CSC = 0.1500 0.3000 l/w = 2.5616

0.2000 0.3500 w/P = 2.8100 *(1 cycle)*.

0.2500

*Trapezoidal geometry

@output01.wk3

*COMMODEL.WK3

Check :

X12 = 28.1002 cm

l12 = 64.9650 cm

w12 = 21.0750 cm

TABLE A.1 (continued)

Sec No	X (cm)	H+ CSC*V^2/2*g (cm)	QL (cm^3/s)	Cd	QN (cm^3/s)	QL/QN	H/P
(17)	(18)	(19)	(20)	(21)	(22)	(23)	(24)
		0.3056		0.9345	130.9939	2.5580	0.0306
		0.3056		0.9344	131.0183	2.5575	0.0306
13	30.4419	0.3057	335.0773	0.9344	131.0427	2.5570	0.0306
		0.3057		0.9343	131.0671	2.5565	0.0306
		0.3058		0.9342	131.0915	2.5561	0.0306
		0.3058		0.9342	131.1159	2.5556	0.0306

INPUT		OUTPUT	
l (cm) =	71.9800	l/w =	2.5616
w (cm) =	28.1000	w/P =	2.8100
a (cm) =	3.5125	QL/QN =	2.5580
P (cm) =	10.0000	H/P =	0.0306
g(cm/det^2) =	981.0000		
n =	12		
CSC =	0.1000		

* delta H is quoted from Open - Channel Hydraulics Ven Te Chow, Ph D., page 346

**delta H = ((Q1*(V2 + V1) delta V)/g (Q2 + Q1)) * (1 - (delta Q/2*Q1))

*CSC = energy loss coefficient due to sudden contraction

1 of 8

TABLE A.2

Table of computation for the determination of discharge of each section

Data :

l =	71.9800 cm	g =	981.0000 cm/s ^ 2	delta l =	2.4136 cm	P =	10.0000 cm	X =	28.1002 cm
w =	28.1000 cm	alpha =	0.2450 radian						o
a =	3.5125 cm	delta x =	2.3417 cm	y =	7.0250 cm	b =	28.9650 cm	alpha =	14.0382
n =	12								

Sec. No	x (cm)	H (cm)	Cd	l (cm)	Q (cm ^ 3/s)	delta Q (cm ^ 3/s)	Q1 + Q2 (cm ^ 3/s)	w (cm)	A (cm ^ 2)	V (cm/s)	(V1 + V2) (cm/s)	delta Q (cm ^ 3/s)	delta V (cm/s)	delta H (cm)	Sec. No
(1)	(2)	(3)	(4)	(5)	(6)	(7)	(8)	(9)	(10)	(11)	(12)	(13)	(14)	(15)	(16)
0	0.0000														0
1	2.3417	1.2192	0.6967	11.8525	326.2762	133.8623		8.1958	91.9507	3.5701				0.0022	1
2	4.6834	1.2214	0.6968		482.1385		790.4147	9.3667	105.1071	4.3968	7.9670	133.8623	0.8267	0.0022	2
2	4.6834	1.2214	0.6968		482.1385	134.2327		9.3667	105.1071	4.3968				0.0023	2
3	7.0250	1.2237			596.3711		1058.5096	10.5375	118.2697	5.0425	9.4393	134.2327	0.6456	0.0023	3
3	7.0250	1.2237	0.6965		596.3711	134.5772		10.5375	118.2697	5.0425				0.0022	3
4	9.3667	1.2259			730.9484		1327.3195	11.7083	131.4366	5.5612	10.6037	134.5772	0.5188	0.0022	4
4	9.3667	1.2259	0.6963		730.9484	134.9068		11.7083	131.4366	5.5612				0.0021	4
5	11.7084	1.2280			865.8551		1596.8035	12.8792	144.6073	5.9876	11.5488	134.9068	0.4264	0.0021	5
5	11.7084	1.2280	0.6962		865.8551	135.2129		12.8792	141.6073	5.9876				0.0019	5
6	14.0501	1.2299			1001.0681		1866.9232	14.0500	157.7801	6.3447	12.3323	135.2129	0.3571	0.0019	6
6	14.0501	1.2299	0.6961		1001.0681	135.4969		14.0500	157.7801	6.3447				0.0018	6
7	16.3918	1.2317			1136.5649		2137.6330	15.2208	170.9559	6.6483	12.9930	135.4969	0.3036	0.0018	7
7	16.3918	1.2317	0.6960		1136.5649	135.7573		15.2208	170.9559	6.6483				0.0016	7
8	18.7335	1.2333			1272.3223		2408.8872	16.3917	184.1325	6.9096	13.5581	135.7573	0.2615	0.0016	8
8	18.7335	1.2333	0.6959		1272.3223	135.9954		16.3917	184.1325	6.9096				0.0015	8
9	21.0751	1.2348			1408.3177		2680.6399	17.5625	197.3112	7.1375	14.0474	135.9954	0.2277	0.0015	9
9	21.0751	1.2348	0.6958		1408.3177	136.2100		17.5625	197.3112	7.1375				0.0013	9
10	23.4168	1.2361			1544.5277		2952.8454	18.7333	210.4896	7.3378	14.4753	136.2100	0.2002	0.0013	10
10	23.4168	1.2361	0.6957		1544.5277	136.4021		18.7333	210.4896	7.3378				0.0012	10
11	25.7585	1.2373			1680.9298		3225.4575	19.9042	223.6691	7.5153	14.8530	136.4021	0.1775	0.0012	11
11	25.7585	1.2373	0.6957		1680.9298	136.5789		19.9042	223.6691	7.5153				0.0011	11
12	28.1002	1.2384	0.6956		1817.5087	136.5789	3498.4386	21.0750	236.8493	7.6737	15.1889	136.5789	0.1564	0.0011	12
12'	28.1002	1.2384			2018.3735										12

*Trapezoidal geometry

@output02.wk3

Check :

X12 = 28.1002 cm

l12 = 64.9550 cm

w12 = 21.0750 cm

* delta H is quoted from Open-Channel Hydraulics, Ven Te Chow, Ph.D., page 348

CSC = 0.1000, 0.1500, 0.2000, 0.2500, 0.3000, 0.3500

l/w = 2.5616

w/P = 2.8100 *(1 cycle).*

*COMMODEL.WK3

TABLE A.2 (continued)

Sec. No.	X (cm)	H+ CSC*V^2/2*g (cm)	QL (cm^3/s)	Cd	QN (cm^3/s)	QL/QN	H/P
(17)	(18)	(19)	(20)	(21)	(22)	(23)	(24)
		1.2414		0.6954	798.1561	2.5263	0.1241
		1.2429		0.6953	799.5059	2.5220	0.1243
13	30.4419	1.2444	2018.3735	0.6953	800.8564	2.5178	0.1244
		1.2459		0.6952	802.2077	2.5135	0.1246
		1.2474		0.6951	803.5598	2.5093	0.1247
		1.2489		0.6950	804.9127	2.5051	0.1249

INPUT		OUTPUT	
l (cm) =	71.9800	l/w =	2.5616
w (cm) =	28.1000	w/P =	2.8100
a (cm) =	3.5125	QL/QN =	2.5263
P (cm) =	10.0000	H/P =	0.1241
g(cm/det^2) =	981.0000		
n =	12		
CSC =	0.1000		

**delta H = ((Q1*(V2 + V1) delta V)/(g (Q2 + Q1)) * (1 − (delta Q/2*Q1))

*CSC = energy loss coefficient due to sudden contraction.

TABLE A.3

Table of computation for the determination of discharge of each section

Data :

l =	71.9600 cm	g =	981.0000 cm/s^2	delta l =	2.4138 cm	P =	10.0000 cm	X =	28.1002 cm
w =	28.1000 cm	alpha =	0.2450 radian						o
a =	3.5125 cm	delta x =	2.3417 cm	y =	7.0250 cm	b =	28.9650 cm	alpha =	14.0362
n =	12								

Sec. No	x (cm)	H (cm)	Cd	l (cm)	Q (cm^3/s)	delta Q (cm^3/s)	Q1 + Q2 (cm^3/s)	w (cm)	A (cm^2)	V (cm/s)	(V1 + V2) (cm/s)	delta Q (cm^3/s)	delta V (cm/s)	delta H (cm)	Sec. No
(1)	(2)	(3)	(4)	(5)	(6)	(7)	(8)	(9)	(10)	(11)	(12)	(13)	(14)	(15)	(16)
0	0.0000														0
1	2.3417	1.8288	0.6743	11.8525	583.6530	238.2867		8.1958	98.9489	6.0203				0.0063	1
2	4.6834	1.8351	0.6741		821.9397		1405.5927	9.3667	110.8554	7.4145	13.4349	238.2867	1.3942	0.0063	2
2	4.6834	1.8351	0.6741		821.9397	239.5462		9.3667	110.8554	7.4145				0.0066	2
3	7.0250	1.8417			1061.4859		1883.4256	10.5375	124.7619	8.5067	15.9212	239.5462	1.0922	0.0066	3
3	7.0250	1.8417	0.6740		1061.4859	240.7670		10.5375	124.7619	8.5067				0.0064	3
4	9.3667	1.8481			1302.2529		2363.7388	11.7083	138.7215	9.3875	17.8943	240.7670	0.6808	0.0064	4
4	9.3667	1.8481	0.6739		1302.2529	241.9328		11.7083	138.7215	9.3875				0.0060	4
5	11.7084	1.8541			1544.1854		2846.4383	12.8792	152.6709	10.1145	19.5020	241.9328	0.7269	0.0060	5
5	11.7084	1.8541	0.6737		1544.1854	243.0149		12.8792	152.6709	10.1145				0.0055	5
6	14.0501	1.8596			1787.2003		3331.3858	14.0500	166.6274	10.7257	20.8402	243.0149	0.6113	0.0055	6
6	14.0501	1.8596	0.6736		1787.2003	244.0143		14.0500	166.6274	10.7257				0.0051	6
7	16.3918	1.8647			2031.2146		3818.4150	15.2208	180.5906	11.2476	21.9733	244.0143	0.5219	0.0051	7
7	16.3918	1.8647	0.6735		2031.2146	244.9394		15.2208	180.5906	11.2476				0.0047	7
8	18.7335	1.8694			2276.1541		4307.3687	16.3917	194.5593	11.8990	22.9466	244.9394	0.4514	0.0047	8
8	18.7335	1.8694	0.6734		2276.1541	245.7901		16.3917	194.5593	11.8990				0.0043	8
9	21.0751	1.8737			2521.9442		4798.0982	17.5625	208.5319	12.0938	23.7928	245.7901	0.3948	0.0043	9
9	21.0751	1.8737	0.6733		2521.9442	246.5757		17.5625	208.5319	12.0938				0.0040	9
10	23.4168	1.8777			2768.5199		5290.4640	18.7333	222.5069	12.4423	24.5361	246.5757	0.3485	0.0040	10
10	23.4168	1.8777	0.6732		2768.5199	247.2954		18.7333	222.5069	12.4423				0.0036	10
11	25.7585	1.8813			3015.8153		5784.3352	19.9042	236.4874	12.7525	25.1948	247.2954	0.3103	0.0036	11
11	25.7585	1.8813	0.6732		3015.8153	247.9586		19.9042	236.4874	12.7525				0.0034	11
12	28.1002	1.8847	0.8731		3263.7749	361.2839	6279.5902	21.0750	250.4701	13.0306	25.7831	247.9586	0.2781	0.0034	12
12'	28.1002	1.8847			3625.0588										12

*Trapezoidal geometry
@output03.wk3

CSC = 0.1000, 0.1500, 0.2000, 0.2500, 0.3000, 0.3500

l/w = 2.5616
w/P = 2.8100 *(1 cycle)*

*COMMODEL.WK3

Check :

X12 = 28.1002 cm

l12 = 64.9550 cm

w12 = 21.0750 cm

TABLE A.3 (continued)

Sec. No.	X (cm)	H+ CSC*V^2/2*g (cm)	QL (cm^3/s)	Cd	QN (cm^3/s)	QL/QN	H/P
(17)	(18)	(19)	(20)	(21)	(22)	(23)	(24)
		1.8934		0.6729	1454.7264	2.4919	0.1893
		1.8977		0.6728	1458.5303	2.4837	0.1898
13	30.4419	1.9020	3625.0588	0.6728	1464.3396	2.4756	0.1902
		1.9063		0.6727	1469.1548	2.4674	0.1906
		1.9107		0.6726	1473.9755	2.4594	0.1911
		1.9150		0.6725	1478.8018	2.4513	0.1915

	INPUT		OUTPUT
l (cm) =	71.9600	l/w =	2.5616
w (cm) =	28.1000	w/P =	2.8100
a (cm) =	3.5125	QL/QN =	2.4919
P (cm) =	10.0000	H/P =	0.1893
g(cm/det^2) =	981.0000		
n =	12		
CSC =	0.1000		

* delta H is quoted from Open-Channel Hydraulics, Ven Te Chow, Ph.D., page 346

**delta H = ((Q1*(V2 + V1) delta V)/(g (Q2 − Q1)) * (1 − (delta Q/2*Q1))

*CSC = energy loss coefficient due to eddies contraction.

TABLE A.4

Table of computation for the determination of discharge of each section

Data

l =	71.9800 cm	g =	981.0000 cm/s^2	delta =	2.4138 cm	P =	10.0000 cm	X =	28.1002 cm
w =	29.1000 cm	alpha =	0.2450 radian						o
a =	3.5125 cm	delta x =	2.3417 cm	y =	7.0250 cm	b =	28.9650 cm	alpha =	14.0362
n =	12								

Sec. No	x (cm)	H (cm)	Cd	l (cm)	Q (cm^3/s)	delta Q (cm^3/s)	Q1 + Q2 (cm^3/s)	w (cm)	A (cm^2)	V (cm/s)	(V1 + V2) (cm/s)	delta Q (cm^3/s)	delta V (cm/s)	delta H (cm)	Sec No
(1)	(2)	(3)	(4)	(5)	(6)	(7)	(8)	(9)	(10)	(11)	(12)	(13)	(14)	(15)	(16)
0	0.0000														0
1	2.3417	2.4384	0.6655	11.8525	886.6858	362.6317		8.1958	101.8431	8.6998				0.0132	1
2	4.6834	2.4516	0.6654		1249.5175		2136.4033	9.3667	116.6300	10.7135	19.4133	362.6317	2.0137	0.0132	2
2	4.6834	2.4516	0.6654		1249.5175	365.6393		9.3667	116.6300	10.7135				0.0138	2
3	7.0250	2.4654			1615.1568		2864.6743	10.5375	131.3542	12.2962	23.0097	365.6393	1.5827	0.0138	3
3	7.0250	2.4654	0.6653		1615.1568	368.6122		10.5375	131.3542	12.2962				0.0134	3
4	9.3667	2.4788			1983.7689		3598.9257	11.7083	146.1060	13.5778	25.8738	368.6122	1.2814	0.0134	4
4	9.3667	2.4788	0.6651		1983.7689	371.4723		11.7083	146.1060	13.5778				0.0127	4
5	11.7084	2.4915			2355.2412		4339.0102	12.8792	160.8801	14.6397	28.2173	371.4723	1.0621	0.0127	5
5	11.7084	2.4915	0.6650		2355.2412	374.1639		12.8792	160.8801	14.6397				0.0118	5
6	14.0501	2.5033			2729.4051		5084.6464	14.0500	175.6714	15.5370	30.1767	374.1639	0.8973	0.0118	6
6	14.0501	2.5033	0.6649		2729.4051	376.6639		14.0500	175.6714	15.5370				0.0109	6
7	16.3918	2.5142			3106.0690		5835.4741	15.2208	190.4766	16.3068	31.8438	376.6639	0.7898	0.0109	7
7	16.3918	2.5142	0.6649		3106.0690	378.9708		15.2208	190.4766	16.3068				0.0100	7
8	18.7335	2.5242			3485.0398		6591.1088	16.3917	205.2925	16.9760	33.2828	378.9708	0.6691	0.0100	8
8	18.7335	2.5242	0.6648		3485.0398	381.1060		16.3917	205.2925	16.9760				0.0093	8
9	21.0751	2.5335			3866.1458		7351.1855	17.5625	220.1196	17.5638	34.5398	381.1060	0.5879	0.0093	9
9	21.0751	2.5335	0.6647		3866.1458	383.0901		17.5625	220.1196	17.5638				0.0086	9
10	23.4168	2.5421			4249.2359		8115.3816	18.7333	234.9554	18.0853	35.6491	383.0901	0.5214	0.0086	10
10	23.4168	2.5421	0.6646		4249.2359	384.9336		18.7333	234.9554	18.0853				0.0080	10
11	25.7585	2.5501			4634.1694		8883.4053	19.9042	249.7993	18.5516	36.6369	384.9336	0.4663	0.0080	11
11	25.7585	2.5501	0.6646		4634.1694	388.6486		19.9042	249.7993	18.5516				0.0074	11
12	28.1002	2.5575	0.6645		5020.8180	563.8271	9654.9654	21.0750	264.6494	18.9718	37.5231	388.6486	0.4200	0.0074	12
12'	28.1002	2.5575			5584.6431										12

*Trapezoidal geometry

@output04.wk3

Check:

X12 = 28.1002 cm

l12 = 84.9550 cm

w12 = 21.0750 cm

* delta H is quoted from Open-Channel Hydraulics, Ven Te Chow, Ph.D., page 348

CSC = 0.1000 / 0.1500 / 0.2000 / 0.2500 / 0.3000 / 0.3500

l/w = 2.5616

w/P = 2.8100 *(1 cycle).*

*COMMODEL.WK3

TABLE A.4 (continued)

Sec. No.	X (cm)	H+ CSC*V^2/2*g (cm)	QL (cm^3/s)	Cd	QN (cm^3/s)	QL/QN	H/P
(17)	(18)	(19)	(20)	(21)	(22)	(23)	(24)
		2.5758		0.6644	2279.1661	2.4503	0.2576
		2.5850		0.6643	2291.1290	2.4375	0.2585
13	30.4419	2.5942	5584.6431	0.6643	2303.1148	2.4248	0.2594
		2.6034		0.6642	2315.1227	2.4122	0.2603
		2.6125		0.6642	2327.1535	2.3998	0.2613
		2.6217		0.6641	2339.2069	2.3874	0.2622

**delta H = ((Q1*(V2 + V1) delta V)/(g (Q2 + Q1)) * (1 - (delta Q/2*Q1))

INPUT		OUTPUT	
l (cm) =	71.9800	l/w =	2.5616
w (cm) =	28.1000	w/P =	2.8100
a (cm) =	3.5125	QL/QN =	2.4503
P (cm) =	10.0000	H/P =	0.2576
g(cm/det^2) =	981.0000		
n =	12		
CSC =	0.1000		

*CSC = energy loss coefficient due to sudden contraction.

TABLE A.5

Table of computation for the determination of discharge of each section

Data :

l =	71.9800 cm	g =	981.0000 cm/s ^2	delta l =	2.4138 cm	P =	10.0000 cm	X =	28.1002 cm
w =	28.1000 cm	alpha =	0.2450 radian						o
a =	3.5125 cm	delta x =	2.3417 cm	y =	7.0250 cm	b =	28.9650 cm	alpha =	14.0362
n =	12								

Sec. No.	x (cm)	H (cm)	Cd	l (cm)	Q (cm^3/s)	delta Q (cm^3/s)	Q1 + Q2 (cm^3/s)	w (cm)	A (cm^2)	V (cm/s)	(V1 + V2) (cm/s)	delta Q (cm^3/s)	delta V (cm/s)	delta H (cm)	Sec. No
(1)	(2)	(3)	(4)	(5)	(6)	(7)	(8)	(9)	(10)	(11)	(12)	(13)	(14)	(15)	(16)
0	0.0000														0
1	2.3417	3.0480	0.6622	11.6525	1233.2773	505.1221		8.1958	106.8392	11.5325				0.0231	1
2	4.6834	3.0711	0.6621		1738.3994		2971.6767	9.3667	122.4326	14.1988	25.7313	505.1221	2.6663	0.0231	2
2	4.6834	3.0711	0.6621		1738.3994	511.0027		9.3667	122.4326	14.1988				0.0243	2
3	7.0250	3.0954			2249.4021		3987.8015	10.5375	137.9928	16.3009	30.4997	511.0027	2.1020	0.0243	3
3	7.0250	3.0954	0.6620		2249.4021	516.9331		10.5375	137.9928	16.3009				0.0237	3
4	9.3667	3.1191			2766.3352		5015.7373	11.7083	153.6028	18.0097	34.3105	516.9331	1.7088	0.0237	4
4	9.3667	3.1191	0.6620		2766.3352	522.6643		11.7083	153.6028	18.0097				0.0225	4
5	11.7084	3.1416			3288.9994		6055.3346	12.8792	169.2529	19.4325	37.4421	522.6643	1.4228	0.0225	5
5	11.7084	3.1416	0.6619		3288.9994	528.0816		12.8792	169.2529	19.4325				0.0210	5
6	14.0501	3.1626			3817.0810		7106.0605	14.0500	184.9348	20.6402	40.0726	528.0816	1.2077	0.0210	6
6	14.0501	3.1626	0.6619		3817.0810	533.1437		14.0500	184.9348	20.6402				0.0195	6
7	16.3918	3.1821			4350.2247		8167.3057	15.2208	200.6426	21.6815	42.3216	533.1437	1.0413	0.0195	7
7	16.3918	3.1821	0.6619		4350.2247	537.8594		15.2208	200.6426	21.6815				0.0181	7
8	18.7335	3.2002			4888.0842		9238.3089	16.3917	216.3733	22.5910	44.2724	537.8594	0.9095	0.0181	8
8	18.7335	3.2002	0.6618		4888.0842	542.2503		16.3917	216.3733	22.5910				0.0168	8
9	21.0751	3.2170			5430.3345		10318.4186	17.5625	232.1236	23.3942	45.9851	542.2503	0.8032	0.0168	9
9	21.0751	3.2170	0.6618		5430.3345	546.3512		17.5625	232.1236	23.3942				0.0157	9
10	23.4168	3.2327			5976.6856		11407.0201	18.7333	247.8926	24.1100	47.5041	546.3512	0.7158	0.0157	10
10	23.4168	3.2327	0.6618		5976.6856	550.1847		18.7333	247.8926	24.1100				0.0148	10
11	25.7585	3.2473			6526.8704		12503.5560	19.9042	263.6765	24.7533	48.8633	550.1847	0.6433	0.0148	11
11	25.7585	3.2473	0.6618		6526.8704	553.7743		19.9042	263.6765	24.7533				0.0137	11
12	28.1002	3.2610	0.6617		7080.6447	808.3767	13607.5151	21.0750	279.4756	25.3355	50.0888	553.7743	0.5821	0.0137	12
12'	28.1002	3.2610			7889.0214										12

*Trapezoidal geometry

@output05.wk3

CSC = 0.1000, 0.1500, 0.2000, 0.2500, 0.3000, 0.3500

l/w = 2.5616

w/P = 2.8100 *(1 cycle)*

*CONMODEL.WK3

Check :

X12 = 28.1002 cm

l12 = 64.9550 cm

w12 = 21.0750 cm

TABLE A.5 (continued)

Sec. No	X (cm)	H+ CSC*V^2/2*g (cm)	QL (cm^3/s)	Cd	QN (cm^3/s)	QL/QN	H/P
(17)	(18)	(19)	(20)	(21)	(22)	(23)	(24)
		3.2907		0.6617	3282.0770	2.4037	0.3294
		3.3101		0.6617	3306.4623	2.3859	0.3310
13	30.4419	3.3264	7889.0214	0.6617	3330.9140	2.3684	0.3326
		3.3428		0.6616	3355.4323	2.3511	0.3343
		3.3591		0.6616	3380.0169	2.3340	0.3359
		3.3755		0.6615	3404.6679	2.3171	0.3376

INPUT		OUTPUT	
l (cm) =	71.9800	l/w =	2.5616
w (cm) =	28.1000	w/P =	2.8100
a (cm) =	3.5125	QL/QN =	2.4037
P (cm) =	10.0000	H/P =	0.3294
g(cm/det^2) =	981.0000		
n =	12		
CSC =	0.1000		

* delta H is quoted from Open - Channel Hydraulics Ven Te Chow, Ph D , page 346

**delta H = ((Q1*(V2 + V1) delta V)/(g (Q2 + Q1)) * (1 - (delta Q2*Q1))

*CSC = energy loss coefficient due to sudden contraction.

TABLE A.6

Table of computation for the determination of discharge of each section

Data :

l =	71 9600 cm	g =	981 0000 cm/s ^ 2	delta l =	2 4138 cm	P =	10 0000 cm	X =	28 1002 cm
w =	28 1000 cm	alpha =	0 2450 radian						o
a =	3 5125 cm	delta x =	2 3417 cm	y =	7 0250 cm	b =	28 9650 cm	alpha =	14 0362
n =	12								

Sec No	x (cm)	H (cm)	Cd	l (cm)	Q (cm ^ 3/s)	delta Q (cm ^ 3/s)	Q1 + Q2 (cm ^ 3/s)	w (cm)	A (cm ^ 2)	V (cm/s)	(V1 + V2) (cm/s)	delta Q (cm ^ 3/s)	delta V (cm/s)	delta H (cm)	Sec No
(1)	(2)	(3)	(4)	(5)	(6)	(7)	(8)	(9)	(10)	(11)	(12)	(13)	(14)	(15)	(16)
0	0 0000														0
1	2.3417	3 8100	0 6617	11 8525	1722.3565	707.0941		8 1958	113.1845	15.2173				0 0400	1
2	4 6834	3 8500	0 6618		2429 4506		4151 8071	9 3667	129 7283	18.7272	33 9445	707 0941	3 5100	0 0400	2
2	4 6834	3 8500	0 6618		2429 4506	718.5203		9 3667	129.7283	18.7272				0 0423	2
3	7.0250	3 8923			3147.9710		5577.4216	10.5375	146.3901	21.5040	40 2312	718 5203	2 7768	0 0423	3
3	7 0250	3 8923	0 6618		3147.9710	730 2795		10 5375	146 3901	21.5040				0 0415	3
4	9 3667	3 9338			3876.2505		7026 2214	11.7063	163.1416	23.7723	45 2783	730 2795	2.2683	0.0415	4
4	9 3667	3 9338	0 6619		3878 2505	741.7149		11.7063	163.1416	23.7723				0 0395	4
5	11 7084	3.9733			4619.9654		8498 2158	12 8792	179 9645	25 6715	49.4438	741.7149	1.8992	0 0395	5
5	11 7084	3 9733	0.6619		4819 9654	752.6053		12 8792	179 9645	25 6715				0 0372	5
6	14 0501	4.0105			5372.5706		9992.5360	14.0500	196 8475	27.2931	52.9646	752 6053	1.6215	0 0372	6
6	14 0501	4 0105	0 6620		5372.5706	782.8831		14 0500	196 8475	27.2931				0.0348	6
7	16 3918	4 0453			6135 4537		11508.0243	15 2208	213.7812	28 8997	55 9927	782.8831	1.4066	0.0348	7
7	16 3918	4.0453	0.6621		6135.4537	772.5520		15 2208	213 7812	28.8997				0 0326	7
8	18 7335	4 0779			6906.0057		13043.4584	16 3917	230 7603	29 9359	58 8355	772.5520	1 2362	0 0326	8
8	18.7335	4.0779	0 6621		6906 0057	781.6458		16 3917	230.7603	29.9359				0.0305	8
9	21.0751	4.1084			7688 6514		14597.6571	17.5625	247.7788	31.0343	60 9702	781.6458	1 0985	0 0305	9
9	21.0751	4 1084	0 6622		7688.6514	790.1996		17 5625	247.7788	31.0343				0 0286	9
10	23 4168	4.1370			8478.8510		16169.5025	18.7333	264.8332	32.0196	63.0539	790.1996	0.9653	0 0286	10
10	23.4168	4.1370	0.6623		8479.8510	798 2500		18.7333	264.8332	32.0196				0.0268	10
11	25.7585	4.1638			9276 1010		17757.9521	19 9042	281.9187	32.9106	64.9302	798 2500	0 8910	0 0268	11
11	25.7585	4.1638	0 6623		9276.1010	805.8468		19.9042	281.9187	32.9106				0 0253	11
12	28.1002	4.1891	0.6624		10083 9498	1178.1088	19362.0508	21.0750	299.0353	33.7216	66.6322	805 8468	0 8110	0 0253	12
12'	28.1002	4.1891			11262.0586										12

*Trapezoidal geometry

CSC = 0.1000, 0.1500, 0.2000, 0.2500, 0.3000, 0.3500

l/w = 2.5616

w/P = 2.8100 *(1 cycle)*

*COMMODEL.WK3

@output06.wk3

Check :

X12 = 28.1002 cm

l12 = 84.9550 cm

w12 = 21.0750 cm

TABLE A.6 (continued)

Sec. No.	X (cm)	H+ CSC*V^2/2*g (cm)	QL (cm ^ 3/s)	Cd	QN (cm ^ 3/s)	QL/QN	H/P
(17)	(18)	(19)	(20)	(21)	(22)	(23)	(24)
		4.2471		0.6625	4811.5747	2.3406	0 4247
		4 2760		0.6626	4861.4363	2 3186	0.4276
13	30.4419	4.3050	11262.0586	0 6627	4911.4921	2.2930	0.4305
		4.3340		0.6627	4961.7417	2.2696	0.4334
		4 3630		0 6628	5012.1848	2.2469	0 4363
		4.3920		0 6629	5062 8210	2.2245	0 4392

INPUT		OUTPUT	
l (cm) =	71.9600	l/w =	2 5616
w (cm) =	28.1000	w/P =	2 8100
a (cm) =	3 5125	QL/QN =	2 3406
P (cm) =	10.0000	H/P =	0.4247
g(cm/det^2) =	981 0000		
n =	12		
CSC =	0.1000		

* delta H is quoted from Open – Channel Hydraulics, Ven Te Chow, Ph.D., page 346

** delta H = ((Q1*(V2 + V1) delta V)/(g (Q2 + Q1)) * (1 – (delta Q/2*Q1))

*CSC = energy loss coefficient due to sudden contraction.

TABLE A.7

Table of computation for the determination of discharge of each section

Data :

l =	71 9800 cm	g =	981 0000 cm/s ^2	delta l =	2 4136 cm	P =	10 0000 cm	X =	28 1002 cm
w =	28 1000 cm	alpha =	0 2450 radian						o
a =	3.5125 cm	delta x =	2 3417 cm	y =	7.0250 cm	b =	28 9650 cm	alpha =	14.0382
n =	12								

Sec. No.	x (cm)	H (cm)	Cd	l (cm)	Q (cm^3/s)	delta Q (cm^3/s)	Q1 + Q2 (cm^3/s)	w (cm)	A (cm^2)	V (cm/s)	(V1 + V2) (cm/s)	delta Q (cm^3/s)	delta V (cm/s)	delta H (cm)	Sec. No.
(1)	(2)	(3)	(4)	(5)	(6)	(7)	(8)	(9)	(10)	(11)	(12)	(13)	(14)	(15)	(16)
0	0 0000														0
1	2 3417	4 5720	0 6634	11.8525	2269.9966	934 3024		8 1958	119.4297	19 0070				0 0622	1
2	4 6834	4.6342	0.6636		3204.2991		5474 2957	9 3667	137 0737	23 3765	42.3834	934 3024	4 3695	0 0622	2
2	4 6834	4.6342	0.6636		3204.2991	953 8554		9.3667	137.0737	23.3785				0 0658	2
3	7.0250	4.7000			4158.1545		7362.4536	10 5375	154.9013	26.8439	50 2204	953 8554	3 4674	0 0658	3
3	7.0250	4.7000	0 6639		4158.1545	974.2738		10.5375	154.9013	26 8439				0 0648	3
4	9 3667	4.7648			5132.4281		9290 5825	11.7083	172.8712	29 6893	56 5332	974.2738	2 8454	0 0648	4
4	9 3667	4 7648	0 6641		5132.4281	994 2783		11 7083	172.8712	29.6893				0 0621	4
5	11.7084	4 8289			6126.7044		11259.1324	12.8792	190 9581	32.0640	61.7733	994 2783	2 3947	0 0621	5
5	11.7084	4.8289	0 6643		6126 7044	1013 4804		12.8792	190 9581	32.0640				0 0588	5
6	14 0501	4 8857			7140 1848		13266.8891	14.0500	209.1441	34 1400	66 2240	1013.4804	2 0560	0 0588	6
6	14 0501	4 8857	0 6645		7140.1848	1031.7510		14.0500	209.1441	34 1400				0 0554	6
7	16 3918	4 9411			8171 9358		15312.1205	15 2206	227.4160	35 9339	70 0739	1031.7510	1 7938	0 0554	7
7	16 3918	4 9411	0.6648		8171.9358	1049 0808		15 2206	227.4160	35 9339				0 0522	7
8	18 7335	4.9933			9221.0165		17392.9523	16 3917	245 7652	37.5196	73.4535	1049 0808	1.5656	0 0522	8
8	18 7335	4 9933	0 6650		9221.0165	1065 5139		16.3917	245.7652	37 5196				0 0492	8
9	21.0751	5 0425			10286 5304		19507 5489	17.5625	264 1839	38 9370	76.4566	1065 5139	1 4174	0 0492	9
9	21.0751	5 0425	0 6652		10286.5304	1081.0974		17 5625	264.1839	38.9370				0 0464	9
10	23 4168	5 0689			11367.6278		21654.1582	18.7333	282 6654	40 2158	79 1526	1081.0974	1 2768	0 0464	10
10	23 4168	5 0689	0 6653		11367.6278	1095 8969		18.7333	282.6654	40 2158				0 0439	10
11	25 7585	5.1326			12463 5247		23831.1525	19 9042	301.2058	41.3788	81 5946	1095 8969	1 1629	0 0439	11
11	25.7585	5.1326	0 6655		12463 5247	1109 9813		19.9042	301.2058	41.3788				0 0416	11
12	28.1002	5 1744	0 6657		13573.5060	1625 4688	26037.0307	21 0750	319.8005	42.4437	83.8224	1109 9813	1 0649	0 0416	12
12	28.1002	5 1744			15198.9747										12

*Trapezoidal geometry

@output07.wk3

Check :

X12 = 28 1002 cm

l12 = 64 9550 cm

w12 = 21 0750 cm

* delta H is quoted from Open – Channel Hydraulics Van Te Chow Ph D., page 346

CSC = 0 1000, 0 1500, 0 2000, 0 2500, 0 3000, 0 3500

l/w = 2 5618

w/P = 2 8100 *(1 cycle)*

*COMMODEL.WK3

TABLE A.7 (continued)

Sec. No	X (cm)	H+ CSC*V^2/2*g (cm)	QL (cm^3/s)	Cd	QN (cm^3/s)	QL/QN	H/P
(17)	(18)	(19)	(20)	(21)	(22)	(23)	(24)
		5 2662		0 6661	6679 6896	2 2754	0 5256
		5 3121		0 6663	6789 2914	2 2453	0 5312
13	30 4419	5 3580	15198 9747	0 6665	6859 3548	2 2158	0 5358
		5 4039		0 6667	6949 8789	2 1869	0 5404
		5 4499		0 6669	7040 8628	2 1567	0 5450
		5 4958		0 6672	7132 3057	2 1310	0 5496

**Delta H = ((Q1*(V2 + V1) delta V) / (Q2 + Q1)) * (1 + (delta Q2*Q1))

INPUT		OUTPUT	
l (cm) =	71 9800	l/w =	2 5618
w (cm) =	28 1000	w/P =	2 8100
a (cm) =	3 5125	QL/QN =	2 2754
P (cm) =	10 0000	H/P =	0 5268
g(cm/del^2) =	981 0000		
n =	12		
CSC =	0 1000		

*CSC = energy loss coefficient due to sudden contraction

TABLE A.8

Table of computation for the determination of discharge of each section

Data :

l =	71.9800 cm	g =	981.0000 cm/s ^2	delta l =	2.4138 cm	P =	10 0000 cm	X =	28 1002 cm
w =	28 1000 cm	alpha =	0 2450 radian						o
a =	3.5125 cm	delta x =	2.3417 cm	y =	7.0250 cm	b =	28 9650 cm	alpha =	14.0362
n =	12								

Sec. No	x (cm)	H (cm)	Cd	l (cm)	Q (cm^3/s)	delta Q (cm^3/s)	Q1 + Q2 (cm^3/s)	w (cm)	A (cm^2)	V (cm/s)	(V1 + V2) (cm/s)	delta Q (cm^3/s)	delta V (cm/s)	delta H (cm)	Sec. No.
(1)	(2)	(3)	(4)	(5)	(6)	(7)	(8)	(9)	(10)	(11)	(12)	(13)	(14)	(15)	(16)
0	0 0000														0
1	2.3417	4 9530	0.6648	11.8525	2564.8506	1057.0533		6.1958	122 5523	20 9286				0 0752	1
2	4.6834	5 0282	0.6651		3621 9038		6186.7544	9 3667	140.7641	25 7303	46.6589	1057.0533	4 8017	0 0752	2
2	4.6834	5 0282	0 6651		3621.9038	1081.7394		9 3667	140.7641	25.7303				0 0766	2
3	7.0250	5.1078			4703 6432		8325 5471	10 5375	159.1965	29 5458	55.2761	1081.7394	3 8155	0 0796	3
3	7.0250	5.1078	0.6654		4703.6432	1107.7012		10.5375	159.1965	29 5458				0.0786	3
4	9 3667	5.1664			5811.3444		10514 9877	11 7083	177 8070	32.6834	62.2292	1107 7012	3 1377	0 0786	4
4	9.3667	5.1664	0 6658		5811.3444	1133.2257		11.7083	177.8070	32 6834				0 0755	4
5	11.7084	5.2619			6944.5702		12755.9146	12 8792	196 5601	35 3305	68 0140	1133 2257	2 6471	0 0.'55	5
5	11.7084	5 2619	0.6661		6944.5702	1157.6274		12 8792	196 5601	35.3305				0 0717	5
6	14 0501	5 3336			8102.3976		15048.9677	14.0500	215 4365	37.6092	72 9397	1157 6274	2.2787	0 0717	6
6	14 0501	5 3336	0 6664		8102 3976	1181.3328		14.0500	215 4365	37.6092				0 0678	6
7	16 3918	5 4014			9283.7304		17386.1279	15 2208	234 4216	39 6027	77 2119	1181 3328	1 9935	0 0678	7
7	16 3918	5 4014	0 6667		9283.7304	1203.7267		15 2206	234.4216	39.6027				0 0641	7
8	18 7335	5 4655			10487.4571		19771.1874	16 3917	253 5047	41 3699	80 9726	1203.7267	1 7672	0 0641	8
8	18.7335	5 4655	0 6670		10487.4571	1225 0490		16.3917	253 5047	41.3699				0 0606	8
9	21.0751	5 5261			11712 5061		22199.9632	17.5625	272 8785	42 9539	84 3237	1225 0490	1 5840	0 0606	9
9	21.0751	5 5261	0 6673		11712.5061	1245 3598		17.5625	272 8785	42 9539				0.0574	9
10	23.4168	5 5835			12957.8659		24870.3721	18.7333	291.9302	44 3869	87.3407	1245 3598	1.4330	0 0574	10
10	23 4168	5.5835	0.6676		12957 8659	1264.7237		18.7333	291.9302	44.3869				0 0544	10
11	25 7585	5 6379			14222 5896		27180 4556	19 9042	311 2586	45 6938	90 0607	1264 7237	1 3069	0 0544	11
11	25.7585	5 6379	0 6678		14222.5896	1283 2078		19 9042	311 2586	45 6938				0 0517	11
12	28 1002	5 6898	0.6681		15505 7974	1860 8394	29728 3870	21 0750	330 6575	46 8938	92 5876	1283.2078	1.2000	0 0517	12
12'	28 1002	5 6898			17386 6368										12

CSC = 0 1000, 0 1500, 0 2000, 0 2500, 0 3000, 0 3500

l/w = 2 5616

w/P = 2 8100 *(1 cycle)*.

*Trapezoidal geometry

@output0* wk3

*COMMODEL.WK3

Check .

X12 = 28 1002 cm

l12 = 64 9550 cm

w12 = 21 0750 cm

TABLE A.8 (continued)

Sec. No	X (cm)	H+ CSC*V^2/2*g (cm)	QL (cm^3/s)	Cd	QN (cm^3/s)	QL/QN	H/P
(17)	(18)	(19)	(20)	(21)	(22)	(23)	(24)
		5 8016		0.6686	7753 2202	2 2425	0 5802
		5 8577		0 6689	7889 1640	2 2095	0 5858
13	30 4419	5 9137	17386 6368	0 6692	7985 7810	2 1772	0 5914
		5 9698		0 6695	8103.0699	2 1457	0 5970
		6 0258		0 6698	8221.0293	2 1149	0 6026
		6 0818		0 6701	8339 8578	2 0848	0 6082

INPUT		OUTPUT	
l (cm) =	71 9800	l/w =	2 5616
w (cm) =	28 1000	w/P =	2 8100
a (cm) =	3.5125	QL/QN =	2 2425
P (cm) =	10 0000	H/P =	0 5802
g(cm/det^2) =	981 0000		
n =	12		
CSC =	0 1000		

* delta H is quoted from Open – Channel Hydraulics, Ven Te Chow, Ph.D., page 346

**delta H = ((Q1*(V2 + V1) delta V)/(g (Q2 + Q1)) * (1 – (delta Q2*Q1))

*CSC = energy loss coefficient due to sudden contraction

APPENDIX B

Listing of QuickBASIC program

```
10  CLS

20  '*************************************************************************
30  'This QuickBASIC program computes the flow magnification (QL/QN) and the depth
40  'to crest height ratio (H/P) of one cycle labyrinth weir.
50  'The program is modified from Hay and Taylor computer program, pp.214-221,
60  'October 1968, Faculty of Applied Science, University of Nottingham.
70  'Modification is made by Adolf Tommy Sitompul, Faculty of Engineering and
80  'Applied Science, Memorial University of Newfoundland.
90  '*************************************************************************

100 DIM H(200), X(200), w(200), A(200), V(200), CD(200), Q(200), delh(200),
    delha(200), delQ(200), delQa(200), delV(200)

110 LPRINT
120 LPRINT
130 LPRINT
140 LPRINT "                              DESIGN DATA "
150 LPRINT "                              ___________ "
160 LPRINT
170 T1$ = "      - Length Magnification ..........................l/w    = ##.#### "
180 T2$ = "      - Vertical aspect ratio ..........................w/P    = ##.#### "
190 T3$ = "      - Angle of side walls ..........................alpha  = ##.#### "
200 T4$ = "                                QL/QN = ##.#### "
210 T5$ = "                                 H/P  =  #.#### "

220 '*************
230 'DATA INPUT
240 '*************

250 INPUT "Length of labyrinth weir, l(cm) = "; l
260 INPUT "Width of labyrinth weir, w(cm) = "; w
270 INPUT "Half length of tip section of labyrinth weir, a(cm) = "; a
280 INPUT "Gravitational acceleration, g(cm/det2) = "; g
290 INPUT "Crest height of labyrinth weir, P(cm) = "; P
300 INPUT "Number of sections, n = "; n
310 INPUT "Energy loss coefficient, CSC = "; CSC

320 LPRINT "       o Labyrinth weir geometry : "
330 LPRINT "         ________________________ "
340 LPRINT
350 LPRINT "       - Length of labyrinth weir ..........l (cm) ="; l
360 LPRINT "       - Width of labyrinth weir ..........w (cm) ="; w
370 LPRINT "       - Crest height of labyrinth weir ..... P (cm) ="; P
```

```
380 LPRINT "       - Half length of tip section of labyrinth weir .... a (cm) ="; a
390 LPRINT

400 '*********************************
410 'CALCULATION OF PARAMETERS
420 '*********************************

430 LWR = l / w
440 WPR = w / P
450 y = (w / 2) - (2 * a)
460 b = (l - (4 * a)) / 2
470 X = ((b) ^ 2 - (y) ^ 2) ^ .5
480 ALPHA = ATN(y / X)
490 delX = X / n
500 delL = delX / COS(ALPHA)
510 ALPHA1 = ALPHA * 57.295779513082 32#

520 LPRINT
530 LPRINT "       o Design Parameter : "
540 LPRINT "         ------------------ "
550 LPRINT
560 LPRINT USING T1$; LWR
570 LPRINT USING T2$; WPR
580 LPRINT USING T3$; ALPHA1
590 LPRINT "       - Energy loss coefficient ..... CSC    ="; CSC
600 LPRINT "       - Gravitational acceleration ..... g (cm/s^2) ="; g
610 LPRINT
620 LPRINT
630 LPRINT "                    HYDRAULIC CALCULATION - RESULTS "
640 LPRINT "                    ------------------------------- "
650 LPRINT
660 LPRINT "                      QL/QN vs H/P Relationship "
670 LPRINT "                      ------------------------ "
680 LPRINT
690 LPRINT "                       H1      QL/QN      H/P    "
700 LPRINT "                      ------------------------- "
710 LPRINT
720 LPRINT

730 INPUT "Initial delta h, delh = "; delh

740 INPUT "The level of acceptable error, E = "; E

750 INPUT "The minimum value of initial depth, Hminimum = "; HMIN
```

```
760 INPUT "The maximum value of initial depth, Hmaximum = "; HMAX

770 IF HMAX < P THEN 810 ELSE PRINT "Sorry, the value exceeds the maximum
    value allowed, Please Try again ": GOTO 790

780 INPUT "The increment of desired initial depth, Increment = "; INC

790 FOR H1 = HMIN TO HMAX STEP INC

800 '****************************************
810 'CALCULATION OF INITIAL DISCHARGE
820 '****************************************

830 H(1) = H1

840 X1 = delX
850 X(1) = X1

860 l1 = (2 * a + 2 * delL)

870 w1 = (2 * a + 2 * X1 * TAN(ALPHA))
880 w(1) = w1

890 CD1 = .605 + .08 * (H1 / P) + 1 / (10.006562# * H1)
900 CD(1) = CD1

910 Q1 = CD1 * l1 * (H1 ^ 1.5) * (2 / 3) * ((2 * g) ^ .5)
920 Q(1) = Q1

930   FOR I = 2 TO n

940     delh(I - 1) = delh
950     X(I) = X(I - 1) + delX

960     w(I) = (2 * a + 2 * X(I) * TAN(ALPHA))

970       WHILE ABS(delh(I - 1) - delha(I - 1)) > E

980         delh(I - 1) = delha(I - 1)

990         H(I) = H(I - 1) + delh(I - 1)

1000        CD(I) = .605 + .08 * (((H(I - 1) + H(I)) / 2) / P)
            + 1 / (10.006562# * ((H(I - 1) + H(I)) / 2))
```

```
1010        delQ(I - 1) = CD(I) * delL * (((H(I - 1) + H(I)) / 2) ^ 1.5) * (2 / 3)
              * ((2 * g) ^ .5)

1020        Q(I) = Q(I - 1) + 2 * delQ(I - 1)

1030        A(I - 1) = (H(I - 1) + P) * w(I - 1)

1040        A(I) = (H(I) + P) * w(I)

1050        V(I - 1) = Q(I - 1) / A(I - 1)

1060        V(I) = Q(I) / A(I)

1070        delV(I - 1) = V(I) - V(I - 1)

1080        delQa(I - 1) = Q(I) - Q(I - 1)

1090        delha(I - 1) = ((Q(I - 1) * (V(I - 1) + V(I)) * delV(I - 1))
            /(g * (Q(I - 1) + Q(I))) * (1 - (delQa(I - 1) / (2 * Q(I - 1))))

1100        delhfix = delha(I - 1)

1110      WEND

1120    H(I) = H(I - 1) + delhfix

1130  NEXT I

1140 HL = H(n)
1150 QLWL = Q(n)

1160 CDLWLS = CD(n)
1170 VLWLS = V(n)

1180 delQtip = CDLWLS * a * (HL ^ 1.5) * (2 / 3) * ((2 * g) ^ .5)

1190 QL = QLWL + 2 * delQtip

1200 ELOSS = CSC * ((VLWLS ^ 2) / (2 * g))

1210 HTOT = HL + ELOSS

1220 CDNW = .605 + .08 * (HTOT / P) + 1 / (10.006562# * HTOT)
```

```
1230 QN = CDNW * W * (HTOT ^ 1.5) * (2 / 3) * ((2 * g) ^ .5)

1240 QLQNR = QL / QN

1250 HPR = HTOT / P

1260 IF HPR > .6 GOTO 1320

1270 '****************
1280 'DATA OUTPUT
1290 '****************

1300 LPRINT USING "          ##.####   ##.####   ##.#### "; H1; QLQNR; HPR

1310 NEXT H1

1320 LPRINT
1330 LPRINT "                                    _____ "
1340 LPRINT
1350 LPRINT "                The level of acceptable error :"; E
1360 LPRINT
1370 IF ALPHA1 = 0 THEN LPRINT " Rectangular Shape " ELSE LPRINT
     Trapezoidal Shape "
1380 LPRINT
1390 LPRINT "                          Filename : COMPUTE1.BAS "
1400 LPRINT
1410 LPRINT "                             End of Results "

1420 END
```

APPENDIX C

Input and output of QuickBASIC program

DESIGN DATA

o Labyrinth weir geometry :

- Length of labyrinth weir ..... l (cm) = 71.98
- Width of labyrinth weir ..... w (cm) = 28.1
- Crest height of labyrinth weir ..... P (cm) = 10
- Half length of tip section of labyrinth weir .... a (cm) = 3.51

o Design Parameter :

- Length Magnification ..... l/w = 2.5616
- Vertical aspect ratio ..... w/P = 2.8100
- Angle of side walls ..... alpha = 14.0439
- Energy loss coefficient ..... CSC = .1
- Gravitational acceleration ..... g (cm/s^2) = 981

HYDRAULIC CALCULATION - RESULTS

QL/QN vs H/P Relationship

H1	QL/QN	H/P
0.4000	2.5557	0.0401
0.7500	2.5457	0.0756
1.1000	2.5317	0.1117
1.4500	2.5141	0.1485
1.8000	2.4937	0.1862
2.1500	2.4708	0.2249
2.5000	2.4459	0.2646
2.8500	2.4193	0.3056
3.2000	2.3915	0.3479
3.5500	2.3627	0.3914
3.9000	2.3332	0.4364
4.2500	2.3033	0.4827
4.6000	2.2732	0.5305
4.9500	2.2431	0.5797

The level of acceptable error : .00005

Trapezoidal Shape

Filename : COMPUTE1.BAS

End of Results

APPENDIX D

Experimental data of

all weir models

Remarks

(for Table D.1 to Table D.13)

1). Column 1 indicates the number of the test.

2). Column 2, Q_{TL} is the experimental total flowrate at the labyrinth weir regardless of the number of cycles. (Note that Q_L is the flowrate over one cycle. At low flow rates (less than 8.1 l/s) Q_{TL} was measured directly by rotameter. At higher flows Q_{TL} was estimated from equation 5.1 whic is :

$$Q_{TL} = 15.21\ H^{2.5}$$

where H is the experimental average flow depth over the V-notch weir crest in cm.

3). Column 3, H is the experimental mean depth over the weir model crest. Three depth measurements were taken 250 mm upstream of weir model (see Figure 5-27). The mean depth, H, is the average.

4). Column 4 indicates the experimental value of C_d. This is calculated by rearranging the standard weir equation (equation 4.1) to give :

$$C_d = \frac{Q_{TL} \times 1000}{\frac{2}{3}\sqrt{2g}\ L\ H^{1.5}}$$

where Q_{TL} is the experimental total flowrate at labyrinth weir (column 2) in l/s; L is the total developed length of labyrinth weir in cm ; g is the acceleration due to gravity = 981 cm/sec^2; and H is the experimental mean depth over the weir model crest (column 3) in cm.

5). Column 5 indicates the theoretical value of C_d. This is estimated from the Rehbock equation (equation 4.3) ie :

$$C_d = 0.605 + 0.08 \frac{H}{P} + \frac{1}{10.007 H}$$

where H is the experimental mean depth over the weir crest (column 3) in cm; and P is the weir height in cm.

6). Column 6 indicates the difference between experimental and theoretical values of C_d. This value, ΔC_d, is obtained from the equation :

$$\Delta C_d = \frac{(Experimental\ C_d - Theoretical\ C_d)}{(Theoretical\ C_d)} \times 100\ \%$$

7). Column 7 indicates the theoretical flowrate Q_{TN} a straight weir constructed across the channel width (sometimes called the presumptive linear weir). This is estimated from the standard weir equation (equation 4.1) using the total channel width, W, and the theoretical value of C_d. This gives by :

$$Q_{TN} = \frac{C_d \frac{2}{3} \sqrt{2g}\ W H^{1.5}}{1000}$$

where Q_{TN} is the theoretical flowrate at the straight weir (column 7) in l/s; C_d is the theoretical discharge coefficient (column 5) and H is the experimental mean depth over the weir crest (column 3) in cm.

Note that Q_{TN} is the flowrate calculated on the basis of full channel width, the value of Q_N, used previously, refers to a straight weir with a crest length equal to the channel width for one cycle only.

8). Column 8 indicates the flow magnification, Q_{TL}/Q_{TN}. This, of course, is equal to Q_L/Q_N. This is calculated from column (2) divided by column (7).

9). Column 9 indicates the depth to weir height ratio, H/P. This is calculated from column (3) divided by weir height, P.

Table D.6 refers to a straight weir and therefore does not have values for flow magnification (Q_{TL}/Q_{TN} or Q_L/Q_N) and theoretical Q_{TN}.

TABLE D.1

Experimental data of model no.1 (see Figure 5-1)

Trapezoidal	two-cycle	
P = 10.00 cm	W = 56.20 cm	g = 981 cm/sec^2
L = 143.96 cm	L/W = 2.56	α = 14.04°

Test no.	Q_{TL} (l/s)	H (cm)	Experimental C_d	Theoretical C_d	Difference in C_d (%)	Theoretical Q_{TN} (l/s)	Q_{TL}/Q_{TN} or Q_L/Q_N	H/P
(1)	(2)	(3)	(4)	(5)	(6)	(7)	(8)	(9)
1.	3.53	1.14	0.68	0.70	-2.67	1.42	2.49	0.11
2.	4.19	1.27	0.69	0.69	-0.37	1.64	2.55	0.13
3.	4.94	1.41	0.69	0.69	0.86	1.91	2.58	0.14
4.	5.57	1.68	0.60	0.68	-11.11	2.44	2.28	0.17
5.	5.63	1.57	0.67	0.68	-0.95	2.22	2.54	0.16
6.	6.39	1.68	0.69	0.68	1.73	2.45	2.61	0.17
7.	7.16	1.84	0.68	0.67	0.23	2.79	2.57	0.18
8.	7.61	1.93	0.67	0.67	-0.75	2.99	2.54	0.19
9.	8.61	2.20	0.62	0.67	-7.09	3.62	2.38	0.22
10.	11.01	2.37	0.71	0.67	6.77	4.03	2.73	0.24
11.	11.89	2.51	0.70	0.66	5.83	4.39	2.71	0.25
12.	12.98	2.67	0.70	0.66	5.28	4.81	2.70	0.27
13.	14.54	3.00	0.66	0.66	-0.47	5.70	2.55	0.30
14.	15.13	3.00	0.68	0.66	3.36	5.71	2.65	0.30
15.	16.80	3.14	0.71	0.66	7.05	6.13	2.74	0.31
16.	19.31	3.49	0.70	0.66	5.35	7.16	2.70	0.35
17.	21.38	3.80	0.68	0.66	2.64	8.13	2.63	0.38
18.	27.18	4.74	0.62	0.66	-6.79	11.38	2.39	0.47
19.	27.94	4.77	0.63	0.66	-5.02	11.48	2.43	0.48
20.	30.00	4.98	0.64	0.66	-4.45	12.26	2.45	0.50
21.	37.92	6.04	0.60	0.67	-10.38	16.52	2.30	0.60

TABLE D.2

Experimental data of model no.2 (see Figure 5-1)

Trapezoidal	four-cycle	
P = 10.00 cm	W = 56.20 cm	g = 981 cm/sec^2
L = 143.95 cm	L/W = 2.56	α = 14.04°

Test no.	Q_{TL} (l/s)	H (cm)	Experimental C_d	Theoretical C_d	Difference in C_d (%)	Theoretical Q_{TN} (l/s)	Q_{TL}/Q_{TN} or Q_L/Q_N	H/P
(1)	(2)	(3)	(4)	(5)	(6)	(7)	(8)	(9)
1.	3.86	1.28	0.63	0.69	-9.74	1.67	2.31	0.13
2.	4.59	1.42	0.64	0.69	-7.03	1.93	2.38	0.14
3.	5.22	1.54	0.64	0.68	-5.50	2.16	2.42	0.15
4.	5.96	1.68	0.64	0.68	-5.29	2.46	2.43	0.17
5.	7.36	1.78	0.73	0.68	7.97	2.66	2.77	0.18
6.	8.14	1.91	0.73	0.67	8.13	2.94	2.77	0.19
7.	9.62	2.18	0.70	0.67	5.16	3.57	2.69	0.22
8.	12.91	2.65	0.70	0.66	6.12	4.75	2.72	0.26
9.	15.50	3.09	0.67	0.66	1.64	5.96	2.60	0.31
10.	19.81	3.65	0.67	0.66	1.05	7.65	2.59	0.36
11.	22.76	4.15	0.63	0.66	-4.45	9.30	2.45	0.42
12.	24.87	4.50	0.61	0.66	-7.53	10.50	2.37	0.45
13.	26.16	4.77	0.59	0.66	-10.96	11.47	2.28	0.48
14.	27.19	4.98	0.58	0.66	-13.46	12.27	2.22	0.50
15.	29.31	5.34	0.56	0.67	-16.07	13.63	2.15	0.53

TABLE D.3

Experimental data of model no.3 (see Figure 5-1)

Trapezoidal	two-cycle	
P = 10.00 cm	W = 56.20 cm	g = 981 cm/sec^2
L = 151.49 cm	L/W = 2.69	α = 9.42°

Test no.	Q_{TL} (l/s)	H (cm)	Experimental C_d	Theoretical C_d	Difference in C_d (%)	Theoretical Q_{TN} (l/s)	Q_{TL}/Q_{TN} or Q_L/Q_N	H/P
(1)	(2)	(3)	(4)	(5)	(6)	(7)	(8)	(9)
1.	4.73	1.34	0.68	0.69	-1.30	1.78	2.66	0.13
2.	6.24	1.59	0.70	0.68	2.62	2.25	2.77	0.16
3.	7.60	1.84	0.68	0.67	1.08	2.79	2.72	0.18
4.	9.46	2.14	0.67	0.67	0.89	3.48	2.72	0.21
5.	11.69	2.51	0.66	0.66	-1.45	4.40	2.66	0.25
6.	16.87	3.10	0.69	0.66	4.17	6.01	2.81	0.31
7.	21.39	3.56	0.71	0.66	7.56	7.38	2.90	0.36
8.	23.90	3.85	0.71	0.66	6.83	8.30	2.88	0.39
9.	29.09	4.60	0.66	0.66	-0.74	10.87	2.68	0.46
10.	31.75	4.99	0.64	0.66	-4.20	12.30	2.58	0.50
11.	35.27	5.51	0.61	0.67	-8.68	14.33	2.46	0.55

TABLE D.4

Experimental data of model no.4 (see Figure 5-1), rectangular-two cycle

P = 10.00 cm	W = 56.20 cm	g = 981 cm/sec²
L = 168.60 cm	L/W = 3.00	α = 0°

Test no. (1)	Q_{TL} (l/s) (2)	H (cm) (3)	Experimental C_d (4)	Theoretical C_d (5)	Difference in C_d (%) (6)	Theoretical Q_{TN} (l/s) (7)	Q_{TL}/Q_{TN} or Q_L/Q_N (8)	H/P (9)
1.	4.24	1.16	0.68	0.70	-3.04	1.46	2.91	0.12
2.	4.88	1.28	0.68	0.69	-2.40	1.67	2.93	0.13
3.	5.49	1.39	0.68	0.69	-1.83	1.87	2.94	0.14
4.	6.28	1.50	0.69	0.68	0.30	2.09	3.01	0.15
5.	6.94	1.61	0.68	0.68	0.37	2.31	3.01	0.16
6.	7.70	1.74	0.67	0.68	-0.60	2.58	2.98	0.17
7.	9.05	1.98	0.65	0.67	-2.53	3.10	2.92	0.20
8.	10.71	2.27	0.63	0.67	-5.74	3.79	2.83	0.23
9.	11.88	2.50	0.60	0.66	-9.49	4.37	2.72	0.25
10.	13.72	2.74	0.61	0.66	-8.57	5.00	2.74	0.27
11.	16.03	3.01	0.62	0.66	-6.80	5.73	2.80	0.30
12.	17.90	3.27	0.61	0.66	-7.97	6.48	2.76	0.33
13.	19.05	3.45	0.60	0.66	-9.72	7.03	2.71	0.34
14.	21.75	3.77	0.60	0.66	-9.77	8.04	2.71	0.38
15.	22.58	3.98	0.57	0.66	-13.65	8.72	2.59	0.40
16.	23.99	4.08	0.58	0.66	-11.83	9.07	2.65	0.41
17.	24.97	4.20	0.58	0.66	-11.93	9.45	2.64	0.42
18.	27.19	4.52	0.57	0.66	-14.36	10.58	2.57	0.45
19.	28.66	4.77	0.55	0.66	-16.66	11.46	2.50	0.48
20.	29.09	4.84	0.55	0.66	-17.30	11.73	2.48	0.48
21.	31.19	5.08	0.55	0.67	-17.65	12.62	2.47	0.51
22.	34.43	5.63	0.52	0.67	-22.45	14.80	2.33	0.56
23.	35.03	5.68	0.52	0.67	-22.29	15.03	2.33	0.57
24.	37.00	5.96	0.51	0.67	-23.80	16.18	2.29	0.60

TABLE D.5

Experimental data of model no.5 (see Figure 5-1), rectangular with a semi-circular connections, 2 cycle

P = 10.00 cm	W = 56.20 cm	g = 981 cm/sec^2
L = 150.51 cm	L/W = 2.68	α = 0°

Test no. (1)	Q_{TL} (l/s) (2)	H (cm) (3)	Experimental C_d (4)	Theoretical C_d (5)	Difference in C_d (%) (6)	Theoretical Q_{TN} (l/s) (7)	Q_{TL}/Q_{TN} or Q_L/Q_N (8)	H/P (9)
1.	3.37	1.06	0.70	0.71	-1.48	1.28	2.64	0.11
2.	4.28	1.22	0.71	0.70	1.97	1.57	2.73	0.12
3.	4.86	1.36	0.69	0.69	0.42	1.81	2.69	0.14
4.	6.28	1.63	0.68	0.68	-0.29	2.35	2.67	0.16
5.	7.58	1.88	0.66	0.67	-2.12	2.89	2.62	0.19
6.	9.79	2.21	0.67	0.67	0.68	3.63	2.70	0.22
7.	11.13	2.37	0.68	0.67	2.82	4.04	2.75	0.24
8.	12.45	2.59	0.67	0.66	1.42	4.58	2.72	0.26
9.	13.45	2.75	0.66	0.66	-0.17	5.03	2.67	0.28
10.	15.58	3.00	0.67	0.66	1.75	5.72	2.72	0.30
11.	17.38	3.26	0.66	0.66	0.41	6.46	2.69	0.33
12.	19.51	3.54	0.66	0.66	-0.39	7.32	2.67	0.35
13.	20.86	3.74	0.65	0.66	-2.10	7.95	2.62	0.37
14.	23.04	4.00	0.65	0.66	-2.10	8.79	2.62	0.40
15.	25.16	4.29	0.64	0.66	-3.87	9.77	2.57	0.43
16.	26.98	4.52	0.63	0.66	-4.63	10.56	2.55	0.45
17.	28.61	4.72	0.63	0.66	-5.54	11.31	2.53	0.47
18.	29.09	4.79	0.63	0.66	-5.86	11.54	2.52	0.48
19.	30.07	5.00	0.61	0.66	-9.01	12.34	2.44	0.50
20.	31.75	5.15	0.61	0.67	-8.06	12.90	2.46	0.51
21.	32.50	5.26	0.61	0.67	-9.13	13.35	2.43	0.53
22.	34.19	5.50	0.60	0.67	-10.56	14.28	2.40	0.55
23.	35.52	5.68	0.59	0.67	-11.74	15.03	2.36	0.57
24.	36.87	5.86	0.58	0.67	-12.64	15.76	2.34	0.59

TABLE D.6

Experimental data of model no.6 (see Figure 5-2)

Straight Weir		
P = 10.00 cm	W = 56.20 cm	g = 981 cm/sec^2
L = 56.20 cm	L/W = 1.00	α = 90°

Test no.	Q_{TL} (l/s)	H (cm)	Experi-mental C_d	Theore-tical C_d	Diffe-rence in C_d (%)	H/P
(1)	(2)	(3)	(4)	(5)	(6)	(7)
1.	2.43	1.52	0.78	0.68	14.11	0.15
2.	2.71	1.76	0.70	0.68	3.28	0.18
3.	3.77	2.08	0.75	0.67	12.72	0.21
4.	4.13	2.32	0.71	0.67	5.83	0.23
5.	4.30	2.51	0.65	0.66	-2.22	0.25
6.	4.87	2.56	0.71	0.66	7.57	0.26
7.	5.46	2.77	0.71	0.66	7.73	0.28
8.	6.21	3.01	0.72	0.66	8.16	0.30
9.	6.22	3.13	0.68	0.66	2.29	0.31
10.	6.94	3.23	0.72	0.66	9.12	0.32
11.	7.63	3.44	0.72	0.66	8.83	0.34
12.	9.43	3.87	0.75	0.66	12.69	0.39
13.	13.55	5.03	0.72	0.67	8.95	0.50
14.	16.69	5.82	0.72	0.67	7.07	0.58
15.	17.66	5.95	0.73	0.67	9.45	0.60

TABLE D.7

Experimental data of model no.7 (see Figure 5-2)

Reverse	trapezoidal shape	two-cycle
P = 10.00 cm	W = 56.20 cm	g = 981 cm/sec^2
L = 200.16 cm	L/W = 3.56	α = 14.04°

Test no.	Q_{TL} (l/s)	H (cm)	Experimental C_d	Theoretical C_d	Difference in C_d (%)	Theoretical Q_{TN} (l/s)	Q_{TL}/Q_{TN} or Q_L/Q_N	H/P
(1)	(2)	(3)	(4)	(5)	(6)	(7)	(8)	(9)
1.	5.07	1.38	0.53	0.69	-23.33	1.86	2.73	0.14
2.	6.41	1.65	0.51	0.68	-24.37	2.38	2.69	0.16
3.	7.89	2.00	0.47	0.67	-29.45	3.14	2.51	0.20
4.	8.92	2.26	0.45	0.67	-33.26	3.75	2.38	0.23
5.	10.07	2.57	0.41	0.66	-37.76	4.54	2.22	0.26
6.	12.19	3.07	0.38	0.66	-42.17	5.92	2.06	0.31
7.	12.26	3.16	0.37	0.66	-44.22	6.17	1.99	0.32
8.	14.78	3.75	0.34	0.66	-47.96	7.97	1.85	0.37
9.	16.03	3.99	0.34	0.66	-48.66	8.77	1.83	0.40
10.	17.18	4.28	0.33	0.66	-50.49	9.75	1.76	0.43
11.	18.80	4.57	0.33	0.66	-50.96	10.76	1.75	0.46
12.	20.95	5.01	0.32	0.67	-52.47	12.37	1.69	0.50
13.	22.67	5.44	0.30	0.67	-54.68	14.05	1.61	0.54
14.	23.80	5.69	0.30	0.67	-55.59	15.05	1.58	0.57

TABLE D.8

Experimental data of model no.8 (see Figure 5-2)

Reverse	trapezoidal shape	two-cycle
P = 10.00 cm	W = 56.20 cm	g = 981 cm/sec^2
L = 143.96 cm	L/W = 2.56	α = 14.04°

Test no.	Q_{TL} (l/s)	H (cm)	Experimental C_d	Theoretical C_d	Difference in C_d (%)	Theoretical Q_{TN} (l/s)	Q_{TL}/Q_{TN} or Q_L/Q_N	H/P
(1)	(2)	(3)	(4)	(5)	(6)	(7)	(8)	(9)
1.	4.73	1.47	0.62	0.68	-9.05	2.03	2.33	0.15
2.	6.24	1.82	0.60	0.67	-11.69	2.76	2.26	0.18
3.	7.65	2.19	0.56	0.67	-16.88	3.59	2.13	0.22
4.	8.65	2.48	0.52	0.67	-21.58	4.31	2.01	0.25
5.	10.95	2.97	0.50	0.66	-24.08	5.63	1.94	0.30
6.	12.45	3.32	0.48	0.66	-26.73	6.63	1.88	0.33
7.	14.49	3.64	0.49	0.66	-25.89	7.63	1.90	0.36
8.	15.73	3.93	0.48	0.66	-28.17	8.55	1.84	0.39
9.	17.42	4.28	0.46	0.66	-30.09	9.73	1.79	0.43
10.	19.64	4.75	0.45	0.66	-32.79	11.41	1.72	0.48
11.	20.77	4.98	0.44	0.66	-33.96	12.28	1.69	0.50
12.	22.39	5.25	0.44	0.67	-34.31	13.31	1.68	0.53
13.	23.14	5.47	0.43	0.67	-36.15	14.15	1.64	0.55
14.	24.19	5.73	0.42	0.67	-37.85	15.19	1.59	0.57

TABLE D.9

Experimental data of model no. 1a (see Figure 5-2)

Trapezoidal			two-cycle					
P = 5.00 cm			W = 56.20 cm			g = 981 cm/sec^2		
L = 143.96 cm			L/W = 2.56			α = 14.04°		
Test no.	Q_{TL} (l/s)	H (cm)	Experimental C_d	Theoretical C_d	Difference in C_d (%)	Theoretical Q_{TN} (l/s)	Q_{TL}/Q_{TN} or Q_L/Q_N	H/P
(1)	(2)	(3)	(4)	(5)	(6)	(7)	(8)	(9)
1.	2.90	1.04	0.64	0.72	-10.33	1.26	2.30	0.21
2.	3.44	1.18	0.63	0.71	-11.06	1.51	2.28	0.24
3.	4.24	1.32	0.65	0.70	-6.68	1.77	2.39	0.26
4.	4.92	1.46	0.66	0.70	-5.56	2.03	2.42	0.29
5.	5.59	1.59	0.66	0.69	-5.21	2.30	2.43	0.32
6.	6.37	1.75	0.65	0.69	-6.36	2.65	2.40	0.35
7.	7.08	1.84	0.67	0.69	-2.76	2.84	2.49	0.37
8.	7.84	1.98	0.66	0.69	-3.71	3.18	2.47	0.40
9.	9.85	2.39	0.63	0.69	-8.74	4.21	2.34	0.48
10.	10.42	2.49	0.62	0.68	-8.88	4.46	2.33	0.50
11.	11.69	2.74	0.61	0.69	-11.70	5.17	2.26	0.55
12.	13.52	3.02	0.61	0.69	-11.71	5.98	2.26	0.60

TABLE D.10

Experimental data of model no.1b (see Figure 5-3)

Trapezoidal	two-cycle	
P = 10.00 cm	W = 56.20 cm	g = 981 cm/sec^2
L = 143.96 cm	L/W = 2.56	α = 14.04°
Top width = 0.7 cm		

Test no.	Q_{TL} (l/s)	H (cm)	Experimental C_d	Theoretical C_d	Difference in C_d (%)	Theoretical Q_{TN} (l/s)	Q_{TL}/Q_{TN} or Q_L/Q_N	H/P
(1)	(2)	(3)	(4)	(5)	(6)	(7)	(8)	(9)
1.	4.84	1.40	0.69	0.69	0.35	1.88	2.57	0.14
2.	6.45	1.64	0.72	0.68	6.38	2.37	2.72	0.16
3.	7.99	1.93	0.70	0.67	4.72	2.98	2.68	0.19
4.	9.96	2.20	0.72	0.67	7.57	3.62	2.76	0.22
5.	12.26	2.53	0.72	0.66	7.87	4.44	2.76	0.25
6.	17.82	3.14	0.75	0.66	13.92	6.11	2.92	0.31
7.	19.47	3.49	0.70	0.66	6.17	7.16	2.72	0.34
8.	21.21	3.72	0.69	0.66	5.05	7.88	2.69	0.37
9.	24.48	4.14	0.68	0.66	3.21	9.26	2.64	0.41
10.	27.71	4.52	0.68	0.66	2.33	10.57	2.62	0.44
11.	32.21	5.09	0.66	0.66	-0.73	12.67	2.54	0.50
12.	35.40	5.43	0.66	0.67	-1.21	13.99	2.53	0.53
13.	38.00	5.74	0.65	0.67	-2.49	15.21	2.50	0.56

TABLE D.11

Experimental data of model no.1c (see Figure 5-3)

Trapezoidal	two-cycle	
P = 10.00 cm	W = 56.20 cm	g = 981 cm/sec^2
L = 143.96 cm	L/W = 2.56	α = 14.04°
Top width = 1 cm		

Test no. (1)	Q_{TL} (l/s) (2)	H (cm) (3)	Experimental C_d (4)	Theoretical C_d (5)	Difference in C_d (%) (6)	Theoretical Q_{TN} (l/s) (7)	Q_{TL}/Q_{TN} or Q_L/Q_N (8)	H/P (9)
1.	4.95	1.50	0.64	0.68	-7.06	2.08	2.38	0.15
2.	6.39	1.73	0.66	0.68	-2.56	2.56	2.50	0.17
3.	7.99	1.97	0.68	0.67	1.23	3.08	2.59	0.19
4.	10.42	2.32	0.69	0.67	4.01	3.91	2.66	0.23
5.	12.98	2.62	0.72	0.66	8.37	4.67	2.78	0.26
6.	17.58	3.26	0.70	0.66	6.18	6.46	2.72	0.32
7.	22.58	3.85	0.70	0.66	6.30	8.29	2.72	0.38
8.	24.97	4.12	0.70	0.66	6.35	9.16	2.72	0.40
9.	28.34	4.48	0.70	0.66	6.12	10.43	2.72	0.44
10.	30.52	4.72	0.70	0.66	5.40	11.30	2.70	0.46
11.	34.67	5.27	0.67	0.67	1.24	13.37	2.59	0.52
12.	34.67	5.27	0.67	0.67	1.24	13.37	2.59	0.52
13.	38.13	5.64	0.67	0.67	0.42	14.82	2.57	0.55
14.	39.15	5.82	0.66	0.67	-1.83	15.57	2.51	0.57

TABLE D.12
Experimental data of model no. 1d (see Figure 5-3)

Trapezoidal	two-cycle	
P = 10.00 cm	W = 56.20 cm	g = 981 cm/sec^2
L = 143.96 cm	L/W = 2.56	α = 14.04°
Top width = 1.50 cm		

Test no.	Q_{TL} (l/s)	H (cm)	Experimental C_d	Theoretical C_d	Difference in C_d (%)	Theoretical Q_{TN} (l/s)	Q_{TL}/Q_{TN} or Q_L/Q_N	H/P
(1)	(2)	(3)	(4)	(5)	(6)	(7)	(8)	(9)
1.	4.92	1.52	0.62	0.68	-9.50	2.12	2.32	0.15
2.	6.50	1.75	0.66	0.68	-2.55	2.60	2.50	0.17
3.	8.04	2.01	0.66	0.67	-1.11	3.17	2.53	0.20
4.	9.02	2.22	0.64	0.67	-3.84	3.66	2.46	0.22
5.	10.48	2.47	0.64	0.66	-4.43	4.28	2.45	0.24
6.	15.06	3.02	0.68	0.66	2.15	5.76	2.62	0.30
7.	16.95	3.26	0.68	0.66	2.37	6.46	2.62	0.32
8.	19.22	3.50	0.69	0.66	4.67	7.17	2.68	0.34
9.	22.67	3.95	0.68	0.66	2.83	8.61	2.63	0.39
10.	24.77	4.23	0.67	0.66	1.32	9.54	2.60	0.41
11.	26.78	4.48	0.67	0.66	0.42	10.41	2.57	0.44
12.	31.98	4.99	0.68	0.66	1.65	12.28	2.60	0.49
13.	35.76	5.46	0.66	0.67	-1.05	14.11	2.53	0.54
14.	38.89	5.81	0.65	0.67	-2.08	15.51	2.51	0.57

TABLE D.13

Experimental data of model no. 1e (see Figure 5-3)

Trapezoidal	two-cycle	
P = 10.00 cm	W = 56.20 cm	g = 981 cm/sec^2
L = 143.96 cm	L/W = 2.56	α = 14.04°
Top width = 2.00 cm		

Test no.	Q_{TL} (l/s)	H (cm)	Experimental C_d	Theoretical C_d	Difference in C_d (%)	Theoretical Q_{TN} (l/s)	Q_{TL}/Q_{TN} or Q_L/Q_N	H/P
(1)	(2)	(3)	(4)	(5)	(6)	(7)	(8)	(9)
1.	4.92	1.62	0.56	0.68	-17.10	2.32	2.12	0.16
2.	6.54	1.92	0.58	0.67	-13.98	2.97	2.20	0.19
3.	7.89	2.13	0.60	0.67	-10.89	3.46	2.28	0.21
4.	8.60	2.29	0.59	0.67	-12.18	3.82	2.25	0.22
5.	10.25	2.53	0.60	0.66	-9.83	4.44	2.31	0.25
6.	12.91	2.96	0.60	0.66	-9.76	5.59	2.31	0.29
7.	15.50	3.27	0.62	0.66	-6.79	6.49	2.39	0.32
8.	17.50	3.49	0.63	0.66	-4.48	7.15	2.45	0.34
9.	21.21	3.99	0.63	0.66	-5.26	8.74	2.43	0.39
10.	23.14	4.22	0.63	0.66	-5.18	9.53	2.43	0.41
11.	24.67	4.38	0.63	0.66	-4.35	10.07	2.45	0.43
12.	29.42	5.00	0.62	0.66	-6.78	12.32	2.39	0.49
13.	33.37	5.44	0.62	0.67	-7.14	14.03	2.38	0.53
14.	35.76	5.66	0.62	0.67	-6.46	14.92	2.40	0.56

TABLE D.14

Depth profile data taken along the centre line of one-cycle on rectangular plan form, model no.4 (see Figure 5-1)

H/P = 0.41 QL/QN = 2.64

QTL = 23.99 l/s
P = 10.00 cm
L/W = 3.00

No.	X (cm)	E (cm)	X/P	E/P
1	0.00	3.50	0.00	0.35
2	-3.00	3.13	-0.30	0.31
3	-6.00	2.73	-0.60	0.27
4	-9.00	2.52	-0.90	0.25
5	-12.00	2.70	-1.20	0.27
6	-15.00	3.77	-1.50	0.38
7	-16.30	4.26	-1.63	0.43
8	-18.00	4.26	-1.80	0.43
9	-20.00	3.62	-2.00	0.36
10	-23.00	3.65	-2.30	0.36
11	-26.00	3.71	-2.60	0.37
12	-28.10	3.34	-2.81	0.33
13	-32.00	1.12	-3.20	0.11
14	-35.00	-2.75	-3.50	-0.28
15	-37.00	-5.50	-3.70	-0.55

*E = water surface elevation relative to crest.
*X = distance.
*P = weir height.
*QTL = total flowrate over the labyrinth weir.

TABLE D.15

Depth profile data taken along the centre line of one–cycle on rectangular plan form, model no.4 (see Figure 5–1)

H/P = 0.48 QL/QN = 2.48

QTL = 29.09 l/s
P = 10.00 cm
L/W = 3.00

No.	X (cm)	E (cm)	X/P	E/P
1	0.00	4.17	0.00	0.42
2	−3.00	3.77	−0.30	0.38
3	−6.00	3.25	−0.60	0.33
4	−9.00	2.79	−0.90	0.28
5	−12.00	2.67	−1.20	0.27
6	−15.00	3.04	−1.50	0.30
7	−18.30	4.74	−1.83	0.47
8	−20.00	5.05	−2.00	0.50
9	−23.00	4.56	−2.30	0.46
10	−25.00	4.26	−2.50	0.43
11	−28.10	3.74	−2.81	0.37
12	−30.00	3.10	−3.00	0.31
13	−32.00	1.67	−3.20	0.17
14	−36.20	−4.43	−3.62	−0.44

*E = water surface elevation relative to crest.
*X = distance.
*P = weir height.
*QTL = total flowrate over the labyrinth weir.

TABLE D.16

Depth profile data taken along the centre line of one–cycle on rectangular plan form, model no.4 (see Figure 5–1)

H/P = 0.56 QL/QN = 2.33

QTL = 34.43 l/s
P = 10.00 cm
L/W = 3.00

No.	X (cm)	E (cm)	X/P	E/P
1	0.00	4.84	0.00	0.48
2	−3.00	4.35	−0.30	0.43
3	−6.00	3.77	−0.60	0.38
4	−9.00	3.25	−0.90	0.33
5	−12.00	2.95	−1.20	0.29
6	−15.00	3.04	−1.50	0.30
7	−18.00	3.65	−1.80	0.36
8	−21.00	4.71	−2.10	0.47
9	−23.70	5.81	−2.37	0.58
10	−25.00	5.90	−2.50	0.59
11	−27.00	5.32	−2.70	0.53
12	−28.10	4.68	−2.81	0.47
13	−30.00	3.83	−3.00	0.38
14	−33.00	1.76	−3.30	0.18
15	−35.00	−0.99	−3.50	−0.10
16	−37.50	−3.79	−3.75	−0.38

*E = water surface elevation relative to crest.
*X = distance.
*P = weir height.
*QTL = total flowrate over the labyrinth weir.

TABLE D.17

Depth profile data taken along the centre line of one–cycle on rectangular geometry with a semi–circular connection, model no.5 (see Figure 5–1)

H/P = 0.48 QL/QN = 2.52

QTL = 29.09 l/s
P = 10.00 cm
L/W = 2.68

No.	X (cm)	E (cm)	X/P	E/P
1	0.00	4.26	0.00	0.43
2	−3.00	3.95	−0.30	0.40
3	−6.00	3.65	−0.60	0.36
4	−9.00	3.40	−0.90	0.34
5	−12.00	3.43	−1.20	0.34
6	−15.00	3.80	−1.50	0.38
7	−18.00	4.56	−1.80	0.46
8	−21.00	4.87	−2.10	0.49
9	−24.00	4.32	−2.40	0.43
10	−27.00	3.86	−2.70	0.39
11	−28.10	3.65	−2.81	0.36
12	−32.00	1.54	−3.20	0.15
13	−35.00	−1.44	−3.50	−0.14
14	−38.00	−2.97	−3.80	−0.30
15	−41.00	−4.09	−4.10	−0.41
16	−44.00	−4.77	−4.40	−0.48
17	3.00	4.47	0.30	0.45
18	6.00	4.62	0.60	0.46
19	9.00	4.65	0.90	0.47
20	12.00	4.68	1.20	0.47
21	15.00	4.74	1.50	0.47
22	18.00	4.78	1.80	0.48

*E = water surface elevation relative to crest.
*X = distance.
*P = weir height.
*QTL = total flowrate over the labyrinth weir.

TABLE D.18

Depth profile data taken along the centre line of one–cycle on rectangular geometry with a semi–circular connection, model no.5 (see Figure 5–1)

H/P = 0.51 QL/QN = 2.46

QTL = 31.75 l/s
P = 10.00 cm
L/W = 2.68

No.	X (cm)	E (cm)	X/P	E/P
1	0.00	4.62	0.00	0.46
2	−3.00	4.35	−0.30	0.43
3	−6.00	3.95	−0.60	0.40
4	−9.00	3.65	−0.90	0.36
5	−12.00	3.56	−1.20	0.36
6	−15.00	3.83	−1.50	0.38
7	−18.00	4.50	−1.80	0.45
8	−21.00	5.20	−2.10	0.52
9	−24.00	4.96	−2.40	0.50
10	−27.00	4.35	−2.70	0.43
11	−28.10	4.04	−2.81	0.40
12	−32.00	2.12	−3.20	0.21
13	−35.00	−0.28	−3.50	−0.03
14	−38.00	−2.11	−3.80	−0.21
15	−41.00	−3.30	−4.10	−0.33
16	−44.00	−3.97	−4.40	−0.40
17	5.00	4.93	0.50	0.49
18	10.00	5.05	1.00	0.50
19	15.00	5.08	1.50	0.51
20	20.00	5.11	2.00	0.51

*E = water surface elevation relative to crest.
*X = distance.
*P = weir height.
*QTL = total flowrate over the labyrinth weir.

TABLE D.19

Depth profile data taken along the centre line of one–cycle on rectangular geometry with a semi–circular connection, model no.5 (see Figure 5–1)

H/P = 0.59 QL/QN = 2.34

QTL = 36.87 l/s
P = 10.00 cm
L/W = 2.68

No.	X (cm)	E (cm)	X/P	E/P
1	0.00	5.20	0.00	0.52
2	−3.00	4.93	−0.30	0.49
3	−6.00	4.56	−0.60	0.46
4	−9.00	4.17	−0.90	0.42
5	−12.00	3.98	−1.20	0.40
6	−15.00	3.95	−1.50	0.40
7	−18.00	4.50	−1.80	0.45
8	−21.00	5.32	−2.10	0.53
9	−24.00	5.87	−2.40	0.59
10	−27.00	5.42	−2.70	0.54
11	−28.10	5.08	−2.81	0.51
12	−32.00	3.19	−3.20	0.32
13	−35.00	1.09	−3.50	0.11
14	−38.00	−0.80	−3.80	−0.08
15	−41.00	−2.02	−4.10	−0.20
16	5.00	5.54	0.50	0.55
17	10.00	5.72	1.00	0.57
18	15.00	5.78	1.50	0.58
19	20.00	5.87	2.00	0.59

*E = water surface elevation relative to crest.
*X = distance.
*P = weir height.
*QTL = total flowrate over the labyrinth weir.

TABLE D.20

Depth profile data taken along the centre line of one–cycle on reverse trapezoidal plan form, model no.7 (see Figure 5–2)

H/P = 0.43 QL/QN = 1.76

QTL = 17.18 l/s
P = 10.00 cm
L/W = 3.56

No.	X (cm)	E (cm)	X/P	E/P
1	−45.00	−5.55	−4.50	−0.55
2	−40.00	−6.37	−4.00	−0.64
3	−37.00	−7.38	−3.70	−0.74
4	−32.00	0.49	−3.20	0.05
5	−31.00	1.62	−3.10	0.16
6	−30.00	1.77	−3.00	0.18
7	−28.10	2.50	−2.81	0.25
8	−25.00	2.44	−2.50	0.24
9	−20.00	2.74	−2.00	0.27
10	−15.00	2.56	−1.50	0.26
11	−10.00	1.28	−1.00	0.13
12	−5.00	2.41	−0.50	0.24
13	0.00	3.57	0.00	0.36
14	5.00	4.02	0.50	0.40
15	10.00	4.15	1.00	0.41
16	15.00	4.21	1.50	0.42
17	20.00	4.24	2.00	0.42

*E = water surface elevation relative to crest.
*X = distance.
*P = weir height.
*QTL = total flowrate over the labyrinth weir.

TABLE D.21

Depth profile data taken along the centre line of one–cycle on reverse trapezoidal plan form, model no.7 (see Figure 5–2)

H/P = 0.50 QL/QN = 1.69

QTL = 20.95 l/s
P = 10.00 cm
L/W = 3.56

No.	X (cm)	E (cm)	X/P	E/P
1	−45.00	−7.68	−4.50	−0.77
2	−40.00	−7.22	−4.00	−0.72
3	−38.00	−6.89	−3.80	−0.69
4	−32.00	1.74	−3.20	0.17
5	−31.00	2.10	−3.10	0.21
6	−30.00	2.65	−3.00	0.27
7	−28.10	3.23	−2.81	0.32
8	−25.00	3.29	−2.50	0.33
9	−20.00	3.75	−2.00	0.37
10	−15.00	2.07	−1.50	0.21
11	−10.00	1.77	−1.00	0.18
12	−5.00	3.14	−0.50	0.31
13	0.00	4.33	0.00	0.43
14	5.00	4.79	0.50	0.48
15	10.00	4.82	1.00	0.48
16	15.00	5.00	1.50	0.50
17	20.00	5.03	2.00	0.50

*E = water surface elevation relative to crest.
*X = distance.
*P = weir height.
*QTL = total flowrate over the labyrinth weir.

TABLE D.22

Depth profile data taken along the centre line of one–cycle on reverse trapezoidal plan form, model no.7 (see Figure 5–2)

H/P = 0.57 QL/QN = 1.58

QTL = 23.80 l/s
P = 10.00 cm
L/W = 3.56

No.	X (cm)	E (cm)	X/P	E/P
1	−45.00	−5.79	−4.50	−0.58
2	−40.00	−7.68	−4.00	−0.77
3	−38.00	−5.97	−3.80	−0.60
4	−32.00	1.98	−3.20	0.20
5	−31.00	2.80	−3.10	0.28
6	−30.00	2.99	−3.00	0.30
7	−28.10	3.47	−2.81	0.35
8	−25.00	4.18	−2.50	0.42
9	−20.00	4.11	−2.00	0.41
10	−15.00	1.95	−1.50	0.20
11	−10.00	2.19	−1.00	0.22
12	−5.00	3.57	−0.50	0.36
13	0.00	4.85	0.00	0.48
14	5.00	5.33	0.50	0.53
15	10.00	5.46	1.00	0.55
16	15.00	5.55	1.50	0.55
17	20.00	5.70	2.00	0.57

*E = water surface elevation relative to crest.
*X = distance.
*P = weir height.
*QTL = total flowrate over the labyrinth weir.

TABLE D.23

Depth profile data taken along the centre line of one–cycle on reverse trapezoidal plan form, model no.8 (see Figure 5–2)

H/P = 0.43 QL/QN = 1.79

QTL = 17.42 l/s
P = 10.00 cm
L/W = 2.56

No.	X (cm)	E (cm)	X/P	E/P
1	−40.00	−6.24	−4.00	−0.62
2	−35.00	−6.76	−3.50	−0.68
3	−28.00	−7.64	−2.80	−0.76
4	−27.00	−6.33	−2.70	−0.63
5	−24.50	−2.18	−2.45	−0.22
6	−21.00	1.47	−2.10	0.15
7	−20.00	2.20	−2.00	0.22
8	−19.00	2.51	−1.90	0.25
9	−17.20	3.21	−1.72	0.32
10	−15.00	3.33	−1.50	0.33
11	−10.00	2.30	−1.00	0.23
12	−5.00	2.60	−0.50	0.26
13	0.00	3.58	0.00	0.36
14	5.00	4.03	0.50	0.40
15	10.00	4.16	1.00	0.42
16	15.00	4.19	1.50	0.42
17	20.00	4.22	2.00	0.42

*E = water surface elevation relative to crest.
*X = distance.
*P = weir height.
*QTL = total flowrate over the labyrinth weir.

TABLE D.24

Depth profile data taken along the centre line of one–cycle on reverse trapezoidal plan form, model no.8 (see Figure 5–2)

H/P = 0.50 QL/QN = 1.69

QTL = 20.77 l/s
P = 10.00 cm
L/W = 2.56

No.	X (cm)	E (cm)	X/P	E/P
1	−40.00	−5.99	−4.00	−0.60
2	−35.00	−7.21	−3.50	−0.72
3	−29.00	−7.24	−2.90	−0.72
4	−27.00	−4.07	−2.70	−0.41
5	−24.50	−0.48	−2.45	−0.05
6	−21.00	2.42	−2.10	0.24
7	−20.00	2.91	−2.00	0.29
8	−19.00	3.39	−1.90	0.34
9	−17.20	3.88	−1.72	0.39
10	−15.00	3.70	−1.50	0.37
11	−10.00	2.24	−1.00	0.22
12	−5.00	3.18	−0.50	0.32
13	0.00	4.19	0.00	0.42
14	5.00	4.67	0.50	0.47
15	10.00	4.77	1.00	0.48
16	15.00	4.92	1.50	0.49
17	20.00	4.92	2.00	0.49

*E = water surface elevation relative to crest.
*X = distance.
*P = weir height.
*QTL = total flowrate over the labyrinth weir.

TABLE D.25

Depth profile data taken along the centre line of one–cycle on reverse trapezoidal plan form, model no.8 (see Figure 5–2)

H/P = 0.57 QL/QN = 1.59

QTL = 24.19 l/s
P = 10.00 cm
L/W = 2.56

No.	X (cm)	E (cm)	X/P	E/P
1	−40.00	−6.27	−4.00	−0.63
2	−33.00	−7.46	−3.30	−0.75
3	−30.00	−5.75	−3.00	−0.58
4	−27.00	−1.39	−2.70	−0.14
5	−24.50	0.62	−2.45	0.06
6	−21.00	3.21	−2.10	0.32
7	−20.00	3.82	−2.00	0.38
8	−19.00	4.09	−1.90	0.41
9	−17.20	4.06	−1.72	0.41
10	−15.00	2.78	−1.50	0.28
11	−10.00	2.88	−1.00	0.29
12	−5.00	3.70	−0.50	0.37
13	0.00	4.89	0.00	0.49
14	5.00	5.41	0.50	0.54
15	10.00	5.47	1.00	0.55
16	15.00	5.56	1.50	0.56
17	20.00	5.59	2.00	0.56

*E = water surface elevation relative to crest.
*X = distance.
*P = weir height.
*QTL = total flowrate over the labyrinth weir.

TABLE D.26

Depth profile data taken along the centre line between two cycles on rectangular plan form, model no.4 (see Figure 5–1)

H/P = 0.41 QL/QN = 2.64

QTL = 23.99 l/s
P = 10.00 cm
L/W = 3.00

No.	X (cm)	E (cm)	X/P	E/P
1	0.00	3.53	0.00	0.35
2	−3.00	2.37	−0.30	0.24
3	−6.00	0.14	−0.60	0.01
4	−9.00	−1.90	−0.90	−0.19
5	−18.50	0.11	−1.85	0.01
6	−24.60	−0.56	−2.46	−0.06
7	−28.10	−1.29	−2.81	−0.13
8	−32.50	−4.06	−3.25	−0.41
9	−35.00	−5.47	−3.50	−0.55

*E = water surface elevation relative to crest.
*X = distance.
*P = weir height.
*QTL = total flowrate over the labyrinth weir.

TABLE D.27

Depth profile data taken along the centre line between two cycles on reverse trapezoidal plan form, model no.7 (see Figure 5–2)

H/P = 0.57 QL/QN = 1.58

QTL = 23.80 l/s
P = 10.00 cm
L/W = 3.56

No.	X (cm)	E (cm)	X/P	E/P
1	−40.00	−6.16	−4.00	−0.62
2	−35.00	−1.77	−3.50	−0.18
3	−30.00	1.92	−3.00	0.19
4	−28.10	3.60	−2.81	0.36
5	−25.00	3.78	−2.50	0.38
6	−15.00	1.43	−1.50	0.14
7	−9.50	1.16	−0.95	0.12
8	−6.00	2.59	−0.60	0.26
9	−4.00	3.60	−0.40	0.36
10	−2.00	4.36	−0.20	0.44
11	0.00	4.94	0.00	0.49
12	5.00	5.46	0.50	0.55
13	10.00	5.55	1.00	0.55
14	15.00	5.61	1.50	0.56
15	20.00	5.64	2.00	0.56

*E = water surface elevation relative to crest.
*X = distance.
*P = weir height.
*QTL = total flowrate over the labyrinth weir.

TABLE D.28

Depth profile data taken along the centre line between two cycles on reverse trapezoidal plan form, model no.8 (see Figure 5–2)

H/P = 0.57 QL/QN = 1.59

QTL = 24.19 l/s
P = 10.00 cm
L/W = 2.56

No.	X (cm)	E (cm)	X/P	E/P
1	−35.00	−5.93	−3.50	−0.59
2	−28.00	−5.26	−2.80	−0.53
3	−21.00	−1.12	−2.10	−0.11
4	−17.20	0.83	−1.72	0.08
5	−15.00	1.02	−1.50	0.10
6	−12.50	−2.76	−1.25	−0.28
7	−9.00	−1.15	−0.90	−0.11
8	−7.00	0.68	−0.70	0.07
9	−5.20	2.30	−0.52	0.23
10	−3.00	3.76	−0.30	0.38
11	−2.00	4.09	−0.20	0.41
12	−1.00	4.49	−0.10	0.45
13	0.00	4.70	0.00	0.47
14	5.00	5.44	0.50	0.54
15	10.00	5.50	1.00	0.55
16	15.00	5.56	1.50	0.56
17	20.00	5.62	2.00	0.56

*E = water surface elevation relative to crest.
*X = distance.
*P = weir height.
*QTL = total flowrate over the labyrinth weir.

Appendix E

This appendix contains a number of graphs which showed a different plotting of the relationship between flow magnification, Q_L/Q_N and depth to crest ratio, H/P; and the relationship between flow magnification, Q_L/Q_N and total head to crest ratio, H_o/P (see section 3.4).

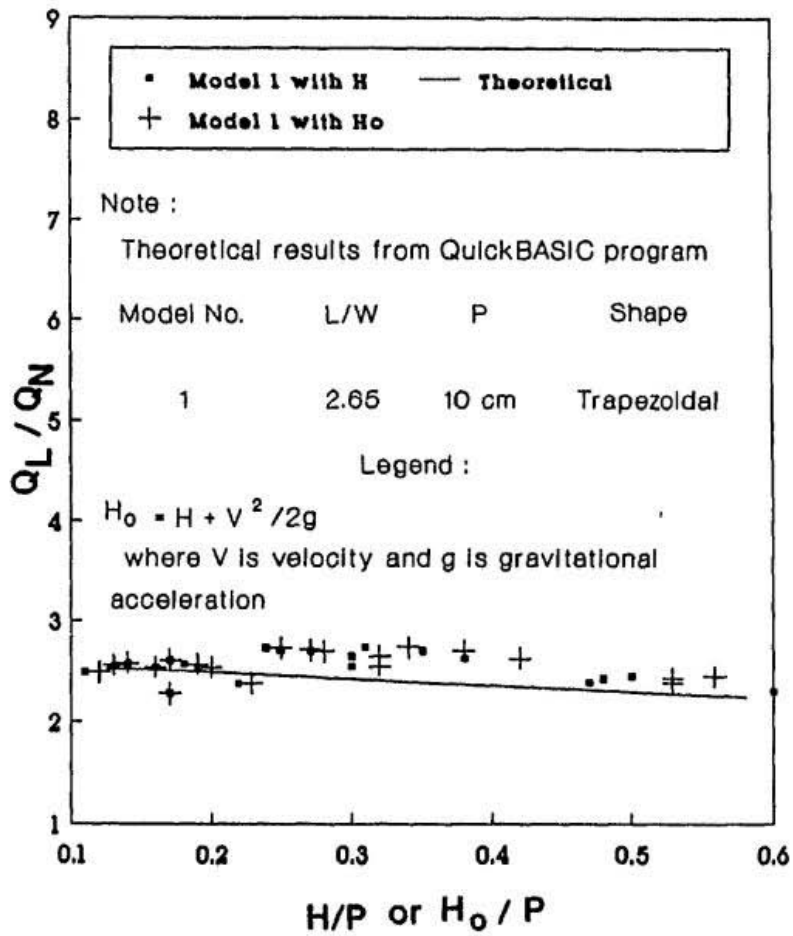

Figure E-1 A comparison of the flow magnification values plotting with H/P and H_o/P for model no.1 (trapezoidal shape, two-cycle-see Figure 5-1).

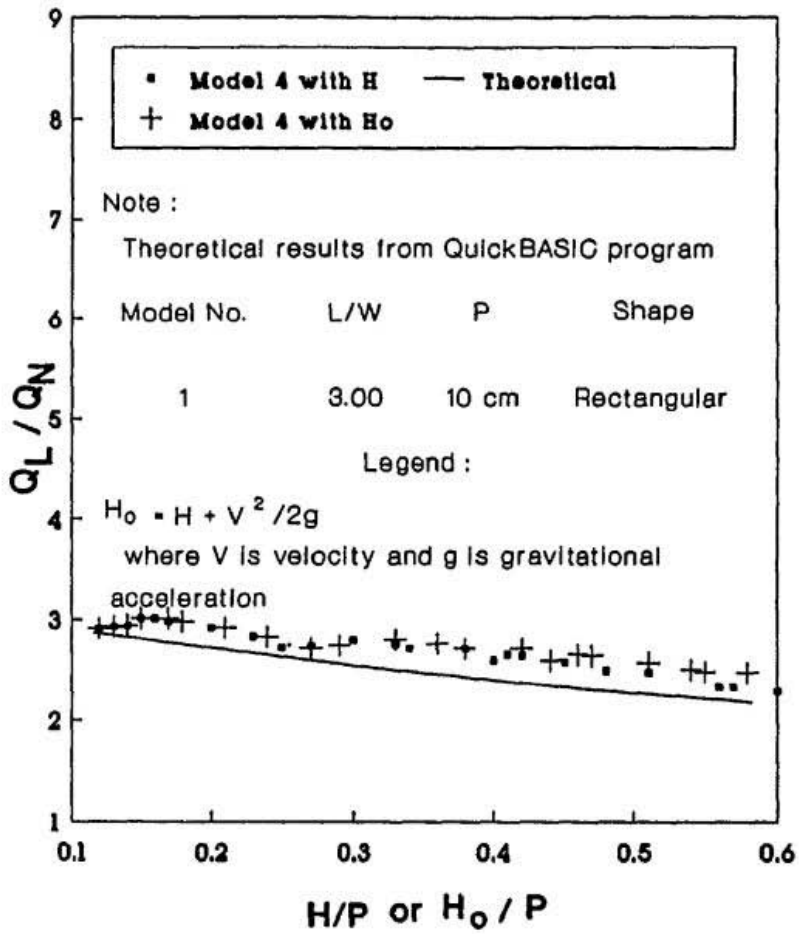

Figure E-2 A comparison of the flow magnification values plotting with H/P and H_o/P for model no.4 (rectangular shape, two-cycle-see Figure 5-1).

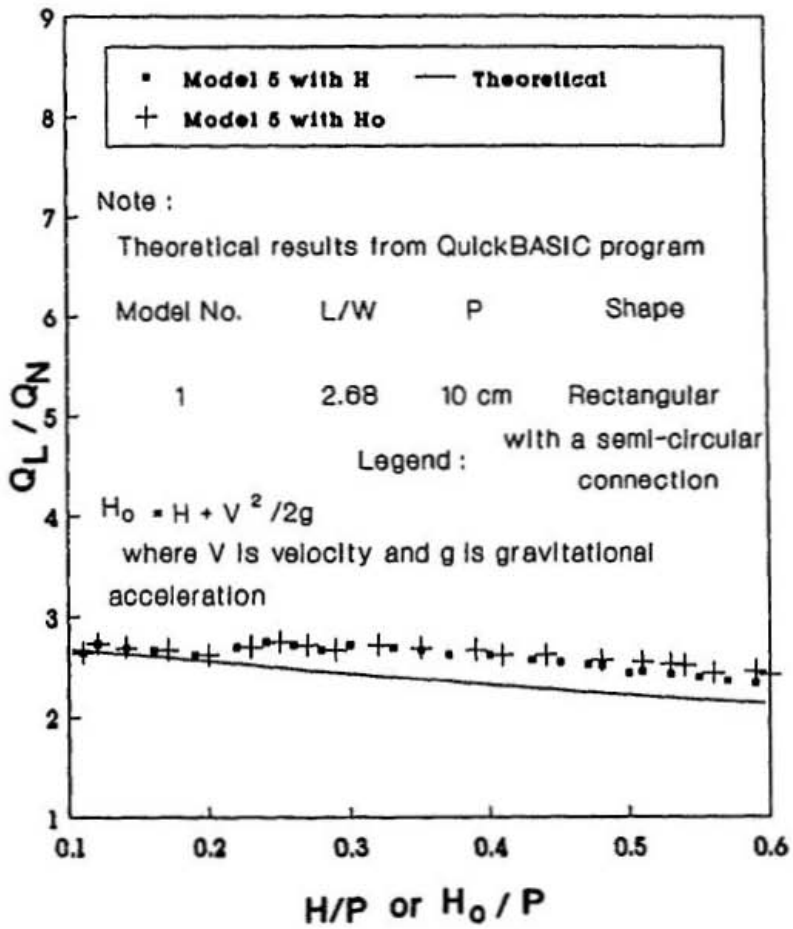

Figure E-3 A comparison of the flow magnification values plotting with H/P and H_o/P for model no.5 (rectangular shape with a semi-circular connection, two-cycle-see Figure 5-1).